144 p.

NASA
Technical
Paper
2364

October 1984

Static Internal Performance of Single-Expansion-Ramp Nozzles With Thrust-Vectoring Capability up to 60°

Bobby L. Berrier and
Laurence D. Leavitt

[redacted]

NASA

NASA Technical Paper 2364

1984

Static Internal Performance of Single-Expansion-Ramp Nozzles With Thrust-Vectoring Capability up to 60°

Bobby L. Berrier and
Laurence D. Leavitt

Langley Research Center
Hampton, Virginia

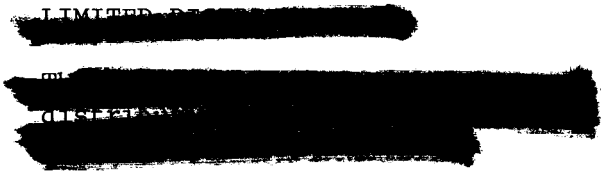

National Aeronautics and Space Administration

Scientific and Technical Information Branch

Summary

An investigation has been conducted at static conditions (wind off) in the static-test facility of the Langley 16-Foot Transonic Tunnel. The effects of geometric thrust-vector angle, sidewall containment, ramp curvature, lower-flap lip angle, and ramp length on the internal performance of nonaxisymmetric single-expansion-ramp nozzles were investigated. Geometric thrust-vector angle was varied from -20° to 60°, and nozzle pressure ratio was varied from 1.0 (jet off) to approximately 10.0.

The results of this investigation indicate that single-expansion-ramp nozzles can provide large positive thrust-vector angles (up to 60°) with little or no loss in resultant thrust ratio. However, exhaust flow separation on the ramp limits the negative thrust-vectoring capability. Nozzle positive thrust-vectoring capability was improved by sidewall containment along the ramp length, by ramp curvature, and by increasing the lower-flap lip angle. Ramp length for maximum flow-turning capability was highly dependent on nozzle pressure ratio.

Introduction

Recent studies on twin-engine fighter airplanes (refs. 1 to 15) have identified potential benefits of nonaxisymmetric or two-dimensional nozzles. This nozzle concept is geometrically amenable to improvements in nozzle integration for reduced installed drag, thrust vectoring for maneuver enhancement and short take-off and landing (STOL), and thrust reversing for improved agility and reduced landing ground roll. The single-expansion-ramp nozzle (SERN) is one of the most promising types of nonaxisymmetric nozzles identified in recent years. (See refs. 7 to 24.) The SERN was originally developed with a jet deflector to provide high vector angles (up to 110°) for vertical take-off and landing (VTOL) operations (refs. 7, 8, and 18 to 21). However, system studies and wind-tunnel tests have shown that the SERN is also competitive with other nozzle types during cruise and combat operating modes (refs. 3, 9, 10, 12 to 17, and 22 to 24). If conventional or moderate STOL performance is desired, the jet deflector can be removed from the SERN design to reduce nozzle weight, and low vector angles can be achieved by deflection of a variable external expansion ramp (VEER) flap (refs. 19 and 21). Because of flow separation at negative thrust-vector angles and large supersonic flow-turning losses at positive thrust-vector angles approaching 30° (refs. 17 and 21), most experimental programs with SERN nozzles have limited VEER flap deflections to ±20°. A recent experimental SERN study (ref. 24), conducted at thrust-vector angles from -10° to 20°, indicated that the large supersonic-flow turning losses associated with VEER flap deflection can be substantially reduced by utilizing the entire upper expansion ramp (as opposed to a short VEER flap) and the nozzle lower flap to obtain thrust vectoring.

This paper presents static internal performance of a single-expansion-ramp nozzle at geometric thrust-vector angles from -20° up to 60°. The entire upper expansion ramp and the nozzle lower flap (for geometric thrust-vector angles greater than 10°) were utilized to obtain thrust vectoring. The effects of sidewall containment and lower-flap lip angle are presented for geometric thrust-vector angles from -20° to 30°. Data are presented showing the effect of parametric variation of upper expansion ramp curvature and length for a geometric thrust-vector angle of 30°. One ramp curvature variation at a geometric thrust-vector angle of 0° (cruise operating mode) was also tested. This investigation was conducted in the static-test facility of the Langley 16-Foot Transonic Tunnel at static conditions and at nozzle pressure ratios up to 10.

Symbols

All forces (with the exception of resultant gross thrust) and angles are referred to the model centerline (body axis). A detailed discussion of the data-reduction and calibration procedures as well as definitions of forces, angles, and propulsion relationships used herein can be found in reference 17.

A_e nozzle-exit area, in^2

A_t nozzle-throat area, in^2

$(A_e/A_t)_i$ internal expansion ratio (A_e measured at end of nozzle lower flap)

C_d nozzle discharge coefficient (ratio of measured weight-flow rate to ideal weight-flow rate)

F measured thrust along body axis, lbf

F_i ideal isentropic gross thrust,

$$w_p\sqrt{\frac{RT_{t,j}}{g}\left(\frac{2\gamma}{\gamma-1}\right)\left[1-\left(\frac{p_a}{p_{t,j}}\right)^{\frac{\gamma-1}{\gamma}}\right]},\ \text{lbf}$$

F_r resultant gross thrust, $\sqrt{F^2+N^2}$, lbf

g gravitational constant, 32.174 ft/sec^2

h_t nozzle-throat height (fig. 3(b)), in.

l_l chord length of nozzle lower flap measured from lower-flap hinge point (fig. 3(d)), in.

$l_{l,\text{nom}}$ nominal lower-flap length (average of all lower-flap lengths), 3.401 in.

l_r chord length of nozzle ramp measured from ramp hinge point (fig. 3(c)), in.

$l_{r,\mathrm{nom}}$ nominal ramp length (average of all ramp lengths), 3.476 in.

$l_{r,o}$ length of ramp downstream and perpendicular to nozzle exit (fig. 3(c)), in.

N measured normal force, lbf

NPR nozzle pressure ratio (ratio of jet total pressure to ambient pressure)

p local static pressure, psi

p_a ambient pressure, psi

$p_{t,j}$ jet total pressure, psi

R gas constant (for $\gamma = 1.3997$), 53.364 ft/°R

$T_{t,j}$ jet total temperature, °R

w half-width of nozzle ramp, 2.00 in.

w_p measured weight-flow rate, lbf/sec

x axial distance measured from nozzle connect station, positive downstream, in.

x' location of ramp pressure orifices (relative to unvectored baseline, configuration 3) on longitudinal axis which rotates with upper ramp (fig. 3(a)), positive downstream of nominal ramp hinge point, in.

x'' location of lower-flap pressure orifices (relative to unvectored baseline, configuration 3) on longitudinal axis which rotates with lower flap (fig. 3(a)), positive downstream of nominal lower-flap hinge point, in.

x_e length from nozzle connect station to ramp or lower-flap exit (figs. 3(c) and 3(d)), in.

x_t length from nozzle connect station to throat location on ramp or lower flap (fig. 3(b)), in.

y vertical distance measured from model centerline, positive up, in.

y_e vertical distance of nozzle ramp or lower-flap trailing edge from model centerline, positive up (figs. 3(c) and 3(d)), in.

y_t vertical distance of nozzle ramp or lower-flap throat location from model centerline, positive up (see fig. 3(b)), in.

z lateral distance measured from model centerline, positive to left looking upstream, in.

$\alpha_{c,u}$ nozzle-ramp chord angle measured from horizontal reference line (fig. 3(c)), deg

α_{term} nozzle-ramp or lower-flap terminal or lip angle measured from horizontal reference line (see figs. 3(c) and 3(d)), deg

γ ratio of specific heats, 1.3997 for air

δ resultant thrust-vector angle, $\tan^{-1}\frac{N}{F}$, deg

δ_v design thrust-vector angle measured from horizontal reference line, positive in downward direction, deg

δ_l lower-flap rotation angle (relative to unvectored baseline, configuration 3, fig. 3(a)), positive in downward direction, deg

δ_u ramp rotation angle (relative to unvectored baseline, configuration 3, fig. 3(a)), positive in downward direction, deg

θ_t rotation angle of nozzle throat plane measured from vertical reference line, positive in clockwise direction (fig. 3(b)), deg

Subscripts:

l lower flap

u upper flap (or ramp)

Abbreviations:

Conf configuration

Curv. curvature

Incr. increased

Max maximum

Med medium

Min minimum

SERN single-expansion-ramp nozzle

Sta. model station, in.

Apparatus and Methods

Static-Test Facility

This investigation was conducted in the static-test facility of the Langley 16-Foot Transonic Tunnel. Testing was conducted in a room with a high ceiling where the jet exhausts to atmosphere through a large open doorway. The control room is remotely located from the test area, and a closed-circuit television camera is

used to observe the model. This facility utilizes the same clean, dry-air supply as that used in the 16-Foot Transonic Tunnel and a similar air-control system—including valving, filters, and a heat exchanger (to operate the jet flow at constant stagnation temperature).

Single-Engine Propulsion Simulation System

A sketch of the single-engine air-powered nacelle model on which various nozzles were mounted is presented in figure 1 with a typical nozzle configuration attached. The body shell forward of model station 20.50 was removed for this investigation.

An external high-pressure air system provided a continuous flow of clean, dry air at a controlled temperature of about 540°R. This high-pressure air was varied up to approximately 148 psi and was brought through the dolly-mounted support strut by six tubes which connect to a high-pressure plenum chamber. As shown in figure 1, the air was then discharged perpendicularly into the model low-pressure plenum through eight multiholed sonic nozzles equally spaced around the high-pressure plenum. This method was designed to minimize any forces imposed by the transfer of axial momentum as the air is passed from the nonmetric high-pressure plenum to the metric (mounted to the force balance) low-pressure plenum. Two flexible metal bellows are used as seals and serve to compensate for axial forces caused by pressurization. The air was then passed from the model low-pressure plenum (circular in cross section) through a transition section, choke plate, and instrumentation section. The transition section provided a smooth flow path for the airflow from the round low-pressure plenum to the rectangular choke plate and instrumentation section. The instrumentation section had a flow-path width-height ratio of 1.437 and was identical in geometry to the nozzle airflow entrance. The nozzles were attached to the instrumentation section at model station 41.13.

Nozzle Description

The single-expansion-ramp nozzle (SERN) is a nonaxisymmetric, variable-area, internal/external expansion exhaust system. A photograph showing a typical SERN test nozzle installed on the single-engine propulsion-simulation system is shown in figure 2. Details of nozzle operation (mechanics of varying throat and exit areas to optimize performance at any given engine power setting and flight condition) and construction are in references 7 and 17 to 20. For the current investigation, all test nozzles had a nominally constant exhaust flow-path width of 4.0 in., throat height h_t of 1.0 in., and throat area A_t of 4.0 in^2. The constant throat area of the current SERN test nozzles simulated a typical dry-power engine setting. Parametric geometry changes were achieved by using interchangeable upper ramps, lower nozzle flaps, and sidewalls.

Figure 3 presents sketches showing the SERN vectoring operation and defining important nozzle geometric parameters. Figure 4 presents sketches showing the geometry of each SERN configuration tested. An index to nozzle geometry sketches and tables and individual component part numbers is provided in table I. Values for the important nozzle-throat, upper-ramp, and lower-flap geometric parameters are summarized in tables II, III, and IV, respectively. Coordinates for each upper ramp, lower flap, and sidewall used to build up a particular configuration (see table I) are given in tables V, VI, and VII, respectively.

The baseline SERN for the current test (configuration 3, fig. 4(c)) simulated an unvectored ($\delta_v = 0°$), dry-power nozzle with minimum sidewall containment. The baseline upper ramp contained a moderate amount of axial ramp curvature (concave shape). For the current test, geometric thrust-vector angle δ_v has been defined as the geometric angle of the upper ramp relative to the baseline configuration δ_u (fig. 3(a)). A range of geometric thrust-vector angles from -20° to 60° were tested on the baseline SERN (configurations 1 to 8). For values of geometric thrust-vector angle from -20° to 10°, the lower flap remains fixed in the unvectored ($\delta_v = 0°$) nozzle position of $\delta_l = 0°$ (see table IV). For geometric thrust-vector angles greater than 10°, the lower-flap angle δ_l is increased (rotated downward). As geometric thrust-vector angle increases, the nozzle geometric throat translates toward the lower-flap exit until, at $\delta_v = 30°$, the nozzle geometric throat is coincident with the lower-flap exit (see throat location on figs. 4(a) to 4(f)). Of course, this also means that nozzle internal expansion ratio varies (approaches unity) with geometric thrust-vector angle (see table II).

In addition to geometric thrust-vector angle, other nozzle geometric parameters investigated were amount of sidewall containment, amount of ramp curvature, lower-flap lip angle, and upper-ramp length. Sidewall containment during vectored-thrust operation was investigated by replacing the baseline nozzle sidewalls with larger sidewalls (configurations 9 to 15, figs. 4(a) to 4(f)). Configurations 16 to 18 (fig. 4(i)) were used in conjunction with baseline configurations 1 to 3 to examine the effect of lower-flap lip angle $\alpha_{\text{term},l}$ on cruise ($\delta_v = 0°$) and negative thrust-vectoring nozzle performance. For all lower-flap lip angle variations during the current investigation, the lower-flap angle δ_l remained in the baseline position for each geometric thrust-vector angle δ_v, and the lip shape was changed to vary $\alpha_{\text{term},l}$ (see tables IV and VI). In addition to the baseline ramp, a straight ramp and a ramp with increased curvature were also tested. The straight ramp was investigated at

$\delta_v = 0°$ (configuration 19, fig. 4(j)) and at $\delta_v = 30°$ with three different lower-flap lip angles (configurations 20 to 22, fig. 4(k)). The increased-curvature ramp was investigated at $\delta_v = 30°$ with three different lower-flap lip angles (configurations 23, 24, and 26; fig. 4(l)) and two amounts of sidewall containment at the baseline lower-flap lip angle of 14.8° (configurations 24 and 25, fig. 4(l)). Configurations 27 to 40 (figs. 4(m) to 4(q)) and the baseline configuration 6 (fig. 4(f)) were used for a parametric study on the effects of ramp length l_r and lower-flap lip angle $\alpha_{\text{term},l}$ on SERN performance at $\delta_v = 30°$. Similar to increasing δ_v, the nozzle throat translates aft to the lower-flap exit as the lower-flap lip rotates upward (figs. 4(m) to 4(o)), and nozzle expansion ratio $(A_e/A_t)_i$ approaches unity (see table II). Although the lower-flap lip angle $\alpha_{\text{term},l}$ varies, the lower-flap angle δ_l remains at the baseline value of 6.1° ($\delta_v = 30°$) for configurations 27 to 40 (see table IV). Configurations 35 (fig. 4(o)) and 40 (fig. 4(q)) have essentially no exposed ramp length $l_{r,o}$ (see table III), and thus are not true single-expansion-ramp nozzles. These configuratons are simple convergent nozzles.

Instrumentation

A three-component strain-gauge balance was used to measure the forces and moments on the model downstream of station 20.50 in. (See fig. 1.) Jet total pressure was measured at a fixed station in the instrumentation section (see fig. 1) by means of a four-probe rake through the upper surface, a three-probe rake through the side, and a three-probe rake through the corner. A thermocouple, also located in the instrumentation section, was used to measure jet total temperature. Flow rate of the high-pressure air supplied to the nozzle was determined from pressure and temperature measurements in the high-pressure plenum (located on top of the support strut) calibrated with standard axisymmetric nozzles. Internal static-pressure orifices were located on all the ramp and lower-flap configurations tested. The locations of these orifices vary for each configuration and are given in table VIII in the form of $x'/l_{r,\text{nom}}$, $x''/l_{l,\text{nom}}$, and z/w. The symbols x' and x'' represent axis systems used to locate pressure orifices on the ramp and lower flaps, respectively. As shown in figure 3, values of x' and x'' are defined as positive downstream of the ramp and lower-flap hinge points and rotate with δ_u and δ_l. Both x' and x'' are parallel to the body axis when $\delta_u = \delta_l = 0°$. Both x' and x'' remain fixed upstream of the hinge points and are independent of δ_u and δ_l. Pressure orifice locations were defined in this manner to allow a more direct comparison of ramp and lower-flap pressure distributions.

Data Reduction

All data were recorded simultaneously on magnetic tape. Approximately 50 frames of data, taken at a rate of 10 frames per second, were used for each data point; average values were used in computations. Data were recorded in an ascending order of $p_{t,j}$. With the exception of resultant gross thrust F_r, all force data in this report are referenced to the model centerline.

The basic performance parameters used for the presentation of results are F/F_i, F_r/F_i, δ, and C_d. The internal thrust ratio F/F_i is the ratio of actual nozzle thrust (along the body axis) to ideal nozzle thrust, where ideal nozzle thrust is based on measured weight-flow rate and total temperature and pressure conditions in the nozzle throat as defined in the section "Symbols." The balance axial-force measurement, from which actual nozzle thrust is subsequently obtained, is initially corrected for model weight tares and balance interactions. Although the bellows arrangement was designed to eliminate pressure and momentum interactions with the balance, small bellows tares on axial-force, normal-force, and pitching-moment balance components still exist. These tares result from a small pressure difference between the ends of the bellows when internal velocities are high, and small differences in the forward and aft bellows spring constants when the bellows are pressurized. As discussed in reference 17, these bellows tares were determined by running calibration nozzles with known performance over a range of expected normal forces and pitching moments. The balance data were then corrected in a manner similar to that discussed in reference 17 to obtain actual nozzle thrust, normal force, and pitching moment. The resultant gross thrust F_r, used in resultant thrust ratio F_r/F_i, and the resultant thrust vector angle δ are then determined from these corrected balance data. Resultant thrust ratio F_r/F_i is equal to internal thrust ratio F/F_i as long as the jet-exhaust flow remains unvectored ($\delta = 0°$). Significant differences between F_r/F_i and F/F_i occur when jet-exhaust flow is turned from the axial direction, and the magnitude of these differences are a function of resultant thrust-vector angle δ. Nozzle discharge coefficient C_d is the ratio of measured weight-flow rate to ideal weight-flow rate, where ideal weight-flow rate is based on jet total pressure $p_{t,j}$, jet total temperature $T_{t,j}$, and measured nozzle-throat area.

Presentation of Results

The table on the following page is a summary of the results shown in figure 5. Other results of this investigation are plotted in the following figures:

Basic data (F/F_i, F_r/F_i, C_d, and δ):

Conf	δ_v, deg	Sidewall containment	Ramp curvature	Nominal l_r, in.	$\alpha_{\text{term},l}$, deg	$(A_e/A_t)_i$	Figure
1	-20	Minimum	Baseline	3.48	8.7	1.34	5(a)
2	-10	↓	↓	↓	↓	1.22	5(b)
3	0	↓	↓	↓	↓	1.12	5(c)
4	10	↓	↓	↓	8.7	1.03	5(d)
5	20	↓	↓	↓	11.3	1.00	5(e)
6	30	↓	↓	↓	14.8	↓	5(f)
7	45	↓	↓	↓	23.2	↓	5(g)
8	60	Minimum	↓	↓	36.2	1.00	5(h)
9	-20	Maximum	↓	↓	8.7	1.34	5(a)
10	-10	↓	↓	↓	↓	1.22	5(b)
11	0	↓	↓	↓	↓	1.12	5(c)
12	10	↓	↓	↓	8.7	1.03	5(d)
13	20	Maximum	↓	↓	11.3	1.00	5(e)
14	30	Medium	↓	↓	14.8	1.00	5(f)
15	30	Maximum	Baseline	3.48	14.8	1.00	5(f)
16	0	Minimum	Baseline	3.51	-8.0	1.04	5(i)
17	-10	Minimum	Baseline	3.51	-8.0	1.12	5(i)
18	-20	Minimum	Baseline	3.51	-8.0	1.21	5(i)
19	0	Minimum	Straight	3.54	8.7	1.07	5(j)
20	30	↓	↓	3.46	33.9	1.02	5(k)
21	↓	↓	↓	↓	14.8	1.00	5(k)
22	↓	↓	Straight	↓	-3.7	1.00	5(k)
23	↓	↓	Increased	↓	33.9	1.03	5(l)
24	↓	Minimum	↓	↓	14.8	1.00	5(l)
25	↓	Medium	↓	↓	14.8	1.00	5(l)
26	30	Minimum	Increased	3.46	-3.7	1.00	5(l)
27	30	Minimum	Baseline	5.74	33.9	1.03	5(m)
28	↓	↓	↓	3.46	33.9	1.03	5(m)
29	↓	↓	↓	4.60	25.1	1.00	5(n)
30	↓	↓	↓	3.46	25.1	↓	5(n)
31	↓	↓	↓	2.32	25.1	↓	5(n)
32	↓	↓	↓	5.74	14.8	↓	5(o)
33	↓	↓	↓	4.60	↓	↓	↓
34	↓	↓	↓	2.32	↓	↓	↓
35	↓	↓	↓	1.17	14.8	↓	5(o)
36	↓	↓	↓	4.60	6.3	↓	5(p)
37	↓	↓	↓	3.46	6.3	↓	5(p)
38	↓	↓	↓	2.32	6.3	↓	5(p)
39	↓	↓	↓	3.46	-3.7	↓	5(q)
40	30	Minimum	Baseline	1.17	-3.7	1.00	5(q)

Results and Discussion

Basic Data

Basic data for the SERN configurations tested are presented in figure 5. Nozzle internal thrust ratio F/F_i, resultant thrust ratio F_r/F_i, discharge coefficient C_d, and resultant thrust-vector angle δ are presented as a function of NPR for each configuration investigated. These basic data are used for the comparisons shown in later sections of this paper. Configuration 6 was tested at periodic intervals during the test program and these data are shown in figure 5(f) as a data band to indicate data repeatability.

The internal performance data shown in figure 5 are typical of other single-expansion-ramp nozzle data (refs. 23 and 24) and are often characterized by a tendency to have two nozzle-thrust-ratio performance peaks. These two peaks occur as a result of two separate exhaust-flow expansion processes. The first (internal expansion) occurs as the exhaust flow expands in the region between the nozzle throat and nozzle exit formed by the downstream edge of the lower flap and the ramp. The second expansion process (external expansion) occurs between the ramp (portion downstream of the exit) and the lower-jet free boundary. The double-peak characteristic is not evident for the high-vector-angle cases ($\delta_v \geq 30°$), because the internal expansion process is eliminated as the nozzle throat translates aft to coincide with the nozzle exit; hence, all expansion takes place externally on the ramp.

As observed previously for SERN nozzles (ref. 24), the resultant thrust-ratio levels of the nozzles of the present investigation remain near peak levels over a much larger nozzle-pressure-ratio range than would be expected of a typical convergent-divergent nozzle. This performance characteristic, which probably results from the two separate exhaust-flow expansion processes (internal and external), could be a significant advantage for SERN nozzles, as less expansion-ratio control may be required (particularly for all subsonic-mission aircraft), and reductions in exhaust-system weight and complexity could be achieved.

Comparison of resultant thrust ratio F_r/F_i and internal (body-axis) thrust ratio F/F_i (fig. 5) illustrates another characteristic of SERN nozzles, that significant differences can occur between resultant and internal thrust ratios on unvectored ($\delta_v = 0°$) configurations. These differences occur only when the resultant thrust-vector angle is nonzero. The nonlinear variation of resultant thrust-vector angle δ with nozzle pressure ratio (NPR) at all values of δ_v is characteristic of SERN nozzles and is caused by changing compression-expansion wave patterns impinging on the ramp as NPR is varied. Since the ramp has a large, unopposed, normal projected area, values of normal force can change significantly with varying NPR. An axial-force (body-axis) performance penalty would be associated with any value of resultant thrust-vector angle which is nonzero, because the thrust is being turned away from the axial direction. The magnitude of this penalty can be assessed by comparing the difference between resultant and internal thrust ratio at a given NPR.

Measured values of nozzle discharge coefficient C_d are below 1.0. These values indicate that, as expected, there are losses due to viscous effects which reduce the amount of weight flow passing through the throat. Discharge coefficient tended to increase slightly throughout the range of nozzle pressure ratio. The magnitude of these increases in C_d are closely related to lower-flap lip (or terminal) angle. As the lower-flap lip is rotated up, increases in nozzle discharge coefficient (over the range of NPR) become larger. Examination of the internal pressure data in table VIII indicates that those configurations for which C_d variations with NPR were largest also had the largest changes in the sonic-pressure-ratio ($p/p_{t,j} = 0.528$ and local Mach number = 1.0) location on the ramp with varying NPR. As NPR increased, the sonic-pressure-ratio location moved upstream along the ramp. Unfortunately, the throat location on the lower flap of these configurations is downstream of the last pressure orifice; hence, it is not known whether the location of the sonic pressure ratio on the lower flap is fixed or moves with changing NPR.

Internal Static-Pressure Distributions

Internal static-pressure data are presented in table VIII for each nozzle pressure ratio and configuration tested. Typical internal static-pressure distributions for various configuration comparisons are shown in figures 6 to 10. All static-pressure data on these figures are presented at NPR = 3.0.

Actual nozzle-throat location can be defined as the location at which the ratio of static pressure to jet total pressure is 0.528 (local Mach number = 1.0). As shown subsequently, actual nozzle-throat location ($p/p_{t,j} = 0.528$) differs from the nozzle geometric throat (minimum geometric area) in some cases. In the following discussion of the internal static pressure distributions, "throat location" refers to the location of the sonic pressure ratio unless otherwise noted.

Effect of geometric thrust-vector angle. Figure 6 shows the effect of thrust-vector angle δ_v on upper-ramp and lower-flap centerline pressures. As noted previously in the section "Nozzle Description," the location of the nozzle geometric throat translates downstream with increasing δ_v until it is coincident with the lower-flap exit for $\delta_v \geq 30°$ (internal expansion ratio approaches unity during throat translation). In addition, as geometric thrust-vector angle increases beyond 30°, the location of the throat on the upper ramp moves closer to the ramp trailing edge because of increasing ramp, lower-flap and throat rotation angles. (See figs. 4(f) to 4(h).) This movement of throat location ($p/p_{t,j} = 0.528$) with increasing δ_v is clearly indicated by the ramp and lower-flap static-pressure distributions shown in figure 6. For $-20° \leq \delta_v \leq 0°$, the ramp pressure distributions indicate a throat location which is upstream of the ramp hinge point ($x'/l_{r,\text{nom}} = 0.0$) and nearly independent of geometric thrust-vector angle. For the configurations with $\delta_v = -10°$ and $\delta_v = -20°$, shock-induced internal flow separation appears to occur on the ramp near $x'/l_{r,\text{nom}} = 0.5$ and 0.4, respectively. As geometric thrust-vector angle increases from 0° to 60°, the throat location translates down the upper-ramp surface from $x'/l_{r,\text{nom}} \approx -0.1$ to $x'/l_{r,\text{nom}} \approx 0.8$. Significant increases in static pressure on the upper ramp occur with increasing δ_v. For $-20° \leq \delta_v \leq 10°$, an exhaust-flow shock stands on the ramp surface and moves aft with increasing geometric thrust-vector angle. For geometric thrust-vector angles greater than 10°, the shock moves aft of the last pressure measurement and may be aft of the ramp trailing edge, particularly for the largest thrust-vector angles.

On the lower flap, throat location is independent of thrust-vector angle for $-20° \leq \delta_v \leq 0°$. For $0° \leq \delta_v \leq 20°$, the throat location translates aft on the lower flap from $x''/l_{l,\text{nom}} \approx 0.78$ to $x''/l_{l,\text{nom}} \approx 0.91$. For thrust-vector angles of 30° or greater, the throat location is aft of the last pressure measurement and is probably located at the lower-flap trailing edge. Static pressure on the lower flap increases with increasing thrust-vector angle.

Effect of sidewall containment. Typical effects of sidewall containment on upper-ramp static-pressure distributions are presented in figure 7 for two thrust-vector angles. Longitudinal centerline distributions are shown on the top of each figure part and lateral distributions at three longitudinal locations are shown on the bottom of each figure part. Lower-flap pressures did not vary with amount of sidewall containment and hence are not presented. The ramp centerline static-pressure data indicate that, for $\delta_v = -20°$, increasing the amount of sidewall containment decreases the static pressures downstream of the exhaust-flow shock at $x'/l_{r,\text{nom}} \approx 0.30$. This decrease in pressure persists across the ramp width except near the ramp trailing edge. There is also a decrease in static pressure near the nozzle sidewall ($z/w = 1.0$) ahead of the exhaust-flow shock at $x'/l_{r,\text{nom}} = 0.25$. These pressure data indicate a smaller (or more negative) normal-force contribution from the ramp surface when sidewall containment is increased. Thus, increased sidewall containment would tend to improve the negative resultant thrust-vector angle δ.

The effects of sidewall containment on the ramp static pressures for $\delta_v = 30°$ (fig. 7(b)) are much smaller than observed for $\delta_v = -20°$ (fig. 7(a)). However, the increase in static pressure on and near the aft-ramp centerline and near the forward-ramp sidewall indicate a potential improvement (increase in ramp normal force) in positive resultant turning angle δ when the amount of sidewall containment is increased. The decrease in static pressure near the aft-ramp sidewall offsets part of this improvement. The aforementioned effects of sidewall containment on static-pressure distributions are, in general, similar to those reported in other studies. (See refs. 23 and 24.)

Effect of ramp curvature. Figure 8 presents typical effects of ramp curvature on upper-ramp centerline static pressures for $\delta_v = 30°$. As ramp curvature is increased from no curvature or straight (configuration 21) to baseline curvature (configuration 6) to increased curvature (configuration 24), ramp static pressures downstream of $x'/l_{r,\text{nom}} \approx 0.3$ are increased. These data infer an increase in resultant thrust-vector angle as ramp curvature increases.

Effect of lower-flap lip angle. Typical effects of lower-flap lip (or terminal) angle on both ramp and lower-flap centerline pressure distributions for $\delta_v = 30°$ are presented in figure 9. Only lip shape and angle

vary—lower-flap angle δ_l (fig. 3(a)) remains constant at 6.1°. (See table IV.) Both ramp and lower-flap pressures decrease as lower-flap lip angle is rotated downward to 33.9°. The exception to this trend occurs on the ramp downstream of $x'/l_{r,\text{nom}} = 0.7$, where pressure trends are reversed. The nozzle-throat location ($p/p_{t,j} = 0.528$) moves downstream on both the ramp and lower flap as lower-flap lip angle is reduced (rotated upward). In fact, the throat is probably at or near the exit of the lower flap for lip angles of 14.8°, 6.3°, and -3.7°. Because both ramp and lower-flap pressures generally decrease as the lower-flap lip angle is rotated downward, any resultant pressure-area forces on these surfaces tend to be self-canceling, and little can be concluded about these effects on nozzle performance. This is especially true in view of the changing pressure trends near the ramp trailing edge. These trends would produce an unopposed force since the lower flap is shorter than the ramp.

Effect of upper-ramp length. The effects of ramp length on ramp centerline pressure distributions for $\delta_v = 30°$ are presented in figure 10. Ramp length has little or no effect on the ramp pressure distribution but would have a significant effect on the integrated pressure-area forces on the ramp because of the large variation in ramp projected normal and axial areas with varying length. Thus, ramp length can be expected to produce large effects on nozzle performance and resultant thrust-vector angle. The data of figure 10 exhibit characteristics typical of single-expansion-ramp nozzles operated at underexpanded conditions. (See refs. 23 and 24.) As discussed previously, the nozzle throat is located at the lower-flap exit for $\delta_v \geq 30°$ (internal expansion ratio equal to unity). Hence, the design nozzle pressure ratio is approximately 1.89 for the configurations shown in figure 10. For NPR > 1.89 (NPR = 3.0 for fig. 10 data), the ambient or back pressure is less than the nozzle-exit pressure, and an adjustment in pressure must occur downstream of the exit plane. This adjustment takes the form of a series of expansion waves radiating from the exit of the lower flap and impinging on the upper ramp. The expansion on the ramp for 0.42 (throat) $< x'/l_{r,\text{nom}} <$ 1.04 is obvious for all configurations shown except configuration 35 which had no external ramp length downstream of the throat or exit. (See fig. 4(o).) If the external ramp is long enough, these expansion waves reflect off the ramp and again off the free jet boundary and form compression waves (or coalesce into a shock wave) which may again intersect the ramp surface. This causes the sharp pressure rise on the ramp between $x'/l_{r,\text{nom}}$ values of 1.04 and 1.20 for the ramp lengths of 4.598 in. and 5.736 in. (configurations 32 and 33). The pattern of alternate expansion and compression is repeated downstream, and the decrease in ramp pressure downstream of $x'/l_{r,\text{nom}} = 1.2$ for configurations 32 and 33 results from another series of expansion waves. For nonviscous flow, the process of alternating expansion and compression waves theoretically extends to infinity. Naturally, in the practical case, at the boundary of the jet a strong turbulent mixing region is produced by viscous effects, and after a finite distance, the expansion and compression waves disappear. (See ref. 25.)

It is obvious from the pressure data shown in figure 10 that ramp normal force and thus resultant thrust-vector angle δ is a strong function of ramp length. The ratio of ambient pressure to jet total pressure (inverse of NPR) is shown on the right-hand side of figure 10; a positive ramp normal-force component is produced for $p/p_{t,j} > p_a/p_{t,j}$, and a negative ramp normal-force component is produced for $p/p_{t,j} < p_a/p_{t,j}$. Thus, one might expect configurations 34 ($l_r = 2.319$ in.) and 33 ($l_r = 4.598$ in.) to provide the largest resultant thrust-vector angles for the test condition shown. High resultant thrust-vector angles are expected for configuration 34, because its relatively short ramp length avoids the negative normal-force contribution caused by the expansion process for approximately $0.70 \leq x'/l_{r,\text{nom}} \leq 1.00 (p/p_{t,j} < p_a/p_{t,j})$. High resultant thrust-vector angles are expected for configuration 33, because its relatively long ramp length takes advantage of the positive normal-force contribution caused by the compression (shock) process for approximately $1.10 \leq x'/l_{r,\text{nom}} \leq 1.32 (p/p_{t,j} > p_a/p_{t,j})$. Somewhat higher resultant thrust-vector angles might be expected for configuration 33 if the ramp length were extended to $x'/l_{r,\text{nom}} = 1.45 (p/p_{t,j} = p_a/p_{t,j})$. The preceding discussion is based on data at a constant NPR = 3.0 (fig. 10). For NPR < 3.0, the period of expansion and compression cycle becomes shorter, and for NPR > 3.0, the period becomes longer. Thus, it is obvious that the ramp length required for maximum resultant thrust-vector angle is probably highly dependent on nozzle pressure ratio and that a compromise ramp length must be selected for a particular airplane mission (or a variable length ramp incorporated).

Performance Comparisons

Effect of geometric thrust-vector angle. The effect of geometric thrust-vector angle δ_v on nozzle performance as a function of nozzle pressure ratio is presented in figure 11. Nozzle performance as a function of δ_v is presented in figure 12 for constant values of NPR. It is obvious from these figures that the current SERN configurations were highly effective in providing large positive (ramp deflected downward) thrust-vector angles (up to 60°). At NPR typical of subsonic combat (NPR = 3 to 5), resultant thrust-vector angles approximately

equal to the design (geometric) thrust-vector angles were obtained. As discussed previously, these resultant thrust-vector angles were a function of NPR (even for $\delta_v = 0°$) because of the changing pressure distribution on the upper ramp. For negative design thrust-vector angles (ramp deflected upward) greater than $-10°$, the flow-turning capability of the current SERN was reduced. (See fig. 12(b).) The reduced flow-turning capability of SERN at negative design thrust-vector angles is caused by exhaust-flow separation from the ramp. The ramp pressure distribution for $\delta_v = -20°$ at NPR = 3.0 (see fig. 6) indicates that flow separation occurs on the rear half of the ramp surface.

With the exception of the $\delta_v = -20°$ configuration and the $\delta_v = -10°$ and 0° configurations at lower NPR, nozzle internal performance F_r/F_i was relatively independent of design thrust-vector angle, and high performance was realized throughout the range of thrust-vector angles. For the exceptions noted, and in particular for the $\delta_v = -20°$ configuration, internal performance penalties (higher ramp drags) are associated with the exhaust-flow separation on the ramp as discussed previously. As shown in figures 11 and 12, nozzle discharge coefficient C_d tends to decrease with increasing δ_v. These data indicate a reduction in effective nozzle throat area as δ_v increases.

Effect of sidewall containment. The effect of sidewall containment on SERN performance at various design thrust-vector angles is shown in figures 5(a) to 5(f) and 5(l). For convenience, resultant thrust-vector-angle data have been cross-plotted at constant values of NPR and are shown in figure 13 as a function of design thrust-vector angle. Increasing the amount of SERN sidewall containment generally improved nozzle flow-turning capability for both negative and positive design thrust-vector angles. This result was indicated by the internal pressure distributions discussed previously. Although only one design thrust-vector angle ($\delta_v = 30°$) was investigated with an alternate ramp with increased curvature, results on this configuration (see fig. 5(l) and isolated symbols in fig. 13) indicate similar trends with increased sidewall containment. Increasing sidewall containment prevents lateral expansion of the exhaust flow before the flow is turned in the pitch plane by the deflected ramp. With minimum sidewall containment, part of the exhaust weight flow escapes laterally before being turned. As indicated in figure 5(f), containment of the flow in proximity to the ramp surface appears to be most important, since the medium and maximum sidewall configurations (fig. 4(f)) have nearly identical flow-turning performance. Sidewall containment had little effect on nozzle internal performance F_r/F_i and no effect on discharge coefficient. The small variations which occur in resultant thrust ratio probably result from variation of nozzle effective expansion ratio as sidewall containment varies.

Effect of ramp curvature. Figure 14 presents the effect of ramp curvature on the static performance characteristics of several SERN configurations. Figure 15 is a summary of ramp curvature effects on resultant thrust-vector angle. Increasing ramp curvature provided significant increases in SERN positive (ramp deflected downward) thrust-vectoring capability. (See $\delta_v = 30°$ data at top of fig. 15.) The favorable effect of ramp curvature on positive resultant thrust-vector angle was inferred by the ramp pressure distributions (fig. 8) discussed previously and was expected, since increased ramp curvature tends to turn the exhaust flow near the ramp trailing edge downward. For the unvectored ($\delta_v = 0°$) baseline nozzle (see fig. 14(a) and bottom plots of fig. 15), increasing ramp curvature increased resultant thrust-vector angle at NPR < 4.2 but decreased δ at higher NPR. It is not currently understood why this trend reversal occurs for the $\delta_v = 0°$ configuration.

Increasing ramp curvature from the straight ramp to the baseline ramp increases nozzle resultant thrust ratio throughout the NPR range tested. A divergence loss (exhaust flow at ramp trailing edge not parallel to thrust axis) is probably associated with the straight-ramp configurations and is eliminated or reduced by the baseline ramp curvature. Increasing ramp curvature beyond the baseline ramp curvature generally had little additional effect on resultant thrust ratio. Although large variations in nozzle discharge coefficient with varying ramp curvature are shown in figure 14, no consistent trend was observed.

Effect of lower-flap lip angle. Figure 16 presents the effect of lower-flap lip (terminal) angle on negative thrust-vectoring performance ($\delta_v < 0°$) and cruise ($\delta_v = 0°$) SERN performance. Figure 17 is a summary of the effects of lower-flap lip angle on resultant thrust-vector angle. Decreasing lower-flap lip angle $\alpha_{\text{term},l}$ increased resultant thrust-vector angle δ at nozzle pressure ratios greater than 4.0 for the cruise configuration (fig. 16(a)), had little effect on the $\delta_v = -10°$ configuration (fig. 16(b)), and decreased δ (improved negative thrust-vectoring capability) for the $\delta_v = -20°$ configuration (fig. 16(c)). The increase in δ which occurred on the cruise configuration when $\alpha_{\text{term},l}$ was decreased (from 8.7° to -8.0°) was unexpected and is similar to the trend reversal with ramp curvature noted previously for the $\delta_v = 0°$ configuration. It was expected that reducing $\alpha_{\text{term},l}$ (similar to rotating lower flap upward) would decrease δ (improve negative thrust-vectoring capability) as observed for the $\delta_v = -20°$. The reason for the trend reversal at $\delta_v = 0°$ is not currently understood.

As lower-flap lip angle is decreased, the amount of internal expansion $(A_e/A_t)_i$ for the $\delta_v \leq 0°$ configurations also decreases (see table II), and peak resultant thrust ratio moves to lower values of nozzle pressure ratio. The majority of the variation in resultant thrust ratio shown in figure 16 is probably caused by varying expansion ratio. For $\delta_v \leq 0°$, lower-flap lip angle had little effect on SERN discharge coefficient.

The effect of lower-flap lip angle on positive thrust-vectoring ($\delta_v = 30°$) SERN performance is presented in figure 18 for several ramp lengths and ramp curvatures. A summary of the $\alpha_{\text{term},l}$ effects on resultant thrust-vector angle is given in figure 19. As expected, increasing $\alpha_{\text{term},l}$ (similar to rotating lower flap down) tended to improve SERN positive thrust-vectoring capability (increase δ). However, there is some indication from the data shown in figure 19, especially for the higher NPR, that positive thrust-vectoring capability may be reduced if the lower-lip angle is increased too much.

For the $\delta_v = 30°$ configurations, $\alpha_{\text{term},l}$ had little (less than 1 percent) effect on resultant thrust ratio. For these configurations, the nozzle throat is very near the lower-flap exit, $(A_e/A_t)_i \approx 1.0$, and little variation in internal expansion occurs with varying lower-flap lip angle (table II). Large variations in nozzle discharge coefficient occur with varying $\alpha_{\text{term},l}$. Peak discharge coefficient occurs for lip angles between 14.8° to 25.1°; increasing or decreasing $\alpha_{\text{term},l}$ beyond this range decreases discharge coefficient.

Effect of upper-ramp length. The effect of ramp length on SERN ($\delta_v = 30°$) performance is shown in figures 5(m) to 5(q). Figure 20 is a summary of the effects of ramp length on resultant thrust-vector angle. As discussed previously, ramp pressure distributions indicate that both ramp length and nozzle pressure ratio will have a significant effect on resultant thrust-vector angle. Examination of figure 20 confirms both of these observations. In fact, the optimum ramp length for maximum δ is highly dependent upon nozzle pressure ratio for the reasons discussed in the section "Internal Static-Pressure Distributions." At NPR = 2.0 and 3.0, maximum resultant thrust-vector angle δ occurs with the longest ramp lengths. At NPR = 4.0 to 6.0, maximum δ occurs when $l_r = 2.319$ in. For the range of nozzle pressure ratio tested, the only result which was independent of NPR was that the lowest δ was always obtained with $l_r = 1.169$ in. The 1.169-in. ramp length was a special case with no exposed external ramp downstream of the nozzle throat (see figs. 4(o) and 4(q)); configurations 35 and 40 (l_r = 1.169 in.) were essentially nonaxisymmetric convergent nozzles at $\delta_v = 30°$. It is obvious from figure 20 that some external ramp length downstream of the nozzle throat is desirable for optimum flow-turning capability. Excluding the special case of $l_r = 1.169$ in., it is interesting to note that the ramp length which gives the lowest flow-turning capability progressively increases with increasing nozzle pressure ratio ($l_r = 2.319$ in. at NPR = 2.0, $l_r = 3.465$ in. at NPR = 3.0, $l_r = 4.594$ in. at NPR = 4.0, and $l_r = 5.763$ in. at NPR = 5.0). It is obvious from the preceding discussion and from the previous discussion of the pressure distributions that ramp length can be designed to provide maximum flow turning at only one specific nozzle pressure ratio. Since NPR varies throughout an airplane mission, a compromise ramp length must be selected or a variable-length ramp must be incorporated.

Examination of figures 5(m) to 5(q) indicates that the highest resultant thrust ratio is generally obtained with the 2.319-in. or 3.465-in. ramp length. Based on this result, the previous discussion of resultant thrust-vector angle, and consideration of nozzle (ramp) weight and cooling, the best compromise ramp length for an airplane which operates over the current test range of nozzle pressure ratio is probably the 2.319-in. SERN configuration. No consistent trends of nozzle discharge coefficient were observed with varying ramp length.

Conclusions

An investigation has been conducted at static conditions (wind off) in the static-test facility of the Langley 16-Foot Transonic Tunnel. The effects of geometric thrust-vector angle, sidewall containment, ramp curvature, lower-flap lip angle, and ramp length on the internal performance of nonaxisymmetric single-expansion-ramp nozzles were investigated. Geometric thrust-vector angle was varied from -20° to 60°, and nozzle pressure ratio was varied from 1.0 (jet off) to approximately 10.0. Results of this study indicate the following conclusions:

1. Single-expansion-ramp nozzles can be highly effective in providing large positive (ramp deflected downward) thrust-vector angles (up to 60°) with little loss in resultant thrust ratio. However, for negative (ramp deflected upward) thrust-vector angles above −10°, exhaust-flow separation on the ramp reduced nozzle flow-turning capability and resultant thrust-ratio performance.

2. Increased sidewall containment along the ramp length generally improved nozzle flow-turning capability and had little effect on resultant thrust ratio.

3. Except for the unvectored cruise configuration, increasing ramp curvature provided significant increases in positive resultant thrust-vector angles. A ramp with some curvature also reduces flow divergence losses and results in higher resultant thrust ratios than can be obtained with a straight ramp.

4. Except for the unvectored cruise configuration, for which a trend reversal occurred, increasing or decreasing the lower-flap lip (terminal) angle in the same direction as the geometric thrust-vector angle tended to improve nozzle thrust-vectoring capability. Lower-flap lip angle had little effect on resultant thrust ratio unless nozzle expansion ratio also varied.

5. The ramp length for maximum resultant thrust-vector angle is highly dependent on nozzle pressure ratio; thus, a compromise ramp length must be selected for a particular airplane mission. However, at all conditions investigated, some external ramp length (downstream of nozzle throat) is preferred over a zero length ramp (special case of a nonaxisymmetric convergent nozzle). For the nozzle-pressure-ratio range of the current test, a short ramp length appears to offer the best compromise when flow-turning capability, internal performance, and nozzle (ramp) weight are considered.

Langley Research Center
National Aeronautics and Space Administration
Hampton, VA 23665
July 11, 1984

References

1. Martens, Richard E.: F-15 Nozzle/Afterbody Integration. *J. Aircr.*, vol. 13, no. 5, May 1976, pp. 327–333.
2. Hiley, P. E.; Wallace, H. W.; and Booz, D. E.: Nonaxisymmetric Nozzles Installed in Advanced Fighter Aircraft. *J. Aircr.*, vol. 13, no. 12, Dec. 1976, pp. 1000–1006.
3. Sedgwick, T. A.: Investigation of Non-Symmetric Two-Dimensional Nozzles Installed in Twin-Engine Tactical Aircraft. AIAA Paper No. 75-1319, Sept.–Oct. 1975.
4. *F-15 2-D Nozzle System Integration Study. Volume I—Technical Report.* NASA CR-145295, 1978.
5. Stevens, H. L.: *F-15/Nonaxisymmetric Nozzle System Integration Study Support Program.* NASA CR-135252, 1978.
6. Bergman, D.; Mace, J. L.; and Thayer, E. B.: Non-Axisymmetric Nozzle Concepts for an F-111 Test Bed. AIAA Paper No. 77-841, July 1977.
7. Schnell, W. C.; Grossman, R. L.; and Hoff, G. E.: Comparison of Non-Axisymmetric and Axisymmetric Nozzles Installed on a V/STOL Fighter Model. [Preprint] 770983, Soc. Automot. Eng., Nov. 1977.
8. Schnell, W. C.; and Grossman, R. L.: Vectoring Non-Axisymmetric Nozzle Jet Induced Effects on a V/STOL Fighter Model. AIAA Paper 78-1080, July 1978.
9. Hiley, P. E.; and Bowers, D. L.: Advanced Nozzle Integration for Supersonic Strike Fighter Application. AIAA-81-1441, July 1981.
10. Capone, Francis J.; Hunt, Brian L.; and Poth, Greg E.: Subsonic/Supersonic Nonvectored Aeropropulsive Characteristics of Nonaxisymmetric Nozzles Installed on an F-18 Model. AIAA-81-1445, July 1981.
11. Berrier, Bobby L.; Palcza, J. Lawrence; and Richey, G. Keith: Nonaxisymmetric Nozzle Technology Program—An Overview. AIAA Paper 77-1225, Aug. 1977.
12. Capone, Francis J.; and Berrier, Bobby L.: *Investigation of Axisymmetric and Nonaxisymmetric Nozzles Installed on a 0.10-Scale F-18 Prototype Airplane Model.* NASA TP-1638, 1980.
13. Capone, Francis J.: *Aeropropulsive Characteristics at Mach Numbers up to 2.2 of Axisymmetric and Nonaxibreak symmetric Nozzles Installed on an F-18 Model.* NASA TP-2044, 1982.
14. Capone, Francis J.; and Reubush, David E.: *Effects of Varying Podded Nacelle-Nozzle Installations on Transonic Aeropropulsive Characteristics of a Supersonic Fighter Aircraft.* NASA TP-2120, 1983.
15. Mason, Mary L.; and Capone, Francis J.: *Aeropropulsive Characteristics of Twin Single-Expansion-Ramp Vectoring Nozzles Installed With Forward-Swept Wings and Canards.* NASA TP-2133, 1983.
16. Wasson, H. R.; Hall, G. R.; and Palcza, J. L.: Results of a Feasibility Study To Add Canards and ADEN Nozzle to the YF-17. AIAA Paper 77-1227, Aug. 1977.
17. Capone, Francis J.: *Static Performance of Five Twin-Engine Nonaxisymmetric Nozzles With Vectoring and Reversing Capability.* NASA TP-1224, 1978.
18. Lander, J. A.; and Palcza, J. Lawrence: Exhaust Nozzle Deflector Systems for V/STOL Fighter Aircraft. AIAA Paper No. 74-1169, Oct. 1974.
19. Lander, J. A.; Nash, D. O.; and Palcza, J. Lawrence: Augmented Deflector Exhaust Nozzle (ADEN) Design for Future Fighters. AIAA Paper No. 75-1318, Sept.–Oct. 1975.
20. Nash, D. O.; Wakeman, T. G.; and Palcza, J. L.: Structural and Cooling Aspects of the ADEN Nonaxisymmetric Exhaust Nozzle. Paper No. 77-GT-110, American Soc. Mech. Eng., Mar. 1977.
21. Berrier, B. L.; and Re, R. J.: A Review of Thrust-Vectoring Schemes for Fighter Aircraft. AIAA Paper No. 78-1023, July 1978.
22. Hutchinson, R. A.; Petit, J. E.; Capone, F. J.; and Whittaker, R. W.: Investigation of Advanced Thrust Vectoring Exhaust Systems for High Speed Propulsive Lift. AIAA-80-1159, June–July 1980.
23. Berrier, Bobby L.; and Re, Richard J.: *Effect of Several Geometric Parameters on the Static Internal Performance of Three Nonaxisymmetric Nozzle Concepts.* NASA TP-1468, 1979.
24. Re, Richard J.; and Berrier, Bobby L.: *Static Internal Performance of Single Expansion-Ramp Nozzles With Thrust Vectoring and Reversing.* NASA TP-1962, 1982.
25. Ferri, Antonio: *Elements of Aerodynamics of Supersonic Flows.* Macmillan Co., 1949, p. 171.

TABLE I. INDEX TO NOZZLE GEOMETRY AND COORDINATE TABLES

Configuration[1]	Figure	Upper-ramp[2]	Lower flap[3]	Sidewalls[4]	
				Number	Amount of containment
1	4(a)	1	1	1	Minimum
2	4(b)	2	1	1	Minimum
3	4(c)	3	1	1	Minimum
4	4(d)	4	1	1	Minimum
5	4(e)	5	2	2	Minimum
6	4(f)	6	3	2	Minimum
7	4(g)	7	4	3	Minimum
8	4(h)	8	5	4	Minimum
9	4(a)	1	1	3	Maximum
10	4(b)	2	1	3	Maximum
11	4(c)	3	1	3	Maximum
12	4(d)	4	1	3	Maximum
13	4(e)	5	2	4	Maximum
14	4(f)	6	3	5	Medium
15	4(f)	6	3	4	Maximum
16	4(i)	3	6	1	Minimum
17	4(i)	2	6	1	Minimum
18	4(i)	1	6	1	Minimum
19	4(j)	9	1	1	Minimum
20	4(k)	10	7	2	Minimum
21	4(k)	10	3	2	Minimum
22	4(k)	10	8	2	Minimum
23	4(l)	11	7	2	Minimum
24	4(l)	11	3	2	Minimum
25	4(l)	11	3	5	Medium
26	4(l)	11	8	2	Minimum
27	4(m)	12	7	2	Minimum
28	4(m)	6	7	2	Minimum
29	4(n)	13	9	2	Minimum
30	4(n)	6	9	2	Minimum
31	4(n)	14	9	2	Minimum
32	4(o)	12	3	2	Minimum
33	4(o)	13	3	2	Minimum
34	4(o)	14	3	2	Minimum
35	4(o)	15	3	2	Minimum
36	4(p)	13	10	2	Minimum
37	4(p)	6	10	2	Minimum
38	4(p)	14	10	2	Minimum
39	4(q)	6	8	2	Minimum
40	4(q)	15	8	2	Minimum

[1]Throat geometry parameters in table II.
[2]Geometry in table III; coordinates in table V.
[3]Geometry in table IV; coordinates in table VI.
[4]Coordinates in table VII.

TABLE II. IMPORTANT THROAT GEOMETRIC PARAMETERS

Conf	δ_v, deg	$x_{t,u}$, in.	$y_{t,u}$, in.	$x_{t,l}$, in.	$y_{t,l}$, in.	θ_t, deg	h_t, in.	A_t, in^2	$(A_e/A_t)_i$
1	−20	4.664	0.155	4.753	−0.811	−5.3	0.971	3.992	1.34
2	−10	4.639	.153	4.753	−.811	−6.7	.972	3.997	1.22
3	0	4.615	.156	4.753	−.811	−8.1	.977	3.992	1.12
4	10	4.931	.171	4.920	−.794	.6	.965	3.909	1.03
5	20	5.457	.011	5.283	−.954	10.2	.980	3.979	1.00
6	30	5.800	−.298	5.394	−1.175	24.9	.965	3.960	1.00
7	45	6.048	−.938	5.407	−1.671	41.2	.976	3.966	1.00
8	60	6.082	−1.865	5.285	−2.429	54.7	.976	3.958	1.00
9	−20	4.664	.155	4.753	−.811	−5.3	.971	3.995	1.34
10	−10	4.639	.153	4.753	−.811	−6.7	.972	3.996	1.22
11	0	4.615	.156	4.753	−.811	−8.1	.977	3.998	1.12
12	10	4.931	.171	4.920	−.794	.6	.965	3.909	1.03
13	20	5.457	.011	5.283	−.954	10.2	.980	3.975	1.00
14	30	5.800	−.298	5.394	−1.175	24.9	.965	3.945	1.00
15	30	5.800	−.298	5.394	−1.175	24.9	.965	3.943	1.00
16	0	4.664	.155	4.837	−.802	−11.1	.972	4.002	1.04
17	−10	4.664	.155	4.837	−.802	−11.1	.972	4.004	1.12
18	−20	4.664	.155	4.837	−.802	−11.1	.972	4.006	1.21
19	0	4.714	.156	4.837	−.801	−7.3	.965	4.004	1.07
20	30	5.600	−.273	5.179	−1.164	25.3	.985	4.010	1.02
21	↓	5.777	−.357	5.393	−1.175	25.1	.904	3.670	1.00
22	↓	5.763	−.352	5.404	−1.083	26.2	.814	3.368	1.00
23	↓	5.517	−.092	5.134	−1.149	19.9	1.124	4.571	1.03
24	↓	5.856	−.227	5.393	−1.175	26.0	1.055	4.280	1.00
25	↓	5.856	−.227	5.393	−1.175	26.0	1.055	4.269	1.00
26	↓	5.760	−.187	5.404	−1.083	21.7	.964	3.951	1.00
27	↓	5.654	−.236	5.215	−1.182	24.9	1.043	4.230	1.03
28	↓	↓	↓	5.215	−1.182	24.9	1.043	4.371	1.03
29	↓	↓	↓	5.294	−1.203	20.4	1.032	4.190	1.00
30	↓	↓	↓	5.294	−1.203	20.4	1.032	4.219	↓
31	↓	5.654	−.236	5.294	−1.203	20.4	1.032	4.196	↓
32	↓	5.800	−.298	5.394	−1.175	24.9	.965	3.920	↓
33	↓	5.800	−.298	↓	−1.175	24.9	.965	3.922	↓
34	↓	5.800	−.298	↓	−1.175	24.9	.965	3.929	↓
35	↓	5.800	−.298	↓	−1.175	24.9	.965	3.926	↓
36	↓	5.760	−.281	↓	−1.142	23.1	.935	3.813	↓
37	↓	5.760	−.281	↓	−1.142	23.1	.935	3.840	↓
38	↓	5.760	−.281	5.394	−1.142	23.1	.935	3.834	↓
39	↓	5.750	−.277	5.404	−1.083	23.3	.877	3.634	↓
40	30	5.750	−.277	5.404	−1.083	23.3	.877	3.611	1.00

TABLE III. IMPORTANT UPPER-RAMP GEOMETRIC PARAMETERS

Conf	δ_v, deg	δ_u, deg	$x_{e,u}$, in.	$y_{e,u}$, in.	l_r, in.	$l_{r,o}$, in.	Ramp curvature	$\alpha_{c,u}$, deg	$\alpha_{\text{term},u}$, deg
1	−20	−20	7.950	1.714	3.525	2.743	Baseline	25.0	22.0
2	−10	−10	8.146	1.118	3.510	2.968	↓	15.1	12.0
3	0	0	8.236	.497	3.496	3.083	↓	5.1	2.0
4	10	10	8.216	−.130	3.484	2.867	↓	−4.9	−8.0
5	20	20	8.088	−.744	3.470	2.590	↓	−15.0	−18.0
6	30	30	7.855	−1.327	3.465	2.268	↓	−25.0	−28.0
7	45	45	7.326	−2.103	3.453	1.698	↓	−40.0	−43.0
8	60	60	6.614	−2.716	3.441	.921	↓	−55.1	−58.0
9	−20	−20	7.950	1.714	3.525	2.743	↓	25.0	22.0
10	−10	−10	8.146	1.118	3.510	2.968	↓	15.1	12.0
11	0	0	8.236	.497	3.496	3.083	↓	5.1	2.0
12	10	10	8.216	−.130	3.484	2.867	↓	−4.9	−8.0
13	20	20	8.088	−.744	3.470	2.590	↓	−15.0	−18.0
14	30	30	7.855	−1.327	3.465	2.268	↓	−25.0	−28.0
15	30	30	7.855	−1.327	3.465	2.268	↓	−25.0	−28.0
16	0	0	8.236	.497	3.496	3.083	↓	5.1	2.0
17	−10	−10	8.146	1.118	3.510	2.968	↓	15.1	12.0
18	−20	−20	7.950	1.714	3.525	2.743	Baseline	25.0	22.0
19	0	0	8.236	.497	3.540	3.088	Straight	5.5	5.5
20	30	30	7.855	−1.327	3.465	2.269	Straight	−25.0	−25.0
21	↓	↓	7.855	↓	↓	2.296	Straight	↓	−25.0
22	↓	↓	7.855	↓	↓	2.332	Straight	↓	−25.0
23	↓	↓	7.854	↓	↓	2.218	Increased	↓	−31.8
24	↓	↓	7.854	↓	↓	2.223	Increased	↓	−31.8
25	↓	↓	7.854	↓	↓	2.223	Increased	↓	−31.8
26	↓	↓	7.854	−1.327	3.465	2.254	Increased	−25.0	−31.8
27	↓	↓	9.850	−2.420	5.736	4.437	Baseline	−26.5	−28.5
28	↓	↓	7.855	−1.327	3.465	2.238	↓	−25.0	−28.0
29	↓	↓	8.850	−1.870	4.598	3.323	↓	−25.9	−28.4
30	↓	↓	7.855	−1.327	3.465	2.262	↓	−25.0	−28.0
31	↓	↓	6.840	−.790	2.319	1.179	↓	−23.6	−26.6
32	↓	↓	9.850	−2.420	5.736	4.466	↓	−26.5	−28.5
33	↓	↓	8.850	−1.870	4.598	3.363	↓	−25.9	−28.4
34	↓	↓	6.840	−.790	2.319	1.147	↓	−23.6	−26.6
35	↓	↓	5.800	−.300	1.169	.000	↓	−22.0	−23.8
36	↓	↓	8.850	−1.870	4.598	3.358	↓	−25.9	−28.4
37	↓	↓	7.855	−1.327	3.465	2.277	↓	−25.0	−28.0
38	↓	↓	6.840	−.790	2.319	1.174	↓	−23.6	−26.6
39	↓	↓	7.855	−1.327	3.465	2.292	↓	−25.0	−28.0
40	30	30	5.800	−.300	1.169	.054	Baseline	−22.0	−23.8

TABLE IV. IMPORTANT LOWER-FLAP GEOMETRIC PARAMETERS

Conf	δ_v, deg	δ_l, deg	$x_{e,l}$, in.	$y_{e,l}$, in.	$\alpha_{\text{term},l}$, deg
1	−20	0.0	5.338	−0.819	8.7
2	−10	.0	5.338	−.819	8.7
3	0	.0	5.338	−.819	8.7
4	10	.0	5.338	−.819	8.7
5	20	2.6	5.366	−.970	11.3
6	30	6.1	5.393	−1.175	14.8
7	45	14.5	5.407	−1.671	23.2
8	60	27.5	5.285	−2.429	36.2
9	−20	.0	5.338	−.819	8.7
10	−10	.0	5.338	−.819	8.7
11	0	.0	5.338	−.819	8.7
12	10	.0	5.338	−.819	8.7
13	20	2.6	5.366	−.970	11.3
14	30	6.1	5.393	−1.175	14.8
15	30	6.1	5.393	−1.175	14.8
16	0	.0	5.354	−.729	−8.0
17	−10	.0	5.354	−.729	−8.0
18	−20	.0	5.354	−.729	−8.0
19	0	.0	5.338	−.819	8.7
20	30	6.1	5.374	−1.280	33.9
21	↓	↓	5.393	−1.175	14.8
22			5.404	−1.083	−3.7
23			5.374	−1.280	33.9
24			5.393	−1.175	14.8
25			5.393	−1.175	14.8
26			5.404	−1.083	−3.7
27			5.374	−1.280	33.9
28			5.374	−1.280	33.9
29			5.374	−1.240	25.1
30			5.374	−1.240	25.1
31			5.374	−1.240	25.1
32			5.393	−1.175	14.8
33			5.393	−1.175	14.8
34			5.393	−1.175	14.8
35			5.393	−1.175	14.8
36			5.394	−1.142	6.3
37			5.394	−1.142	6.3
38			5.394	−1.142	6.3
39			5.404	−1.083	−3.7
40	30	6.1	5.404	−1.083	−3.7

TABLE V. UPPER-RAMP COORDINATES

Upper ramp 1

x, in.	y, in.
0.0000	1.3896
1.4374	1.3896
1.5210	1.3758
1.6882	1.3128
1.8553	1.2301
1.8832	1.2148
3.5549	.2744
3.7221	.1967
3.8893	.1485
4.0565	.1248
4.2236	.1215
4.3908	.1334
4.5580	.1560
[a]4.7561	.2226
4.9542	.3323
5.2006	.4703
5.4494	.6012
5.6992	.7294
5.9497	.8558
6.2016	.9786
6.3538	1.0488
6.5838	1.1503
6.8393	1.2629
7.0193	1.3385
7.9500	1.7142

Upper ramp 2

x, in.	y, in.
0.0000	1.3896
1.4374	1.3896
1.5210	1.3758
1.6882	1.3128
1.8553	1.2301
1.8832	1.2148
3.5549	.2744
3.7221	.1967
3.8893	.1485
4.0565	.1248
4.2236	.1215
4.3908	.1334
4.5580	.1560
[a]4.7570	.2060
4.9559	.2775
5.2224	.3706
5.4902	.4563
5.7585	.5392
6.0271	.6202
6.2965	.6974
6.4587	.7401
6.7028	.8001
6.9739	.8666
7.1643	.9098
8.1461	1.1182

[a]Denotes x station closest to ramp hinge point.

TABLE V. Continued

Upper ramp 3

x, in.	y, in.
0.0000	1.3896
1.4374	1.3896
1.5210	1.3758
1.6882	1.3128
1.8553	1.2301
1.8832	1.2148
3.5549	.2744
3.7221	.1967
3.8893	.1485
4.0565	.1248
4.2236	.1215
4.3908	.1334
4.5580	.1560
[a]4.7530	.1883
4.9480	.2232
5.2267	.2686
5.5053	.3065
5.7839	.3416
6.0625	.3747
6.3412	.4040
6.5083	.4179
6.7591	.4346
7.0377	.4530
7.2327	.4625
8.2358	.4973

Upper ramp 4

x, in.	y, in.
0.0000	1.3896
1.4374	1.3896
1.5210	1.3758
1.6882	1.3128
1.8553	1.2301
1.8832	1.2148
3.5549	.2744
3.7221	.1967
3.8893	.1485
4.0565	.1248
4.2236	.1215
4.3908	.1334
4.5580	.1560
[a]4.7444	.1705
4.9308	.1711
5.2132	.1674
5.4941	.1564
5.7746	.1426
6.0547	.1268
6.3343	.1073
6.5012	.0919
6.7511	.0649
7.0287	.0346
7.2224	.0101
8.2163	−.1298

[a]Denotes x station closest to ramp hinge point.

TABLE V. Continued

Upper ramp 5

x, in.	y, in.
0.0000	1.3896
1.4374	1.3896
1.5210	1.3758
1.6882	1.3128
1.8553	1.2301
1.8832	1.2148
3.5549	.2744
3.7221	.1967
3.8893	.1485
4.0565	.1248
4.2236	.1215
4.3908	.1334
4.5580	.1560
[a]4.7315	.1535
4.9049	.1228
5.1823	.0701
5.4571	.0105
5.7309	−.0518
6.0040	−.1160
6.2759	−.1837
6.4377	−.2278
6.6791	−.2979
6.9472	−.3759
7.1337	−.4336
8.0882	−.7439

Upper ramp 6

x, in.	y, in.
0.0000	1.3896
1.4374	1.3896
1.5210	1.3758
1.6882	1.3128
1.8553	1.2301
1.8832	1.2148
3.5549	.2744
3.7221	.1967
3.8893	.1485
4.0565	.1248
4.2236	.1215
4.3908	.1334
4.5580	.1560
[a]4.7144	.1379
4.8709	.0797
5.1350	−.0203
5.3952	−.1268
5.6541	−.2357
5.9119	−.3463
6.1679	−.4602
6.3196	−.5317
6.5452	−.6426
6.7956	−.7660
6.9693	−.8552
7.8554	−1.3265

[a]Denotes x station closest to ramp hinge point.

TABLE V. Continued

Upper ramp 7

x, in.	y, in.
0.0000	1.3896
1.4374	1.3896
1.5210	1.3758
1.6882	1.3128
1.8553	1.2301
1.8832	1.2148
3.5549	.2744
3.7221	.1967
3.8893	.1485
4.0565	.1248
4.2236	.1215
4.3908	.1334
4.5580	.1560
[a]4.6826	.1182
4.8073	.0277
5.0365	−.1372
5.2603	−.3074
5.4822	−.4796
5.7026	−.6531
5.9204	−.8294
6.0484	−.9378
6.2376	−1.1033
6.4476	−1.2872
6.5923	−1.4184
7.3263	−2.1029

[a]Denotes x station closest to ramp hinge point.

Upper ramp 8

x, in.	y, in.
0.0000	1.3896
1.4374	1.3896
1.5210	1.3758
1.6882	1.3128
1.8553	1.2301
1.8832	1.2148
3.5549	.2744
3.7221	.1967
3.8893	.1485
4.0565	.1248
4.2236	.1215
4.3908	.1334
4.5580	.1560
[a]4.6452	.1039
4.7324	−.0061
4.9111	−.2247
5.0833	−.4470
5.2530	−.6707
5.4210	−.8954
5.5858	−1.1221
5.6814	−1.2598
5.8213	−1.4686
5.9766	−1.7007
6.0824	−1.8648
6.6142	−2.7160

TABLE V. Continued

Upper ramp 9

x, in.	y, in.
0.0000	1.3896
1.4374	1.3896
1.5210	1.3758
1.6882	1.3128
1.8553	1.2301
1.8832	1.2148
3.5549	.2744
3.7221	.1967
3.8893	.1485
4.0565	.1248
4.2236	.1215
4.3908	.1334
4.5580	.1560
[a]4.7144	.1560
8.2358	.4973

Upper ramp 10

x, in.	y, in.
0.0000	1.3896
1.4374	1.3896
1.5210	1.3758
1.6882	1.3128
1.8553	1.2301
1.8832	1.2148
3.5549	.2744
3.7221	.1967
3.8893	.1485
4.0565	.1248
4.2236	.1215
4.3908	.1334
4.5580	.1560
[a]4.7144	.1379
7.8554	−1.3265

[a]Denotes x station closest to ramp hinge point.

TABLE V. Continued

Upper ramp 11

x, in.	y, in.
0.0000	1.3896
1.4374	1.3896
1.5210	1.3758
1.6882	1.3128
1.8553	1.2301
1.8832	1.2148
3.5549	.2744
3.7221	.1967
3.8893	.1485
4.0565	.1248
4.2236	.1215
4.3908	.1334
4.5580	.1560
[a]4.7144	.1379
4.9998	−.0726
5.2853	−.0109
5.5707	−.1113
5.8562	−.2269
6.1416	−.3561
6.4271	−.4973
6.7125	−.6488
6.9980	−.8091
7.2834	−.9765
7.5689	−1.1495
7.8544	−1.3265

Upper ramp 12

x, in.	y, in.
0.0000	1.3896
1.4374	1.3896
1.5210	1.3758
1.6882	1.3128
1.8553	1.2301
1.8832	1.2148
3.5549	.2744
3.7221	.1967
3.8893	.1485
4.0565	.1248
4.2236	.1215
4.3908	.1334
4.5580	.1560
[a]4.7144	.1379
4.8709	.0797
5.1350	−.0203
5.3952	−.1268
5.6541	−.2357
5.9119	−.3463
6.1679	−.4602
6.3196	−.5317
6.5452	−.6426
6.7956	−.7660
6.9693	−.8552
9.8500	−2.4200

[a]Denotes x station closest to ramp hinge point.

TABLE V. Concluded

Upper ramp 13

x, in.	y, in.
0.0000	1.3896
1.4374	1.3896
1.5210	1.3758
1.6882	1.3128
1.8553	1.2301
1.8832	1.2148
3.5549	.2744
3.7221	.1967
3.8893	.1485
4.0565	.1248
4.2236	.1215
4.3908	.1334
4.5580	.1560
[a]4.7144	.1379
4.8709	.0797
5.1350	−.0203
5.3952	−.1268
5.6541	−.2357
5.9119	−.3463
6.1679	−.4602
6.3196	−.5317
6.5452	−.6426
6.7956	−.7660
6.9693	−.8552
8.8500	−1.8700

Upper ramp 14

x, in.	y, in.
0.0000	1.3896
1.4374	1.3896
1.5210	1.3758
1.6882	1.3128
1.8553	1.2301
1.8832	1.2148
3.5549	.2744
3.7221	.1967
3.8893	.1485
4.0565	.1248
4.2236	.1215
4.3908	.1334
4.5580	.1560
[a]4.7144	.1379
4.8709	.0797
5.1350	−.0203
5.3952	−.1268
5.6541	−.2357
5.9119	−.3463
6.1679	−.4602
6.3196	−.5317
6.5452	−.6426
6.7956	−.7660
6.8000	−.7700
6.8400	−.7900

Upper ramp 15

x, in.	y, in.
0.0000	1.3896
1.4374	1.3896
1.5210	1.3758
1.6882	1.3128
1.8553	1.2301
1.8832	1.2148
3.5549	.2744
3.7221	.1967
3.8893	.1485
4.0565	.1248
4.2236	.1215
4.3908	.1334
4.5580	.1560
[a]4.7144	.1379
4.8709	.0797
5.1350	−.0203
5.3952	−.1268
5.6541	−.2357
5.8000	−.3000

[a]Denotes x station closest to ramp hinge point.

TABLE VI. LOWER-FLAP COORDINATES

Lower flap 1

x, in.	y, in.
0.0000	−1.3910
.6967	−1.3910
1.1866	−1.3973
1.2145	−1.3973
1.3816	−1.3834
1.5489	−1.3541
1.7160	−1.3287
1.8832	−1.3211
1.9668	−1.3207
2.4404	−1.3026
2.9977	−1.2371
3.5549	−1.1296
4.1122	−.9863
4.6694	−.8250
4.7530	−.8114
4.8366	−.8008
4.9202	−.7938
5.0038	−.7913
5.0874	−.7927
5.1709	−.7977
5.2545	−.8064
5.3381	−.8192

Lower flap 2

x, in.	y, in.
0.0000	−1.3910
.6967	−1.3910
1.1866	−1.3973
1.2145	−1.3973
1.3816	−1.3834
1.5489	−1.3541
1.7160	−1.3287
1.8832	−1.3211
1.9668	−1.3207
2.4496	−1.3218
3.0093	−1.2816
3.5708	−1.1995
4.1341	−1.0816
4.6980	−.9458
4.7821	−.9360
4.8661	−.9292
4.9500	−.9260
5.0336	−.9273
5.1170	−.9325
5.2002	−.9412
5.2833	−.9537
5.3663	−.9703

Lower flap 3

x, in.	y, in.
0.0000	−1.3910
.6967	−1.3910
1.1866	−1.3973
1.2145	−1.3973
1.3816	−1.3834
1.5489	−1.3541
1.7160	−1.3287
1.8832	−1.3211
1.9668	−1.3207
2.4607	−1.3482
3.0218	−1.3423
3.5872	−1.2946
4.1566	−1.2113
4.7278	−1.1101
4.8124	−1.1055
4.8966	−1.1038
4.9805	−1.1057
5.0639	−1.1121
5.1469	−1.1224
5.2294	−1.1363
5.3116	−1.1538
5.3933	−1.1754

Lower flap 4

x, in.	y, in.
0.0000	−1.3910
.6967	−1.3910
1.1866	−1.3973
1.2145	−1.3973
1.3816	−1.3834
1.5489	−1.3541
1.7160	−1.3287
1.8832	−1.3211
1.9668	−1.3207
2.4804	−1.4140
3.0364	−1.4901
3.6028	−1.5255
4.1782	−1.5263
4.7580	−1.5096
4.8424	−1.5174
4.9260	−1.5280
5.0087	−1.5422
5.0902	−1.5607
5.1708	−1.5830
5.2504	−1.6087
5.3292	−1.6381
5.4069	−1.6714

TABLE VI. Continued

Lower flap 5

x, in.	y, in.
0.0000	−1.3910
.6967	−1.3910
1.1866	−1.3973
1.2145	−1.3973
1.3816	−1.3834
1.5489	−1.3541
1.7160	−1.3287
1.8832	−1.3211
1.9668	−1.3207
2.4916	−1.5196
3.0162	−1.7188
3.5601	−1.8807
4.1206	−2.0108
4.6893	−2.1250
4.7698	−2.1515
4.8488	−2.1807
4.9262	−2.2131
5.0015	−2.2495
5.0750	−2.2893
5.1468	−2.3323
5.2169	−2.3786
5.2852	−2.4286

Lower flap 6

x, in.	y, in.
0.0000	−1.3910
.6967	−1.3910
1.1866	−1.3973
1.2145	−1.3973
1.3816	−1.3834
1.5489	−1.3541
1.7160	−1.3287
1.8832	−1.3211
1.9668	−1.3207
2.4404	−1.3026
2.9977	−1.2371
3.5549	−1.1296
4.1122	−.9863
4.6694	−.8250
4.7530	−.8132
4.8366	−.8015
4.9202	−.7897
5.0038	−.7779
5.0874	−.7662
5.1709	−.7545
5.2545	−.7427
5.3543	−.7287

Lower flap 7

x, in.	y, in.
0.0000	−1.3910
.6967	−1.3910
1.1866	−1.3973
1.2145	−1.3973
1.3816	−1.3834
1.5489	−1.3541
1.7160	−1.3287
1.8832	−1.3211
1.9668	−1.3207
2.4607	−1.3482
3.0218	−1.3423
3.5872	−1.2946
4.1566	−1.2113
4.7278	−1.1101
4.8124	−1.1055
4.8966	−1.1038
4.9761	−1.1096
5.0557	−1.1245
5.1353	−1.1487
5.2148	−1.1824
5.2944	−1.2260
5.3740	−1.2795

Lower flap 8

x, in.	y, in.
0.0000	−1.3910
.6967	−1.3910
1.1866	−1.3973
1.2145	−1.3973
1.3816	−1.3834
1.5489	−1.3541
1.7160	−1.3287
1.8832	−1.3211
1.9668	−1.3207
2.4607	−1.3482
3.0218	−1.3423
3.5872	−1.2946
4.1566	−1.2113
4.7278	−1.1101
4.8124	−1.1055
4.8966	−1.1038
4.9810	−1.1039
5.0655	−1.1019
5.1500	−1.0983
5.2345	−1.0935
5.3190	−1.0882
5.4035	−1.0827

TABLE VI. Concluded

Lower flap 9

x, in.	y, in.
0.0000	−1.3910
.6967	−1.3910
1.1866	−1.3973
1.2145	−1.3973
1.3816	−1.3834
1.5489	−1.3541
1.7160	−1.3287
1.8832	−1.3211
1.9668	−1.3207
2.4607	−1.3482
3.0218	−1.3423
3.5872	−1.2946
4.1566	−1.2113
4.7278	−1.1101
4.8124	−1.1055
4.8966	−1.1038
4.9761	−1.1093
5.0557	−1.1228
5.1353	−1.1434
5.2148	−1.1703
5.2944	−1.2029
5.3740	−1.2402

Lower flap 10

x, in.	y, in.
0.0000	−1.3910
.6967	−1.3910
1.1866	−1.3973
1.2145	−1.3973
1.3816	−1.3834
1.5489	−1.3541
1.7160	−1.3287
1.8832	−1.3211
1.9668	−1.3207
2.4607	−1.3482
3.0218	−1.3423
3.5872	−1.2946
4.1566	−1.2113
4.7278	−1.1101
4.8124	−1.1055
4.8966	−1.1038
4.9794	−1.1062
5.0623	−1.1107
5.1451	−1.1168
5.2280	−1.1242
5.3108	−1.1326
5.3937	−1.1417

TABLE VII. SIDEWALL COORDINATES

Sidewall 1

x, in.	y, in.
0.0000	2.3750
4.6960	2.3750
5.3939	.8248
5.8675	.0168
5.3381	−.8192
3.2130	−2.3750
.0000	−2.3750

Sidewall 2

x, in.	y, in.
0.0000	2.3750
4.6960	2.3750
7.9500	1.7142
8.1461	1.1182
8.2358	.4973
8.2163	−.1298
6.1366	−.9645
5.4069	−1.6714
3.2130	−2.3750
.0000	−2.3750

Sidewall 3

x, in.	y, in.
0.0000	2.3750
4.6960	2.3750
5.5709	.4921
5.9646	−.3740
5.3740	−1.2795
3.2130	−2.3750
.0000	−2.3750

Sidewall 4

x, in.	y, in.
0.0000	2.3750
4.6960	2.3750
8.0882	−.7439
7.8554	−1.3265
6.1366	−1.9291
5.2852	−2.4286
3.2130	−2.3750
.0000	−2.3750

Sidewall 5

x, in.	y, in.
0.0000	2.3750
4.6960	2.3750
7.8554	−1.3265
5.3740	−1.2795
3.2130	−2.3750
.0000	−2.3750

TABLE VIII. RATIO OF INTERNAL STATIC PRESSURE TO JET TOTAL PRESSURE FOR SINGLE-EXPANSION-RAMP NOZZLES

(a) Configuration 1

Ramp pressures, $p/p_{t,j}$

NPR	z/w = 0.0											
	$x'/l_{r,nom}$											
	-.351	-.207	-.135	-.063	.010	.090	.171	.252	.412	.571	.727	.882
2.000	.8504	.6472	.5665	.4696	.2407	.3693	.3800	.3983	.4532	.4956	.5014	.5208
2.503	.8511	.6465	.5663	.4682	.2322	.1870	.3189	.3256	.3590	.3821	.4007	.4421
3.015	.8507	.6461	.5663	.4671	.2318	.1869	.1823	.1731	.2783	.3071	.3325	.3753
3.501	.8504	.6458	.5663	.4664	.2315	.1864	.1814	.1721	.1686	.2470	.2861	.3649
4.009	.8495	.6449	.5661	.4659	.2311	.1860	.1807	.1714	.1395	.2192	.2496	.2813
4.981	.8487	.6446	.5658	.4654	.2304	.1854	.1796	.1704	.1393	.1174	.2009	.1612
5.992	.8485	.6443	.5654	.4653	.2299	.1850	.1791	.1697	.1395	.1175	.1663	.0755
7.021	.8481	.6437	.5649	.4652	.2293	.1847	.1786	.1694	.1395	.1175	.1420	.0757
8.013	.8480	.6434	.5648	.4653	.2291	.1845	.1784	.1693	.1396	.1176	.1245	.0759
9.006	.8478	.6430	.5645	.4655	.2288	.1844	.1782	.1691	.1397	.1176	.1106	.0760
10.021	.8474	.6427	.5643	.4658	.2287	.1843	.1780	.1691	.1398	.1176	.0995	.0760

NPR	$x'/l_{r,nom}$ = .252			$x'/l_{r,nom}$ = .571			$x'/l_{r,nom}$ = .882		
	z/w			z/w			z/w		
	0	.450	.875	0	.450	.875	0	.450	.875
2.000	.3983	.3994	.4991	.4956	.5295	.4983	.5208	.5231	.4982
2.503	.3256	.2956	.3641	.3821	.4444	.3999	.4421	.4117	.3975
3.015	.1731	.1701	.2494	.3071	.3161	.3401	.3753	.3658	.3325
3.501	.1721	.1697	.1805	.2470	.2775	.2885	.3649	.3097	.2873
4.009	.1714	.1694	.1733	.2192	.2455	.2556	.2813	.2709	.2507
4.981	.1704	.1692	.1732	.1174	.1164	.2073	.1612	.1575	.2035
5.992	.1697	.1693	.1730	.1175	.1165	.1675	.0755	.1201	.1718
7.021	.1694	.1692	.1728	.1175	.1166	.1411	.0757	.0867	.1449
8.013	.1693	.1691	.1728	.1176	.1167	.1210	.0759	.0720	.1247
9.006	.1691	.1691	.1726	.1176	.1168	.1055	.0760	.0712	.1072
10.021	.1691	.1690	.1725	.1176	.1167	.0923	.0760	.0712	.0928

Lower-flap pressures, $p/p_{t,j}$

NPR	z/w = 0.0								
	$x''/l_{l,nom}$								
	0	.294	.441	.588	.735	.809	.853	.897	.941
2.000	.8855	.9260	.8935	.8278	.6164	.4674	.3903	.3591	.4795
2.503	.8729	.9256	.8939	.8270	.6172	.4656	.3895	.3000	.3103
3.015	.8645	.9255	.8940	.8250	.6167	.4644	.3889	.2994	.2759
3.501	.8584	.9252	.8936	.8254	.6163	.4634	.3886	.2988	.2742
4.009	.8546	.9254	.8937	.8246	.6162	.4627	.3884	.2984	.2740
4.981	.8495	.9251	.8935	.8238	.6159	.4618	.3883	.2980	.2740
5.992	.8462	.9252	.8930	.8240	.6161	.4615	.3886	.2980	.2737
7.021	.8436	.9249	.8926	.8241	.6158	.4610	.3887	.2978	.2735
8.013	.8420	.9247	.8924	.8242	.6158	.4607	.3890	.2979	.2733
9.006	.8409	.9244	.8920	.8244	.6156	.4605	.3892	.2979	.2732
10.021	.8399	.9243	.8918	.8246	.6153	.4603	.3893	.2978	.2729

TABLE VIII. Continued

(b) Configuration 2

Ramp pressures, $p/p_{t,j}$

NPR	z/w = 0.0											
	$x'/l_{r,nom}$											
	-.351	-.207	-.135	-.063	.005	.080	.155	.230	.379	.528	.675	.823
2.035	.8618	.6336	.5642	.4893	.3306	.2973	.2927	.4464	.5421	.5659	.5327	.5110
2.496	.8610	.6316	.5630	.4880	.3301	.2959	.2907	.2606	.3975	.4524	.4903	.4447
3.019	.8611	.6309	.5631	.4871	.3296	.2950	.2896	.2589	.2047	.3596	.3844	.3802
3.500	.8603	.6297	.5626	.4864	.3293	.2942	.2886	.2578	.2035	.2787	.3203	.3491
3.985	.8600	.6291	.5615	.4850	.3289	.2937	.2881	.2569	.2038	.1614	.2368	.2766
4.996	.8594	.6273	.5607	.4857	.3284	.2929	.2874	.2559	.2043	.1615	.1292	.1062
5.985	.8590	.6266	.5596	.4855	.3282	.2924	.2870	.2552	.2046	.1616	.1288	.1065
7.009	.8588	.6256	.5590	.4855	.3280	.2919	.2868	.2547	.2046	.1617	.1285	.1067
7.988	.8582	.6246	.5580	.4858	.3285	.2916	.2867	.2544	.2046	.1621	.1285	.1070
9.028	.8579	.6240	.5573	.4859	.3279	.2913	.2868	.2543	.2046	.1621	.1284	.1071
10.037	.8573	.6234	.5566	.4859	.3283	.2909	.2868	.2545	.2047	.1623	.1285	.1073

NPR	$x'/l_{r,nom}$ = .230			$x'/l_{r,nom}$ = .528			$x'/l_{r,nom}$ = .823		
	z/w			z/w			z/w		
	0	.450	.875	0	.450	.875	0	.450	.875
2.035	.4464	.4501	.4576	.5659	.5562	.5156	.5110	.5117	.4946
2.496	.2606	.2638	.2639	.4524	.4899	.4278	.4447	.4441	.4036
3.019	.2589	.2634	.2637	.3596	.3419	.3444	.3802	.3709	.3399
3.500	.2578	.2633	.2634	.2787	.1629	.2917	.3491	.4077	.2907
3.985	.2569	.2633	.2631	.1614	.1628	.2488	.2766	.3374	.2524
4.996	.2559	.2634	.2628	.1615	.1630	.1916	.1062	.1150	.1989
5.985	.2552	.2636	.2625	.1616	.1632	.1545	.1065	.0969	.1611
7.009	.2547	.2635	.2625	.1617	.1632	.1274	.1067	.0970	.1302
7.988	.2544	.2636	.2621	.1621	.1635	.1075	.1070	.0972	.1085
9.028	.2543	.2637	.2626	.1621	.1636	.0962	.1071	.0975	.0929
10.037	.2545	.2638	.2622	.1623	.1637	.0934	.1073	.0977	.0783

Lower-flap pressures, $p/p_{t,j}$

NPR	z/w = 0.0								
	$x''/l_{l,nom}$								
	0	.294	.441	.588	.735	.809	.853	.897	.941
2.035	.8851	.9262	.8943	.8282	.6186	.4699	.3935	.3134	.4759
2.496	.8729	.9258	.8944	.8269	.6178	.4678	.3928	.3036	.3182
3.019	.8639	.9262	.8945	.8265	.6181	.4665	.3924	.3028	.2596
3.500	.8581	.9256	.8940	.8255	.6174	.4655	.3920	.3023	.2517
3.985	.8537	.9254	.8940	.8248	.6173	.4646	.3918	.3018	.2516
4.996	.8486	.9254	.8936	.8245	.6172	.4637	.3917	.3013	.2517
5.985	.8456	.9254	.8932	.8246	.6172	.4631	.3919	.3012	.2518
7.009	.8431	.9253	.8929	.8247	.6171	.4627	.3920	.3010	.2519
7.988	.8416	.9248	.8926	.8249	.6167	.4623	.3921	.3010	.2517
9.028	.8400	.9245	.8922	.8248	.6165	.4621	.3922	.3010	.2518
10.037	.8391	.9239	.8917	.8249	.6161	.4619	.3922	.3011	.2519

TABLE VIII. Continued

(c) Configuration 3

Ramp pressures, $p/p_{t,j}$

NPR	z/w = 0.0											
	$x'/l_{r,nom}$											
	-.351	-.207	-.135	-.063	.009	.081	.152	.224	.368	.512	.656	.800
1.992	.8532	.6343	.5554	.5234	.4968	.4595	.4256	.5241	.5557	.5513	.5401	.5183
2.507	.8538	.6344	.5546	.5190	.4961	.4594	.4241	.3736	.2720	.5005	.5040	.4007
3.006	.8536	.6341	.5542	.5196	.4961	.4592	.4233	.3732	.2721	.2091	.4059	.5011
3.481	.8533	.6338	.5533	.5180	.4955	.4589	.4225	.3726	.2720	.2086	.2483	.2869
4.027	.8526	.6330	.5525	.5173	.4951	.4588	.4219	.3721	.2718	.2085	.1650	.2026
5.007	.8523	.6322	.5517	.5170	.4953	.4592	.4217	.3722	.2721	.2086	.1647	.1294
5.971	.8521	.6316	.5508	.5169	.4956	.4597	.4218	.3726	.2723	.2090	.1646	.1298
7.005	.8513	.6308	.5496	.5158	.4957	.4599	.4219	.3729	.2724	.2089	.1644	.1299
7.967	.8509	.6303	.5487	.5158	.4958	.4602	.4221	.3732	.2726	.2089	.1645	.1302
8.997	.8501	.6295	.5477	.5169	.4958	.4605	.4222	.3738	.2725	.2088	.1645	.1304
10.024	.8497	.6288	.5468	.5173	.4960	.4609	.4226	.3744	.2727	.2090	.1646	.1305

NPR	$x'/l_{r,nom}$ = .224			$x'/l_{r,nom}$ = .512			$x'/l_{r,nom}$ = .800		
	z/w			z/w			z/w		
	0	.450	.875	0	.450	.875	0	.450	.875
1.992	.5241	.5256	.5236	.5513	.5543	.5362	.5183	.5170	.5160
2.507	.3736	.3732	.3699	.5005	.5011	.4385	.4007	.3896	.4078
3.006	.3732	.3732	.3701	.2091	.2145	.3568	.5011	.4692	.3540
3.481	.3726	.3732	.3701	.2096	.2125	.2798	.2869	.3290	.3041
4.027	.3721	.3733	.3696	.2085	.2125	.2309	.2026	.2482	.2668
5.007	.3722	.3738	.3694	.2086	.2130	.1774	.1294	.1177	.1981
5.971	.3726	.3743	.3696	.2090	.2131	.1479	.1298	.1180	.1564
7.005	.3729	.3745	.3694	.2089	.2132	.1330	.1299	.1182	.1285
7.967	.3732	.3748	.3695	.2089	.2132	.1299	.1302	.1184	.1063
8.997	.3738	.3749	.3694	.2088	.2132	.1292	.1304	.1186	.0838
10.024	.3744	.3751	.3698	.2090	.2133	.1290	.1305	.1188	.0605

Lower-flap pressures, $p/p_{t,j}$

NPR	z/w = 0.0								
	$x''/l_{l,nom}$								
	0	.294	.441	.588	.735	.809	.853	.897	.941
1.992	.8837	.9229	.8918	.8253	.6161	.4694	.3955	.3183	.4855
2.507	.8693	.9230	.8931	.8244	.6163	.4671	.3946	.3113	.2515
3.006	.8605	.9235	.8933	.8239	.6157	.4656	.3942	.3108	.2352
3.481	.8543	.9230	.8926	.8232	.6152	.4644	.3934	.3103	.2347
4.027	.8494	.9232	.8923	.8223	.6148	.4632	.3929	.3097	.2345
5.007	.8438	.9234	.8924	.8222	.6148	.4623	.3925	.3093	.2344
5.971	.8407	.9237	.8923	.8223	.6150	.4618	.3926	.3093	.2345
7.005	.8376	.9235	.8917	.8222	.6145	.4610	.3924	.3090	.2344
7.967	.8358	.9232	.8914	.8227	.6145	.4604	.3922	.3089	.2343
8.997	.8342	.9228	.8907	.8224	.6142	.4597	.3922	.3087	.2340
10.024	.8331	.9227	.8906	.8226	.6139	.4594	.3924	.3087	.2340

TABLE VIII. Continued

(d) Configuration 4

Ramp pressures, $p/p_{t,j}$

NPR	z/w = 0.0											
	$x'/l_{r,nom}$											
	-.351	-.207	-.135	-.063	.008	.079	.150	.221	.365	.508	.653	.798
2.013	.8636	.6737	.6323	.6726	.6848	.6229	.5563	.4838	.5635	.5505	.5355	.5198
2.498	.8629	.6729	.6314	.6717	.6830	.6218	.5543	.4825	.3629	.4055	.5427	.4447
3.016	.8629	.6736	.6308	.6721	.6822	.6213	.5534	.4817	.3629	.2899	.3014	.3362
3.490	.8611	.6746	.6307	.6725	.6816	.6212	.5532	.4815	.3630	.2747	.2355	.2370
3.991	.8593	.6742	.6302	.6725	.6813	.6213	.5534	.4816	.3632	.2749	.1947	.1841
4.985	.8565	.6729	.6301	.6722	.6806	.6211	.5537	.4821	.3630	.2749	.1916	.1355
6.045	.8531	.6728	.6297	.6722	.6806	.6213	.5545	.4831	.3633	.2752	.1919	.1357
6.990	.8504	.6721	.6290	.6719	.6805	.6214	.5549	.4839	.3634	.2754	.1920	.1360
8.021	.8484	.6718	.6289	.6717	.6810	.6217	.5555	.4847	.3637	.2756	.1921	.1363
8.987	.8463	.6714	.6284	.6714	.6816	.6217	.5562	.4848	.3640	.2760	.1924	.1366
9.483	.8455	.6711	.6282	.6713	.6817	.6218	.5566	.4848	.3641	.2761	.1925	.1368

NPR	$x'/l_{r,nom}$ = .221			$x'/l_{r,nom}$ = .508			$x'/l_{r,nom}$ = .798		
	z/w			z/w			z/w		
	0	.450	.875	0	.450	.875	0	.450	.875
2.013	.4838	.4842	.4725	.5505	.5485	.5295	.5198	.5181	.5160
2.498	.4825	.4836	.4722	.4055	.4156	.4300	.4447	.4351	.4091
3.016	.4817	.4840	.4721	.2899	.2927	.3432	.3362	.3889	.3596
3.490	.4815	.4844	.4718	.2747	.2769	.2678	.2370	.2441	.3016
3.991	.4816	.4849	.4708	.2749	.2771	.2230	.1841	.1536	.2591
4.985	.4821	.4849	.4698	.2749	.2770	.1629	.1355	.1168	.1673
6.045	.4831	.4853	.4694	.2752	.2773	.1577	.1357	.1172	.1313
6.990	.4839	.4854	.4689	.2754	.2775	.1568	.1360	.1175	.1100
8.021	.4847	.4856	.4687	.2756	.2778	.1563	.1363	.1178	.0870
8.987	.4848	.4858	.4687	.2760	.2777	.1561	.1366	.1181	.0625
9.483	.4848	.4859	.4689	.2751	.2781	.1560	.1368	.1182	.0600

Lower-flap pressures, $p/p_{t,j}$

NPR	z/w = 0.0								
	$x''/l_{l,nom}$								
	0	.294	.441	.588	.735	.809	.853	.897	.941
2.013	.8881	.9305	.9017	.8407	.6588	.5407	.4826	.4096	.3414
2.498	.8751	.9298	.9014	.8437	.6575	.5384	.4812	.4084	.3399
3.016	.8662	.9300	.9016	.8398	.6579	.5367	.4806	.4078	.3398
3.490	.8610	.9300	.9014	.8388	.6567	.5356	.4803	.4074	.3396
3.991	.8571	.9300	.9021	.8386	.6570	.5350	.4802	.4074	.3394
4.985	.8512	.9301	.9011	.8379	.6566	.5338	.4799	.4071	.3390
6.045	.8478	.9303	.9009	.8382	.6562	.5330	.4801	.4072	.3388
6.990	.8454	.9300	.9003	.8379	.6559	.5321	.4800	.4073	.3384
8.021	.8439	.9295	.9000	.8382	.6557	.5313	.4800	.4075	.3383
8.987	.8427	.9293	.8994	.8381	.6552	.5307	.4801	.4077	.3382
9.483	.8423	.9292	.8991	.8382	.6550	.5304	.4801	.4078	.3381

TABLE VIII. Continued

(e) Configuration 5

Ramp pressures, $p/p_{t,j}$

NPR	z/w = 0.0								
	$x'/l_{r,nom}$								
	-.207	-.063	.080	.152	.225	.373	.520	.669	.819
1.990	.7257	.7963	.7511	.6889	.6277	.5043	.5534	.5344	.5179
2.522	.7250	.7953	.7485	.6842	.6175	.3985	.4142	.3926	.4882
3.012	.7244	.7947	.7476	.6832	.6168	.3335	.3349	.2985	.2940
3.496	.7240	.7946	.7475	.6831	.6169	.2875	.3312	.2406	.2298
4.017	.7238	.7941	.7470	.6828	.6166	.2502	.3312	.2110	.1847
5.037	.7229	.7929	.7467	.6824	.6166	.1996	.3315	.2101	.1447
6.002	.7219	.7930	.7470	.6824	.6169	.1673	.3323	.2101	.1452
7.007	.7214	.7924	.7476	.6823	.6174	.1432	.3329	.2103	.1456
7.289	.7210	.7924	.7479	.6822	.6175	.1376	.3332	.2103	.1457

NPR	$x'/l_{r,nom}$ = .225			$x'/l_{r,nom}$ = .520			$x'/l_{r,nom}$ = .819		
	z/w			z/w			z/w		
	0	.450	.875	0	.450	.875	0	.450	.875
1.990	.6277	.6141	.6101	.5534	.5382	.5200	.5179	.5152	.5093
2.522	.6175	.6015	.5973	.4142	.4010	.3972	.4882	.4490	.4136
3.012	.6168	.5994	.5957	.3349	.3233	.2905	.2940	.3224	.3450
3.496	.6169	.5983	.5950	.3312	.3202	.2481	.2298	.2020	.2895
4.017	.6166	.5971	.5945	.3312	.3200	.2339	.1847	.1664	.2426
5.037	.6166	.5958	.5939	.3315	.3200	.2235	.1447	.1318	.1576
6.002	.6169	.5953	.5940	.3323	.3203	.2182	.1452	.1323	.1234
7.007	.6174	.5951	.5940	.3329	.3207	.2161	.1456	.1326	.0897
7.289	.6175	.5950	.5938	.3332	.3208	.2159	.1457	.1328	.0793

Lower-flap pressures, $p/p_{t,j}$

NPR	z/w = 0.0								
	$x''/l_{l,nom}$								
	0	.293	.493	.585	.730	.803	.847	.891	.935
1.990	.8837	.9316	.9089	.8642	.7219	.6533	.5983	.5437	.4959
2.522	.8697	.9317	.9088	.8633	.7202	.6504	.5950	.5396	.4925
3.012	.8611	.9316	.9085	.8624	.7186	.6494	.5941	.5388	.4920
3.496	.8551	.9316	.9087	.8619	.7184	.6489	.5940	.5385	.4919
4.017	.8500	.9313	.9081	.8617	.7181	.6484	.5935	.5382	.4916
5.037	.8437	.9311	.9075	.8608	.7172	.6476	.5929	.5379	.4915
6.002	.8407	.9312	.9073	.8608	.7167	.6470	.5929	.5379	.4917
7.007	.8382	.9312	.9068	.8613	.7168	.6466	.5927	.5379	.4916
7.289	.8376	.9310	.9068	.8613	.7166	.6466	.5927	.5379	.4916

TABLE VIII. Continued

(f) Configuration 6

Ramp pressures, $p/p_{t,j}$

NPR	z/w = 0.0								
	$x'/l_{r,nom}$								
	.009	.085	.161	.239	.316	.392	.551	.713	.874
2.015	.8987	.8444	.7941	.7270	.6560	.6072	.5387	.5387	.4890
2.503	.8957	.8408	.7877	.7153	.6320	.5594	.4571	.3917	.4042
2.993	.8953	.8406	.7875	.7155	.6306	.5545	.3971	.3309	.2670
3.510	.8954	.8409	.7874	.7155	.6301	.5545	.3834	.2791	.2210
4.019	.8955	.8405	.7872	.7153	.6299	.5543	.3834	.2441	.1876
5.008	.8966	.8408	.7875	.7156	.6303	.5540	.3838	.2395	.1483
5.987	.8976	.8408	.7873	.7153	.6307	.5542	.3843	.2400	.1425
6.203	.8979	.8407	.7873	.7155	.6307	.5541	.3844	.2401	.1425

NPR	$x'/l_{r,nom}$ = .392			$x'/l_{r,nom}$ = .713			$x'/l_{r,nom}$ = .874		
	z/w			z/w			z/w		
	0	.450	.875	0	.450	.875	0	.450	.875
2.015	.6072	.6114	.5702	.5387	.5221	.5263	.4890	.4983	.4980
2.503	.5594	.5705	.5404	.3917	.3835	.4264	.4042	.4168	.4100
2.993	.5545	.5675	.5396	.3309	.2835	.3476	.2670	.3107	.3404
3.510	.5545	.5675	.5397	.2791	.2440	.2676	.2210	.1839	.2785
4.019	.5543	.5676	.5398	.2441	.2145	.1846	.1876	.1590	.2378
5.008	.5540	.5684	.5405	.2395	.2117	.1374	.1483	.1263	.1587
5.987	.5542	.5689	.5409	.2400	.2113	.1227	.1425	.1233	.1294
6.203	.5541	.5690	.5410	.2401	.2104	.1225	.1425	.1234	.1238

Lower-flap pressures, $p/p_{t,j}$

NPR	z/w = 0.0								
	$x''/l_{l,nom}$								
	0	.293	.438	.582	.723	.797	.841	.885	.930
2.015	.8817	.9384	.9208	.8880	.8000	.7349	.6857	.6338	.5562
2.503	.8685	.9369	.9195	.8870	.7963	.7299	.6795	.6261	.5472
2.993	.8601	.9368	.9193	.8859	.7961	.7293	.6789	.6253	.5455
3.510	.8542	.9371	.9193	.8855	.7957	.7289	.6787	.6251	.5446
4.019	.8498	.9366	.9189	.8853	.7954	.7286	.6783	.6248	.5437
5.008	.8444	.9371	.9188	.8858	.7954	.7294	.6783	.6249	.5421
5.987	.8412	.9365	.9184	.8859	.7950	.7282	.6780	.6246	.5446
6.203	.8404	.9367	.9183	.8859	.7948	.7281	.6779	.6246	.5444

TABLE VIII. Continued

(g) Configuration 7

Ramp pressures, $p/p_{t,j}$

NPR	z/w = 0.0						
	$x'/l_{r,nom}$						
	.010	.185	.276	.368	.462	.651	.846
2.012	.9480	.8840	.8471	.7929	.7148	.5577	.4941
2.504	.9453	.8789	.8407	.7822	.6914	.4821	.3664
3.004	.9454	.8782	.8402	.7801	.6835	.4524	.3193
3.516	.9460	.8785	.8414	.7832	.6830	.4272	.2874
4.017	.9462	.8784	.8420	.7799	.6825	.4267	.2600
5.000	.9468	.8793	.8432	.7796	.6824	.4268	.2329

NPR	$x'/l_{r,nom}$ = .462			$x'/l_{r,nom}$ = .651			$x'/l_{r,nom}$ = .846		
	z/w			z/w			z/w		
	0	.450	.875	0	.450	.875	0	.450	.875
2.012	.7148	.7186	.6948	.5577	.5698	.5343	.4941	.5009	.5093
2.504	.6914	.6985	.6796	.4821	.4908	.4271	.3664	.3735	.4075
3.004	.6835	.6932	.6779	.4524	.4606	.3379	.3193	.2885	.3288
3.516	.6830	.6933	.6781	.4272	.4406	.2972	.2874	.2621	.2676
4.017	.6825	.6933	.6781	.4267	.4405	.2800	.2600	.2381	.1721
5.000	.6824	.6937	.6788	.4268	.4412	.2784	.2329	.2171	.1353

Lower-flap pressures, $p/p_{t,j}$

NPR	z/w = 0.0								
	$x''/l_{l,nom}$								
	.075	.297	.442	.585	.726	.797	.841	.885	.930
2.012	.8798	.9419	.9321	.9139	.8529	.8046	.7641	.7181	.6723
2.504	.8647	.9404	.9336	.9116	.8475	.7973	.7551	.7071	.6594
3.004	.8564	.9404	.9336	.9107	.8463	.7959	.7535	.7055	.6574
3.516	.8504	.9406	.9339	.9105	.8460	.7962	.7532	.7053	.6575
4.017	.8461	.9400	.9333	.9105	.8450	.7960	.7527	.7049	.6573
5.000	.8409	.9401	.9330	.9114	.8451	.7957	.7523	.7049	.6571

TABLE VIII. Continued

(h) Configuration 8

Ramp pressures, $p/p_{t,j}$

NPR	z/w = 0.0						
	$x'/l_{r,nom}$						
	.012	.246	.366	.492	.618	.726	.837
1.983	.9656	.9367	.9063	.8604	.7756	.6787	.5740
2.505	.9633	.9330	.9019	.8527	.7577	.6438	.5078
3.026	.9635	.9327	.9023	.8511	.7523	.6285	.4831
3.507	.9639	.9335	.9036	.8513	.7520	.6260	.4582
3.965	.9643	.9339	.9047	.8515	.7523	.6266	.4580
4.310	.9647	.9349	.9058	.8517	.7526	.6271	.4585
4.374	.9640	.9342	.9053	.8511	.7522	.6267	.4581

NPR	$x'/l_{r,nom}$ = .618			$x'/l_{r,nom}$ = .726			$x'/l_{r,nom}$ = .837		
	z/w			z/w			z/w		
	0	.450	.875	0	.450	.875	0	.450	.875
1.983	.7756	.7717	.7531	.6787	.6727	.5993	.5740	.5659	.5242
2.505	.7577	.7551	.7393	.6438	.6375	.5453	.5078	.4938	.4126
3.026	.7523	.7505	.7367	.6285	.6230	.5389	.4831	.4719	.3384
3.507	.7520	.7505	.7368	.6260	.6212	.5388	.4582	.4504	.3041
3.965	.7523	.7508	.7371	.6266	.6216	.5398	.4580	.4500	.2939
4.310	.7526	.7512	.7374	.6271	.6223	.5404	.4585	.4519	.2930
4.374	.7522	.7507	.7370	.6267	.6217	.5401	.4581	.4516	.2927

Lower-flap pressures, $p/p_{t,j}$

NPR	z/w = 0.0								
	$x''/l_{l,nom}$								
	.079	.315	.466	.611	.755	.815	.860	.909	.959
1.983	.8741	.9483	.9444	.9286	.8723	.8305	.7934	.7429	.6865
2.505	.8553	.9460	.9434	.9258	.8661	.8224	.7839	.7303	.6719
3.026	.8464	.9457	.9430	.9242	.8646	.8208	.7816	.7276	.6692
3.507	.8408	.9459	.9432	.9237	.8644	.8210	.7816	.7278	.6693
3.965	.8366	.9461	.9431	.9235	.8638	.8206	.7818	.7280	.6697
4.310	.8345	.9461	.9440	.9233	.8635	.8209	.7820	.7283	.6700
4.374	.8330	.9456	.9430	.9223	.8630	.8204	.7814	.7278	.6694

TABLE VIII. Continued

(i) Configuration 9

Ramp pressures, $p/p_{t,j}$

NPR	z/w = 0.0											
	$x'/l_{r,nom}$											
	-.351	-.207	-.135	-.063	.010	.090	.171	.252	.412	.571	.727	.882
2.006	.8503	.6466	.5670	.4698	.2326	.3495	.3603	.3698	.4124	.4739	.4980	.5374
2.511	.8504	.6459	.5668	.4681	.2318	.1872	.1836	.3043	.3124	.3337	.3977	.4464
3.011	.8496	.6455	.5664	.4670	.2314	.1869	.1820	.1729	.2542	.2758	.3311	.3340
3.517	.8493	.6453	.5662	.4654	.2313	.1863	.1810	.1722	.1393	.2142	.2835	.2558
4.016	.8487	.6448	.5665	.4659	.2309	.1858	.1803	.1715	.1393	.1171	.2485	.2166
5.027	.8482	.6441	.5660	.4652	.2301	.1851	.1794	.1705	.1394	.1172	.1983	.1731
6.023	.8481	.6441	.5658	.4648	.2297	.1847	.1788	.1699	.1395	.1174	.1655	.0746
6.999	.8476	.6435	.5656	.4646	.2293	.1844	.1784	.1695	.1396	.1175	.1423	.0748
8.023	.8472	.6432	.5652	.4646	.2290	.1841	.1780	.1693	.1397	.1176	.1241	.0749
8.988	.8469	.6429	.5649	.4647	.2291	.1840	.1779	.1693	.1399	.1178	.1108	.0750
9.020	.8468	.6429	.5650	.4647	.2291	.1840	.1779	.1693	.1399	.1178	.1104	.0750
10.037	.8466	.6426	.5648	.4649	.2291	.1840	.1777	.1692	.1400	.1178	.0995	.0751

NPR	$x'/l_{r,nom}$ = .252			$x'/l_{r,nom}$ = .571			$x'/l_{r,nom}$ = .882		
	z/w			z/w			z/w		
	0	.450	.875	0	.450	.875	0	.450	.875
2.006	.3698	.3763	.3759	.4739	.4634	.4999	.5374	.5363	.5294
2.511	.3043	.3129	.2179	.3337	.3276	.3697	.4464	.4380	.4358
3.011	.1729	.1699	.1743	.2758	.2564	.2853	.3340	.3683	.3532
3.517	.1722	.1696	.1741	.2142	.2122	.1188	.2558	.2575	.3045
4.016	.1715	.1695	.1738	.1171	.1165	.1189	.2166	.2155	.2090
5.027	.1705	.1694	.1734	.1172	.1166	.1187	.1731	.1763	.1707
6.023	.1699	.1694	.1732	.1174	.1167	.1187	.0746	.0773	.0773
6.999	.1695	.1693	.1729	.1175	.1167	.1186	.0748	.0776	.0773
8.023	.1693	.1694	.1727	.1176	.1168	.1186	.0749	.0778	.0774
8.988	.1693	.1695	.1725	.1178	.1168	.1184	.0750	.0780	.0774
9.020	.1693	.1695	.1726	.1178	.1168	.1185	.0750	.0780	.0775
10.007	.1692	.1695	.1723	.1178	.1169	.1186	.0751	.0781	.0775

Lower-flap pressures, $p/p_{t,j}$

NPR	z/w = 0.0								
	$x''/l_{l,nom}$								
	0	.294	.441	.588	.735	.809	.853	.897	.941
2.006	.8868	.9269	.8943	.8278	.6176	.4692	.3907	.3817	.4733
2.511	.8733	.9264	.8943	.8272	.6171	.4669	.3897	.2998	.3274
3.011	.8647	.9258	.8943	.8250	.6167	.4655	.3892	.2991	.2740
3.517	.8591	.9259	.8938	.8256	.6166	.4646	.3889	.2985	.2707
4.016	.8547	.9256	.8937	.8251	.6166	.4638	.3887	.2981	.2709
5.027	.8492	.9256	.8932	.8248	.6166	.4629	.3885	.2975	.2707
6.023	.8458	.9253	.8931	.8246	.6168	.4624	.3886	.2974	.2706
6.999	.8434	.9250	.8926	.8247	.6165	.4620	.3888	.2973	.2703
8.023	.8416	.9246	.8924	.8247	.6162	.4615	.3890	.2974	.2699
8.988	.8405	.9243	.8920	.8247	.6161	.4613	.3894	.2975	.2693
9.020	.8406	.9243	.8920	.8249	.6161	.4613	.3894	.2975	.2693
10.007	.8394	.9240	.8917	.8250	.6158	.4611	.3896	.2974	.2689

TABLE VIII. Continued

(j) Configuration 10

Ramp pressures, $p/p_{t,j}$

NPR	z/w = 0.0											
	$x'/l_{r,nom}$											
	-.351	-.207	-.135	-.063	.005	.080	.155	.230	.379	.528	.675	.823
2.000	.8614	.6342	.5634	.4894	.3305	.2972	.2933	.4551	.5618	.5731	.5426	.5196
2.513	.8614	.6326	.5628	.4880	.3301	.2957	.2906	.2600	.3729	.4596	.5092	.4579
3.003	.8613	.6316	.5621	.4873	.3301	.2949	.2894	.2585	.2029	.3210	.3897	.4288
3.503	.8604	.6313	.5615	.4857	.3298	.2940	.2886	.2573	.2028	.1603	.2510	.3302
3.990	.8602	.6301	.5610	.4854	.3294	.2936	.2881	.2565	.2029	.1603	.1301	.1799
5.006	.8596	.6289	.5599	.4851	.3290	.2928	.2875	.2555	.2030	.1603	.1295	.1055
5.993	.8592	.6281	.5590	.4859	.3289	.2923	.2872	.2549	.2032	.1605	.1293	.1059
7.006	.8589	.6271	.5585	.4858	.3287	.2918	.2870	.2545	.2032	.1606	.1290	.1061
8.021	.8586	.6264	.5575	.4859	.3286	.2915	.2869	.2542	.2034	.1606	.1288	.1064
9.016	.8581	.6256	.5567	.4860	.3285	.2911	.2869	.2541	.2034	.1607	.1287	.1066
10.020	.8577	.6249	.5559	.4850	.3284	.2908	.2869	.2540	.2035	.1607	.1287	.1068

NPR	$x'/l_{r,nom}$ = .230			$x'/l_{r,nom}$ = .528			$x'/l_{r,nom}$ = .823		
	z/w			z/w			z/w		
	0	.450	.875	0	.450	.875	0	.450	.875
2.000	.4551	.4585	.4626	.5731	.5724	.5653	.5196	.5212	.5074
2.513	.2600	.2638	.2662	.4596	.4468	.4713	.4579	.4584	.4373
3.003	.2585	.2635	.2659	.3210	.3269	.3172	.4288	.4369	.4140
3.503	.2573	.2634	.2657	.1603	.1630	.1644	.3302	.3240	.3380
3.990	.2565	.2634	.2657	.1603	.1631	.1644	.1799	.1837	.1856
5.006	.2555	.2634	.2648	.1603	.1635	.1639	.1055	.1056	.1038
5.993	.2549	.2636	.2644	.1605	.1636	.1637	.1059	.1061	.1040
7.006	.2545	.2635	.2640	.1606	.1636	.1635	.1061	.1064	.1041
8.021	.2542	.2636	.2638	.1606	.1636	.1636	.1064	.1067	.1042
9.016	.2541	.2635	.2636	.1607	.1636	.1635	.1066	.1069	.1041
10.020	.2540	.2635	.2636	.1607	.1637	.1635	.1068	.1071	.1042

Lower-flap pressures, $p/p_{t,j}$

NPR	z/w = 0.0								
	$x''/l_{l,nom}$								
	0	.294	.441	.588	.735	.809	.853	.897	.941
2.000	.8864	.9259	.8938	.8283	.6160	.4704	.3930	.3702	.4789
2.513	.8725	.9259	.8943	.8279	.6162	.4684	.3924	.3031	.3187
3.003	.8640	.9257	.8945	.8257	.6161	.4673	.3920	.3025	.2627
3.503	.8583	.9257	.8937	.8253	.6153	.4663	.3917	.3018	.2544
3.990	.8545	.9255	.8938	.8256	.6153	.4654	.3916	.3013	.2508
5.006	.8489	.9255	.8938	.8252	.6150	.4645	.3915	.3008	.2511
5.993	.8457	.9254	.8934	.8252	.6148	.4640	.3916	.3003	.2514
7.006	.8433	.9250	.8929	.8251	.6142	.4632	.3915	.3000	.2516
8.021	.8415	.9247	.8929	.8255	.6139	.4629	.3912	.2996	.2519
9.016	.8401	.9244	.8925	.8253	.6136	.4626	.3923	.2994	.2525
10.020	.8391	.9240	.8919	.8252	.6131	.4623	.3924	.2993	.2525

TABLE VIII. Continued

(k) Configuration 11

Ramp pressures, $p/p_{t,j}$

NPR	z/w = 0.0											
	$x'/l_{r,nom}$											
	-.351	-.207	-.135	-.063	.009	.081	.152	.224	.368	.512	.656	.800
1.989	.8536	.6353	.5555	.5207	.4974	.4604	.4254	.5248	.5594	.5547	.5422	.5196
2.499	.8539	.6347	.5538	.5189	.4962	.4592	.4232	.3735	.2722	.4999	.5141	.4170
3.005	.8540	.6340	.5534	.5186	.4963	.4593	.4226	.3731	.2725	.2091	.3526	.4990
3.516	.8537	.6338	.5524	.5180	.4957	.4589	.4218	.3725	.2725	.2088	.2327	.2756
4.033	.8534	.6333	.5525	.5179	.4957	.4591	.4215	.3724	.2726	.2087	.1649	.2018
4.992	.8529	.6323	.5510	.5170	.4955	.4591	.4209	.3722	.2726	.2086	.1645	.1297
6.003	.8521	.6317	.5495	.5164	.4956	.4594	.4209	.3724	.2727	.2086	.1642	.1300
7.000	.8516	.6307	.5489	.5165	.4958	.4598	.4211	.3730	.2729	.2087	.1644	.1302
7.984	.8512	.6301	.5479	.5166	.4961	.4602	.4216	.3736	.2732	.2087	.1642	.1304
9.006	.8504	.6294	.5468	.5165	.4959	.4603	.4217	.3741	.2733	.2088	.1643	.1306
10.031	.8497	.6285	.5458	.5167	.4959	.4606	.4221	.3748	.2735	.2089	.1643	.1308

NPR	$x'/l_{r,nom}$ = .224			$x'/l_{r,nom}$ = .512			$x'/l_{r,nom}$ = .800		
	z/w			z/w			z/w		
	0	.450	.875	0	.450	.875	0	.450	.875
1.989	.5248	.5248	.5339	.5547	.5604	.5588	.5196	.5189	.5241
2.499	.3735	.3719	.3715	.4999	.4998	.5042	.4170	.4095	.4307
3.005	.3731	.3723	.3720	.2091	.2130	.2143	.4990	.4986	.4856
3.516	.3725	.3724	.3718	.2088	.2130	.2143	.2756	.2766	.2832
4.033	.3724	.3728	.3719	.2087	.2131	.2140	.2018	.1979	.2047
4.992	.3722	.3731	.3713	.2086	.2131	.2135	.1297	.1285	.1332
6.003	.3724	.3732	.3710	.2086	.2132	.2131	.1300	.1288	.1333
7.000	.3730	.3736	.3710	.2087	.2133	.2131	.1302	.1292	.1335
7.984	.3736	.3753	.3708	.2087	.2134	.2130	.1304	.1294	.1337
9.006	.3741	.3756	.3708	.2088	.2134	.2137	.1306	.1296	.1338
10.031	.3748	.3758	.3710	.2089	.2136	.2135	.1308	.1299	.1341

Lower-flap pressures, $p/p_{t,j}$

NPR	z/w = 0.0								
	$x''/l_{l,nom}$								
	0	.294	.441	.588	.735	.809	.853	.897	.941
1.989	.8872	.9265	.8942	.8258	.6168	.4694	.3955	.3204	.4844
2.499	.8730	.9260	.8936	.8247	.6161	.4667	.3941	.3121	.3039
3.005	.8644	.9265	.8944	.8244	.6161	.4656	.3939	.3116	.2346
3.516	.8594	.9256	.8938	.8236	.6153	.4643	.3933	.3109	.2341
4.033	.8547	.9263	.8939	.8236	.6156	.4637	.3932	.3105	.2339
4.992	.8492	.9258	.8930	.8229	.6151	.4625	.3926	.3099	.2333
6.003	.8457	.9252	.8925	.8226	.6152	.4617	.3923	.3095	.2329
7.000	.8434	.9252	.8921	.8229	.6149	.4613	.3924	.3094	.2327
7.984	.8418	.9249	.8920	.8233	.6147	.4610	.3925	.3094	.2326
9.036	.8402	.9244	.8911	.8231	.6144	.4602	.3923	.3093	.2323
10.031	.8391	.9239	.8907	.8229	.6141	.4596	.3924	.3092	.2323

TABLE VIII. Continued

(l) Configuration 12

Ramp pressures, $p/p_{t,j}$

NPR	z/w = 0.0											
	$x'/l_{r,nom}$											
	-.351	-.207	-.135	-.063	.008	.079	.150	.221	.365	.508	.653	.798
2.000	.8578	.6720	.6298	.6715	.6844	.6228	.5560	.4847	.5658	.5554	.5399	.5231
2.499	.8562	.6713	.6296	.6715	.6825	.6219	.5541	.4833	.3633	.4056	.5416	.4605
3.007	.8557	.6717	.6298	.6724	.6820	.6217	.5536	.4829	.3635	.2901	.3033	.3415
3.495	.8551	.6714	.6295	.6721	.6813	.6214	.5528	.4824	.3632	.2751	.2354	.2369
4.030	.8542	.6707	.6292	.6717	.6805	.6211	.5523	.4822	.3629	.2749	.1946	.1815
4.994	.8523	.6706	.6291	.6715	.6802	.6215	.5527	.4827	.3631	.2752	.1929	.1360
5.996	.8503	.6702	.6285	.6715	.6802	.6217	.5529	.4836	.3632	.2754	.1927	.1361
7.002	.8489	.6700	.6283	.6714	.6806	.6221	.5533	.4846	.3634	.2756	.1929	.1364
7.996	.8472	.6696	.6280	.6713	.6810	.6223	.5537	.4854	.3637	.2759	.1931	.1367
8.690	.8460	.6695	.6278	.6709	.6812	.6224	.5542	.4855	.3639	.2761	.1933	.1369

NPR	$x'/l_{r,nom}$ = .221			$x'/l_{r,nom}$ = .508			$x'/l_{r,nom}$ = .798		
	z/w			z/w			z/w		
	0	.450	.875	0	.450	.875	0	.450	.875
2.000	.4847	.4837	.4873	.5554	.5562	.5569	.5231	.5215	.5213
2.499	.4833	.4832	.4866	.4056	.4065	.4066	.4605	.4547	.4471
3.007	.4829	.4840	.4865	.2901	.2931	.3065	.3415	.3404	.3801
3.495	.4824	.4838	.4862	.2751	.2771	.2810	.2369	.2361	.2386
4.030	.4822	.4838	.4854	.2749	.2770	.2806	.1815	.1799	.1847
4.994	.4827	.4843	.4857	.2752	.2774	.2804	.1360	.1337	.1390
5.996	.4836	.4845	.4857	.2754	.2776	.2799	.1361	.1339	.1385
7.002	.4846	.4847	.4860	.2756	.2779	.2799	.1364	.1342	.1387
7.996	.4854	.4850	.4863	.2759	.2782	.2800	.1367	.1345	.1389
8.690	.4855	.4850	.4864	.2751	.2784	.2800	.1369	.1347	.1390

Lower-flap pressures, $p/p_{t,j}$

NPR	z/w = 0.0								
	$x''/l_{l,nom}$								
	0	.294	.441	.588	.735	.809	.853	.897	.941
2.000	.8898	.9311	.9015	.8407	.6575	.5402	.4816	.4090	.3388
2.499	.8757	.9307	.9014	.8408	.6568	.5378	.4803	.4078	.3377
3.007	.8675	.9313	.9022	.8398	.6573	.5367	.4801	.4076	.3376
3.495	.8619	.9304	.9014	.8388	.6565	.5355	.4796	.4069	.3373
4.030	.8571	.9302	.9010	.8379	.6560	.5343	.4790	.4065	.3365
4.994	.8521	.9305	.9009	.8377	.6561	.5334	.4792	.4065	.3363
5.996	.8484	.9302	.9002	.8377	.6557	.5327	.4793	.4065	.3359
7.002	.8463	.9301	.9002	.8379	.6557	.5319	.4796	.4067	.3359
7.996	.8446	.9298	.8998	.8379	.6554	.5312	.4797	.4069	.3358
8.690	.8434	.9295	.8994	.8377	.6550	.5308	.4796	.4070	.3356

TABLE VIII. Continued

(m) Configuration 13

Ramp pressures, $p/p_{t,j}$

NPR	z/w = 0.0								
	$x'/l_{r,nom}$								
	-.207	-.063	.080	.152	.225	.373	.520	.669	.819
2.001	.7257	.7966	.7498	.6877	.6262	.5013	.5531	.5328	.5158
2.505	.7239	.7946	.7471	.6830	.6163	.4002	.4180	.4039	.4629
3.016	.7240	.7943	.7466	.6823	.6160	.3324	.3340	.2977	.2998
3.517	.7236	.7942	.7461	.6820	.6160	.2850	.3302	.2387	.2296
4.010	.7236	.7944	.7461	.6823	.6161	.2500	.3305	.2105	.1864
5.002	.7226	.7935	.7458	.6817	.6163	.2006	.3308	.2094	.1451
6.012	.7220	.7929	.7463	.6815	.6165	.1667	.3314	.2096	.1453
6.864	.7214	.7928	.7472	.6817	.6170	.1458	.3322	.2099	.1469

NPR	$x'/l_{r,nom}$ = .225			$x'/l_{r,nom}$ = .520			$x'/l_{r,nom}$ = .819		
	z/w			z/w			z/w		
	0	.450	.875	0	.450	.875	0	.450	.875
2.001	.6262	.6131	.6093	.5531	.5410	.5400	.5158	.5130	.5098
2.505	.6163	.6010	.5967	.4180	.4098	.4078	.4629	.4510	.4440
3.016	.6160	.5992	.5956	.3340	.3243	.3254	.2998	.3009	.3004
3.517	.6160	.5980	.5948	.3302	.3211	.3188	.2296	.2307	.2294
4.010	.6161	.5974	.5945	.3305	.3216	.3185	.1864	.1886	.1881
5.002	.6163	.5963	.5941	.3308	.3216	.3175	.1451	.1459	.1462
6.012	.6165	.5956	.5944	.3314	.3220	.3172	.1453	.1462	.1459
6.864	.6170	.5956	.5952	.3322	.3226	.3174	.1469	.1468	.1461

Lower-flap pressures, $p/p_{t,j}$

NPR	z/w = 0.0								
	$x''/l_{l,nom}$								
	0	.293	.493	.585	.730	.803	.847	.891	.935
2.001	.8827	.9310	.9074	.8625	.7216	.6512	.5977	.5429	.4964
2.505	.8687	.9314	.9086	.8628	.7197	.6485	.5943	.5390	.4926
3.016	.8598	.9315	.9080	.8621	.7200	.6476	.5937	.5383	.4924
3.517	.8539	.9313	.9081	.8618	.7192	.6472	.5935	.5378	.4921
4.010	.8497	.9320	.9084	.8614	.7190	.6469	.5934	.5378	.4922
5.002	.8439	.9314	.9079	.8612	.7181	.6463	.5929	.5374	.4918
6.012	.8402	.9311	.9073	.8608	.7179	.6454	.5926	.5372	.4915
6.864	.8382	.9313	.9072	.8613	.7177	.6452	.5926	.5374	.4916

TABLE VIII. Continued

(n) Configuration 14

Ramp pressures, $p/p_{t,j}$

NPR	z/w = 0.0								
	$x'/l_{r,nom}$								
	.009	.085	.161	.239	.316	.392	.551	.713	.874
2.012	.8982	.8451	.7947	.7288	.6587	.6122	.5441	.5402	.4906
2.518	.8948	.8403	.7873	.7150	.6316	.5592	.4579	.4064	.3842
3.031	.8946	.8404	.7871	.7154	.6302	.5550	.3933	.3292	.2838
3.535	.8949	.8409	.7874	.7155	.6299	.5553	.3831	.2811	.2292
4.018	.8949	.8406	.7873	.7154	.6298	.5550	.3832	.2453	.1932
5.034	.8961	.8409	.7875	.7157	.6302	.5548	.3835	.2401	.1519
5.699	.8967	.8407	.7872	.7150	.6303	.5544	.3838	.2404	.1453

NPR	$x'/l_{r,nom}$ = .392			$x'/l_{r,nom}$ = .713			$x'/l_{r,nom}$ = .874		
	z/w			z/w			z/w		
	0	.450	.875	0	.450	.875	0	.450	.875
2.012	.6122	.6205	.6179	.5402	.5386	.5382	.4906	.4974	.4888
2.518	.5592	.5712	.5695	.4064	.3948	.4031	.3842	.3861	.3955
3.031	.5550	.5683	.5661	.3292	.3234	.3280	.2838	.2786	.2969
3.535	.5553	.5686	.5663	.2811	.2743	.2818	.2292	.2327	.2194
4.018	.5550	.5688	.5663	.2453	.2406	.2448	.1932	.1988	.1867
5.034	.5548	.5693	.5667	.2401	.2343	.2374	.1519	.1537	.1486
5.699	.5544	.5696	.5669	.2404	.2326	.2374	.1453	.1449	.1411

Lower-flap pressures, $p/p_{t,j}$

NPR	z/w = 0.0								
	$x''/l_{l,nom}$								
	0	.293	.438	.582	.723	.797	.841	.885	.930
2.012	.8823	.9378	.9191	.8835	.8006	.7371	.6874	.6358	.5593
2.518	.8679	.9369	.9189	.8864	.7966	.7305	.6794	.6262	.5480
3.031	.8601	.9370	.9190	.8853	.7963	.7298	.6788	.6254	.5469
3.535	.8543	.9370	.9192	.8855	.7960	.7297	.6789	.6254	.5470
4.018	.8499	.9366	.9188	.8851	.7956	.7293	.6785	.6251	.5465
5.034	.8448	.9369	.9189	.8859	.7958	.7292	.6784	.6252	.5462
5.699	.8421	.9368	.9184	.8857	.7954	.7287	.6781	.6250	.5456

TABLE VIII. Continued

(o) Configuration 15

Ramp pressures, $p/p_{t,j}$

NPR	z/w = 0.0								
	$x'/l_{r,nom}$								
	.009	.085	.161	.239	.316	.392	.551	.713	.874
2.012	.8980	.8457	.7949	.7292	.6587	.6126	.5437	.5409	.4892
2.523	.8951	.8410	.7875	.7163	.6315	.5589	.4567	.4058	.3806
3.027	.8950	.8412	.7875	.7159	.6305	.5554	.3933	.3298	.2834
3.503	.8951	.8414	.7875	.7157	.6302	.5554	.3826	.2815	.2283
4.020	.8954	.8416	.7875	.7157	.6301	.5553	.3826	.2453	.1922
5.013	.8962	.8417	.7875	.7159	.6303	.5549	.3828	.2402	.1509
5.689	.8971	.8418	.7876	.7164	.6307	.5548	.3831	.2406	.1446

NPR	$x'/l_{r,nom}$ = .392			$x'/l_{r,nom}$ = .713			$x'/l_{r,nom}$ = .874		
	z/w			z/w			z/w		
	0	.450	.875	0	.450	.875	0	.450	.875
2.012	.6126	.6204	.6184	.5439	.5418	.5413	.4892	.4946	.4893
2.523	.5589	.5716	.5703	.4058	.3991	.4041	.3806	.3832	.3874
3.027	.5554	.5685	.5670	.3298	.3323	.3305	.2834	.2837	.2838
3.503	.5554	.5685	.5670	.2815	.2831	.2824	.2283	.2323	.2313
4.020	.5553	.5689	.5671	.2453	.2418	.2447	.1922	.1986	.1960
5.013	.5549	.5693	.5673	.2402	.2365	.2369	.1509	.1528	.1527
5.689	.5548	.5699	.5677	.2406	.2366	.2371	.1446	.1458	.1454

Lower-flap pressures, $p/p_{t,j}$

NPR	z/w = 0.0								
	$x''/l_{l,nom}$								
	0	.293	.438	.582	.723	.797	.841	.885	.930
2.012	.8821	.9367	.9205	.8885	.8014	.7368	.6876	.6355	.5592
2.523	.8679	.9369	.9191	.8857	.7969	.7300	.6798	.6259	.5480
3.027	.8597	.9368	.9194	.8857	.7966	.7299	.6794	.6253	.5475
3.503	.8540	.9372	.9193	.8857	.7968	.7296	.6793	.6252	.5470
4.020	.8499	.9367	.9194	.8856	.7964	.7293	.6791	.6251	.5468
5.013	.8445	.9370	.9190	.8859	.7963	.7291	.6789	.6252	.5462
5.689	.8420	.9369	.9187	.8861	.7961	.7291	.6790	.6253	.5463

TABLE VIII. Continued

(p) Configuration 16

Ramp pressures, $p/p_{t,j}$

NPR	z/w = 0.0											
	$x'/l_{r,nom}$											
	-.351	-.207	-.135	-.063	.009	.081	.152	.224	.368	.512	.656	.800
2.016	.8513	.6332	.5518	.5144	.4904	.4626	.4955	.5588	.5358	.5477	.5354	.5142
2.513	.8500	.6320	.5507	.5128	.4895	.4616	.4759	.4872	.4169	.4168	.4472	.4647
2.984	.8503	.6318	.5505	.5124	.4892	.4611	.4739	.4860	.3709	.3292	.3173	.3140
3.490	.8509	.6318	.5499	.5118	.4887	.4605	.4718	.4849	.3708	.2566	.2627	.2404
3.988	.8519	.6309	.5495	.5119	.4887	.4606	.4709	.4834	.3715	.2565	.1943	.2094
4.997	.8516	.6303	.5483	.5113	.4884	.4602	.4689	.4822	.3720	.2567	.1771	.1284
6.005	.8505	.6296	.5468	.5106	.4881	.4599	.4674	.4816	.3720	.2568	.1771	.1274
7.004	.8504	.6287	.5460	.5108	.4885	.4601	.4666	.4815	.3726	.2571	.1774	.1278
8.008	.8498	.6281	.5448	.5107	.4885	.4601	.4658	.4814	.3728	.2575	.1776	.1281
8.981	.8494	.6273	.5438	.5109	.4885	.4603	.4651	.4808	.3734	.2578	.1780	.1284
10.002	.8489	.6267	.5429	.5111	.4887	.4604	.4650	.4796	.3739	.2581	.1783	.1287

NPR	$x'/l_{r,nom}$ = .224			$x'/l_{r,nom}$ = .512			$x'/l_{r,nom}$ = .800		
	z/w			z/w			z/w		
	0	.450	.875	0	.450	.875	0	.450	.875
2.016	.5588	.5543	.5425	.5477	.5507	.5308	.5142	.5117	.5097
2.513	.4872	.4851	.4883	.4168	.4158	.4259	.4647	.4288	.4101
2.984	.4860	.4845	.4868	.3292	.3304	.3574	.3140	.3695	.3596
3.490	.4849	.4839	.4859	.2566	.2558	.2505	.2404	.2524	.3049
3.988	.4834	.4843	.4849	.2565	.2562	.2035	.2094	.1715	.2666
4.997	.4822	.4832	.4835	.2557	.2569	.1652	.1284	.1115	.1919
6.005	.4816	.4820	.4824	.2568	.2573	.1537	.1274	.1109	.1387
7.004	.4815	.4812	.4812	.2571	.2579	.1518	.1278	.1111	.1115
8.008	.4814	.4803	.4809	.2575	.2584	.1515	.1281	.1114	.1023
8.981	.4808	.4798	.4804	.2578	.2590	.1515	.1284	.1117	.0870
10.002	.4796	.4789	.4800	.2581	.2595	.1515	.1287	.1119	.0591

Lower-flap pressures, $p/p_{t,j}$

NPR	z/w = 0.0								
	$x''/l_{l,nom}$								
	0	.294	.441	.588	.735	.809	.853	.897	.941
2.016	.8855	.9304	.6939	.8248	.5951	.4928	.4838	.4704	.4607
2.513	.8716	.9291	.8930	.8229	.5932	.4908	.4815	.4681	.4593
2.984	.8628	.9288	.8933	.8227	.5932	.4901	.4802	.4667	.4587
3.490	.8562	.9285	.8933	.8218	.5921	.4893	.4788	.4655	.4577
3.988	.8520	.9268	.8935	.8216	.5920	.4893	.4781	.4650	.4577
4.997	.8456	.9285	.8928	.8211	.5913	.4898	.4766	.4639	.4567
6.005	.8412	.9276	.8920	.8202	.5901	.4882	.4753	.4630	.4556
7.004	.8388	.9274	.8920	.8202	.5897	.4881	.4746	.4625	.4550
8.008	.8364	.9268	.8913	.8202	.5889	.4879	.4739	.4620	.4544
8.981	.8351	.9264	.8910	.8200	.5885	.4876	.4733	.4616	.4535
10.002	.8337	.9257	.8906	.8200	.5878	.4874	.4728	.4611	.4528

TABLE VIII. Continued

(q) Configuration 17

Ramp pressures, $p/p_{t,j}$

NPR	z/w = 0.0											
	$x'/l_{r,nom}$											
	-.351	-.207	-.135	-.063	.005	.080	.155	.230	.379	.528	.675	.823
2.018	.8611	.6324	.5600	.4852	.3256	.2931	.2970	.4625	.5709	.5665	.5354	.5149
2.496	.8603	.6312	.5599	.4839	.3253	.2919	.2947	.2909	.4571	.5265	.4432	.4418
3.005	.8601	.6303	.5589	.4832	.3249	.2909	.2933	.2891	.2833	.4057	.4903	.4167
3.518	.8596	.6298	.5585	.4826	.3246	.2901	.2922	.2878	.2833	.2242	.3315	.4037
4.011	.8595	.6286	.5581	.4823	.3242	.2898	.2916	.2867	.2834	.2245	.1603	.2877
5.000	.8589	.6274	.5573	.4818	.3238	.2889	.2908	.2854	.2834	.2249	.1601	.1191
5.995	.8583	.6264	.5561	.4815	.3236	.2884	.2902	.2846	.2835	.2253	.1600	.1196
6.994	.8581	.6257	.5554	.4816	.3234	.2879	.2899	.2840	.2835	.2257	.1601	.1200
7.991	.8575	.6249	.5546	.4817	.3233	.2875	.2897	.2837	.2835	.2260	.1602	.1204
8.981	.8572	.6238	.5538	.4818	.3232	.2872	.2895	.2833	.2835	.2264	.1601	.1211
9.921	.8569	.6232	.5533	.4821	.3232	.2869	.2895	.2831	.2834	.2268	.1604	.1214
10.013	.8565	.6231	.5531	.4820	.3231	.2869	.2894	.2830	.2832	.2267	.1604	.1214

NPR	$x'/l_{r,nom}$ = .230			$x'/l_{r,nom}$ = .528			$x'/l_{r,nom}$ = .823		
	z/w			z/w			z/w		
	0	.450	.875	0	.450	.875	0	.450	.875
2.018	.4625	.4691	.4643	.5655	.5571	.5281	.5149	.5128	.5010
2.496	.2909	.3018	.3050	.5255	.5136	.4367	.4418	.4292	.4085
3.005	.2891	.3011	.3044	.4057	.4153	.3672	.4167	.4090	.3575
3.518	.2878	.3009	.3039	.2242	.2216	.2824	.4037	.3835	.3100
4.011	.2867	.3009	.3036	.2245	.2217	.2389	.2877	.3268	.2709
5.000	.2854	.3009	.3027	.2249	.2221	.1852	.1191	.1011	.1904
5.995	.2846	.3006	.3019	.2253	.2224	.1561	.1196	.1009	.1458
6.994	.2840	.3005	.3014	.2257	.2228	.1370	.1200	.1013	.1192
7.991	.2837	.3002	.3008	.2260	.2230	.1272	.1204	.1016	.0975
8.981	.2833	.3001	.3004	.2264	.2233	.1247	.1211	.1020	.0760
9.921	.2831	.3001	.3002	.2268	.2236	.1245	.1214	.1023	.0574
10.013	.2830	.3000	.3001	.2267	.2242	.1245	.1214	.1023	.0565

Lower-flap pressures, $p/p_{t,j}$

NPR	z/w = 0.0								
	$x''/l_{l,nom}$								
	0	.294	.441	.588	.735	.809	.853	.897	.941
2.018	.8862	.9268	.8934	.8250	.5946	.5037	.4763	.4575	.4359
2.496	.8741	.9269	.8936	.8238	.5937	.5024	.4751	.4560	.4372
3.005	.8651	.9268	.8936	.8233	.5933	.5015	.4743	.4550	.4380
3.518	.8590	.9266	.8934	.8226	.5925	.5009	.4736	.4543	.4384
4.011	.8550	.9268	.8935	.8221	.5922	.5008	.4736	.4541	.4386
5.000	.8498	.9270	.8929	.8214	.5920	.5006	.4733	.4540	.4389
5.995	.8467	.9267	.8924	.8212	.5912	.5006	.4732	.4539	.4390
6.994	.8446	.9268	.8921	.8213	.5907	.5006	.4732	.4538	.4392
7.991	.8428	.9263	.8918	.8212	.5902	.5006	.4730	.4537	.4391
8.981	.8416	.9261	.8915	.8212	.5895	.5007	.4729	.4537	.4390
9.921	.8409	.9262	.8913	.8215	.5891	.5009	.4728	.4537	.4389
10.013	.8407	.9261	.8910	.8214	.5889	.5008	.4727	.4535	.4387

TABLE VIII. Continued

(r) Configuration 18

Ramp pressures, $p/p_{t,j}$

NPR	z/w = 0.0											
	$x'/l_{r,nom}$											
	-.351	-.207	-.135	-.063	.010	.090	.171	.252	.412	.571	.727	.882
1.999	.8492	.6437	.5648	.4664	.2746	.3903	.3938	.3984	.4265	.4665	.4996	.5144
2.515	.8493	.6431	.5645	.4647	.2286	.1836	.3190	.3269	.3657	.3896	.3972	.4339
3.506	.8490	.6425	.5638	.4631	.2279	.1829	.1803	.1822	.1805	.3140	.2848	.3730
3.006	.8492	.6424	.5640	.4634	.2283	.1834	.1813	.1835	.3164	.3479	.3322	.3613
3.495	.8489	.6424	.5639	.4630	.2281	.1829	.1805	.1824	.1805	.3153	.2855	.3733
4.011	.8483	.6421	.5633	.4625	.2275	.1824	.1795	.1813	.1802	.1686	.2487	.3128
5.015	.8476	.6414	.5634	.4620	.2268	.1818	.1785	.1798	.1799	.1686	.1989	.0944
5.997	.8471	.6414	.5628	.4617	.2263	.1813	.1779	.1788	.1798	.1686	.1663	.0946
7.146	.8462	.6399	.5609	.4596	.2231	.1778	.1742	.1750	.1766	.1656	.1396	.0915
8.011	.8466	.6407	.5622	.4617	.2257	.1806	.1770	.1775	.1795	.1686	.1247	.0952
9.031	.8461	.6404	.5617	.4617	.2253	.1803	.1766	.1770	.1793	.1686	.1105	.0953
10.022	.8458	.6401	.5614	.4620	.2252	.1801	.1763	.1766	.1793	.1687	.0995	.0955

NPR	$x'/l_{r,nom}$ = .252			$x'/l_{r,nom}$ = .571			$x'/l_{r,nom}$ = .882		
	z/w			z/w			z/w		
	0	.450	.875	0	.450	.875	0	.450	.875
1.999	.3984	.4016	.3929	.4655	.4613	.5014	.5144	.5217	.5050
2.515	.3269	.3016	.3721	.3896	.4547	.4000	.4339	.4106	.3981
3.506	.1822	.1863	.1925	.3140	.3137	.2937	.3730	.3788	.2909
3.036	.1835	.1868	.2567	.3479	.3837	.3476	.3613	.3354	.3358
3.495	.1824	.1863	.1927	.3153	.3146	.2946	.3733	.3771	.2918
4.011	.1813	.1856	.1900	.1686	.1817	.2577	.3128	.3584	.2558
5.015	.1798	.1856	.1897	.1686	.1697	.2072	.0944	.1412	.2044
5.997	.1788	.1852	.1894	.1686	.1697	.1746	.0946	.0979	.1672
7.146	.1750	.1819	.1860	.1656	.1668	.1481	.0915	.0835	.1355
8.011	.1775	.1847	.1886	.1686	.1701	.1340	.0952	.0845	.1152
9.031	.1770	.1844	.1882	.1686	.1702	.1200	.0953	.0844	.0984
10.022	.1766	.1840	.1878	.1687	.1703	.1091	.0955	.0846	.0835

Lower-flap pressures, $p/p_{t,j}$

NPR	z/w = 0.0								
	$x''/l_{l,nom}$								
	0	.294	.441	.588	.735	.809	.853	.897	.941
1.999	.8884	.9274	.8940	.8256	.5930	.4931	.4721	.4452	.4154
2.515	.8749	.9276	.8938	.8245	.5916	.4910	.4703	.4442	.4144
3.506	.8613	.9274	.8934	.8229	.5901	.4893	.4682	.4431	.4135
3.006	.8672	.9280	.8944	.8233	.5909	.4903	.4691	.4438	.4140
3.495	.8610	.9274	.8935	.8226	.5896	.4894	.4682	.4432	.4133
4.011	.8565	.9274	.8935	.8220	.5892	.4889	.4675	.4426	.4129
5.015	.8514	.9275	.8927	.8216	.5887	.4885	.4668	.4424	.4128
5.997	.8482	.9276	.8921	.8213	.5881	.4883	.4665	.4422	.4127
7.146	.8453	.9274	.8914	.8207	.5861	.4862	.4641	.4400	.4106
8.011	.8442	.9272	.8917	.8215	.5873	.4890	.4657	.4420	.4127
9.031	.8428	.9270	.8912	.8213	.5866	.4878	.4654	.4419	.4126
10.022	.8416	.9265	.8909	.8213	.5860	.4877	.4650	.4416	.4127

TABLE VIII. Continued

(s) Configuration 19

Ramp pressures, $p/p_{t,j}$

NPR	z/w = 0.0											
	$x'/l_{r,nom}$											
	-.351	-.207	-.135	-.063	.009	.081	.152	.224	.368	.512	.656	.800
2.021	.8642	.6631	.6034	.6524	.5195	.5049	.4476	.3828	.5440	.5162	.5025	.4969
2.523	.8639	.6622	.6031	.6508	.5189	.5038	.4460	.3812	.2684	.3744	.5018	.4292
2.995	.8637	.6620	.6023	.6501	.5184	.5032	.4452	.3806	.2685	.1932	.2477	.4219
3.512	.8642	.6618	.6025	.6497	.5182	.5029	.4446	.3799	.2685	.1933	.1480	.1795
4.011	.8638	.6617	.6020	.6493	.5182	.5029	.4443	.3797	.2685	.1934	.1416	.1259
5.002	.8635	.6611	.6016	.6488	.5185	.5027	.4442	.3796	.2683	.1934	.1412	.1009
5.989	.8629	.6607	.6006	.6488	.5188	.5027	.4441	.3797	.2682	.1936	.1410	.1014
6.994	.8628	.6602	.6001	.6492	.5191	.5028	.4444	.3801	.2682	.1936	.1409	.1016
7.996	.8626	.6600	.5999	.6498	.5194	.5031	.4446	.3806	.2683	.1937	.1411	.1019
8.982	.8620	.6592	.5991	.6502	.5193	.5030	.4448	.3810	.2683	.1938	.1410	.1021
10.012	.8616	.6589	.5986	.6506	.5193	.5032	.4454	.3815	.2684	.1940	.1410	.1025

NPR	$x'/l_{r,nom}$ = .224			$x'/l_{r,nom}$ = .512			$x'/l_{r,nom}$ = .800		
	z/w			z/w			z/w		
	0	.450	.875	0	.450	.875	0	.450	.875
2.021	.3828	.3799	.3756	.5162	.5106	.5038	.4969	.4955	.4958
2.523	.3812	.3793	.3754	.3744	.4026	.4016	.4292	.4190	.4017
2.995	.3806	.3794	.3752	.1932	.1916	.3279	.4219	.3895	.3377
3.512	.3799	.3796	.3756	.1933	.1918	.2558	.1795	.2542	.2861
4.011	.3797	.3798	.3757	.1934	.1918	.2127	.1259	.1460	.2479
5.002	.3796	.3798	.3743	.1934	.1915	.1537	.1009	.0934	.1754
5.989	.3797	.3798	.3741	.1936	.1918	.1296	.1014	.0937	.1374
6.994	.3801	.3797	.3750	.1936	.1924	.1201	.1016	.0939	.1158
7.996	.3806	.3797	.3759	.1937	.1924	.1179	.1019	.0942	.0978
8.982	.3810	.3798	.3754	.1938	.1925	.1173	.1021	.0945	.0875
10.012	.3815	.3798	.3765	.1940	.1925	.1172	.1025	.0947	.0823

Lower-flap pressures, $p/p_{t,j}$

NPR	z/w = 0.0								
	$x''/l_{l,nom}$								
	0	.294	.441	.588	.735	.809	.853	.897	.941
2.021	.8874	.9301	.8997	.8352	.6464	.5160	.4518	.3674	.4306
2.523	.8746	.9292	.8997	.8359	.6455	.5135	.4507	.3662	.2791
2.995	.8664	.9294	.8995	.8352	.6452	.5121	.4504	.3654	.2791
3.512	.8607	.9291	.8999	.8346	.6448	.5109	.4499	.3653	.2791
4.011	.8565	.9292	.8999	.8347	.6449	.5102	.4498	.3650	.2789
5.002	.8509	.9291	.8989	.8340	.6445	.5090	.4496	.3642	.2786
5.989	.8475	.9287	.8986	.8339	.6442	.5080	.4497	.3646	.2783
6.994	.8451	.9285	.8982	.8340	.6441	.5074	.4498	.3648	.2785
7.996	.8435	.9283	.8977	.8344	.6440	.5069	.4501	.3654	.2786
8.982	.8420	.9280	.8972	.8342	.6437	.5062	.4499	.3648	.2786
10.012	.8411	.9276	.8966	.8343	.6434	.5059	.4501	.3649	.2786

TABLE VIII. Continued

(t) Configuration 20

Ramp pressures, $p/p_{t,j}$

NPR	z/w = 0.0								
	$x'/l_{r,nom}$								
	.009	.087	.168	.246	.324	.405	.560	.720	.878
2.006	.9015	.8363	.7594	.6670	.5696	.5350	.4925	.5020	.5066
2.520	.8995	.8359	.7589	.6651	.5682	.4706	.3018	.3367	.4958
3.023	.8992	.8360	.7589	.6648	.5678	.4708	.3019	.2604	.2353
3.546	.8994	.8364	.7592	.6647	.5679	.4714	.3020	.1980	.1795
4.055	.8994	.8365	.7592	.6648	.5679	.4716	.3019	.1980	.1502
5.097	.9008	.8369	.7597	.6653	.5690	.4722	.3019	.1982	.1310
5.039	.9006	.8369	.7597	.6654	.5690	.4724	.3020	.1983	.1311
6.037	.9025	.8371	.7602	.6660	.5700	.4727	.3021	.1984	.1314
6.306	.9030	.8372	.7604	.6663	.5703	.4729	.3023	.1985	.1315

NPR	$x'/l_{r,nom}$ = .405			$x'/l_{r,nom}$ = .720			$x'/l_{r,nom}$ = .878		
	z/w			z/w			z/w		
	0	.450	.875	0	.450	.875	0	.450	.875
2.006	.5350	.5353	.5131	.5020	.5042	.5032	.5066	.5052	.5023
2.520	.4706	.4683	.4049	.3367	.3491	.3944	.4958	.4670	.4070
3.023	.4708	.4681	.4643	.2604	.2413	.3198	.2353	.2729	.3280
3.546	.4714	.4679	.4646	.1990	.1866	.2315	.1795	.1456	.2650
4.055	.4716	.4677	.4646	.1980	.1862	.1987	.1502	.1243	.2180
5.097	.4722	.4678	.4653	.1982	.1863	.1422	.1310	.1103	.1576
5.039	.4724	.4679	.4654	.1983	.1862	.1454	.1311	.1104	.1593
6.037	.4727	.4683	.4660	.1984	.1862	.0949	.1314	.1108	.1299
6.306	.4729	.4683	.4662	.1985	.1862	.0934	.1315	.1109	.1258

Lower-flap pressures, $p/p_{t,j}$

NPR	z/w = 0.0								
	$x''/l_{l,nom}$								
	0	.293	.438	.582	.725	.797	.856	.901	.946
2.006	.8803	.9339	.9163	.8819	.7825	.6939	.5426	.4188	.4133
2.520	.8659	.9336	.9174	.8831	.7816	.6932	.5410	.4180	.3028
3.023	.8579	.9339	.9176	.8818	.7812	.6927	.5404	.4180	.3026
3.546	.8516	.9346	.9177	.8819	.7809	.6927	.5400	.4185	.3025
4.055	.8472	.9340	.9171	.8810	.7811	.6924	.5395	.4187	.3018
5.097	.8417	.9339	.9171	.8818	.7808	.6926	.5394	.4191	.3014
5.039	.8419	.9338	.9171	.8818	.7808	.6926	.5395	.4191	.3015
6.037	.8387	.9341	.9169	.8820	.7805	.6926	.5393	.4190	.3011
6.306	.8381	.9341	.9168	.8824	.7808	.6928	.5392	.4189	.3010

TABLE VIII. Continued

(u) Configuration 21

Ramp pressures, $p/p_{t,j}$

NPR	z/w = 0.0								
	$x'/l_{r,nom}$								
	.009	.087	.168	.246	.324	.405	.560	.720	.878
2.014	.9184	.8675	.8076	.7351	.6594	.5852	.4935	.5150	.5051
2.525	.9159	.8650	.8032	.7260	.6402	.5429	.3987	.3302	.3344
3.031	.9154	.8651	.8033	.7255	.6400	.5403	.3419	.2647	.2259
3.533	.9152	.8651	.8035	.7255	.6402	.5406	.3259	.2246	.1788
4.048	.9158	.8655	.8038	.7259	.6410	.5412	.3261	.1947	.1504
5.030	.9166	.8656	.8040	.7262	.6422	.5415	.3263	.1877	.1188
6.066	.9185	.8658	.8044	.7271	.6436	.5421	.3269	.1880	.1138
6.697	.9195	.8659	.8046	.7278	.6440	.5422	.3273	.1882	.1140

NPR	$x'/l_{r,nom}$ = .405			$x'/l_{r,nom}$ = .720			$x'/l_{r,nom}$ = .878		
	z/w			z/w			z/w		
	0	.450	.875	0	.450	.875	0	.450	.875
2.014	.5852	.5831	.5456	.5150	.5140	.5047	.5051	.5053	.5025
2.525	.5429	.5418	.5042	.3302	.3313	.3888	.3344	.4184	.4053
3.031	.5403	.5393	.5036	.2647	.2388	.3108	.2259	.2547	.3229
3.533	.5406	.5390	.5035	.2246	.2065	.2570	.1786	.1465	.2640
4.048	.5412	.5394	.5040	.1947	.1791	.1850	.1504	.1267	.2185
5.030	.5415	.5397	.5044	.1877	.1738	.1150	.1188	.1001	.1482
6.066	.5421	.5403	.5051	.1880	.1740	.0936	.1138	.0971	.1309
6.697	.5422	.5407	.5053	.1882	.1741	.0933	.1140	.0973	.1235

Lower-flap pressures, $p/p_{t,j}$

NPR	z/w = 0.0								
	$x''/l_{l,nom}$								
	0	.293	.438	.582	.725	.797	.841	.885	.930
2.014	.8892	.9468	.9280	.9013	.8228	.7758	.7171	.6621	.6405
2.525	.8752	.9460	.9277	.8998	.8207	.7745	.7118	.6554	.6348
3.031	.8664	.9463	.9286	.8993	.8207	.7753	.7113	.6550	.6351
3.533	.8605	.9458	.9287	.8991	.8204	.7756	.7111	.6546	.6349
4.048	.8565	.9467	.9289	.8993	.8206	.7759	.7111	.6548	.6354
5.030	.8515	.9464	.9285	.8989	.8201	.7755	.7108	.6548	.6357
6.066	.8480	.9465	.9283	.8995	.8198	.7754	.7107	.6548	.6360
6.697	.8467	.9463	.9282	.8998	.8196	.7752	.7105	.6548	.6363

TABLE VIII. Continued

(v) Configuration 22

Ramp pressures, $p/p_{t,j}$

NPR	z/w = 0.0								
	$x'/l_{r,nom}$								
	.009	.087	.168	.246	.324	.405	.560	.720	.878
2.017	.9393	.9012	.8559	.7933	.7166	.6283	.4995	.5170	.5076
2.522	.9352	.8967	.8481	.7797	.6924	.5857	.4015	.3285	.4360
3.023	.9341	.8956	.8462	.7750	.6832	.5681	.3605	.2569	.2261
3.529	.9336	.8951	.8455	.7736	.6793	.5550	.3384	.2263	.1721
4.043	.9338	.8954	.8457	.7737	.6797	.5532	.3185	.2072	.1480
5.052	.9350	.8957	.8462	.7744	.6813	.5538	.2974	.1834	.1249
6.045	.9365	.8959	.8465	.7754	.6825	.5544	.2972	.1675	.1127
7.083	.9380	.8962	.8469	.7759	.6827	.5547	.2977	.1627	.1043
7.302	.9385	.8964	.8471	.7774	.6828	.5550	.2980	.1627	.1027

NPR	$x'/l_{r,nom}$ = .405			$x'/l_{r,nom}$ = .720			$x'/l_{r,nom}$ = .878		
	z/w			z/w			z/w		
	0	.450	.875	0	.450	.875	0	.450	.875
2.017	.6283	.6235	.5735	.5170	.5134	.5056	.5076	.5071	.4961
2.522	.5857	.5810	.5266	.3285	.3301	.3935	.4360	.4416	.4067
3.023	.5681	.5635	.5185	.2569	.2310	.3113	.2261	.2685	.3267
3.529	.5550	.5506	.5131	.2263	.2082	.2524	.1721	.1411	.2664
4.043	.5532	.5485	.5129	.2072	.1928	.2056	.1480	.1243	.2183
5.052	.5538	.5491	.5134	.1834	.1714	.1431	.1249	.1068	.1451
6.045	.5544	.5499	.5139	.1675	.1577	.0840	.1127	.0972	.1330
7.083	.5547	.5505	.5142	.1627	.1533	.0826	.1043	.0900	.1279
7.302	.5550	.5508	.5144	.1627	.1533	.0826	.1027	.0888	.1247

Lower-flap pressures, $p/p_{t,j}$

NPR	z/w = 0.0								
	$x''/l_{l,nom}$								
	0	.293	.438	.582	.725	.797	.856	.899	.943
2.017	.8989	.9588	.9491	.9264	.8793	.8348	.8292	.8119	.7609
2.522	.8850	.9574	.9471	.9233	.8725	.8266	.8206	.8028	.7491
3.023	.8768	.9571	.9464	.9217	.8712	.8237	.8181	.8004	.7461
3.529	.8708	.9571	.9464	.9209	.8707	.8224	.8172	.7997	.7452
4.043	.8666	.9568	.9460	.9206	.8705	.8221	.8170	.7998	.7451
5.052	.8613	.9570	.9462	.9207	.8704	.8217	.8169	.8003	.7449
6.045	.8582	.9571	.9454	.9212	.8702	.8211	.8166	.8005	.7446
7.083	.8558	.9567	.9450	.9214	.8697	.8212	.8165	.8006	.7437
7.302	.8555	.9568	.9452	.9216	.8698	.8215	.8165	.8007	.7437

TABLE VIII. Continued

(w) Configuration 23

Ramp pressures, $p/p_{t,j}$

NPR	z/w = 0.0								
	$x'/l_{r,nom}$								
	.009	.080	.151	.225	.303	.381	.540	.705	.871
1.994	.8338	.7936	.7461	.6954	.6517	.6224	.5774	.5509	.5283
2.518	.8300	.7889	.7369	.6758	.6046	.5343	.5168	.4263	.4268
2.983	.8301	.7891	.7373	.6757	.6045	.5347	.3864	.3907	.3183
3.508	.8302	.7896	.7375	.6756	.6046	.5352	.3864	.2756	.2792
3.989	.8301	.7896	.7376	.6757	.6048	.5353	.3864	.2757	.2461
5.015	.8310	.7898	.7381	.6763	.6059	.5356	.3865	.2757	.1926
5.550	.8316	.7901	.7383	.6767	.6065	.5359	.3867	.2758	.1928

NPR	$x'/l_{r,nom}$ = .381			$x'/l_{r,nom}$ = .705			$x'/l_{r,nom}$ = .871		
	z/w			z/w			z/w		
	0	.450	.875	0	.450	.875	0	.450	.875
1.994	.6224	.6184	.5782	.5509	.5487	.5301	.5283	.5258	.5182
2.518	.5343	.5327	.5125	.4263	.4227	.4277	.4268	.4261	.4184
2.983	.5347	.5326	.5097	.3907	.3485	.3649	.3183	.3362	.3566
3.508	.5352	.5324	.5090	.2756	.2559	.2621	.2792	.2264	.2937
3.989	.5353	.5321	.5087	.2757	.2564	.2223	.2461	.2039	.2614
5.015	.5356	.5325	.5086	.2757	.2559	.1617	.1926	.1619	.1600
5.550	.5359	.5328	.5089	.2758	.2557	.1447	.1928	.1622	.1341

Lower-flap pressures, $p/p_{t,j}$

NPR	z/w = 0.0								
	$x''/l_{l,nom}$								
	0	.293	.438	.582	.725	.797	.856	.901	.946
1.994	.8667	.9143	.8900	.8491	.7257	.6329	.4786	.3347	.4527
2.518	.8525	.9141	.8909	.8467	.7213	.6285	.4746	.3280	.3106
2.983	.8457	.9141	.8918	.8458	.7218	.6280	.4738	.3272	.2338
3.508	.8397	.9143	.8914	.8454	.7216	.6231	.4735	.3269	.2337
3.989	.8357	.9142	.8911	.8456	.7208	.6279	.4729	.3265	.2334
5.015	.8298	.9141	.8910	.8450	.7200	.6278	.4725	.3260	.2328
5.550	.8284	.9143	.8911	.8452	.7206	.6279	.4723	.3259	.2326

TABLE VIII. Continued

(x) Configuration 24

Ramp pressures, $p/p_{t,j}$

NPR	z/w = 0.0								
	$x'/l_{r,nom}$								
	.009	.080	.151	.225	.303	.381	.540	.705	.871
2.004	.8581	.8265	.7877	.7442	.6967	.6534	.5811	.5475	.5244
2.518	.8532	.8203	.7791	.7300	.6712	.6113	.4997	.4121	.4225
3.009	.8529	.8205	.7791	.7293	.6692	.6028	.4431	.3679	.2957
3.506	.8529	.8209	.7793	.7295	.6695	.6033	.4296	.3202	.2599
3.994	.8529	.8207	.7795	.7295	.6698	.6033	.4298	.2834	.2287
5.056	.8538	.8212	.7799	.7303	.6713	.6036	.4309	.2785	.1820
5.023	.8538	.8212	.7799	.7303	.6713	.6039	.4311	.2786	.1831
5.794	.8546	.8214	.7801	.7312	.6721	.6040	.4319	.2789	.1759

NPR	$x'/l_{r,nom}$ = .381			$x'/l_{r,nom}$ = .705			$x'/l_{r,nom}$ = .871		
	z/w			z/w			z/w		
	0	.450	.875	0	.450	.875	0	.450	.875
2.004	.6534	.6496	.6030	.5475	.5467	.5299	.5244	.5228	.5173
2.518	.6113	.6084	.5676	.4121	.4175	.4234	.4225	.4273	.4190
3.009	.6028	.6015	.5648	.3679	.3298	.3617	.2957	.3286	.3520
3.506	.6033	.6015	.5644	.3202	.2918	.2487	.2599	.2164	.2974
3.994	.6033	.6014	.5640	.2834	.2595	.2035	.2287	.1924	.2622
5.056	.6036	.6019	.5641	.2785	.2573	.1606	.1820	.1528	.1431
5.023	.6039	.6020	.5643	.2786	.2575	.1616	.1831	.1536	.1451
5.794	.6040	.6022	.5644	.2789	.2572	.1495	.1759	.1506	.1022

Lower-flap pressures, $p/p_{t,j}$

NPR	z/w = 0.0								
	$x''/l_{l,nom}$								
	0	.293	.438	.582	.723	.797	.841	.885	.930
2.004	.8739	.9251	.9025	.8646	.7629	.6951	.6482	.5924	.5472
2.518	.8596	.9240	.9019	.8625	.7570	.6865	.6386	.5803	.5343
3.009	.8524	.9245	.9021	.8615	.7575	.6856	.6378	.5795	.5331
3.506	.8471	.9246	.9020	.8617	.7573	.6853	.6376	.5792	.5325
3.994	.8429	.9245	.9021	.8610	.7565	.6851	.6375	.5790	.5328
5.056	.8368	.9247	.9018	.8619	.7566	.6847	.6373	.5790	.5324
5.023	.8365	.9247	.9019	.8620	.7567	.6847	.6374	.5791	.5324
5.794	.8351	.9245	.9016	.8619	.7564	.6844	.6372	.5789	.5287

TABLE VIII. Continued

(y) Configuration 25

Ramp pressures, $p/p_{t,j}$

NPR	z/w = 0.0								
	$x'/l_{r,nom}$								
	.009	.080	.151	.225	.303	.381	.540	.705	.871
1.991	.8603	.8295	.7910	.7491	.7030	.6614	.5907	.5527	.5261
2.514	.8541	.8215	.7797	.7313	.6732	.6143	.5066	.4337	.4117
3.011	.8536	.8213	.7796	.7301	.6702	.6039	.4455	.3747	.3288
3.512	.8533	.8214	.7797	.7300	.6702	.6042	.4297	.3207	.2742
4.002	.8534	.8215	.7797	.7300	.6706	.6042	.4298	.2838	.2387
4.998	.8542	.8220	.7802	.7308	.6719	.6047	.4308	.2783	.1915
5.038	.8540	.8216	.7798	.7305	.6717	.6044	.4305	.2782	.1894
5.289	.8543	.8218	.7801	.7309	.6721	.6046	.4308	.2783	.1825

NPR	$x'/l_{r,nom}$ = .381			$x'/l_{r,nom}$ = .705			$x'/l_{r,nom}$ = .871		
	z/w			z/w			z/w		
	0	.450	.875	0	.450	.875	0	.450	.875
1.991	.6614	.6639	.6599	.5527	.5521	.5468	.5261	.5227	.5144
2.514	.6143	.6156	.6117	.4337	.4358	.4328	.4117	.4062	.4064
3.011	.6039	.6053	.6013	.3747	.3808	.3787	.3288	.3219	.3214
3.512	.6042	.6048	.6015	.3207	.3284	.3276	.2742	.2742	.2660
4.002	.6042	.6047	.6014	.2838	.2856	.2878	.2387	.2422	.2368
4.998	.6047	.6050	.6017	.2783	.2819	.2827	.1915	.1902	.1903
5.038	.6044	.6048	.6014	.2782	.2817	.2826	.1894	.1882	.1884
5.289	.6046	.6049	.6016	.2783	.2818	.2828	.1825	.1818	.1827

Lower-flap pressures, $p/p_{t,j}$

NPR	z/w = 0.0								
	$x''/l_{l,nom}$								
	0	.293	.438	.582	.723	.797	.841	.885	.930
1.991	.8760	.9265	.9036	.8670	.7648	.7106	.6520	.5970	.5588
2.514	.8605	.9241	.9020	.8626	.7563	.7000	.6388	.5811	.5422
3.011	.8527	.9243	.9021	.8621	.7568	.6995	.6375	.5797	.5407
3.512	.8471	.9246	.9017	.8617	.7566	.6990	.6372	.5791	.5399
4.002	.8428	.9243	.9015	.8607	.7560	.6987	.6368	.5788	.5392
4.998	.8374	.9250	.9017	.8619	.7559	.6984	.6368	.5788	.5389
5.038	.8371	.9247	.9014	.8616	.7560	.6981	.6365	.5786	.5386
5.289	.8373	.9246	.9011	.8618	.7563	.6981	.6364	.5785	.5385

TABLE VIII. Continued

(z) Configuration 26

Ramp pressures, $p/p_{t,j}$

NPR	z/w = 0.0								
	$x'/l_{r,nom}$								
	.009	.080	.151	.225	.303	.381	.540	.705	.871
2.020	.8945	.8714	.8407	.8011	.7563	.6951	.5882	.5435	.5158
2.516	.8880	.8633	.8302	.7854	.7254	.6567	.5098	.4092	.4088
3.036	.8861	.8615	.8270	.7799	.7150	.6388	.4765	.3485	.2793
3.530	.8854	.8610	.8263	.7786	.7110	.6268	.4519	.3267	.2415
4.061	.8855	.8611	.8264	.7782	.7114	.6252	.4266	.3038	.2218
5.048	.8865	.8614	.8269	.7789	.7131	.6256	.4153	.2700	.1953
6.048	.8876	.8619	.8273	.7803	.7140	.6259	.4163	.2496	.1768
6.237	.8878	.8618	.8274	.7806	.7140	.6261	.4165	.2488	.1740

NPR	$x'/l_{r,nom}$ = .381			$x'/l_{r,nom}$ = .705			$x'/l_{r,nom}$ = .871		
	z/w			z/w			z/w		
	0	.450	.875	0	.450	.875	0	.450	.875
2.020	.6951	.6885	.6345	.5435	.5390	.5293	.5158	.5162	.5151
2.516	.6567	.6502	.5984	.4092	.4135	.4309	.4088	.4252	.4296
3.036	.6388	.6334	.5886	.3485	.3163	.3423	.2793	.3100	.3548
3.530	.6268	.6225	.5841	.3257	.2999	.2809	.2415	.2058	.2931
4.061	.6252	.6216	.5836	.3038	.2810	.2101	.2218	.1890	.2449
5.048	.6256	.6223	.5838	.2700	.2519	.1490	.1953	.1675	.1750
6.048	.6259	.6231	.5839	.2496	.2347	.1363	.1768	.1524	.1155
6.237	.6261	.6232	.5839	.2488	.2342	.1360	.1740	.1499	.1044

Lower-flap pressures, $p/p_{t,j}$

NPR	z/w = 0.0								
	$x''/l_{l,nom}$								
	0	.293	.438	.582	.725	.797	.856	.899	.943
2.020	.8871	.9432	.9287	.8987	.8373	.7891	.7912	.7801	.7315
2.516	.8722	.9404	.9259	.8936	.8287	.7767	.7790	.7676	.7168
3.036	.8635	.9405	.9243	.8919	.8258	.7726	.7758	.7644	.7133
3.530	.8576	.9399	.9241	.8911	.8246	.7712	.7747	.7635	.7121
4.061	.8533	.9401	.9239	.8909	.8245	.7707	.7745	.7634	.7121
5.048	.8481	.9402	.9237	.8906	.8242	.7702	.7744	.7637	.7120
6.048	.8447	.9402	.9236	.8908	.8239	.7698	.7742	.7639	.7116
6.237	.8441	.9400	.9233	.8909	.8238	.7699	.7742	.7638	.7116

TABLE VIII. Continued

(aa) Configuration 27

Ramp pressures, $p/p_{t,j}$

NPR	z/w = 0.0												
	$x'/l_{r,nom}$												
	.009	.086	.162	.239	.316	.394	.553	.713	.877	1.042	1.204	1.368	1.532
1.988	.8734	.8138	.7575	.6731	.5981	.5712	.5371	.5333	.5184	.5128	.5114	.5045	.5017
2.490	.8718	.8132	.7558	.6649	.5736	.4902	.3753	.4162	.4994	.4161	.3595	.4021	.4391
3.013	.8729	.8136	.7558	.6653	.5736	.4897	.3445	.3217	.2883	.3419	.4573	.3622	.2874
3.489	.8723	.8139	.7557	.6652	.5733	.4895	.3441	.2365	.2340	.2038	.3201	.4147	.3676
4.008	.8726	.8140	.7557	.6645	.5733	.4893	.3436	.2363	.1955	.1654	.1408	.2641	.3325
5.014	.8706	.8141	.7557	.6644	.5734	.4894	.3436	.2367	.1614	.1231	.1000	.0804	.1637
6.004	.8689	.8143	.7560	.6646	.5738	.4900	.3439	.2373	.1615	.1088	.0807	.1308	.1460
6.676	.8679	.8144	.7557	.6648	.5741	.4903	.3443	.2377	.1616	.1090	.0744	.1161	.1345

NPR	$x'/l_{r,nom}$ = .553			$x'/l_{r,nom}$ = 1.042			$x'/l_{r,nom}$ = 1.532		
	z/w			z/w			z/w		
	0	.450	.875	0	.450	.875	0	.450	.875
1.988	.5371	.5347	.5198	.5128	.5155	.5118	.5017	.5032	.5092
2.490	.3753	.3714	.4368	.4151	.4260	.4067	.4391	.4356	.4134
3.013	.3445	.3462	.3031	.3419	.3653	.3463	.2874	.2966	.3402
3.489	.3441	.3455	.2550	.2038	.2734	.2912	.3676	.3540	.3034
4.008	.3438	.3453	.2208	.1654	.1403	.2436	.3325	.3081	.2628
5.014	.3436	.3448	.2027	.1231	.0964	.1714	.1637	.1895	.1980
6.004	.3439	.3449	.2017	.1088	.0871	.1326	.1460	.1208	.1599
6.676	.3443	.3453	.2016	.1090	.0872	.1183	.1345	.1215	.1411

Lower-flap pressures, $p/p_{t,j}$

NPR	z/w = 0.0								
	$x''/l_{l,nom}$								
	0	.293	.438	.582	.725	.797	.856	.901	.946
1.988	.8761	.9248	.9050	.8693	.7645	.6696	.5159	.3783	.4496
2.490	.8613	.9255	.9077	.8688	.7632	.6683	.5136	.3753	.2753
3.013	.8535	.9253	.9077	.8681	.7637	.6672	.5128	.3744	.2746
3.489	.8491	.9254	.9074	.8675	.7634	.6670	.5124	.3739	.2742
4.008	.8436	.9257	.9076	.8673	.7630	.6668	.5121	.3735	.2740
5.014	.8371	.9255	.9071	.8679	.7632	.6666	.5116	.3730	.2731
6.004	.8350	.9256	.9068	.8681	.7628	.6662	.5111	.3723	.2723
6.676	.8335	.9254	.9068	.8682	.7625	.6658	.5108	.3719	.2718

TABLE VIII. Continued

(bb) Configuration 28

Ramp pressures, $p/p_{t,j}$

NPR	z/w = 0.0								
	$x'/l_{r,nom}$								
	.009	.085	.161	.239	.316	.392	.551	.713	.874
2.015	.8787	.8136	.7456	.6624	.5737	.5594	.5337	.5389	.4916
2.510	.8777	.8130	.7444	.6592	.5584	.4826	.3492	.4165	.5061
2.987	.8773	.8132	.7440	.6587	.5567	.4826	.3478	.3337	.2875
3.519	.8779	.8133	.7441	.6584	.5557	.4824	.3477	.2430	.2289
4.025	.8785	.8139	.7441	.6584	.5552	.4826	.3477	.2432	.1933
4.995	.8793	.8137	.7437	.6583	.5547	.4821	.3474	.2431	.1607
5.977	.8813	.8141	.7440	.6589	.5549	.4818	.3474	.2432	.1608

NPR	$x'/l_{r,nom}$ = .392			$x'/l_{r,nom}$ = .713			$x'/l_{r,nom}$ = .874		
	z/w			z/w			z/w		
	0	.450	.875	0	.450	.875	0	.450	.875
2.015	.5594	.5652	.5284	.5339	.5391	.5240	.4916	.4961	.4967
2.510	.4826	.4973	.4853	.4155	.4190	.4276	.5061	.4708	.4171
2.987	.4826	.4970	.4847	.3337	.3007	.3536	.2875	.3245	.3357
3.519	.4824	.4970	.4845	.2430	.2268	.2526	.2289	.1856	.2748
4.025	.4826	.4972	.4847	.2432	.2269	.2115	.1933	.1621	.2354
4.995	.4821	.4974	.4846	.2431	.2261	.1506	.1607	.1368	.1644
5.977	.4818	.4981	.4849	.2432	.2257	.1194	.1608	.1371	.1300

Lower-flap pressures, $p/p_{t,j}$

NPR	z/w = 0.0								
	$x''/l_{l,nom}$								
	0	.293	.438	.582	.725	.797	.856	.901	.946
2.015	.8736	.9258	.9066	.8687	.7584	.6682	.5148	.3772	.4339
2.510	.8607	.9258	.9071	.8682	.7575	.6667	.5133	.3750	.2746
2.987	.8530	.9261	.9071	.8674	.7568	.6662	.5127	.3741	.2739
3.519	.8467	.9261	.9072	.8670	.7564	.6659	.5120	.3738	.2735
4.025	.8428	.9265	.9070	.8672	.7565	.6661	.5119	.3739	.2732
4.995	.8371	.9261	.9061	.8658	.7563	.6658	.5113	.3736	.2723
5.977	.8336	.9262	.9061	.8672	.7559	.6660	.5111	.3737	.2717

TABLE VIII. Continued

(cc) Configuration 29

Ramp pressures, $p/p_{t,j}$

NPR	z/w = 0.0										
	$x'/l_{r,nom}$										
	.009	.084	.162	.240	.317	.394	.554	.713	.877	1.040	1.204
1.992	.8868	.8205	.7520	.6735	.5928	.5667	.5369	.5370	.5186	.5114	.5026
2.512	.8851	.8197	.7501	.6682	.5852	.5040	.4434	.3997	.4750	.4389	.3602
3.003	.8859	.8197	.7498	.6683	.5849	.5031	.3717	.3173	.2837	.2522	.4605
3.497	.8861	.8198	.7497	.6678	.5848	.5025	.3714	.2660	.2287	.1961	.1641
4.036	.8863	.8201	.7497	.6680	.5848	.5022	.3710	.2483	.1907	.1600	.1324
5.019	.8867	.8196	.7495	.6682	.5851	.5022	.3706	.2486	.1608	.1176	.0934
5.985	.8870	.8194	.7504	.6689	.5856	.5028	.3710	.2489	.1612	.1035	.0884
6.379	.8872	.8195	.7507	.6691	.5860	.5031	.3714	.2490	.1614	.1034	.0731

NPR	$x'/l_{r,nom}$ = .554			$x'/l_{r,nom}$ = .877			$x'/l_{r,nom}$ = 1.204		
	z/w			z/w			z/w		
	0	.450	.875	0	.450	.875	0	.450	.875
1.992	.5369	.5352	.5197	.5196	.5185	.5142	.5026	.5052	.5085
2.512	.4434	.4348	.4350	.4750	.4477	.4219	.3602	.3792	.4176
3.003	.3717	.3684	.3173	.2837	.3182	.3453	.4605	.3865	.3516
3.497	.3714	.3684	.2661	.2287	.1842	.2817	.1641	.2955	.2937
4.036	.3710	.3689	.2292	.1907	.1569	.2390	.1324	.2186	.2486
5.019	.3706	.3692	.2077	.1608	.1362	.1604	.0934	.1664	.1898
5.985	.3710	.3697	.2075	.1612	.1365	.1223	.0884	.1339	.1416
6.379	.3714	.3699	.2074	.1614	.1367	.1035	.0731	.1326	.1260

Lower-flap pressures, $p/p_{t,j}$

NPR	z/w = 0.0								
	$x''/l_{l,nom}$								
	0	.293	.438	.582	.725	.797	.856	.901	.946
1.992	.8738	.9266	.9065	.8715	.7607	.6721	.5239	.4323	.3699
2.512	.8597	.9261	.9079	.8711	.7590	.6707	.5221	.4306	.3695
3.003	.8516	.9259	.9078	.8707	.7593	.6701	.5219	.4304	.3699
3.497	.8457	.9262	.9077	.8705	.7588	.6700	.5216	.4302	.3696
4.036	.8411	.9266	.9077	.8697	.7585	.6701	.5216	.4303	.3694
5.019	.8351	.9259	.9070	.8698	.7578	.6700	.5214	.4299	.3690
5.985	.8322	.9264	.9069	.8703	.7580	.6704	.5216	.4298	.3691
6.379	.8313	.9262	.9066	.8706	.7580	.6705	.5215	.4297	.3689

TABLE VIII. Continued

(dd) Configuration 30

Ramp pressures, $p/p_{t,j}$

NPR	z/w = 0.0								
	$x'/l_{r,nom}$								
	.009	.085	.161	.239	.316	.392	.551	.713	.874
2.033	.8800	.8116	.7476	.6691	.5821	.5603	.5367	.5338	.4966
2.504	.8784	.8110	.7462	.6656	.5721	.4994	.4448	.4023	.4685
2.998	.8785	.8112	.7462	.6651	.5711	.4994	.3774	.3167	.2813
3.521	.8786	.8112	.7461	.6656	.5702	.4991	.3771	.2639	.2217
4.011	.8789	.8114	.7458	.6656	.5698	.4990	.3770	.2495	.1864
4.997	.8801	.8116	.7459	.6657	.5697	.4986	.3768	.2497	.1577
6.014	.8814	.8114	.7458	.6659	.5698	.4980	.3767	.2498	.1578

NPR	$x'/l_{r,nom}$ = .392			$x'/l_{r,nom}$ = .713			$x'/l_{r,nom}$ = .874		
	z/w			z/w			z/w		
	0	.450	.875	0	.450	.875	0	.450	.875
2.033	.5603	.5666	.5323	.5338	.5415	.5265	.4966	.4990	.4974
2.504	.4994	.5156	.4993	.4023	.4180	.4289	.4685	.4481	.4158
2.998	.4994	.5157	.4989	.3157	.2911	.3432	.2813	.3161	.3378
3.521	.4991	.5156	.4987	.2639	.2437	.2458	.2217	.1813	.2736
4.011	.4990	.5155	.4988	.2495	.2349	.2096	.1864	.1555	.2321
4.997	.4986	.5159	.4991	.2497	.2347	.1532	.1577	.1351	.1573
6.014	.4980	.5162	.4993	.2498	.2345	.1270	.1578	.1353	.1170

Lower-flap pressures, $p/p_{t,j}$

NPR	z/w = 0.0								
	$x''/l_{l,nom}$								
	0	.293	.438	.582	.725	.797	.856	.901	.946
2.033	.8747	.9261	.9061	.8710	.7584	.6723	.5238	.4321	.3687
2.504	.8621	.9266	.9070	.8702	.7576	.6710	.5228	.4307	.3684
2.998	.8538	.9269	.9077	.8702	.7572	.6705	.5226	.4306	.3683
3.521	.8476	.9269	.9077	.8698	.7570	.6703	.5222	.4302	.3678
4.011	.8435	.9268	.9073	.8697	.7571	.6701	.5219	.4301	.3673
4.997	.8377	.9271	.9070	.8698	.7564	.6701	.5220	.4298	.3668
6.014	.8340	.9266	.9066	.8698	.7558	.6699	.5218	.4294	.3663

TABLE VIII. Continued

(ee) Configuration 31

Ramp pressures, $p/p_{t,j}$

NPR	z/w = 0.0							
	$x'/l_{r,nom}$							
	.009	.084	.162	.239	.317	.394	.489	.585
2.009	.8786	.8158	.7456	.6673	.5925	.5632	.5561	.5283
2.538	.8773	.8156	.7448	.6649	.5855	.5102	.4319	.4311
3.005	.8774	.8159	.7450	.6647	.5851	.5101	.4320	.3516
3.546	.8768	.8155	.7448	.6641	.5846	.5096	.4315	.3514
4.025	.8773	.8158	.7450	.6643	.5849	.5095	.4316	.3516
4.991	.8791	.8165	.7455	.6649	.5860	.5100	.4318	.3521
5.910	.8805	.8166	.7458	.6656	.5869	.5103	.4321	.3525

NPR	$x'/l_{r,nom}$ = .394			$x'/l_{r,nom}$ = .489			$x'/l_{r,nom}$ = .585		
	z/w			z/w			z/w		
	0	.450	.875	0	.450	.875	0	.450	.875
2.009	.5632	.5621	.5340	.5561	.5516	.5265	.5283	.5267	.5146
2.538	.5102	.5140	.5027	.4319	.4290	.3890	.4311	.4148	.4193
3.005	.5101	.5141	.5024	.4320	.4284	.3252	.3516	.3436	.3102
3.546	.5096	.5135	.5020	.4315	.4276	.2920	.3514	.3434	.2573
4.025	.5095	.5136	.5022	.4316	.4271	.2892	.3516	.3437	.2208
4.991	.5100	.5138	.5029	.4318	.4270	.2882	.3521	.3442	.1901
5.910	.5103	.5141	.5033	.4321	.4271	.2880	.3525	.3446	.1890

Lower-flap pressures, $p/p_{t,j}$

NPR	z/w = 0.0								
	$x''/l_{l,nom}$								
	0	.293	.438	.582	.725	.797	.856	.901	.946
2.009	.8745	.9267	.9066	.8710	.7591	.6723	.5244	.4327	.3692
2.538	.8614	.9267	.9073	.8709	.7584	.6712	.5233	.4313	.3689
3.005	.8537	.9272	.9076	.8704	.7577	.6710	.5229	.4313	.3688
3.546	.8468	.9268	.9071	.8697	.7570	.6703	.5221	.4307	.3679
4.025	.8428	.9270	.9073	.8697	.7567	.6704	.5222	.4306	.3676
4.991	.8377	.9273	.9073	.8700	.7569	.6706	.5225	.4305	.3673
5.910	.8346	.9273	.9070	.8704	.7563	.6706	.5226	.4302	.3669

TABLE VIII. Continued

(ff) Configuration 32

Ramp pressures, $p/p_{t,j}$

NPR	z/w = 0.0												
	$x'/l_{r,nom}$												
	.009	.086	.162	.239	.316	.394	.553	.713	.877	1.042	1.204	1.368	1.532
2.012	.8922	.8466	.8036	.7331	.6668	.6139	.5352	.5262	.5102	.5062	.5064	.5009	.4971
2.518	.8902	.8436	.7981	.7239	.6445	.5643	.4515	.3797	.3890	.4698	.3885	.3662	.3974
3.035	.8907	.8444	.7983	.7240	.6439	.5613	.3851	.3154	.2669	.2388	.4582	.3901	.2859
3.010	.8902	.8441	.7977	.7237	.6438	.5612	.3890	.3183	.2697	.2551	.4599	.3840	.2844
3.518	.8904	.8438	.7980	.7244	.6436	.5610	.3761	.2706	.2226	.1869	.3098	.3942	.3738
3.997	.8895	.8440	.7977	.7242	.6435	.5612	.3759	.2369	.1895	.1567	.2014	.2731	.3382
5.015	.8887	.8437	.7979	.7241	.6436	.5615	.3758	.2295	.1495	.1180	.0966	.0774	.1659
6.043	.8870	.8434	.7977	.7242	.6438	.5619	.3764	.2300	.1431	.0978	.0774	.1377	.1474
6.033	.8867	.8433	.7976	.7243	.6438	.5620	.3764	.2301	.1431	.0985	.0779	.1384	.1483
6.859	.8853	.8436	.7975	.7243	.6442	.5624	.3770	.2307	.1433	.0929	.0684	.1308	.1365

NPR	$x'/l_{r,nom}$ = .553			$x'/l_{r,nom}$ = 1.042			$x'/l_{r,nom}$ = 1.532		
	z/w			z/w			z/w		
	0	.450	.875	0	.450	.875	0	.450	.875
2.012	.5352	.5321	.5166	.5052	.5088	.5081	.4974	.4990	.5044
2.518	.4515	.4361	.4128	.4598	.4457	.4080	.3974	.4133	.4194
3.035	.3851	.3793	.3096	.2388	.3592	.3545	.2859	.2951	.3518
3.010	.3890	.3814	.3121	.2551	.3661	.3569	.2844	.2937	.3461
3.518	.3761	.3731	.2653	.1869	.2551	.2915	.3738	.3767	.3062
3.997	.3759	.3725	.2372	.1567	.1260	.2446	.3382	.3244	.2691
5.015	.3758	.3723	.2251	.1180	.0952	.1758	.1659	.1823	.2034
6.043	.3764	.3728	.2241	.0978	.0784	.1205	.1474	.1383	.1598
6.033	.3764	.3728	.2242	.0985	.0789	.1212	.1483	.1385	.1612
6.859	.3770	.3735	.2239	.0929	.0760	.1129	.1365	.1303	.1358

Lower-flap pressures, $p/p_{t,j}$

NPR	z/w = 0.0								
	$x''/l_{l,nom}$								
	0	.293	.438	.582	.723	.797	.841	.885	.930
2.012	.8835	.9363	.9195	.8875	.7983	.7373	.6876	.6339	.5513
2.518	.8703	.9369	.9186	.8854	.7955	.7310	.6805	.6257	.5429
3.035	.8622	.9376	.9187	.8851	.7953	.7303	.6802	.6252	.5441
3.010	.8624	.9373	.9189	.8852	.7951	.7301	.6802	.6249	.5439
3.518	.8565	.9372	.9192	.8848	.7949	.7297	.6799	.6250	.5448
3.997	.8527	.9374	.9190	.8846	.7947	.7294	.6798	.6249	.5454
5.015	.8470	.9375	.9185	.8849	.7947	.7289	.6794	.6248	.5460
6.043	.8437	.9373	.9181	.8852	.7940	.7277	.6788	.6246	.5460
6.033	.8438	.9373	.9182	.8851	.7941	.7276	.6788	.6246	.5460
6.859	.8417	.9369	.9175	.8854	.7939	.7265	.6784	.6244	.5458

TABLE VIII. Continued

(gg) Configuration 33

Ramp pressures, $p/p_{t,j}$

NPR	z/w = 0.0										
	$x'/l_{r,nom}$										
	.009	.084	.162	.240	.317	.394	.554	.713	.877	1.040	1.204
2.038	.9041	.8497	.7934	.7284	.6646	.6098	.5373	.5338	.5131	.5075	.5003
2.487	.9020	.8467	.7877	.7182	.6422	.5615	.4546	.3863	.4229	.4611	.3773
3.013	.9022	.8461	.7871	.7177	.6415	.5543	.3899	.3194	.2729	.2517	.4591
3.488	.9020	.8466	.7871	.7177	.6417	.5543	.3752	.2726	.2273	.1905	.2660
4.028	.9024	.8468	.7873	.7182	.6420	.5545	.3748	.2357	.1912	.1560	.1280
5.031	.9027	.8467	.7875	.7185	.6424	.5550	.3749	.2309	.1514	.1193	.0941
6.037	.9030	.8465	.7883	.7190	.6432	.5559	.3756	.2313	.1448	.0983	.0844
6.589	.9034	.8465	.7888	.7192	.6434	.5564	.3761	.2316	.1451	.0930	.1046

NPR	$x'/l_{r,nom}$ = .554			$x'/l_{r,nom}$ = .877			$x'/l_{r,nom}$ = 1.204		
	z/w			z/w			z/w		
	0	.450	.875	0	.450	.875	0	.450	.875
2.038	.5373	.5351	.5182	.5131	.5141	.4965	.5003	.5015	.5055
2.487	.4546	.4360	.4185	.4229	.4245	.4047	.3773	.3929	.4232
3.013	.3899	.3780	.3100	.2729	.3077	.3264	.4591	.3693	.3477
3.488	.3752	.3683	.2657	.2273	.1862	.2743	.2660	.3225	.3085
4.028	.3748	.3688	.2314	.1912	.1600	.2354	.1280	.2137	.2560
5.031	.3749	.3694	.2184	.1514	.1272	.1627	.0941	.1686	.1956
6.037	.3756	.3701	.2181	.1448	.1240	.1310	.0844	.1483	.1421
6.589	.3761	.3706	.2181	.1451	.1241	.1112	.1046	.1438	.1329

Lower-flap pressures, $p/p_{t,j}$

NPR	z/w = 0.0								
	$x''/l_{l,nom}$								
	0	.293	.438	.582	.723	.797	.841	.885	.930
2.038	.8817	.9373	.9180	.8877	.7987	.7348	.6857	.6329	.5746
2.487	.8678	.9362	.9191	.8871	.7953	.7297	.6794	.6255	.5662
3.013	.8587	.9362	.9193	.8858	.7948	.7292	.6788	.6248	.5653
3.488	.8535	.9364	.9197	.8850	.7947	.7299	.6787	.6248	.5650
4.028	.8490	.9371	.9195	.8858	.7947	.7290	.6788	.6250	.5650
5.031	.8434	.9368	.9191	.8862	.7951	.7289	.6788	.6250	.5645
6.037	.8405	.9369	.9190	.8867	.7951	.7290	.6788	.6251	.5642
6.589	.8391	.9371	.9191	.8872	.7949	.7290	.6787	.6252	.5640

TABLE VIII. Continued

(hh) Configuration 34

Ramp pressures, $p/p_{t,j}$

NPR	z/w = 0.0							
	$x'/l_{r,nom}$							
	.009	.084	.162	.239	.317	.394	.489	.585
2.022	.8971	.8452	.7885	.7248	.6633	.6099	.5667	.5273
2.497	.8937	.8419	.7829	.7142	.6417	.5637	.5004	.4398
3.006	.8939	.8423	.7832	.7139	.6415	.5591	.4578	.3771
3.522	.8938	.8422	.7834	.7138	.6417	.5589	.4576	.3468
3.990	.8944	.8424	.7835	.7140	.6423	.5591	.4579	.3471
5.011	.8957	.8431	.7841	.7148	.6437	.5597	.4587	.3478
5.985	.8972	.8433	.7845	.7157	.6451	.5602	.4595	.3484
6.183	.8976	.8434	.7846	.7159	.6454	.5604	.4597	.3485

NPR	$x'/l_{r,nom}$ = .394			$x'/l_{r,nom}$ = .489			$x'/l_{r,nom}$ = .585		
	z/w			z/w			z/w		
	0	.450	.875	0	.450	.875	0	.450	.875
2.022	.6099	.6080	.5677	.5667	.5605	.5251	.5273	.5264	.5126
2.497	.5637	.5668	.5394	.5004	.4903	.4205	.4398	.4149	.4147
3.006	.5591	.5640	.5391	.4578	.4504	.3359	.3771	.3638	.3009
3.522	.5589	.5640	.5391	.4576	.4498	.3065	.3468	.3362	.2533
3.990	.5591	.5643	.5394	.4579	.4500	.3037	.3471	.3365	.2214
5.011	.5597	.5648	.5400	.4587	.4502	.3032	.3478	.3374	.1950
5.985	.5602	.5653	.5405	.4595	.4510	.3031	.3484	.3381	.1944
6.183	.5604	.5656	.5407	.4597	.4513	.3033	.3485	.3383	.1945

Lower-flap pressures, $p/p_{t,j}$

NPR	z/w = 0.0								
	$x''/l_{l,nom}$								
	0	.293	.438	.582	.723	.797	.841	.885	.930
2.022	.8810	.9370	.9194	.8870	.7983	.7343	.6849	.6326	.5705
2.497	.8669	.9356	.9194	.8856	.7945	.7288	.6786	.6250	.5622
3.006	.8593	.9363	.9196	.8853	.7946	.7287	.6785	.6248	.5617
3.522	.8533	.9366	.9194	.8847	.7942	.7282	.6780	.6242	.5613
3.990	.8495	.9365	.9189	.8847	.7946	.7282	.6780	.6242	.5612
5.011	.8436	.9370	.9191	.8858	.7953	.7280	.6779	.6243	.5610
5.985	.8406	.9368	.9188	.8858	.7945	.7280	.6778	.6245	.5599
6.183	.8404	.9371	.9187	.8854	.7945	.7281	.6778	.6244	.5599

TABLE VIII. Continued

(ii) Configuration 35

Ramp pressures, $p/p_{t,j}$

NPR	z/w = 0.0			
	$x'/l_{r,nom}$			
	.009	.084	.162	.302
1.996	.9013	.8395	.7806	.6180
2.521	.9007	.8382	.7786	.6126
3.041	.9008	.8375	.7787	.6115
3.016	.9000	.8374	.7787	.6115
3.506	.9002	.8371	.7786	.6109
4.031	.9006	.8369	.7788	.6107
5.003	.9011	.8374	.7792	.6109
5.995	.9010	.8379	.7792	.6109
6.997	.9012	.8387	.7793	.6109
8.026	.9014	.8399	.7796	.6111
9.000	.9014	.8406	.7799	.6115
9.940	.9011	.8415	.7802	.6117
10.020	.9012	.8415	.7802	.6117

Lower-flap pressures, $p/p_{t,j}$

NPR	z/w = 0.0								
	$x''/l_{l,nom}$								
	0	.293	.438	.582	.723	.797	.841	.885	.930
1.996	.8809	.9361	.9181	.8857	.7937	.7288	.6734	.6224	.5152
2.521	.8681	.9356	.9178	.8848	.7932	.7267	.6709	.6194	.5138
3.041	.8591	.9359	.9178	.8843	.7924	.7257	.6703	.6185	.5143
3.016	.8592	.9361	.9180	.8840	.7925	.7258	.6703	.6186	.5144
3.506	.8536	.9358	.9181	.8841	.7925	.7254	.6699	.6182	.5146
4.031	.8494	.9358	.9179	.8837	.7921	.7251	.6698	.6181	.5149
5.003	.8442	.9360	.9179	.8841	.7925	.7249	.6698	.6182	.5155
5.995	.8411	.9361	.9172	.8843	.7921	.7237	.6694	.6181	.5154
6.997	.8386	.9359	.9169	.8847	.7917	.7228	.6691	.6181	.5150
8.026	.8369	.9358	.9170	.8854	.7913	.7231	.6690	.6182	.5146
9.000	.8356	.9355	.9166	.8857	.7909	.7234	.6687	.6182	.5139
9.940	.8346	.9353	.9162	.8858	.7905	.7255	.6684	.6181	.5130
10.020	.8345	.9353	.9162	.8859	.7905	.7255	.6684	.6180	.5129

TABLE VIII. Continued

(jj) Configuration 36

Ramp pressures, $p/p_{t,j}$

NPR	z/w = 0.0										
	$x'/l_{r,nom}$										
	.009	.084	.162	.240	.317	.394	.554	.713	.877	1.040	1.204
2.017	.9157	.8669	.8187	.7603	.6979	.6361	.5392	.5341	.5122	.5066	.4990
2.509	.9125	.8628	.8105	.7468	.6740	.5929	.4526	.3799	.3947	.4646	.3671
3.004	.9118	.8626	.8087	.7440	.6673	.5711	.4158	.3235	.2684	.2520	.4621
3.503	.9117	.8624	.8083	.7440	.6672	.5705	.3724	.2854	.2259	.1874	.2858
4.016	.9120	.8621	.8085	.7442	.6675	.5707	.3656	.2553	.1974	.1555	.1277
5.033	.9121	.8621	.8086	.7447	.6680	.5714	.3654	.2213	.1625	.1229	.0934
5.996	.9122	.8619	.8094	.7449	.6685	.5724	.3658	.2215	.1409	.1059	.0787
6.683	.9124	.8620	.8101	.7451	.6688	.5732	.3664	.2219	.1385	.0972	.0720

NPR	$x'/l_{r,nom}$ = .554			$x'/l_{r,nom}$ = .877			$x'/l_{r,nom}$ = 1.204		
	z/w			z/w			z/w		
	0	.450	.875	0	.450	.875	0	.450	.875
2.017	.5392	.5365	.5159	.5122	.5134	.5124	.4990	.5017	.5055
2.509	.4526	.4353	.4096	.3947	.4216	.4254	.3671	.3817	.4239
3.004	.4158	.4055	.3244	.2684	.3013	.3450	.4621	.3782	.3503
3.503	.3724	.3681	.2615	.2259	.1859	.2848	.2858	.3251	.3035
4.016	.3656	.3620	.2331	.1974	.1647	.2420	.1277	.2279	.2581
5.033	.3654	.3627	.2166	.1625	.1376	.1643	.0934	.1679	.1948
5.996	.3658	.3633	.2159	.1409	.1207	.1333	.0787	.1369	.1503
6.693	.3664	.3639	.2160	.1385	.1193	.1183	.0720	.1396	.1234

Lower-flap pressures, $p/p_{t,j}$

NPR	z/w = 0.0								
	$x''/l_{l,nom}$								
	0	.293	.438	.582	.725	.797	.856	.900	.944
2.017	.8874	.9433	.9286	.8999	.8209	.7704	.7353	.7090	.6173
2.509	.8739	.9419	.9266	.8956	.8155	.7615	.7256	.6981	.6025
3.004	.8657	.9418	.9265	.8958	.8140	.7598	.7243	.6967	.6008
3.503	.8599	.9416	.9259	.8959	.8141	.7594	.7240	.6964	.6004
4.016	.8561	.9416	.9261	.8954	.8138	.7592	.7242	.6967	.6004
5.033	.8503	.9419	.9254	.8954	.8138	.7590	.7242	.6969	.5999
5.996	.8473	.9415	.9251	.8959	.8136	.7585	.7241	.6971	.5996
6.693	.8458	.9416	.9247	.8951	.8134	.7579	.7240	.6970	.5996

TABLE VIII. Continued

(kk) Configuration 37

Ramp pressures, $p/p_{t,j}$

NPR	z/w = 0.0								
	$x'/l_{r,nom}$								
	.009	.085	.161	.239	.316	.392	.551	.713	.874
2.000	.9082	.8616	.8171	.7588	.6903	.6354	.5486	.5415	.4977
2.512	.9049	.8560	.8088	.7443	.6631	.5904	.4571	.3873	.3875
2.982	.9037	.8548	.8071	.7413	.6552	.5691	.4239	.3342	.2630
3.508	.9037	.8549	.8070	.7411	.6548	.5685	.3792	.2937	.2206
4.025	.9039	.8551	.8072	.7411	.6548	.5684	.3753	.2627	.1932
5.002	.9055	.8555	.8077	.7418	.6556	.5684	.3755	.2301	.1606
6.039	.9067	.8554	.8076	.7423	.6559	.5678	.3757	.2298	.1380
6.507	.9075	.8557	.8075	.7429	.6557	.5678	.3761	.2301	.1365

NPR	$x'/l_{r,nom}$ = .392			$x'/l_{r,nom}$ = .713			$x'/l_{r,nom}$ = .874		
	z/w			z/w			z/w		
	0	.450	.875	0	.450	.875	0	.450	.875
2.000	.6354	.6394	.5845	.5415	.5422	.5314	.4977	.5019	.5014
2.512	.5904	.5996	.5489	.3873	.3961	.4263	.3875	.4155	.4162
2.982	.5691	.5822	.5424	.3342	.2953	.3441	.2630	.3074	.3454
3.508	.5685	.5819	.5423	.2937	.2644	.2838	.2206	.1841	.2787
4.025	.5684	.5822	.5425	.2627	.2393	.1945	.1932	.1632	.2361
5.002	.5684	.5830	.5431	.2301	.2114	.1311	.1606	.1372	.1633
6.039	.5678	.5837	.5433	.2298	.2111	.1190	.1380	.1193	.1323
6.507	.5678	.5842	.5436	.2301	.2111	.1188	.1365	.1184	.1234

Lower-flap pressures, $p/p_{t,j}$

NPR	z/w = 0.0								
	$x''/l_{l,nom}$								
	0	.293	.438	.582	.725	.797	.856	.900	.944
2.000	.8878	.9432	.9283	.9003	.8215	.7689	.7354	.7094	.6691
2.512	.8731	.9418	.9269	.8970	.8159	.7600	.7253	.6978	.6559
2.982	.8649	.9413	.9260	.8957	.8143	.7576	.7237	.6958	.6542
3.508	.8589	.9409	.9255	.8949	.8140	.7570	.7236	.6957	.6541
4.025	.8546	.9410	.9255	.8947	.8140	.7565	.7239	.6959	.6542
5.002	.8498	.9415	.9255	.8952	.8140	.7563	.7248	.6963	.6545
6.039	.8458	.9411	.9246	.8951	.8134	.7556	.7243	.6963	.6540
6.507	.8447	.9409	.9244	.8952	.8135	.7554	.7243	.6963	.6541

TABLE VIII. Continued

(ll) Configuration 38

Ramp pressures , $p/p_{t,j}$

NPR	z/w = 0.0							
	$x'/l_{r,nom}$							
	.009	.084	.162	.239	.317	.394	.489	.585
2.021	.9083	.8630	.8136	.7566	.6964	.6381	.5797	.5309
2.504	.9035	.8578	.8054	.7424	.6725	.5960	.5130	.4390
3.021	.9032	.8572	.8044	.7398	.6664	.5756	.4724	.3978
3.496	.9042	.8582	.8053	.7404	.6671	.5758	.4569	.3573
4.005	.9041	.8583	.8053	.7405	.6677	.5757	.4569	.3380
5.033	.9051	.8586	.8057	.7413	.6691	.5761	.4575	.3382
5.988	.9068	.8589	.8063	.7421	.6705	.5770	.4583	.3389
6.388	.9076	.8592	.8066	.7428	.6707	.5772	.4586	.3391

NPR	$x'/l_{r,nom}$ = .394			$x'/l_{r,nom}$ = .489			$x'/l_{r,nom}$ = .585		
	z/w			z/w			z/w		
	0	.450	.875	0	.450	.875	0	.450	.875
2.021	.6381	.6318	.5859	.5797	.5721	.5288	.5309	.5285	.5130
2.504	.5960	.5929	.5539	.5130	.5007	.4292	.4390	.4149	.4088
3.021	.5756	.5751	.5480	.4724	.4655	.3371	.3978	.3818	.3190
3.496	.5758	.5757	.5486	.4569	.4491	.3093	.3573	.3478	.2518
4.005	.5757	.5756	.5486	.4569	.4487	.3057	.3380	.3295	.2160
5.033	.5761	.5759	.5489	.4575	.4487	.3053	.3382	.3298	.1932
5.988	.5770	.5767	.5495	.4583	.4496	.3056	.3389	.3305	.1929
6.388	.5772	.5769	.5497	.4586	.4500	.3057	.3391	.3307	.1930

Lower-flap pressures , $p/p_{t,j}$

NPR	z/w = 0.0								
	$x''/l_{l,nom}$								
	0	.293	.438	.582	.725	.797	.856	.900	.944
2.021	.9041	.9428	.9265	.8984	.8210	.7670	.7337	.7069	.6508
2.504	.9167	.9417	.9250	.8955	.8146	.7582	.7241	.6960	.6378
3.021	.9273	.9415	.9249	.8942	.8136	.7568	.7225	.6946	.6363
3.496	.9349	.9420	.9259	.8945	.8138	.7569	.7230	.6951	.6370
4.005	.8844	.9415	.9252	.8942	.8134	.7564	.7229	.6953	.6369
5.033	.8718	.9412	.9248	.8944	.8136	.7558	.7229	.6957	.6369
5.988	.8645	.9410	.9251	.8949	.8139	.7558	.7232	.6962	.6370
6.388	.8625	.9415	.9251	.8952	.8136	.7559	.7234	.6964	.6370

TABLE VIII. Continued

(mm) Configuration 39

Ramp pressures, $p/p_{t,j}$

NPR	z/w = 0.0								
	$x'/l_{r,nom}$								
	.009	.085	.161	.239	.316	.392	.551	.713	.874
1.999	.9211	.8844	.8450	.7892	.7172	.6542	.5485	.5401	.5013
2.504	.9177	.8775	.8354	.7730	.6882	.6067	.4599	.3840	.4099
3.000	.9162	.8753	.8320	.7672	.6760	.5862	.4218	.3177	.2574
3.501	.9159	.8748	.8313	.7655	.6715	.5717	.3965	.2875	.2114
4.000	.9163	.8751	.8315	.7658	.6714	.5704	.3730	.2654	.1874
4.983	.9176	.8755	.8318	.7654	.6721	.5704	.3565	.2348	.1602
5.993	.9189	.8756	.8320	.7671	.6726	.5701	.3567	.2141	.1439
6.833	.9200	.8757	.8319	.7680	.6721	.5698	.3569	.2117	.1343

NPR	$x'/l_{r,nom}$ = .392			$x'/l_{r,nom}$ = .713			$x'/l_{r,nom}$ = .874		
	z/w			z/w			z/w		
	0	.450	.875	0	.450	.875	0	.450	.875
1.999	.6542	.6569	.5972	.5401	.5416	.5329	.5013	.4995	.5039
2.504	.6067	.6141	.5577	.3840	.3942	.4282	.4099	.4238	.4213
3.000	.5862	.5967	.5493	.3177	.2836	.3395	.2574	.3034	.3416
3.501	.5717	.5846	.5445	.2875	.2607	.2721	.2114	.1758	.2832
4.000	.5704	.5842	.5446	.2654	.2429	.2156	.1874	.1579	.2348
4.983	.5704	.5849	.5450	.2348	.2167	.1280	.1602	.1369	.1645
5.993	.5701	.5857	.5453	.2141	.1989	.1102	.1439	.1239	.1351
6.833	.5698	.5863	.5454	.2117	.1961	.1097	.1343	.1160	.1244

Lower-flap pressures, $p/p_{t,j}$

NPR	z/w = 0.0								
	$x''/l_{l,nom}$								
	0	.293	.438	.582	.725	.797	.856	.899	.943
1.999	.8947	.9526	.9409	.9151	.8580	.8148	.8119	.7971	.7603
2.504	.8799	.9504	.9387	.9109	.8503	.8042	.8014	.7857	.7474
3.000	.8709	.9499	.9372	.9086	.8476	.8005	.7981	.7826	.7442
3.501	.8648	.9494	.9368	.9080	.8466	.7991	.7974	.7820	.7436
4.000	.8610	.9494	.9370	.9078	.8466	.7989	.7972	.7823	.7437
4.983	.8559	.9498	.9368	.9082	.8468	.7984	.7973	.7827	.7438
5.993	.8523	.9496	.9364	.9083	.8462	.7978	.7971	.7827	.7432
6.833	.8503	.9493	.9359	.9083	.8458	.7976	.7967	.7827	.7425

TABLE VIII. Concluded

(nn) Configuration 40

Ramp pressures, $p/p_{t,j}$

NPR	z/w = 0.0			
	$x'/l_{r,nom}$			
	.009	.084	.162	.302
2.001	.9252	.8765	.8292	.6522
2.505	.9234	.8725	.8242	.6407
3.010	.9229	.8715	.8231	.6377
3.508	.9223	.8710	.8230	.6371
4.008	.9227	.8709	.8233	.6371
5.003	.9231	.8714	.8236	.6374
6.023	.9230	.8724	.8238	.6378
7.004	.9229	.8733	.8240	.6380
7.968	.9232	.8746	.8247	.6385
7.997	.9232	.8745	.8246	.6385
9.019	.9231	.8755	.8249	.6388
10.021	.9230	.8766	.8255	.6393

Lower-flap pressures, $p/p_{t,j}$

NPR	z/w = 0.0								
	$x''/l_{l,nom}$								
	0	.293	.438	.582	.725	.797	.856	.899	.943
2.001	.8922	.9501	.9377	.9100	.8533	.8012	.8003	.7841	.7349
2.505	.8786	.9486	.9367	.9077	.8489	.7954	.7940	.7777	.7261
3.010	.8700	.9486	.9363	.9056	.8479	.7943	.7928	.7764	.7247
3.508	.8643	.9485	.9362	.9053	.8473	.7939	.7923	.7763	.7242
4.008	.8601	.9485	.9360	.9060	.8470	.7943	.7921	.7764	.7241
5.003	.8547	.9487	.9356	.9059	.8471	.7936	.7918	.7766	.7239
6.023	.8513	.9486	.9355	.9064	.8470	.7925	.7916	.7769	.7234
7.004	.8490	.9485	.9347	.9065	.8464	.7923	.7913	.7769	.7228
7.968	.8478	.9485	.9349	.9070	.8464	.7938	.7914	.7774	.7224
7.997	.8476	.9483	.9347	.9068	.8462	.7937	.7913	.7772	.7222
9.019	.8462	.9479	.9341	.9070	.8457	.7957	.7910	.7770	.7210
10.021	.8454	.9480	.9339	.9074	.8456	.7963	.7912	.7771	.7201

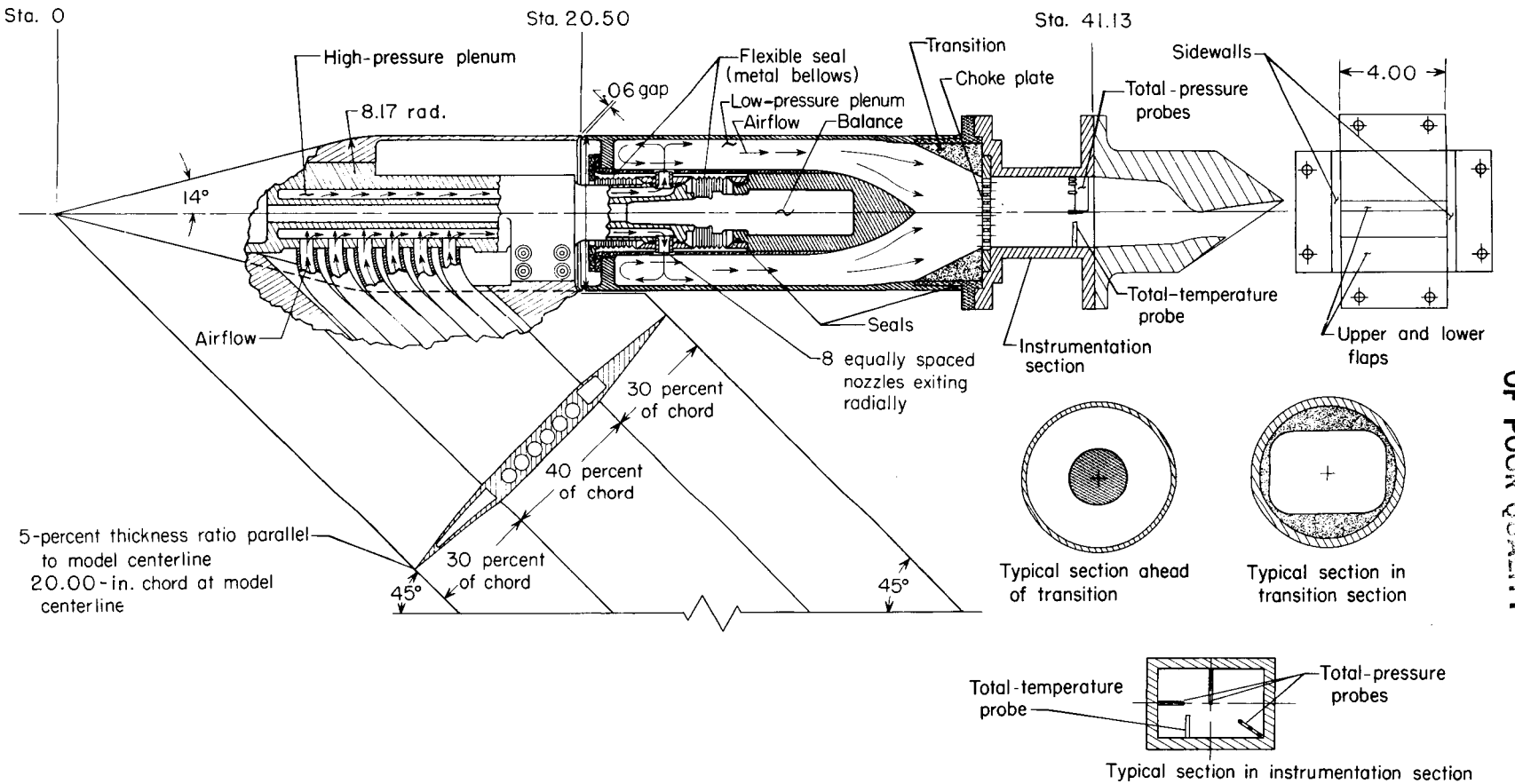

Figure 1. Sketch of air-powered nacelle model with typical SERN installed. All dimensions are in inches unless otherwise noted.

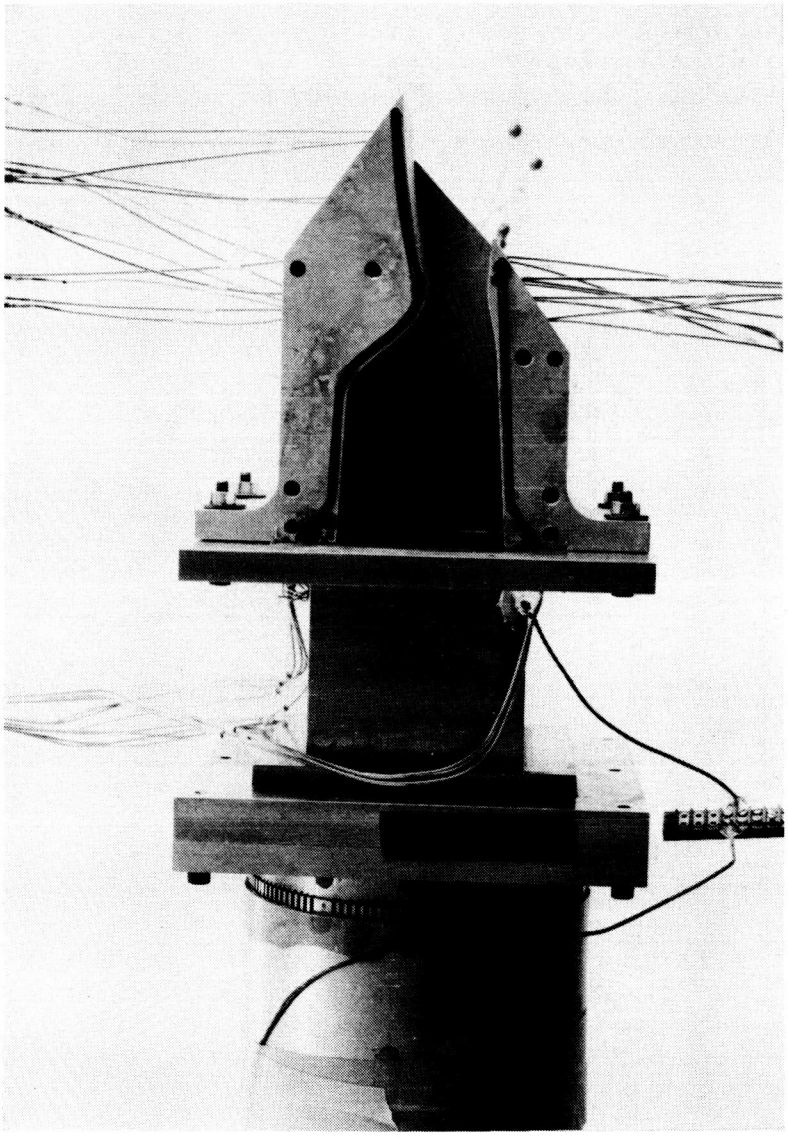

L-82-116

Figure 2. Typical SERN mounted on air-powered nacelle model. Sidewall removed for clarity.

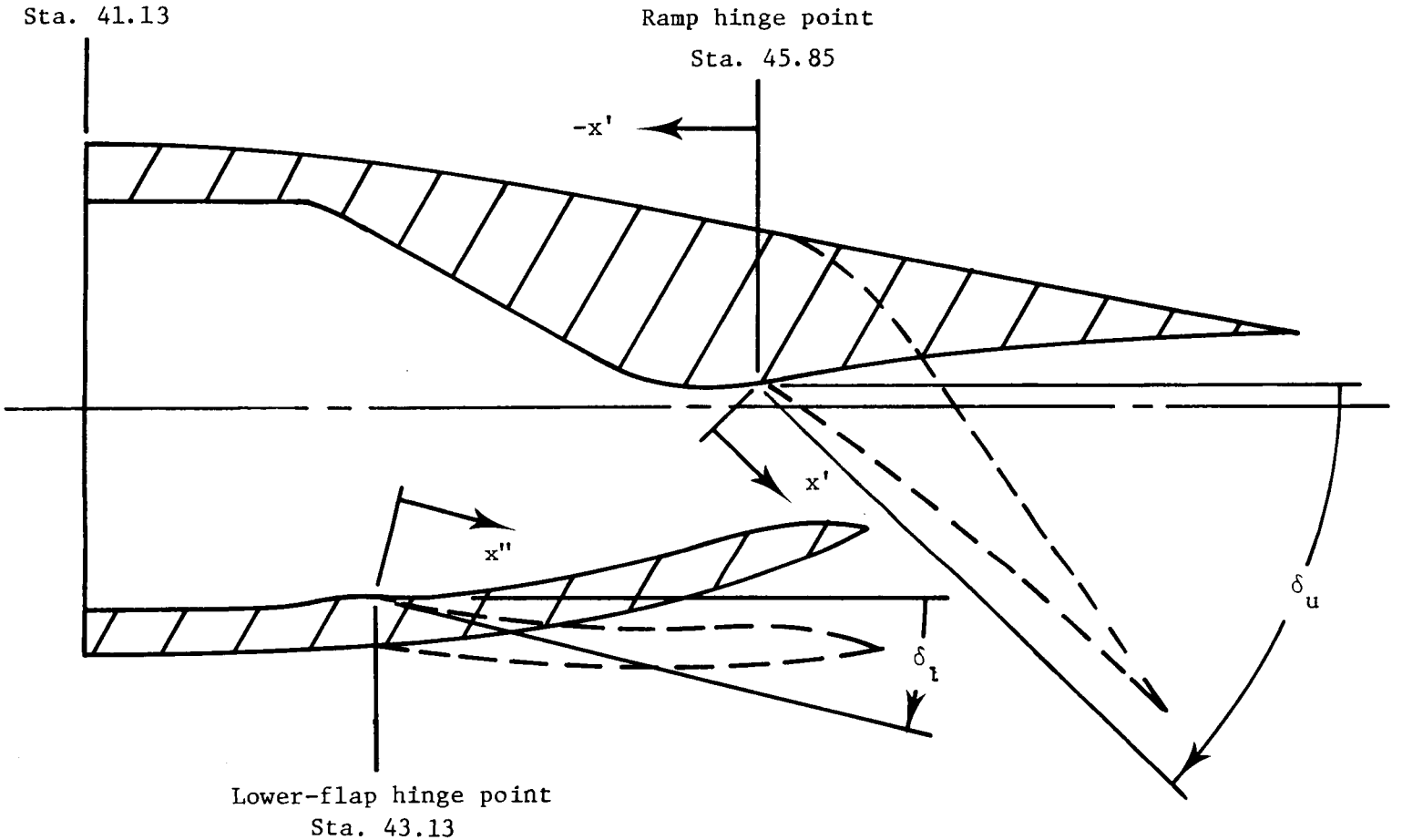

Note: Flap rotation angles, δ_l and δ_u, are defined relative to unvectored baseline (configuration 3; $\delta_l = \delta_u = 0°$).

(a) Nozzle vectoring operation and flap rotation angles.

Figure 3. Sketches defining nozzle geometric parameters. Sidewall removed for clarity.

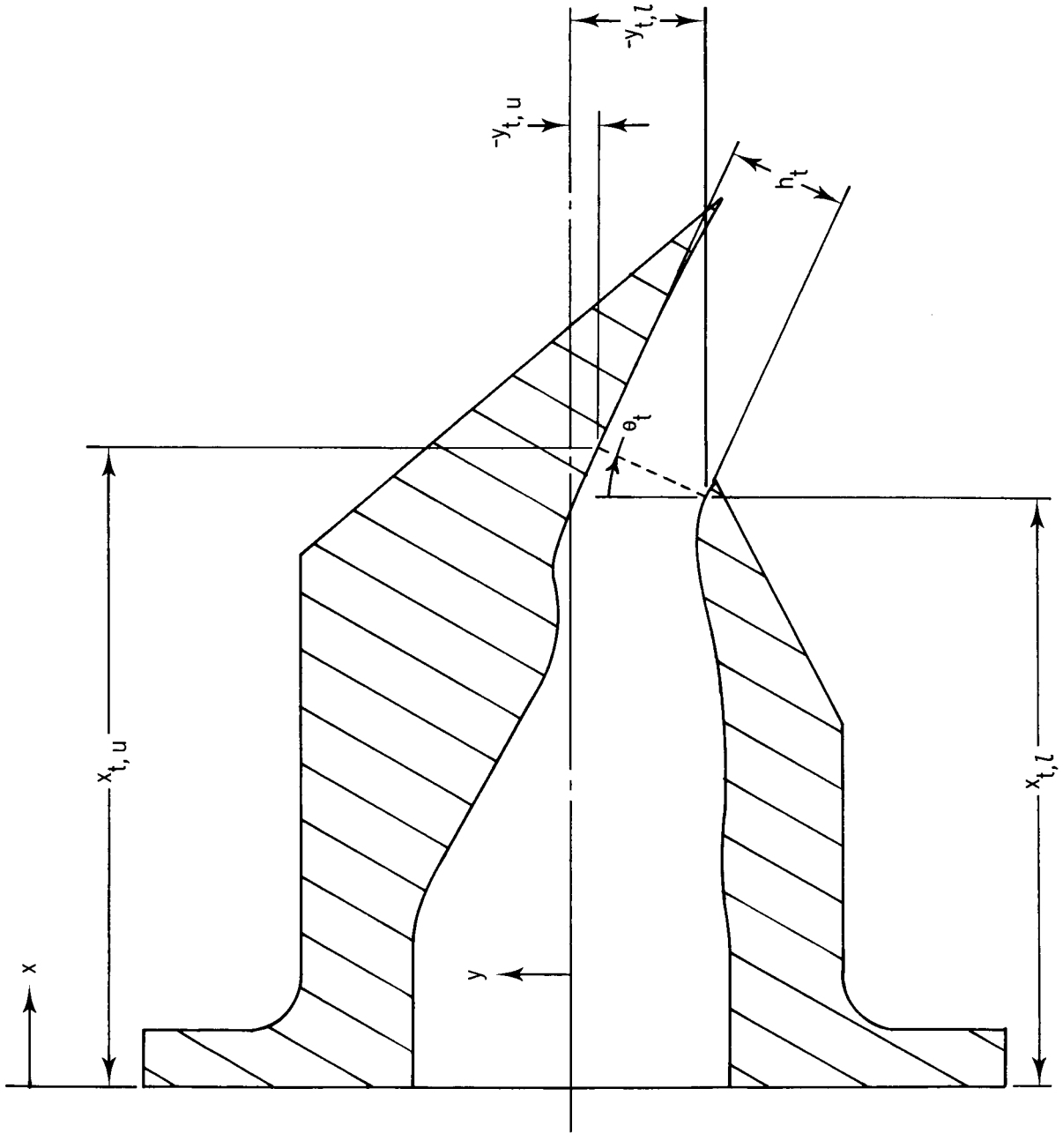

(b) Throat geometric parameters.

Figure 3. Continued.

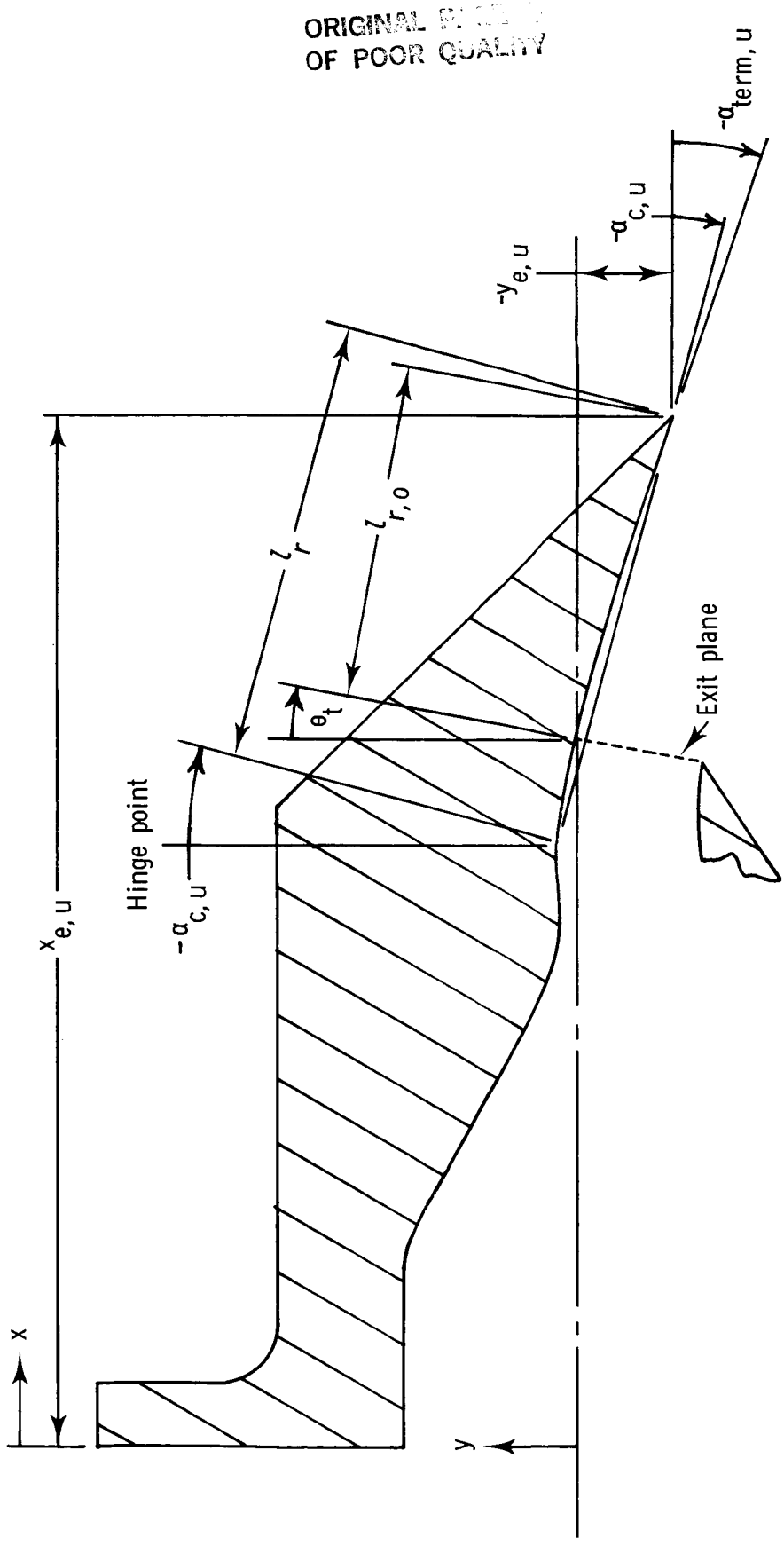

(c) Upper-ramp geometric parameters.

Figure 3. Continued.

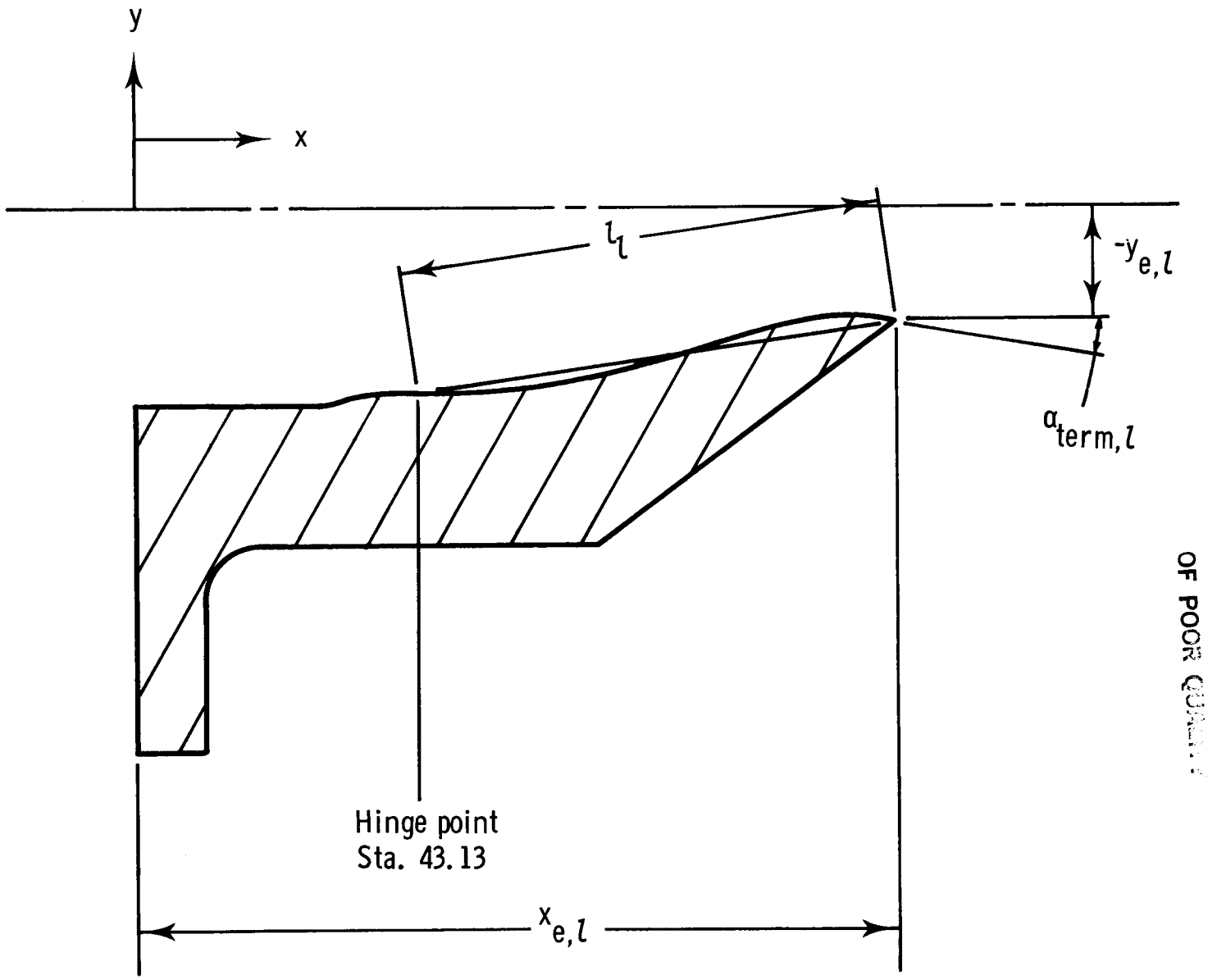

(d) Lower-flap geometric parameters.

Figure 3. Concluded.

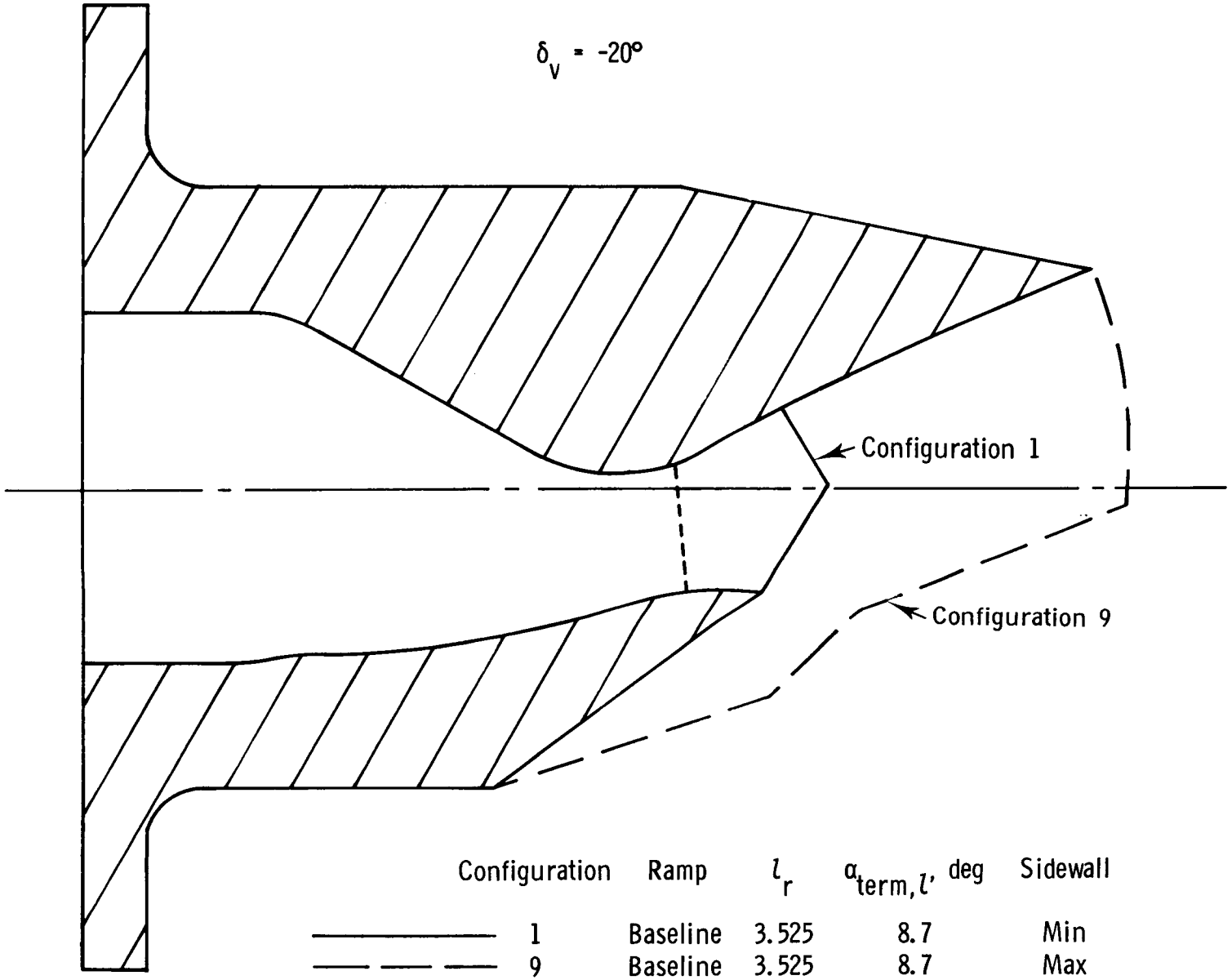

(a) Configurations 1 and 9.

Figure 4. Sketches showing geometry of single-expansion-ramp nozzle configurations. All dimensions are in inches unless otherwise noted. Throat location is indicated by short dashed line.

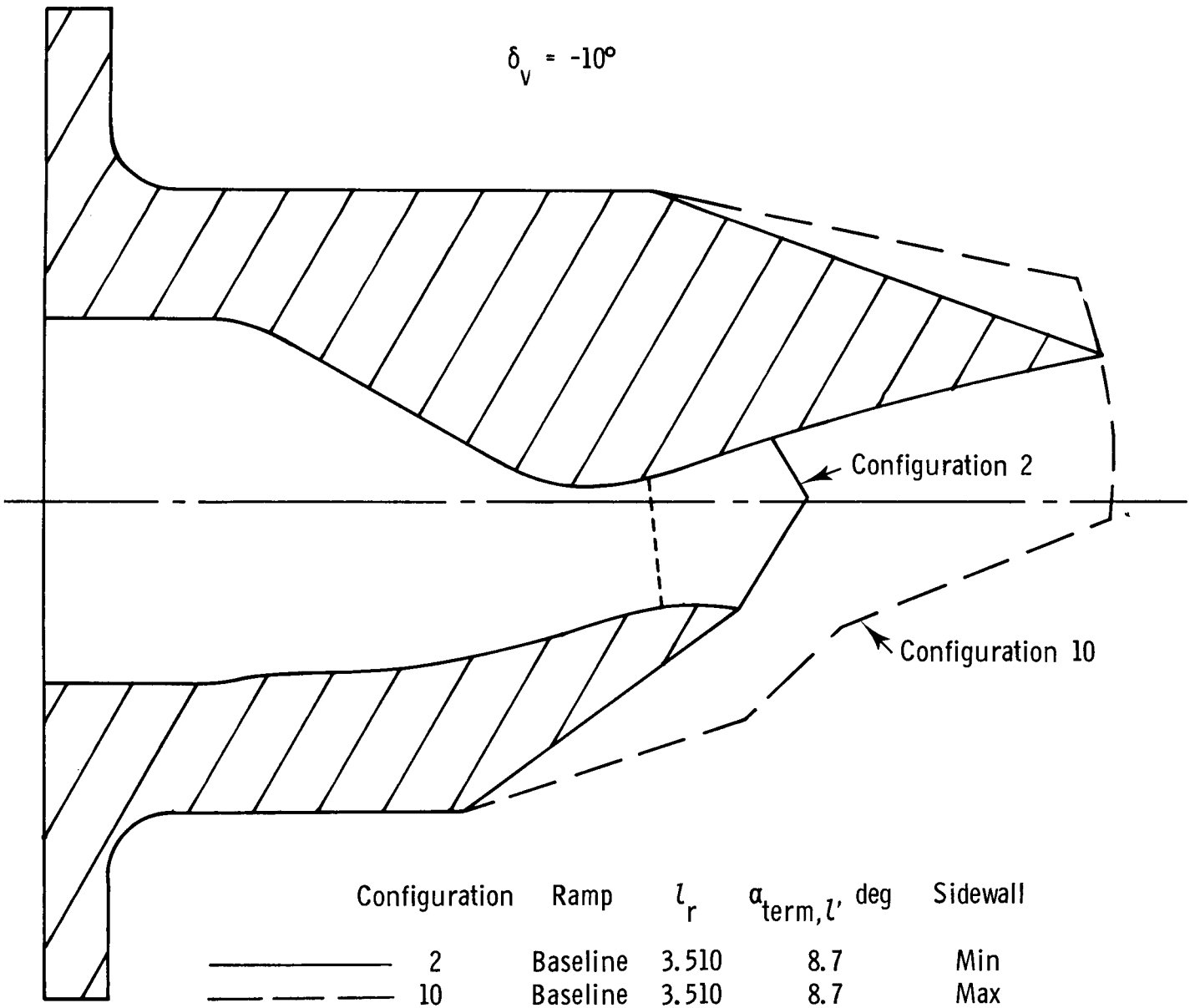

(b) Configurations 2 and 10.

Figure 4. Continued.

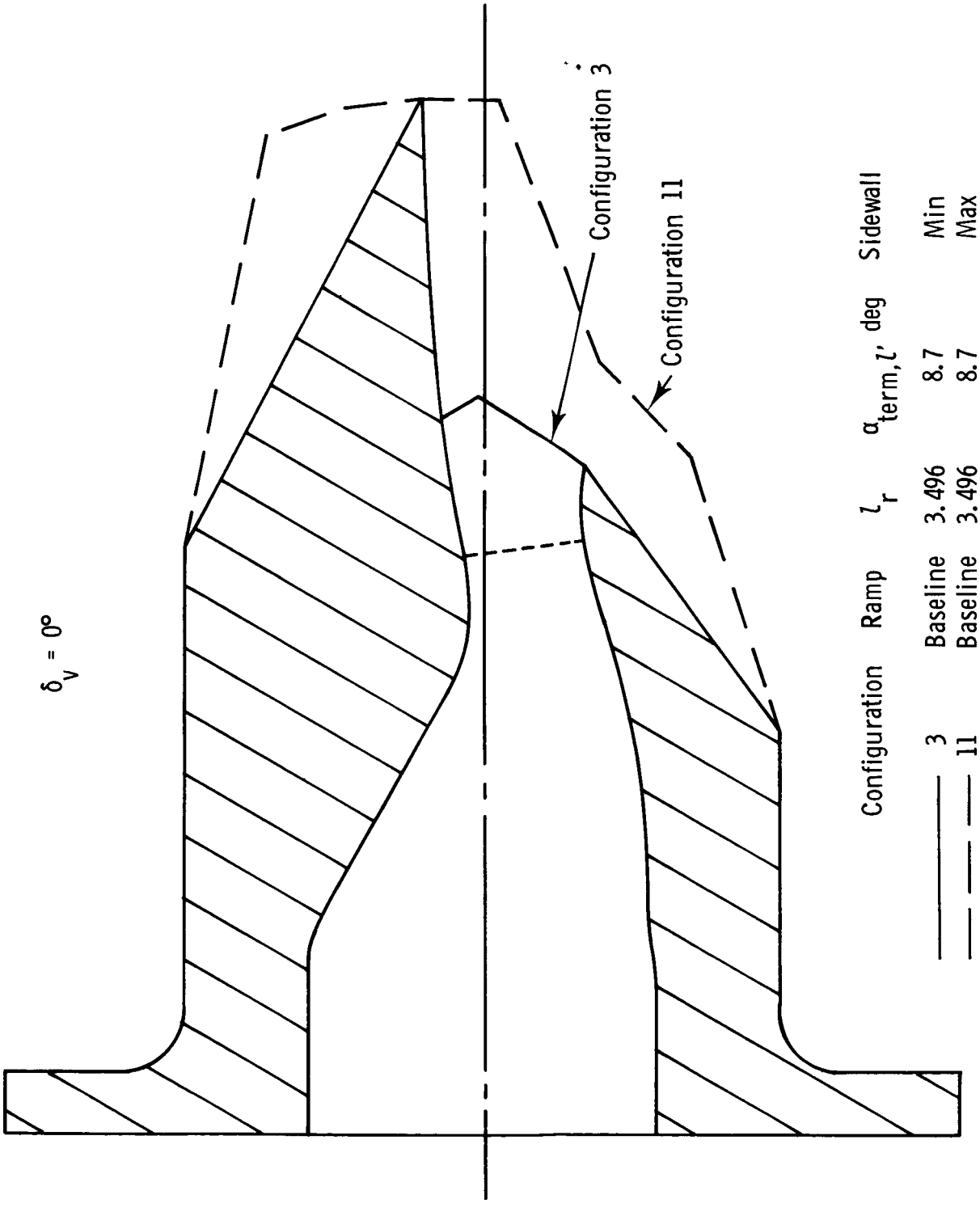

(c) Configurations 3 and 11.

Figure 4. Continued.

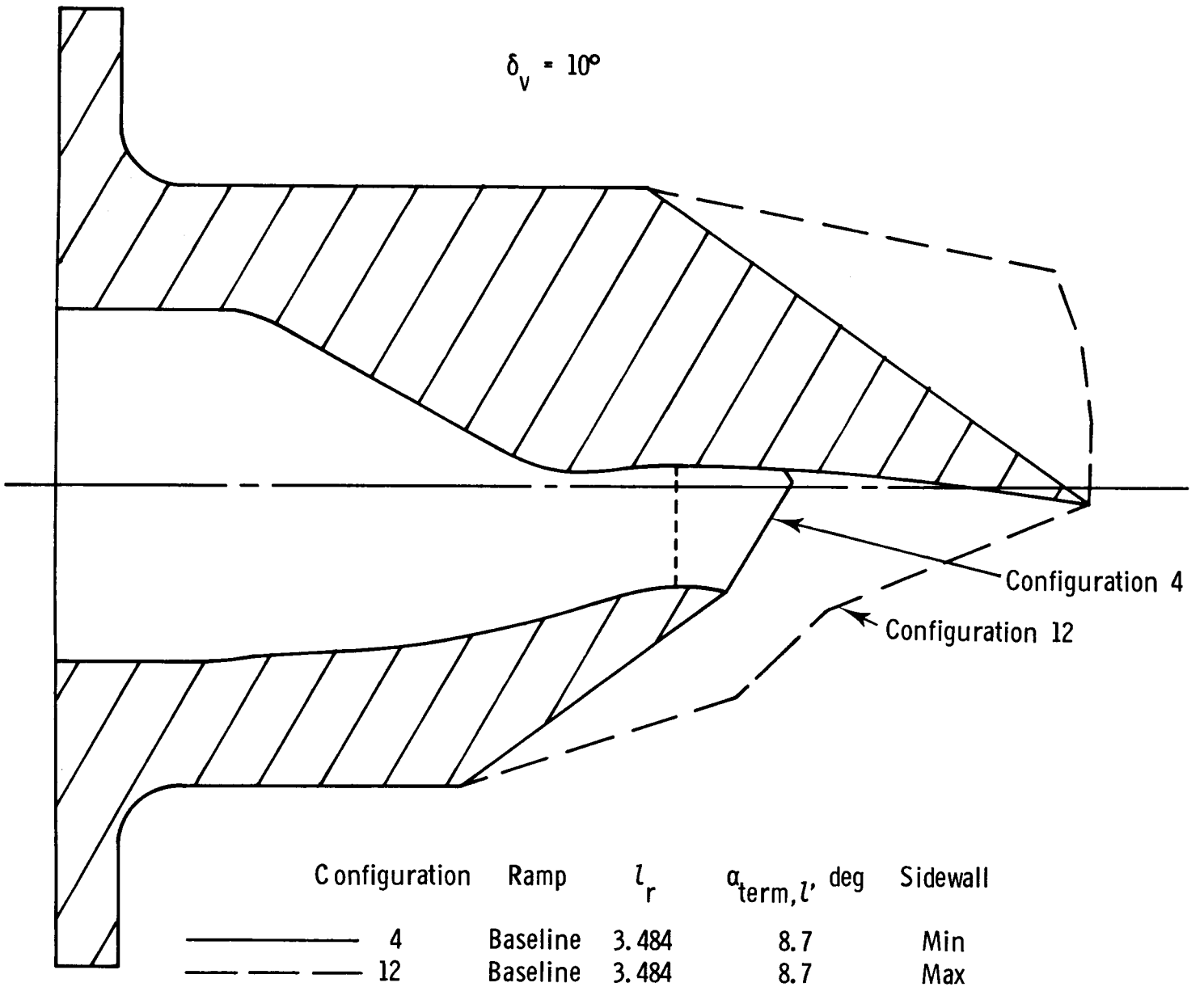

(d) Configurations 4 and 12.

Figure 4. Continued.

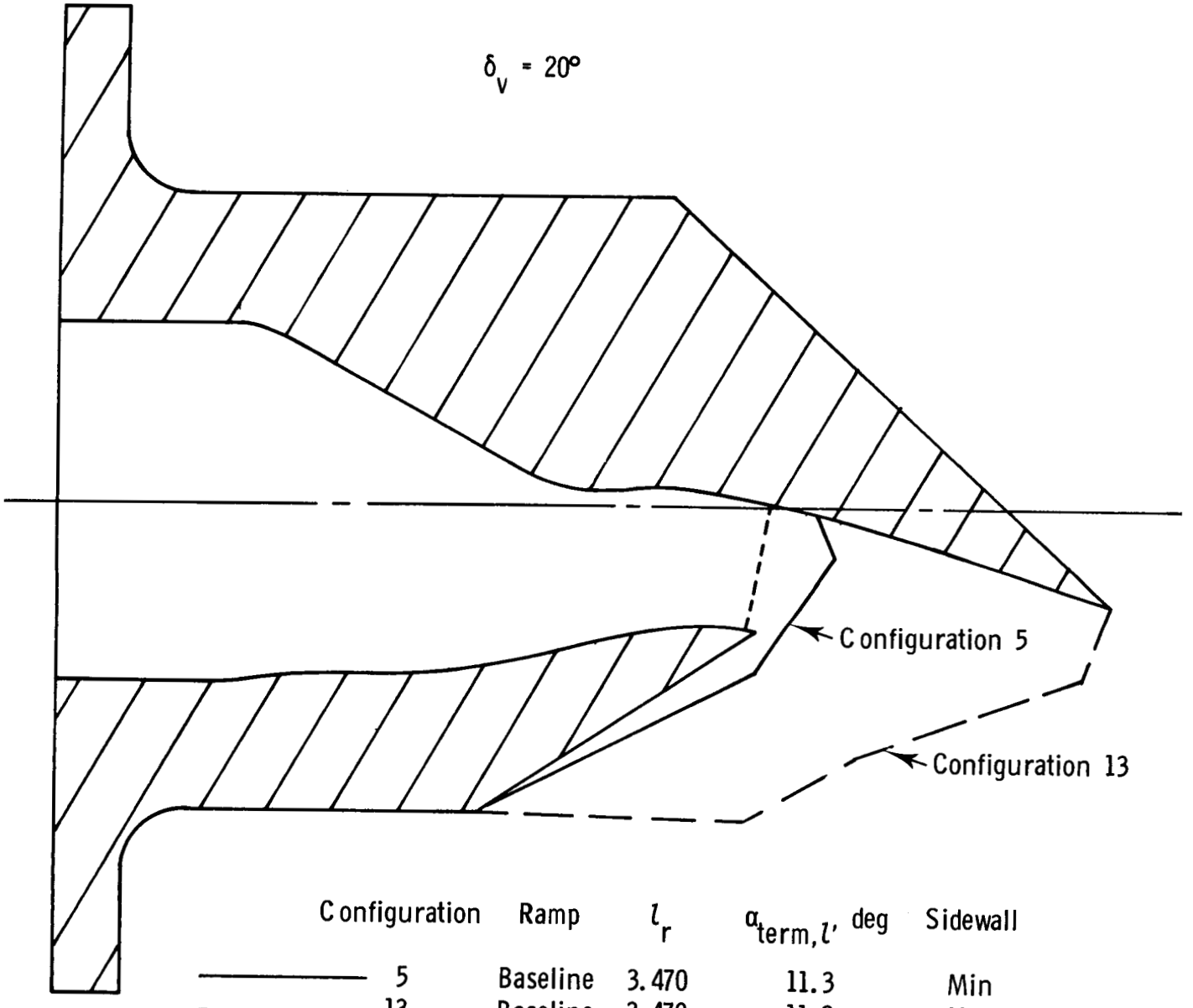

Configuration		Ramp	l_r	$\alpha_{term,l}$, deg	Sidewall
———	5	Baseline	3.470	11.3	Min
— — —	13	Baseline	3.470	11.3	Max

(e) Configurations 5 and 13.

Figure 4. Continued.

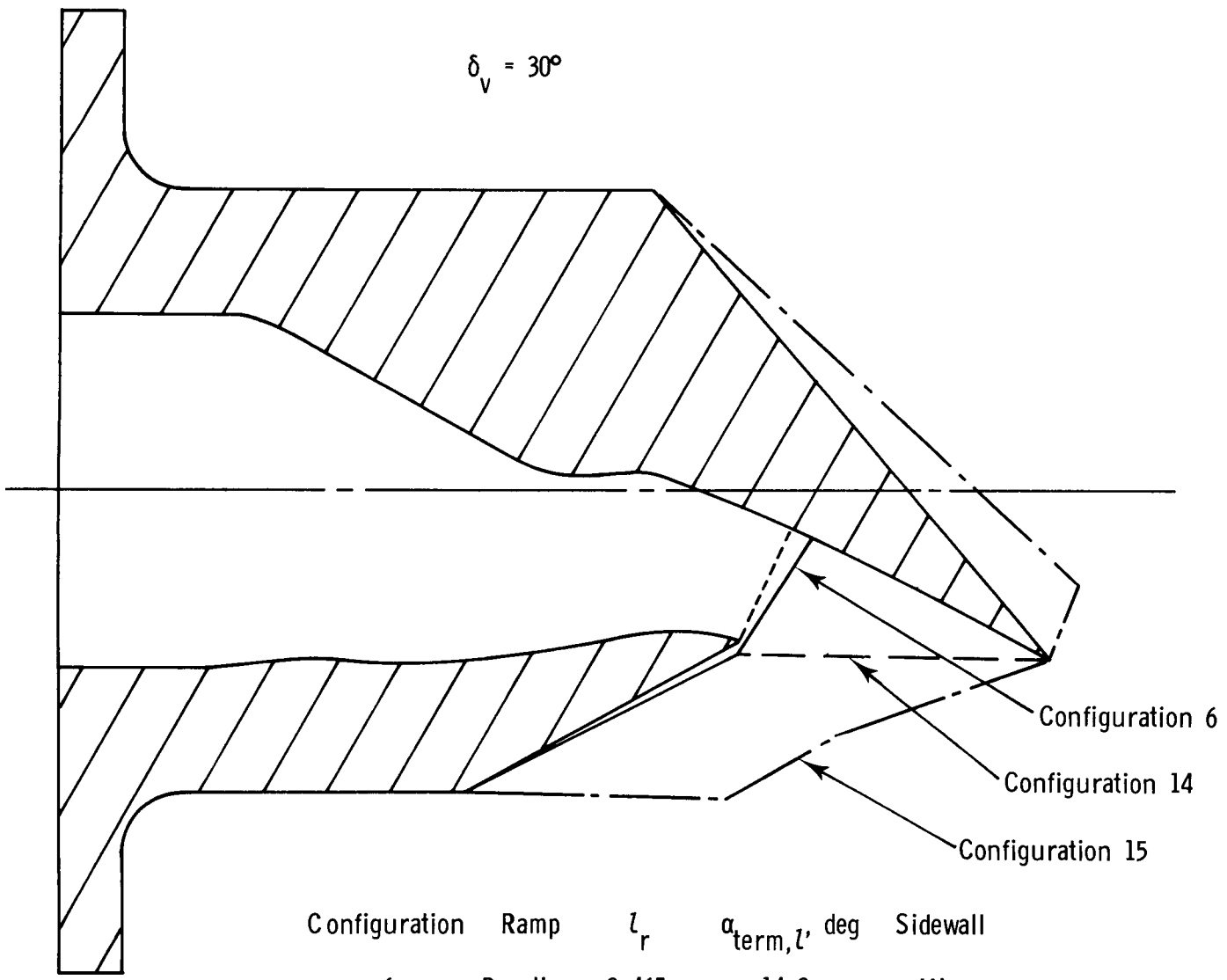

Configuration	Ramp	l_r	$\alpha_{term,l'}$, deg	Sidewall
6	Baseline	3.465	14.8	Min
14	Baseline	3.465	14.8	Med
15	Baseline	3.465	14.8	Max

(f) Configurations 6, 14, and 15.

Figure 4. Continued.

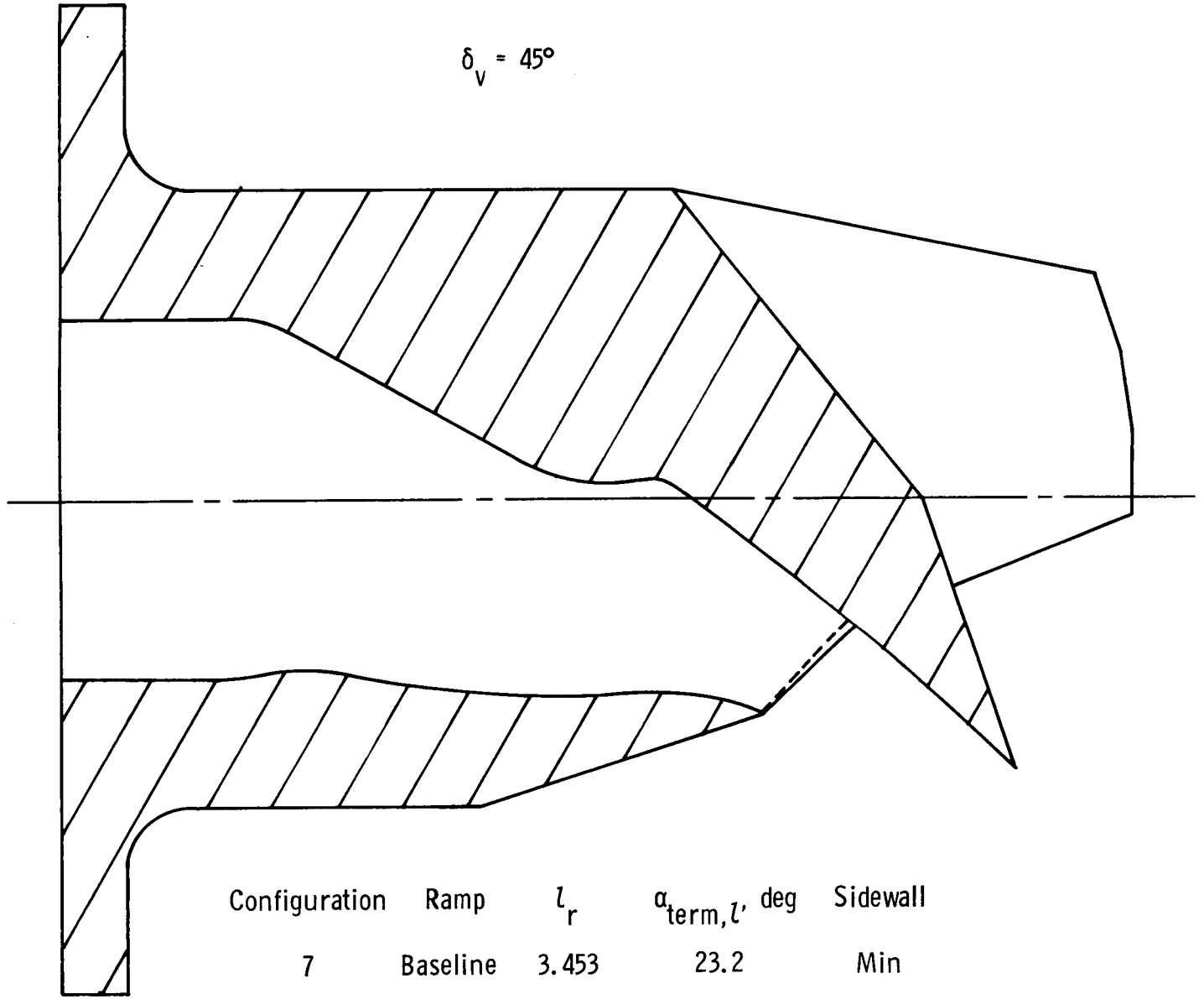

Configuration	Ramp	l_r	$\alpha_{term,l'}$, deg	Sidewall
7	Baseline	3.453	23.2	Min

(g) Configuration 7.

Figure 4. Continued.

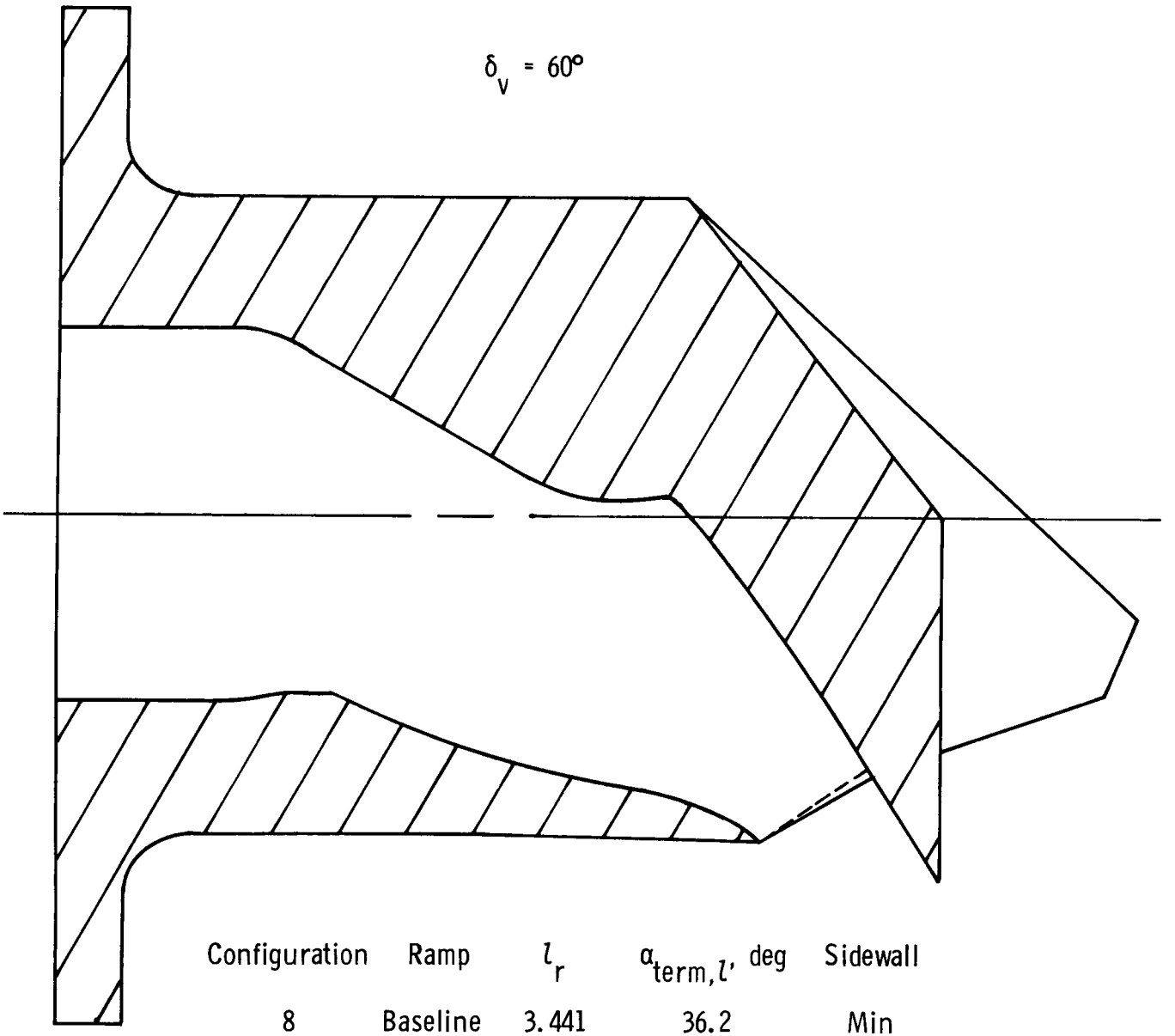

Configuration	Ramp	l_r	$\alpha_{term,l}$, deg	Sidewall
8	Baseline	3.441	36.2	Min

(h) Configuration 8.

Figure 4. Continued.

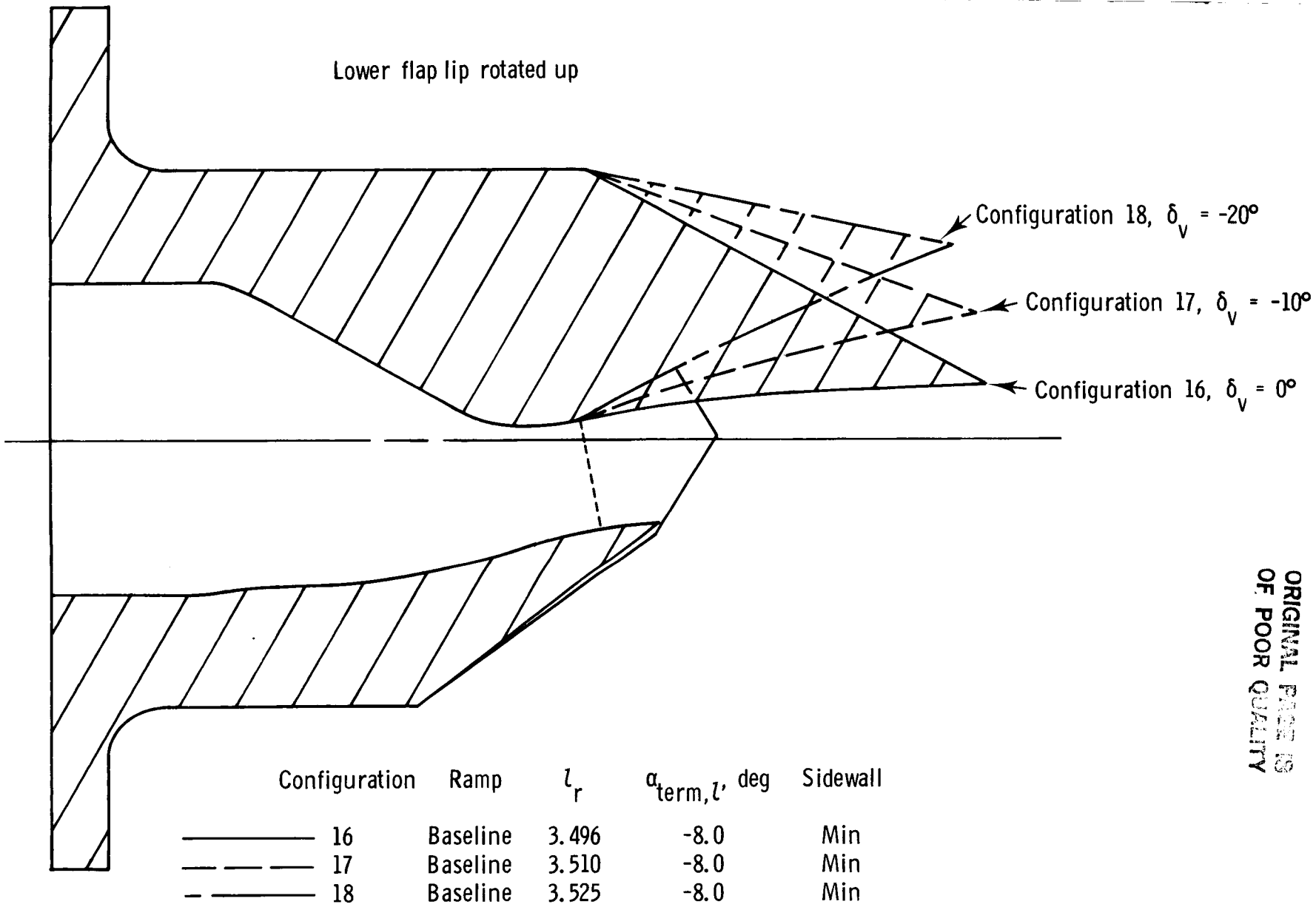

Configuration	Ramp	l_r	$\alpha_{term,l}$, deg	Sidewall
16	Baseline	3.496	-8.0	Min
17	Baseline	3.510	-8.0	Min
18	Baseline	3.525	-8.0	Min

(i) Configurations 16 to 18.

Figure 4. Continued.

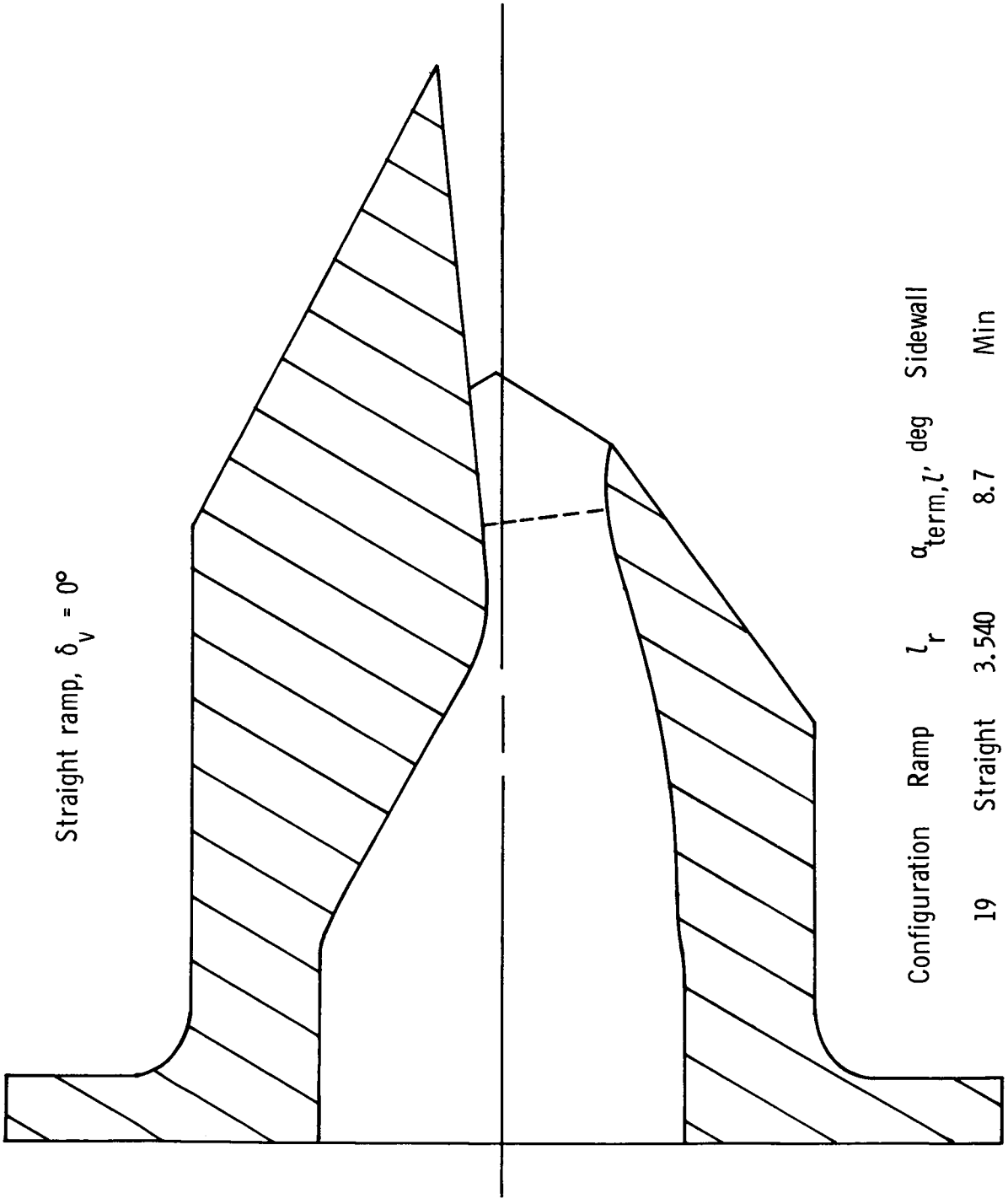

(j) Configuration 19.

Figure 4. Continued.

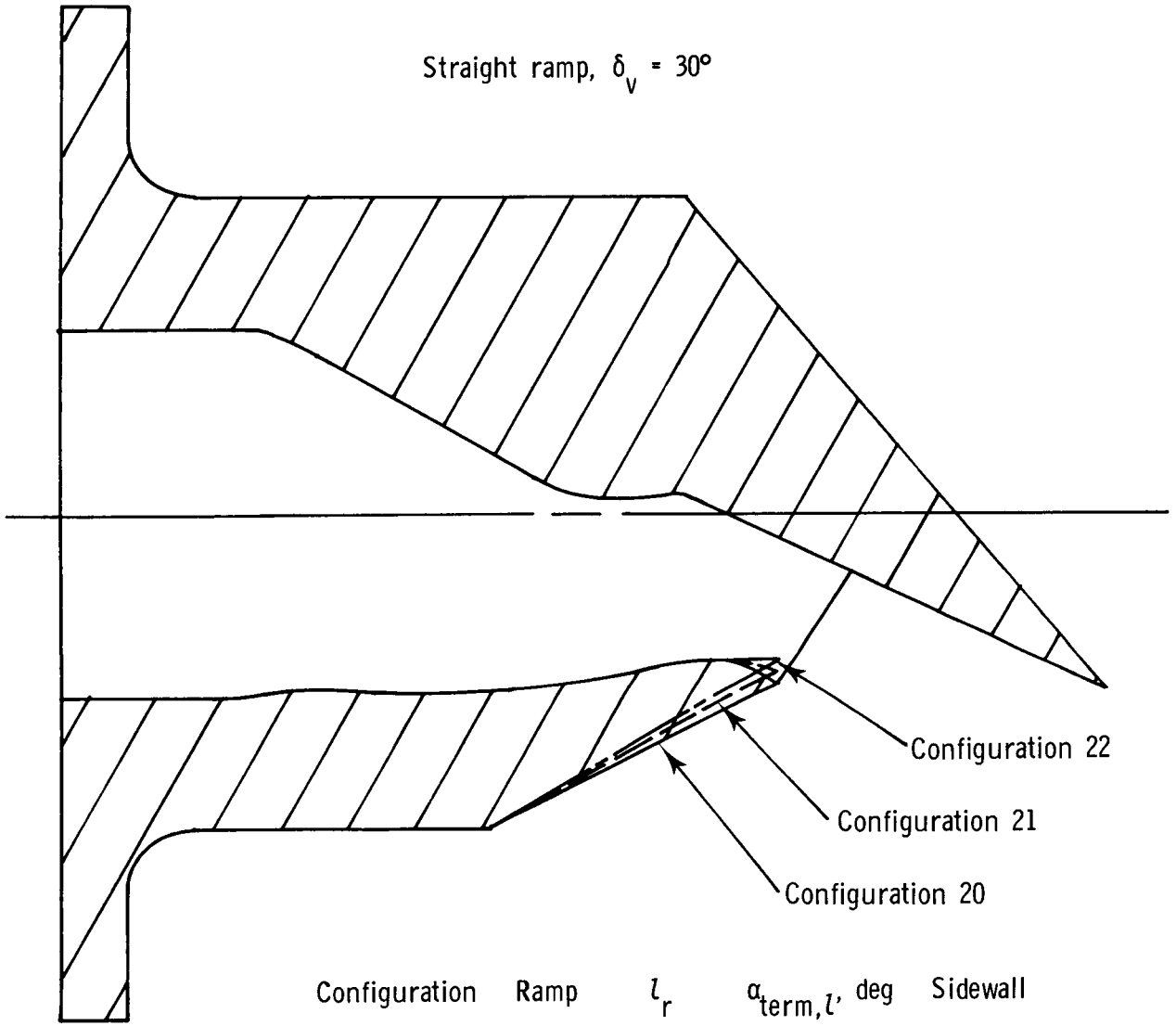

Configuration	Ramp	l_r	$\alpha_{term,l}$, deg	Sidewall
20	Straight	3.465	33.9	Min
21	Straight	3.465	14.8	Min
22	Straight	3.465	- 3.7	Min

(k) Configurations 20 to 22.

Figure 4. Continued.

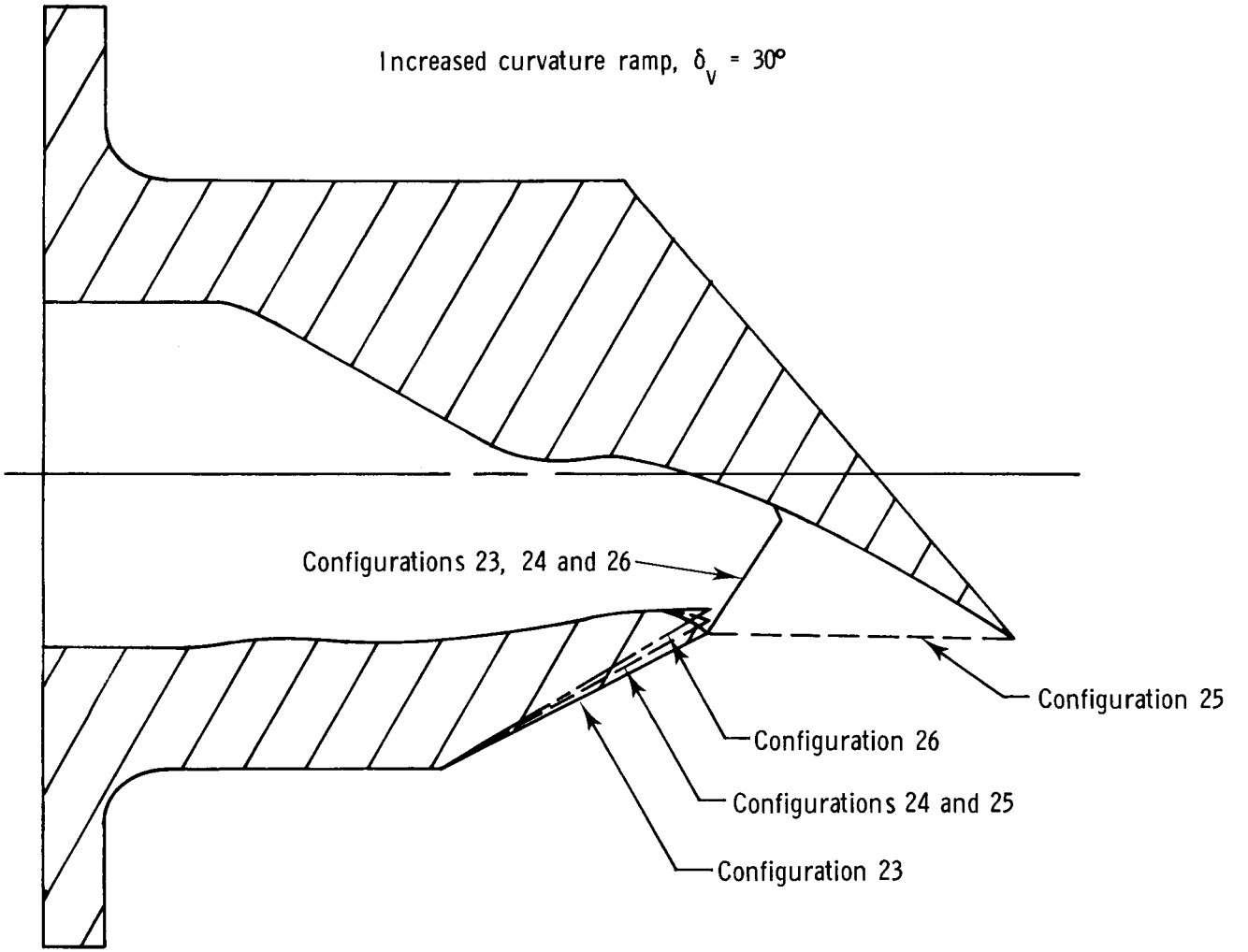

Configuration	Ramp	l_r	$\alpha_{term,l'}$, deg	Sidewall
23	Increased	3.465	33.9	Min
24	Increased	3.465	14.8	Min
25	Increased	3.465	14.8	Med
26	Increased	3.465	-3.7	Min

(l) Configurations 23 to 26.

Figure 4. Continued.

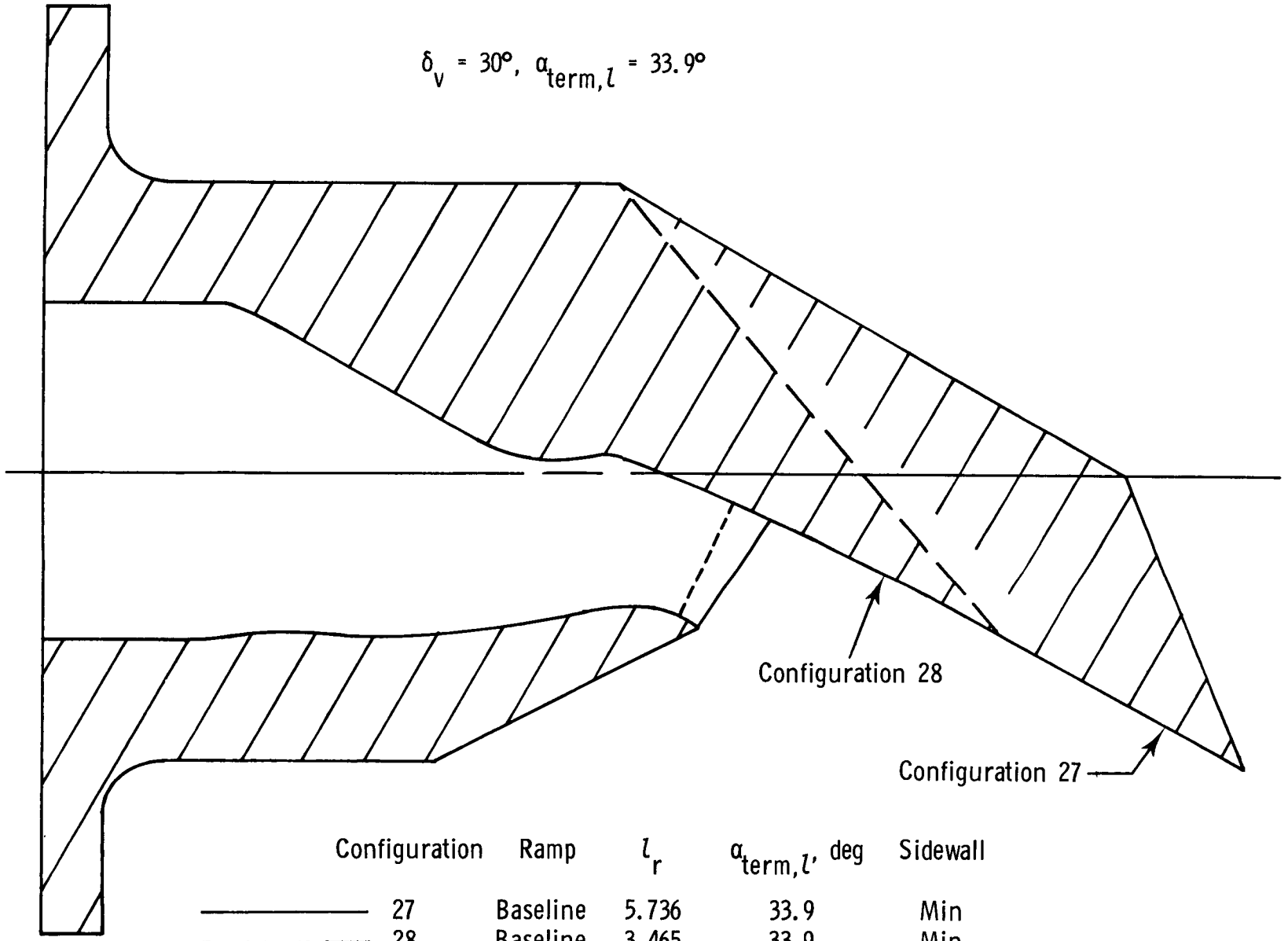

Configuration	Ramp	l_r	$\alpha_{term,l}$, deg	Sidewall
27	Baseline	5.736	33.9	Min
28	Baseline	3.465	33.9	Min

(m) Configurations 27 and 28.

Figure 4. Continued.

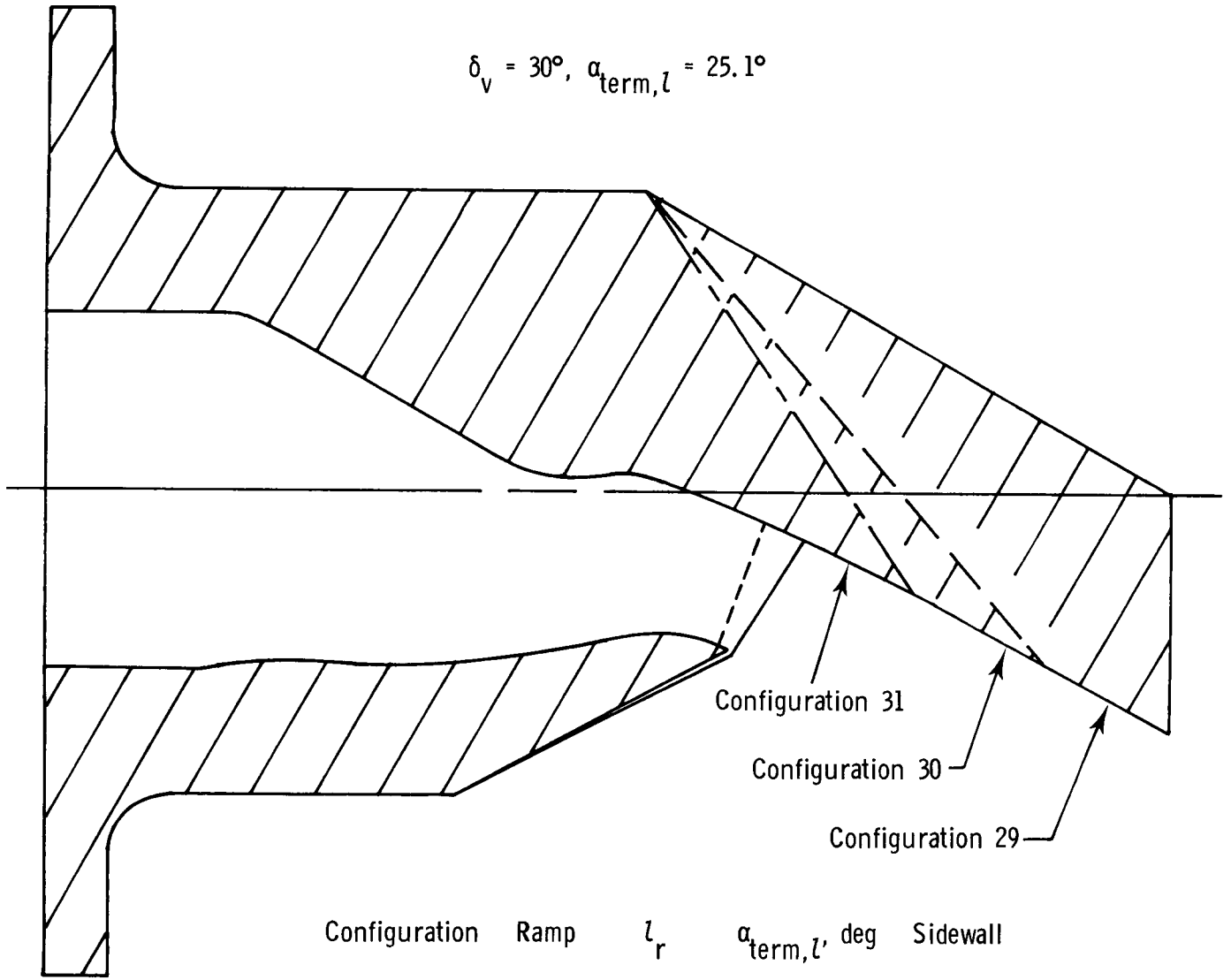

Configuration	Ramp	l_r	$\alpha_{term,l}$, deg	Sidewall
29	Baseline	4.598	25.1	Min
30	Baseline	3.465	25.1	Min
31	Baseline	2.319	25.1	Min

(n) Configurations 29 to 31.

Figure 4. Continued.

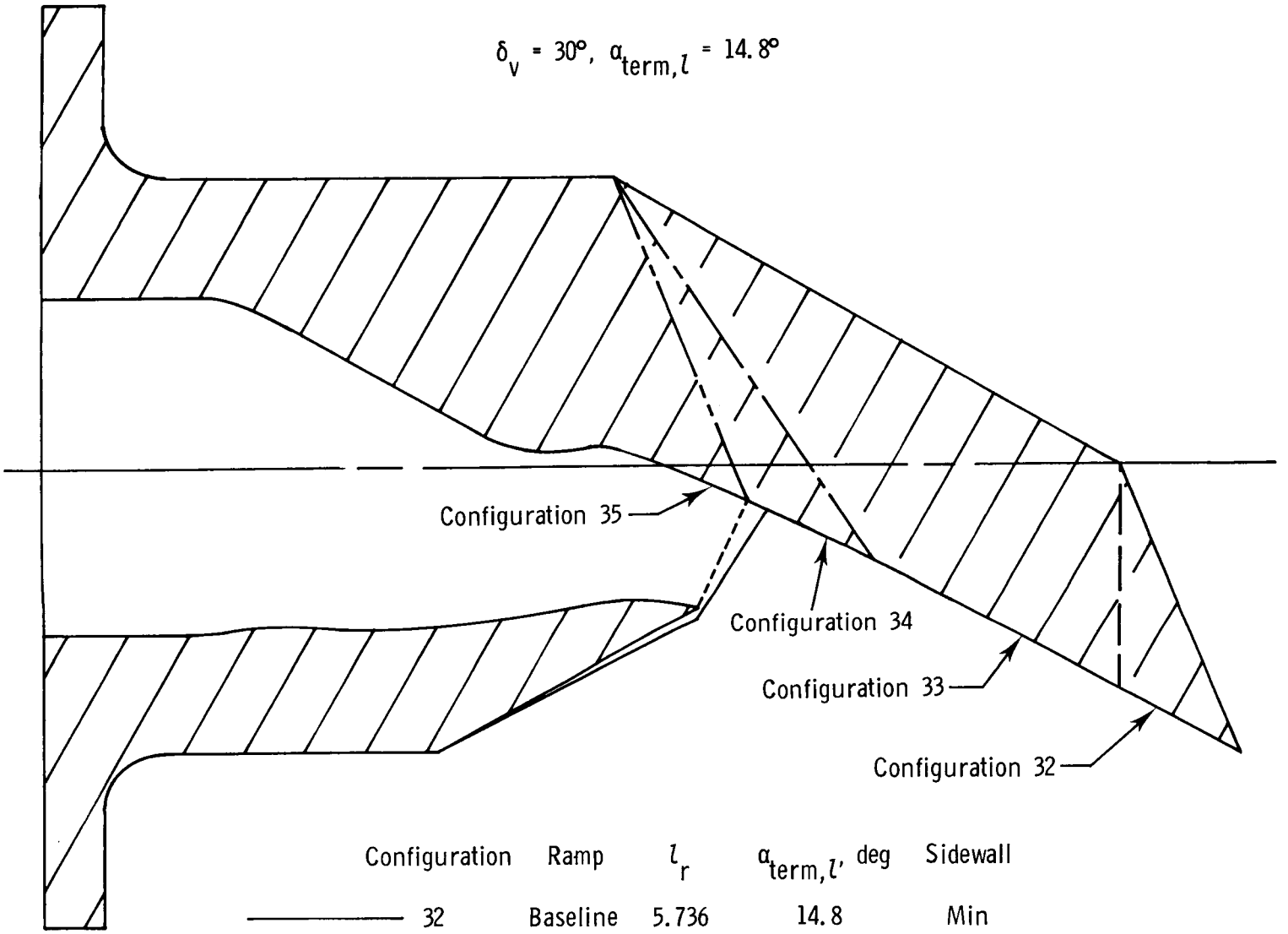

Configuration	Ramp	l_r	$\alpha_{term,l}$, deg	Sidewall
32	Baseline	5.736	14.8	Min
33	Baseline	4.598	14.8	Min
34	Baseline	2.319	14.8	Min
35	Baseline	1.169	14.8	Min

(o) Configurations 32 to 35.

Figure 4. Continued.

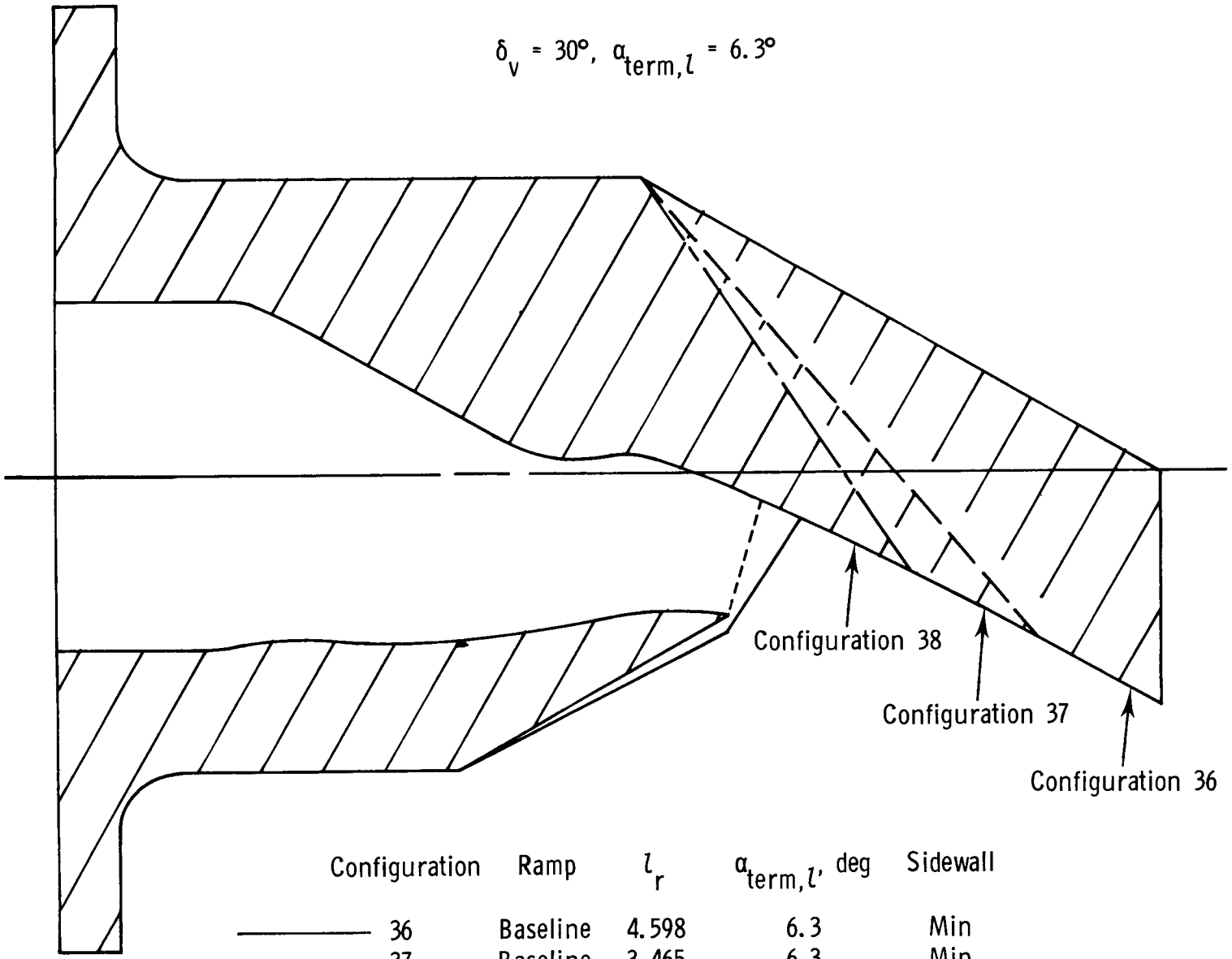

Configuration	Ramp	l_r	$\alpha_{term,l}$, deg	Sidewall
——— 36	Baseline	4.598	6.3	Min
— — — 37	Baseline	3.465	6.3	Min
– ——— 38	Baseline	2.319	6.3	Min

(p) Configurations 36 to 38.

Figure 4. Continued.

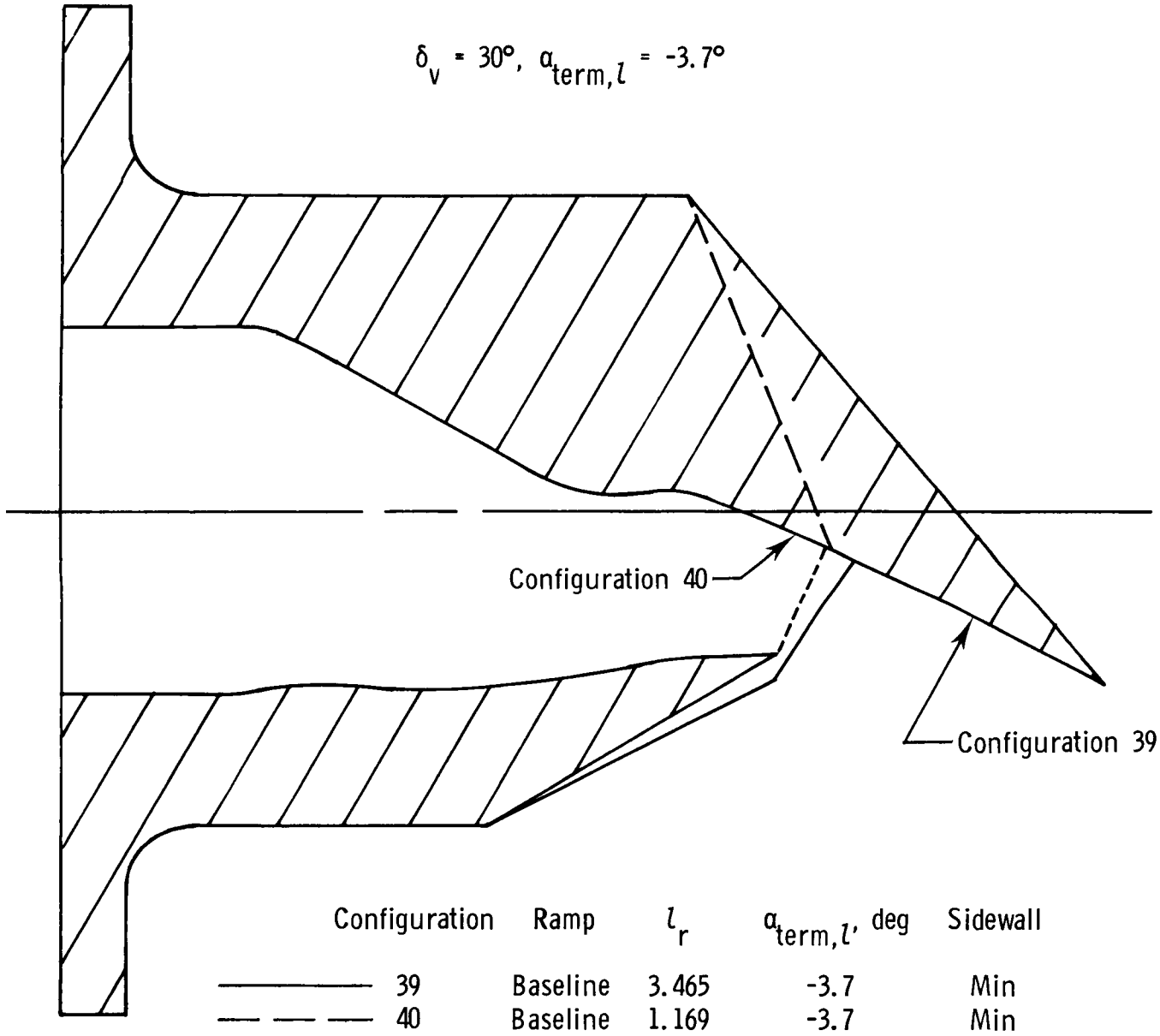

Configuration	Ramp	l_r	$\alpha_{term,l}$, deg	Sidewall
39	Baseline	3.465	-3.7	Min
40	Baseline	1.169	-3.7	Min

(q) Configurations 39 and 40.

Figure 4. Concluded.

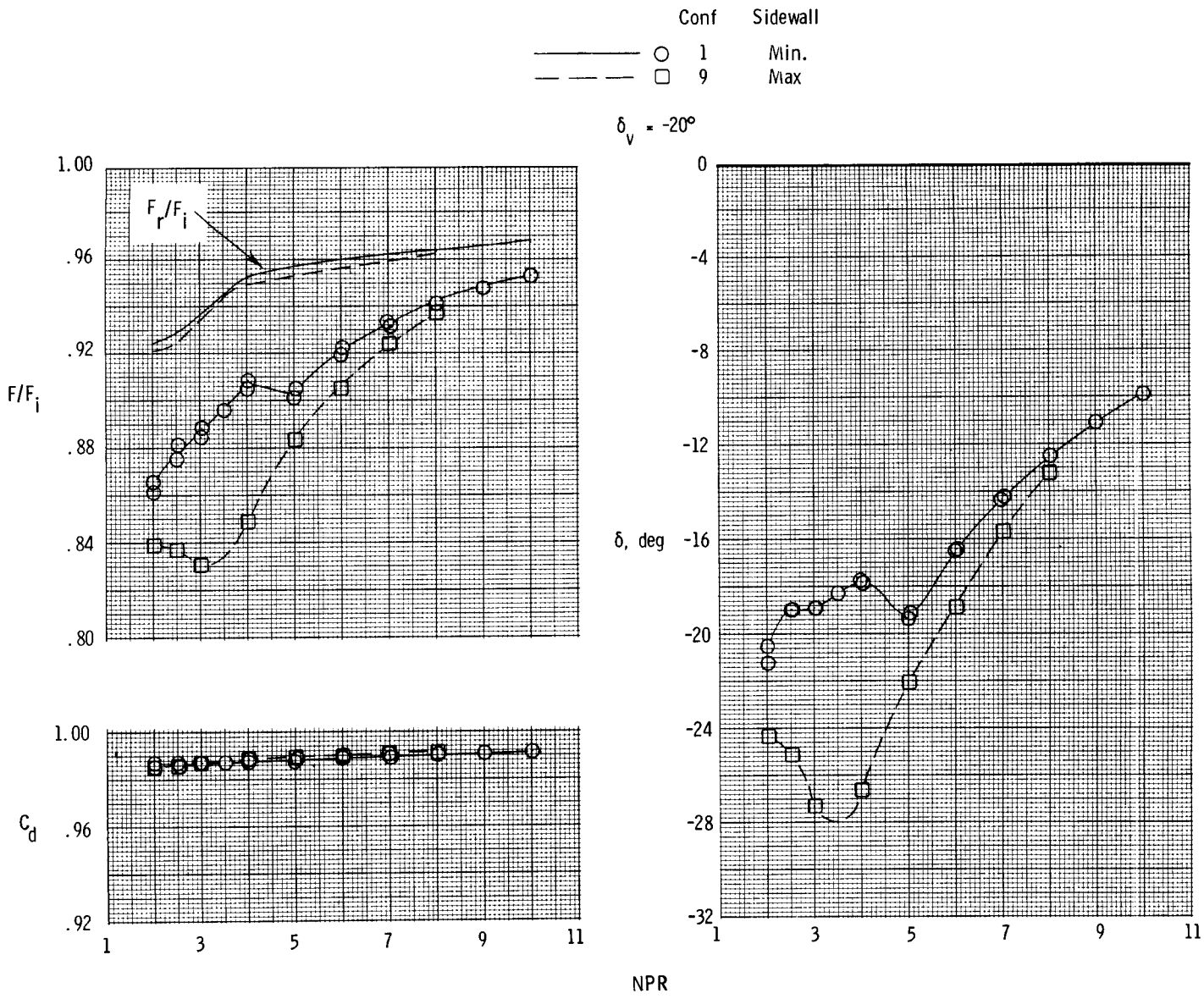

(a) Configurations 1 and 9.

Figure 5. Variation of nozzle thrust ratio, discharge coefficient, and resultant thrust-vector angle with nozzle pressure ratio. Faired lines with no symbols indicate resultant thrust ratio F_r/F_i.

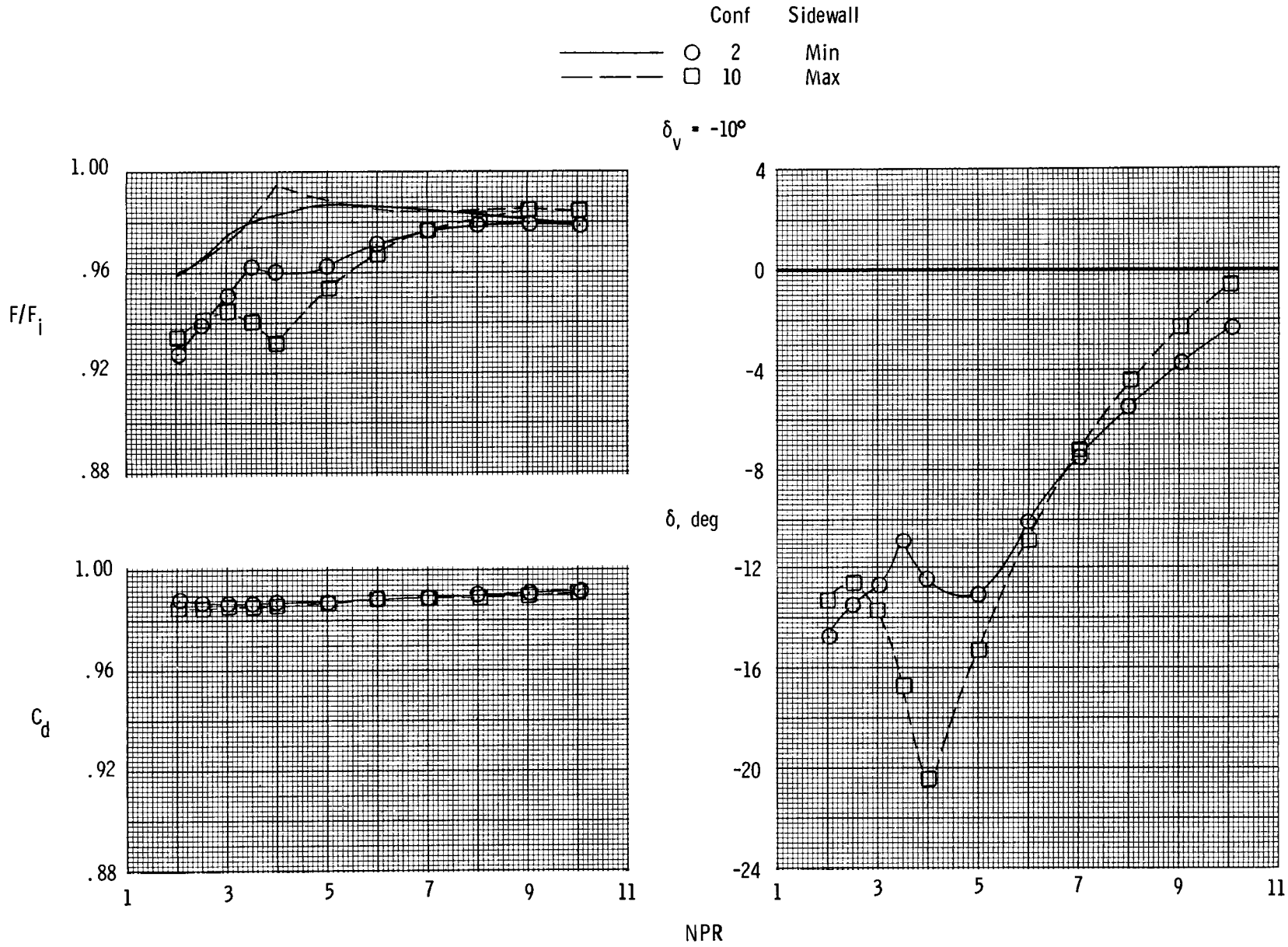

(b) Configurations 2 and 10.

Figure 5. Continued.

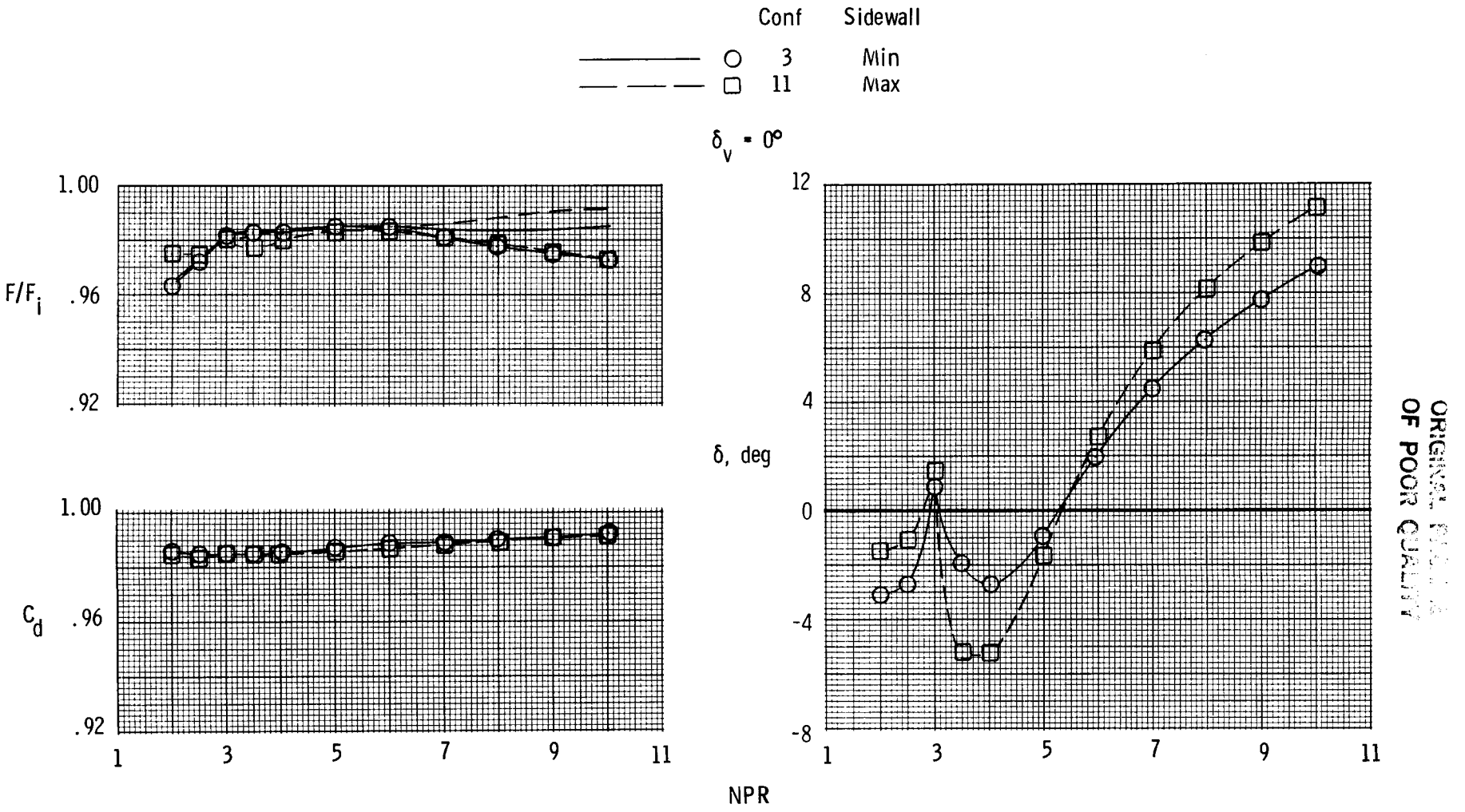

(c) Configurations 3 and 11.

Figure 5. Continued.

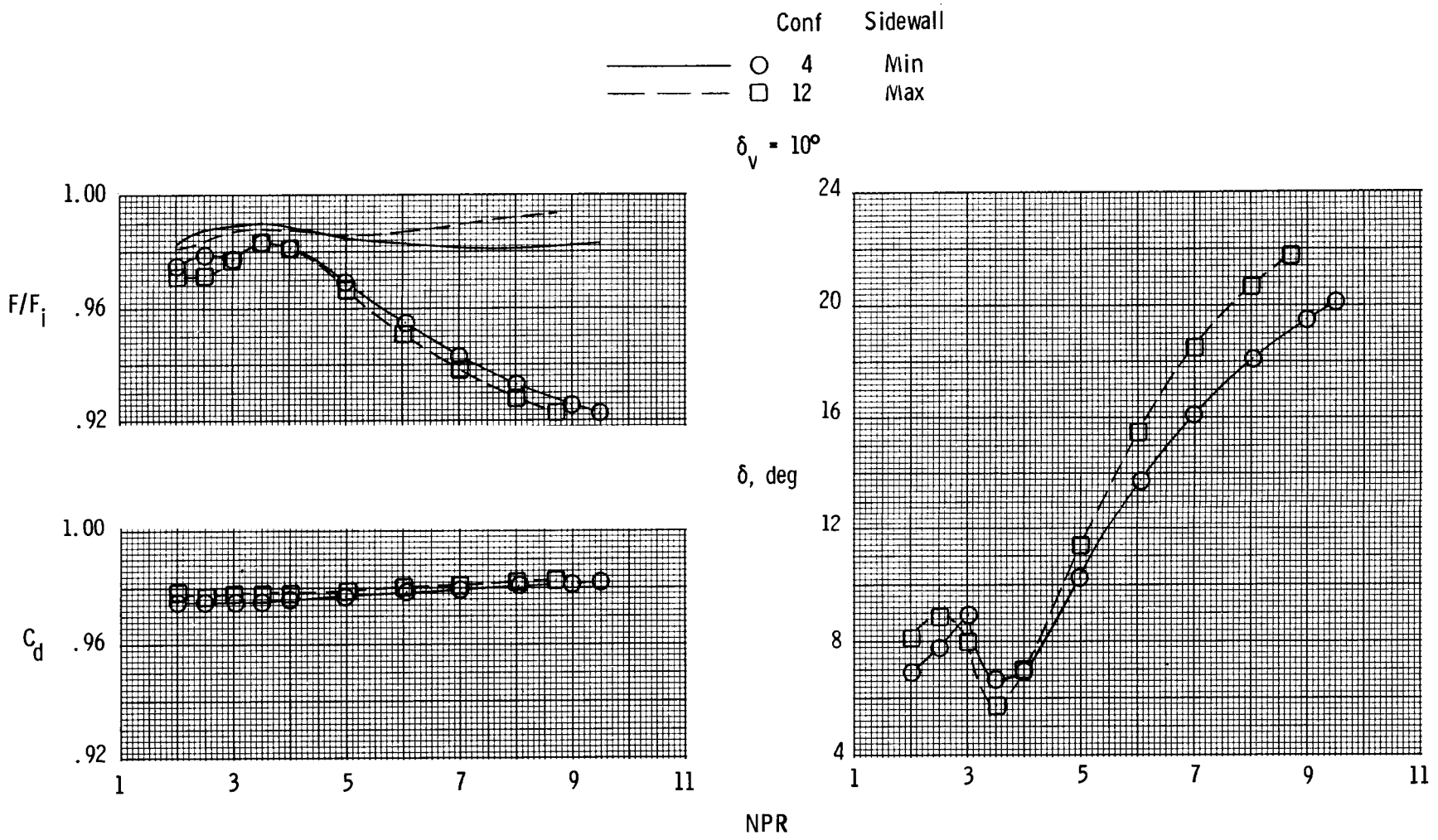

(d) Configurations 4 and 12.

Figure 5. Continued.

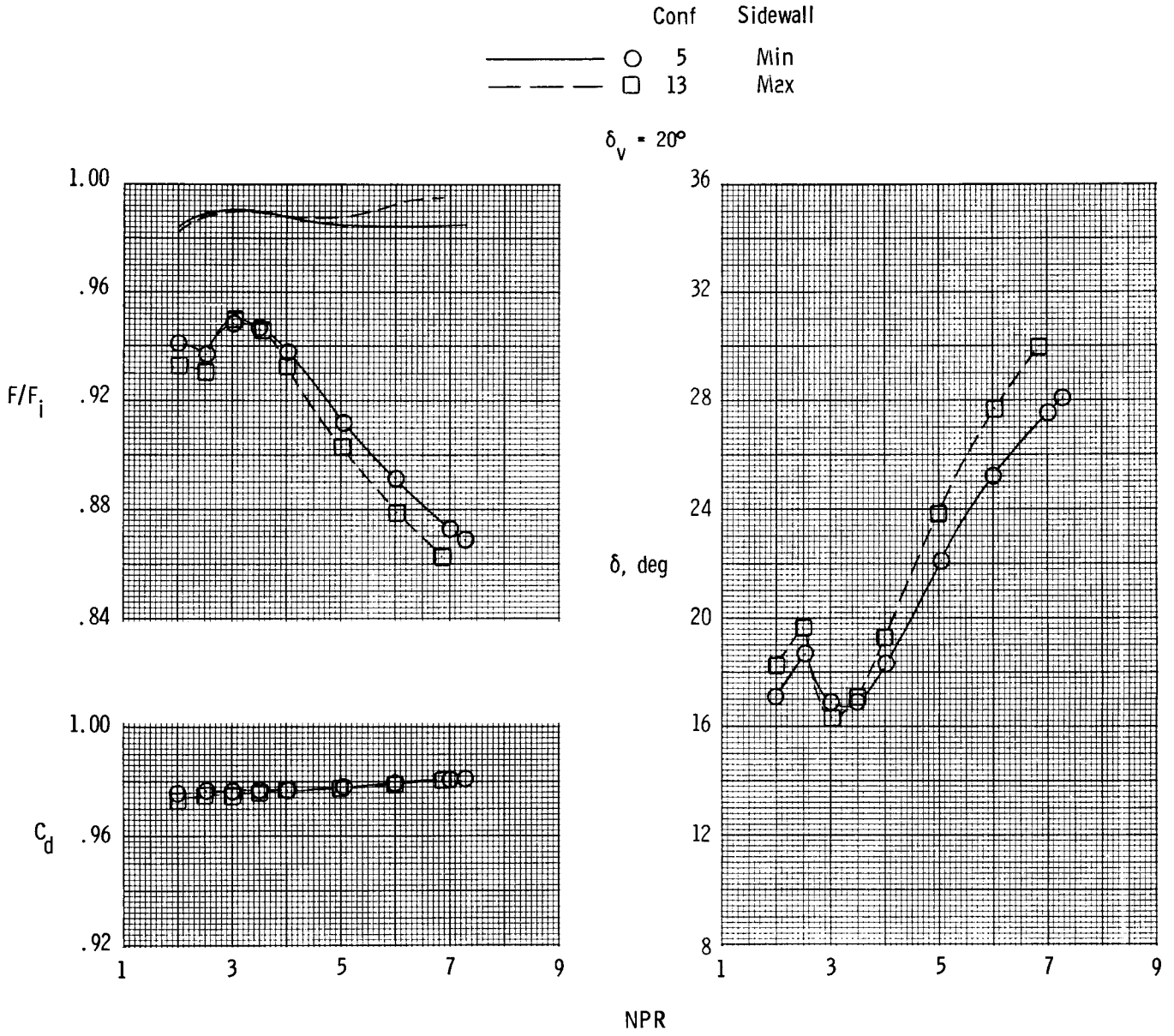

(e) Configurations 5 and 13.

Figure 5. Continued.

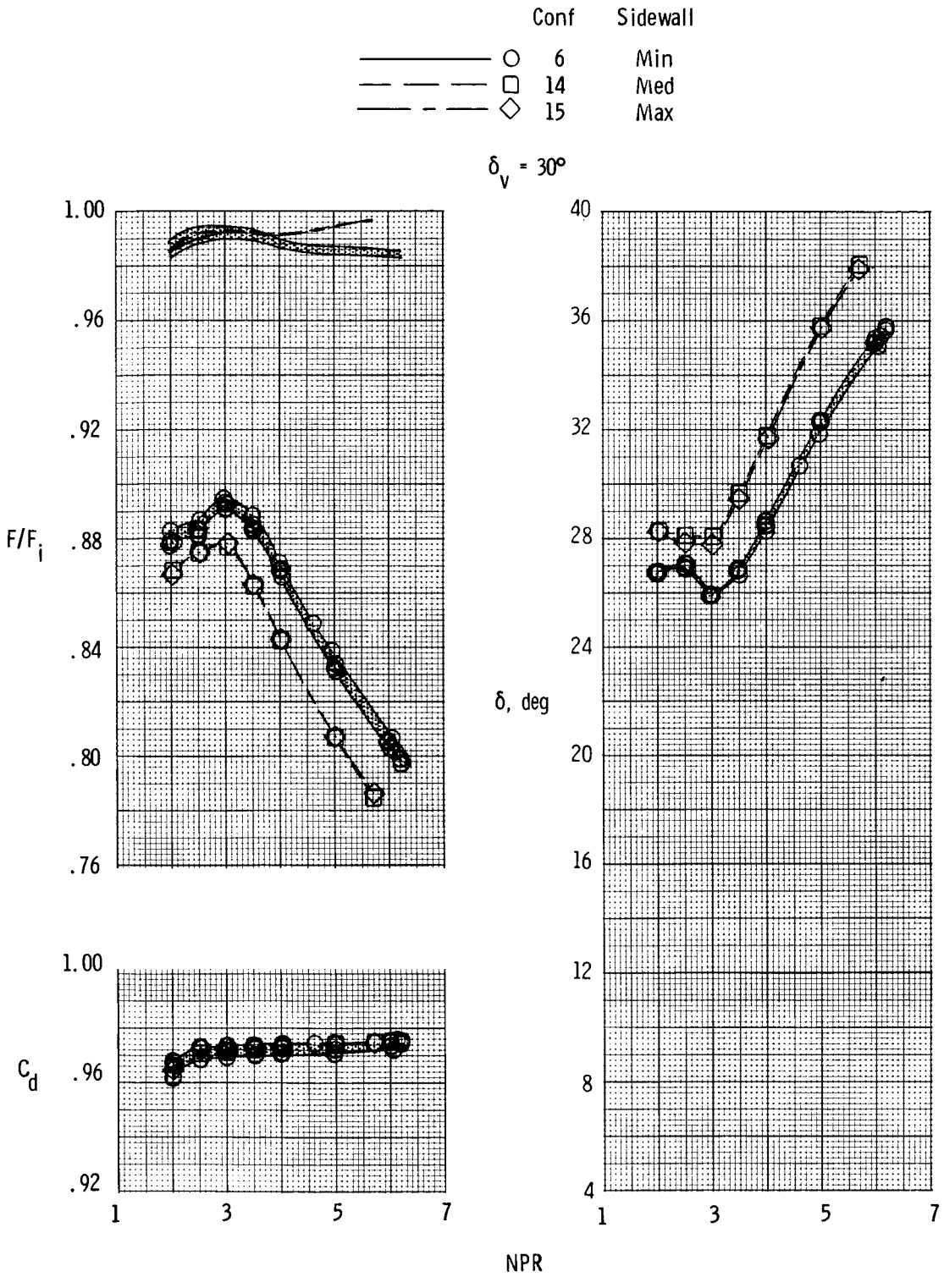

(f) Configurations 6, 14, and 15.

Figure 5. Continued.

C-2

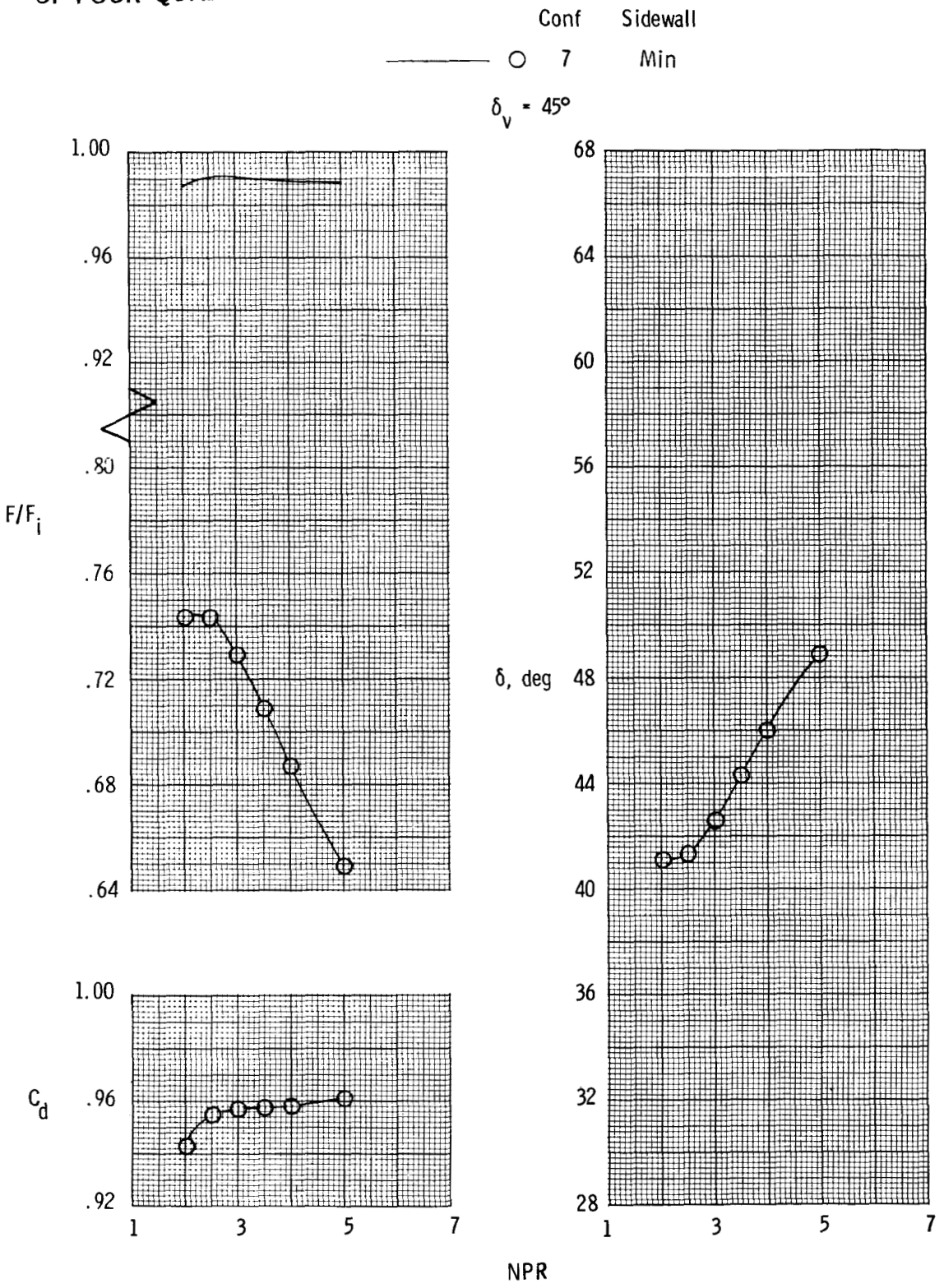

(g) Configuration 7.

Figure 5. Continued.

C2

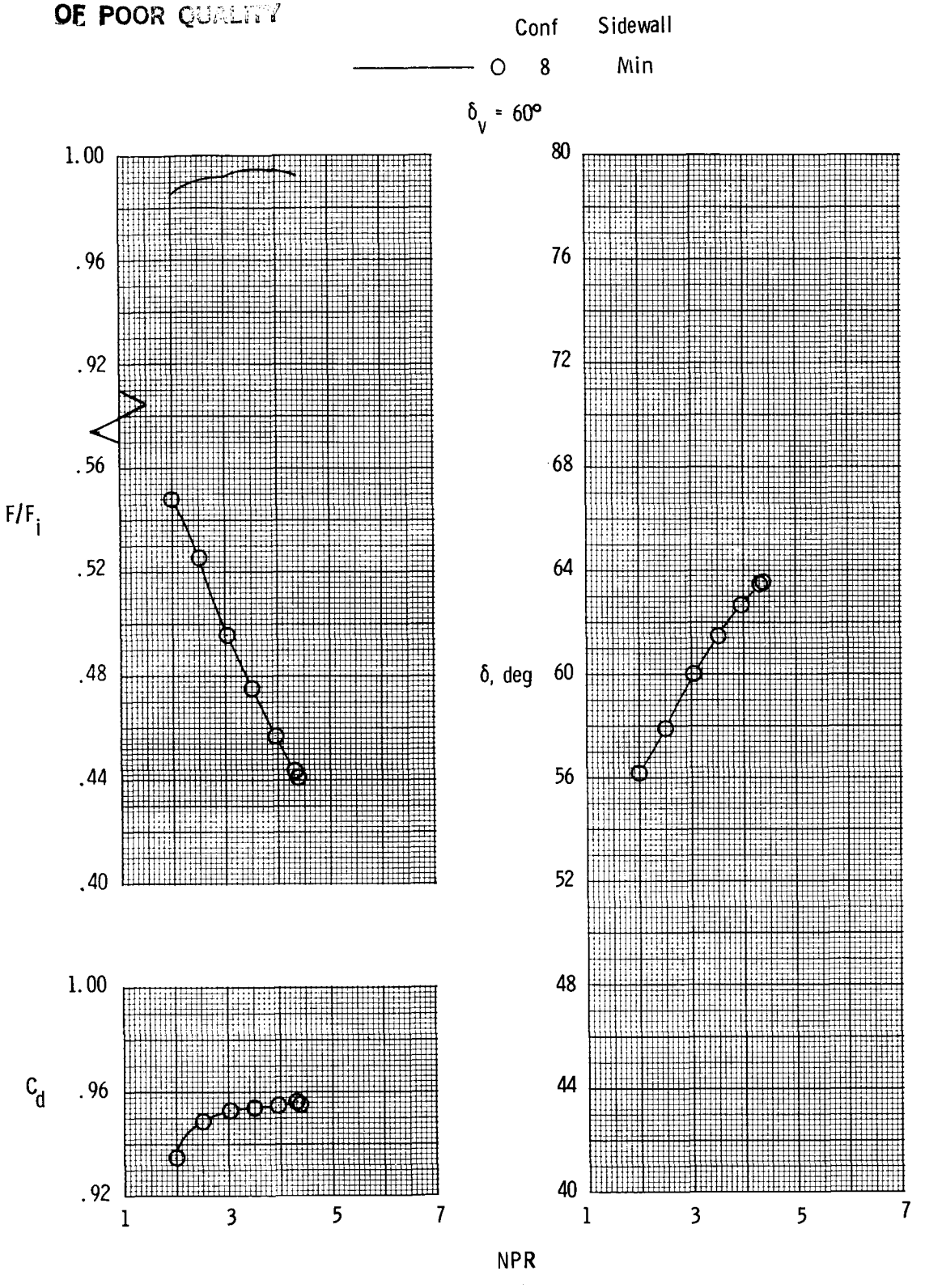

(h) Configuration 8.

Figure 5. Continued.

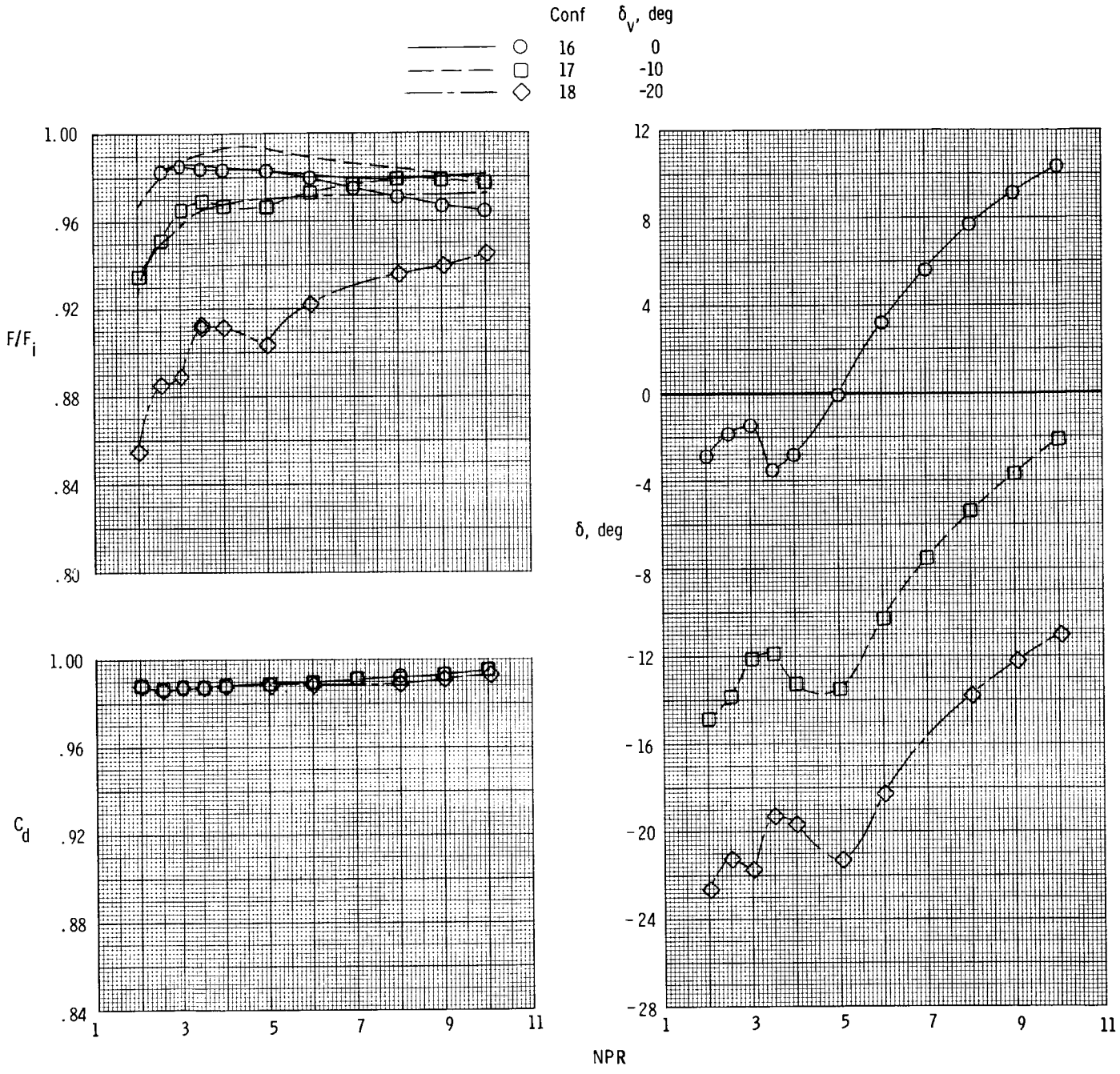

(i) Configurations 16 to 18.

Figure 5. Continued.

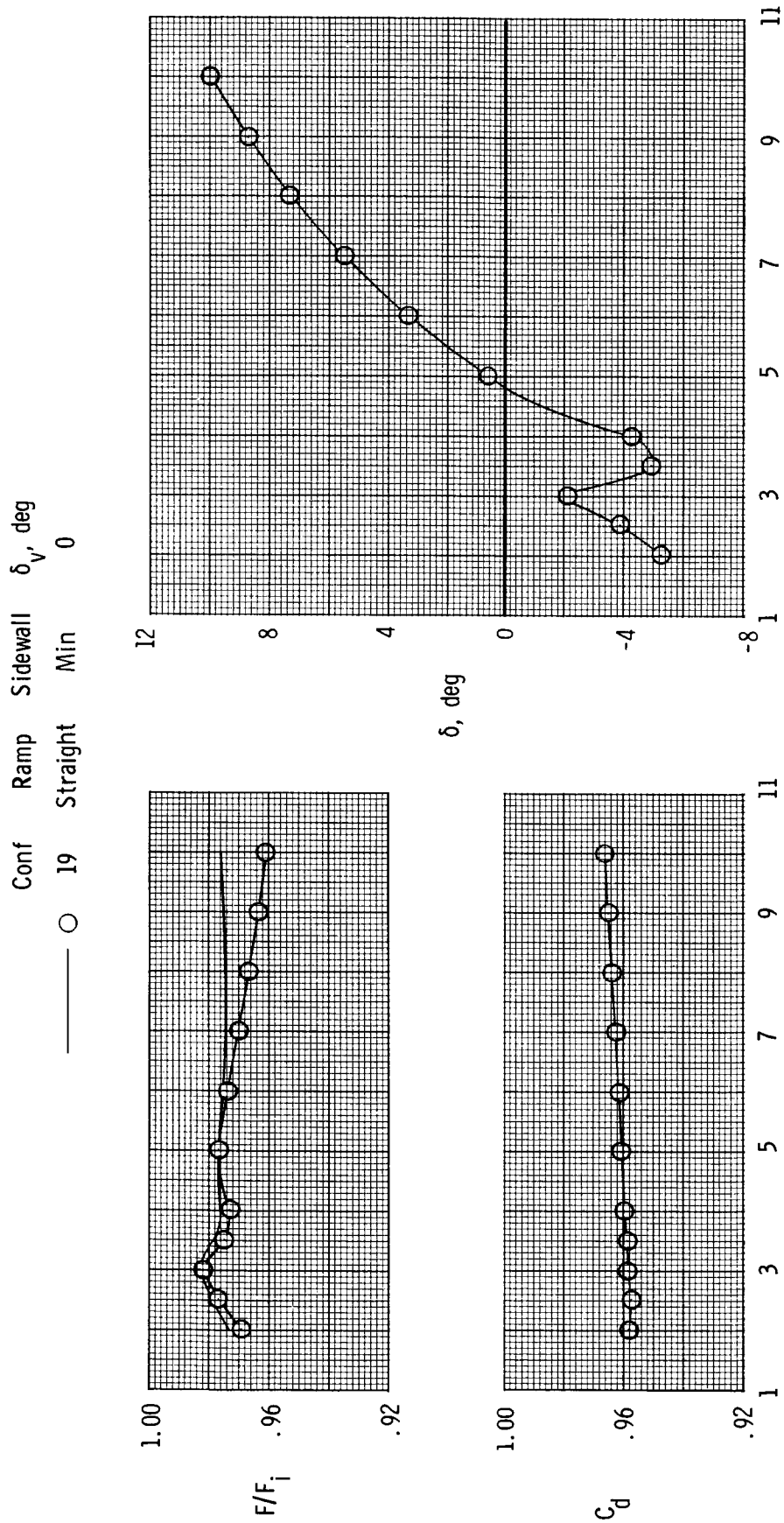

(j) Configuration 19.

Figure 5. Continued.

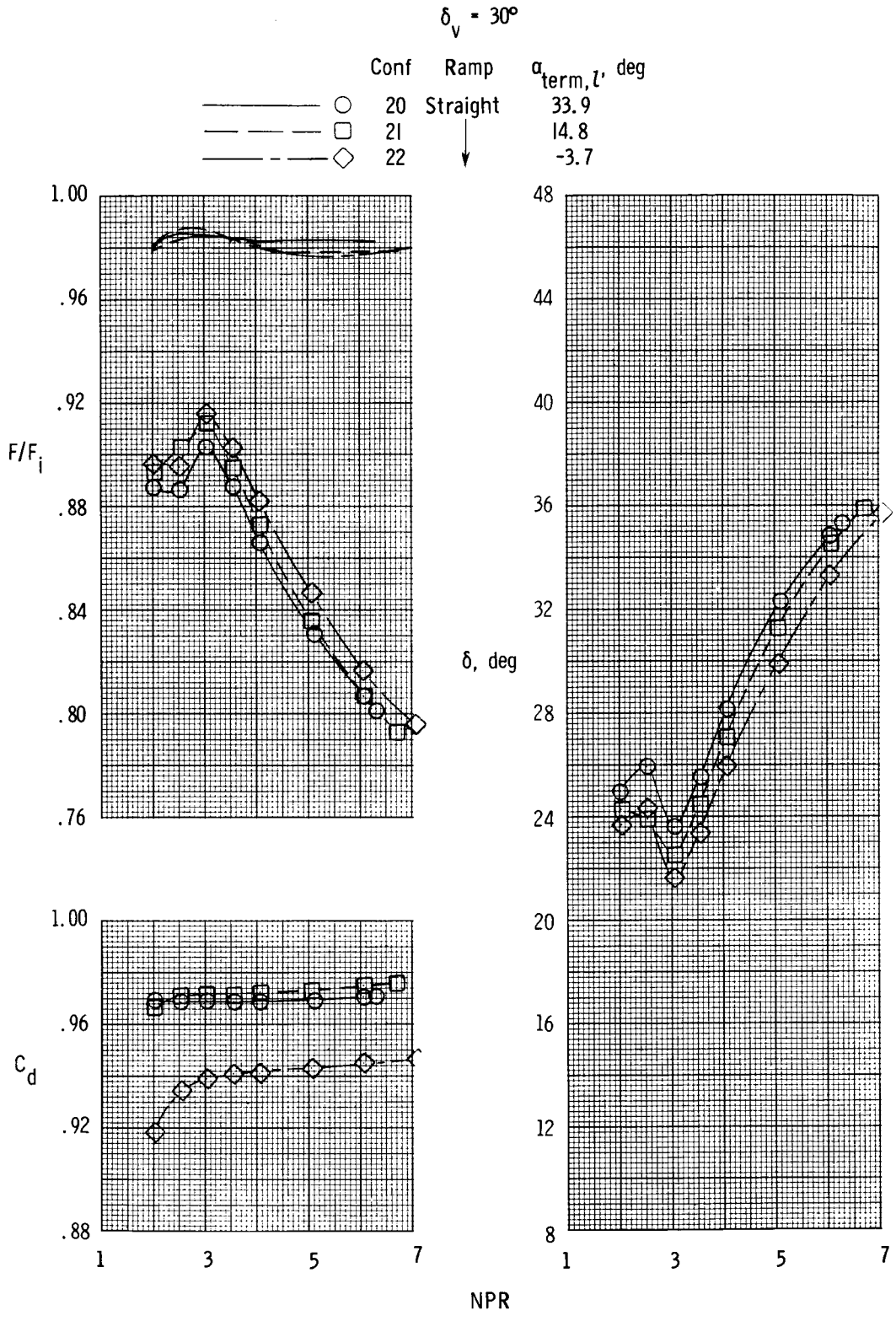

(k) Configurations 20 to 22.

Figure 5. Continued.

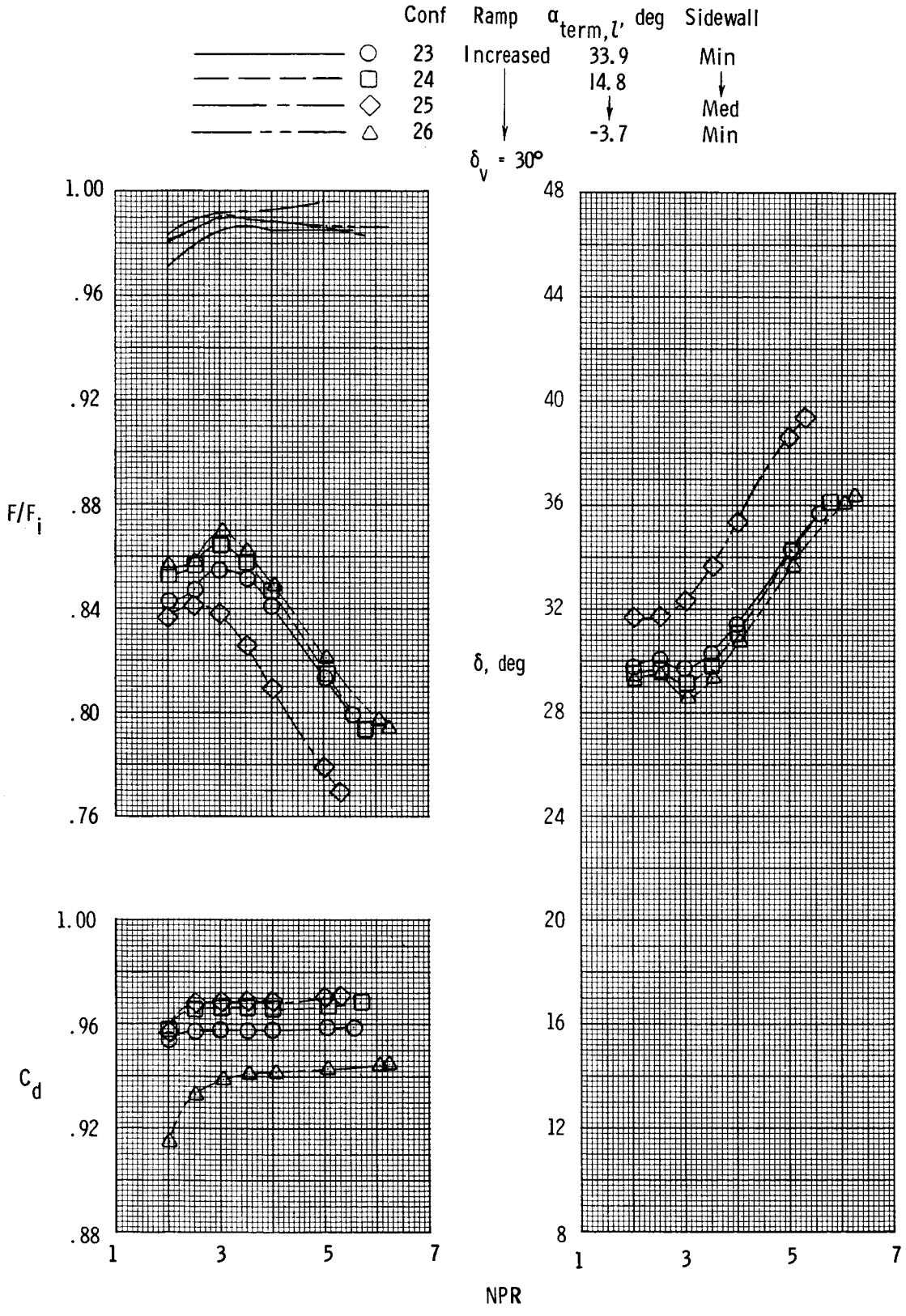

(l) Configurations 23 to 26.

Figure 5. Continued.

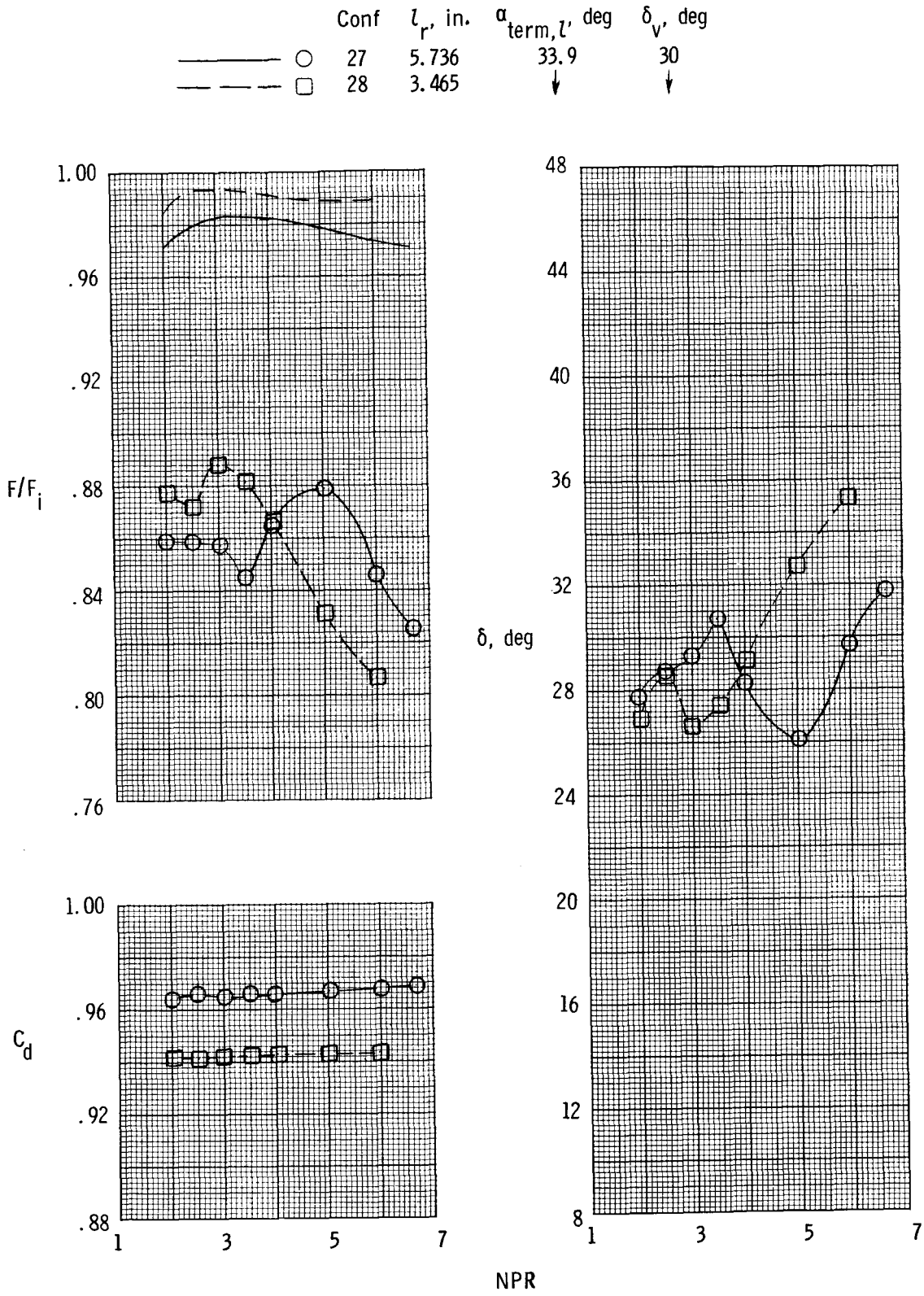

(m) Configurations 27 and 28.

Figure 5. Continued.

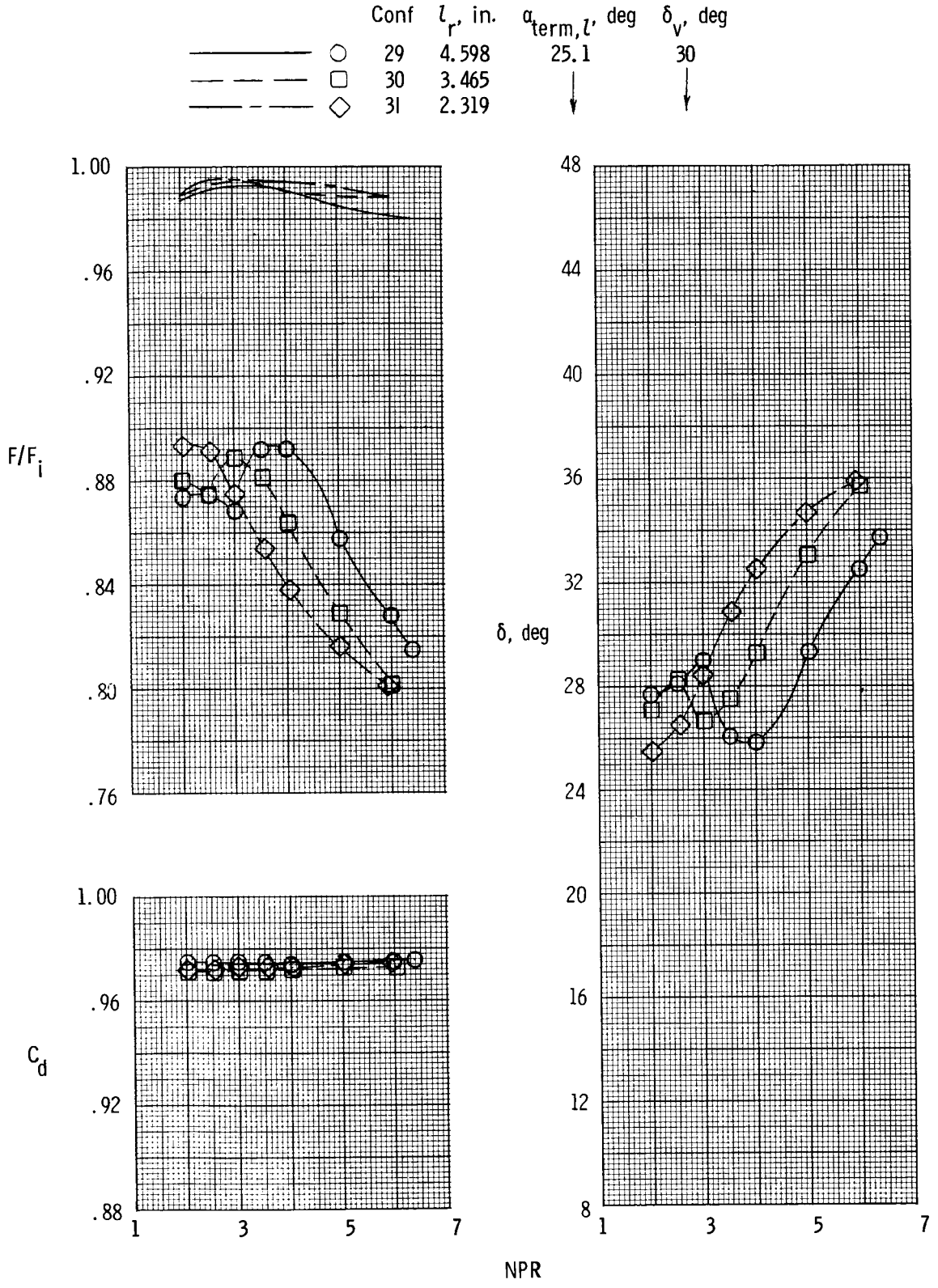

(n) Configurations 29 to 31.

Figure 5. Continued.

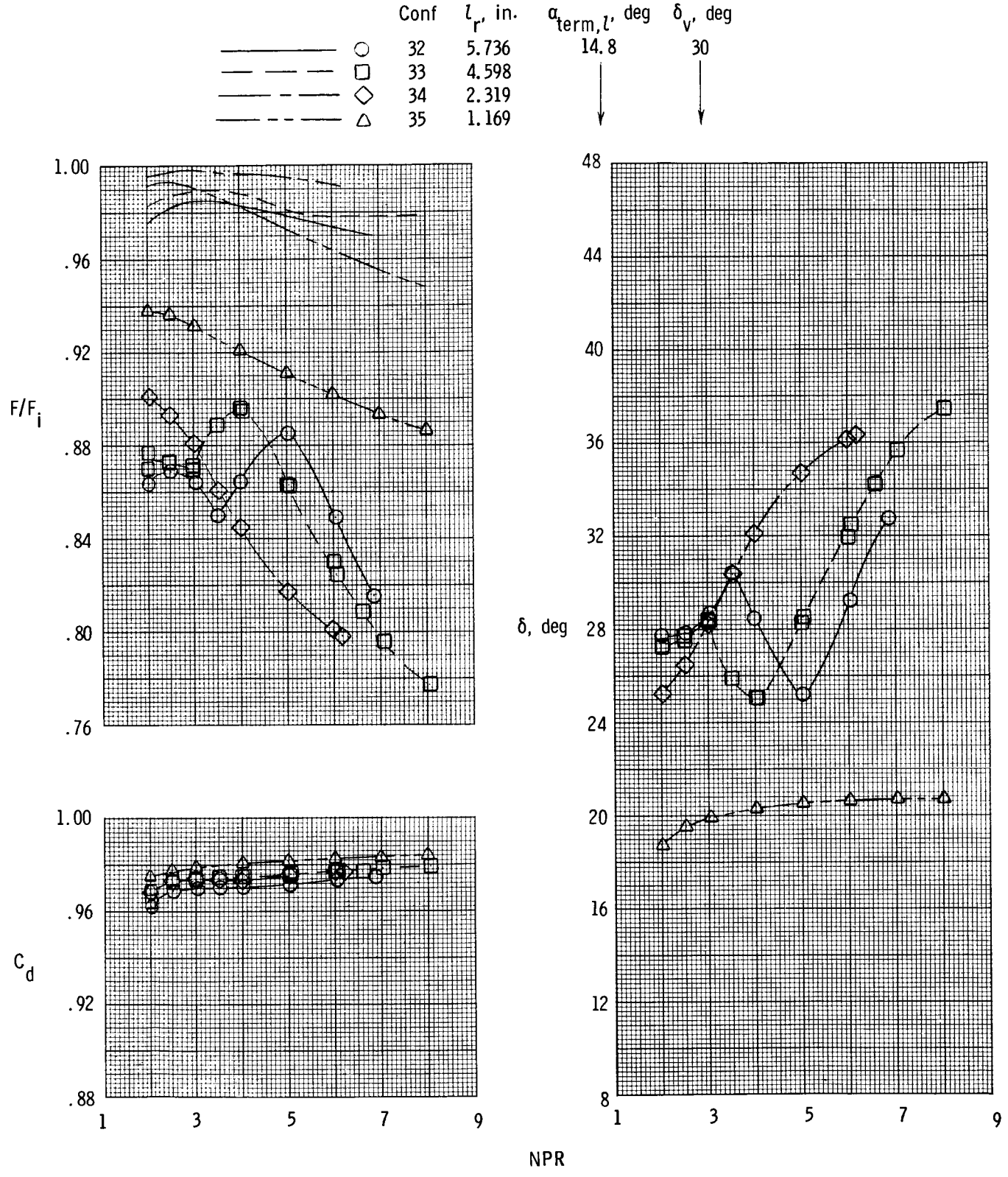

(o) Configurations 32 to 35.

Figure 5. Continued.

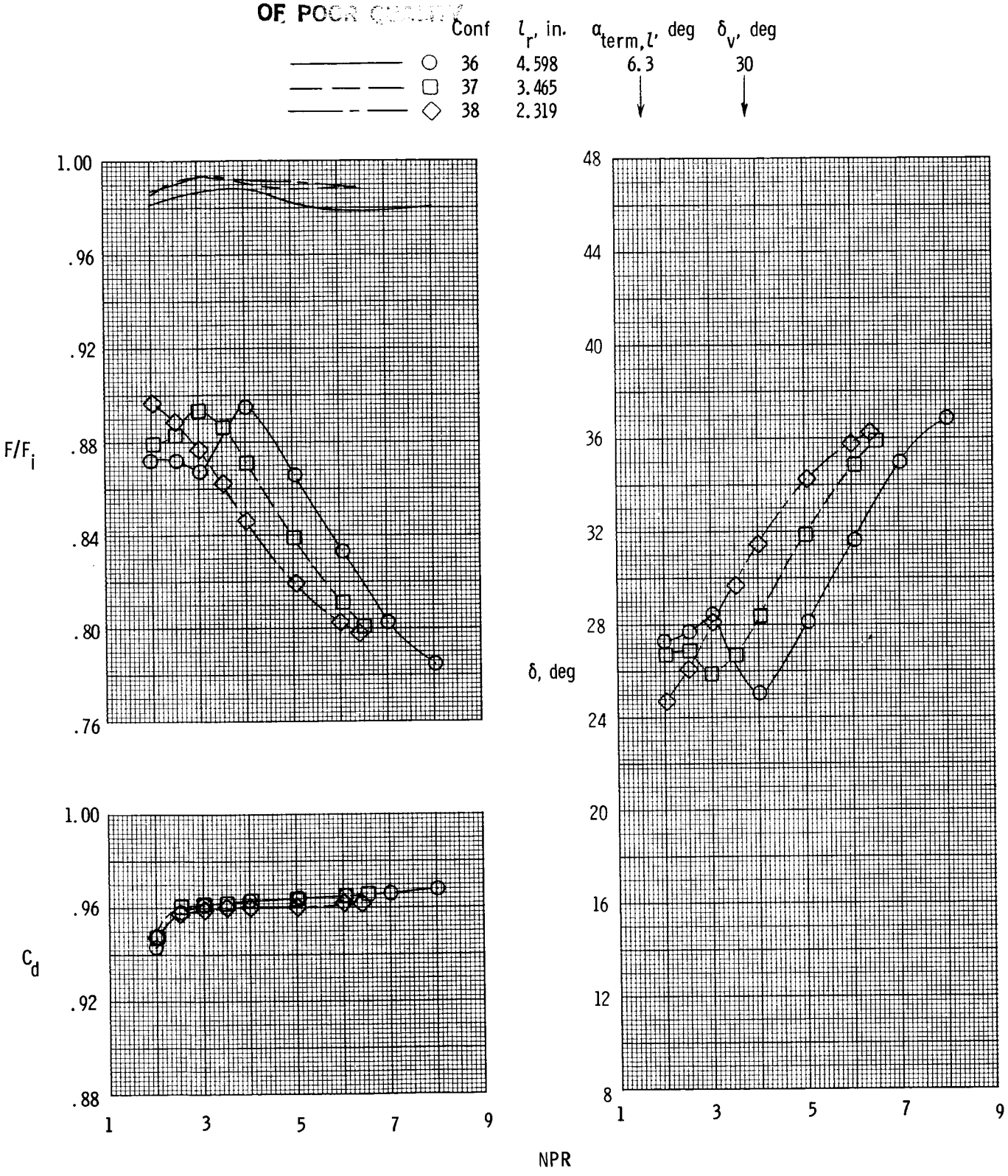

(p) Configurations 36 to 38.

Figure 5. Continued.

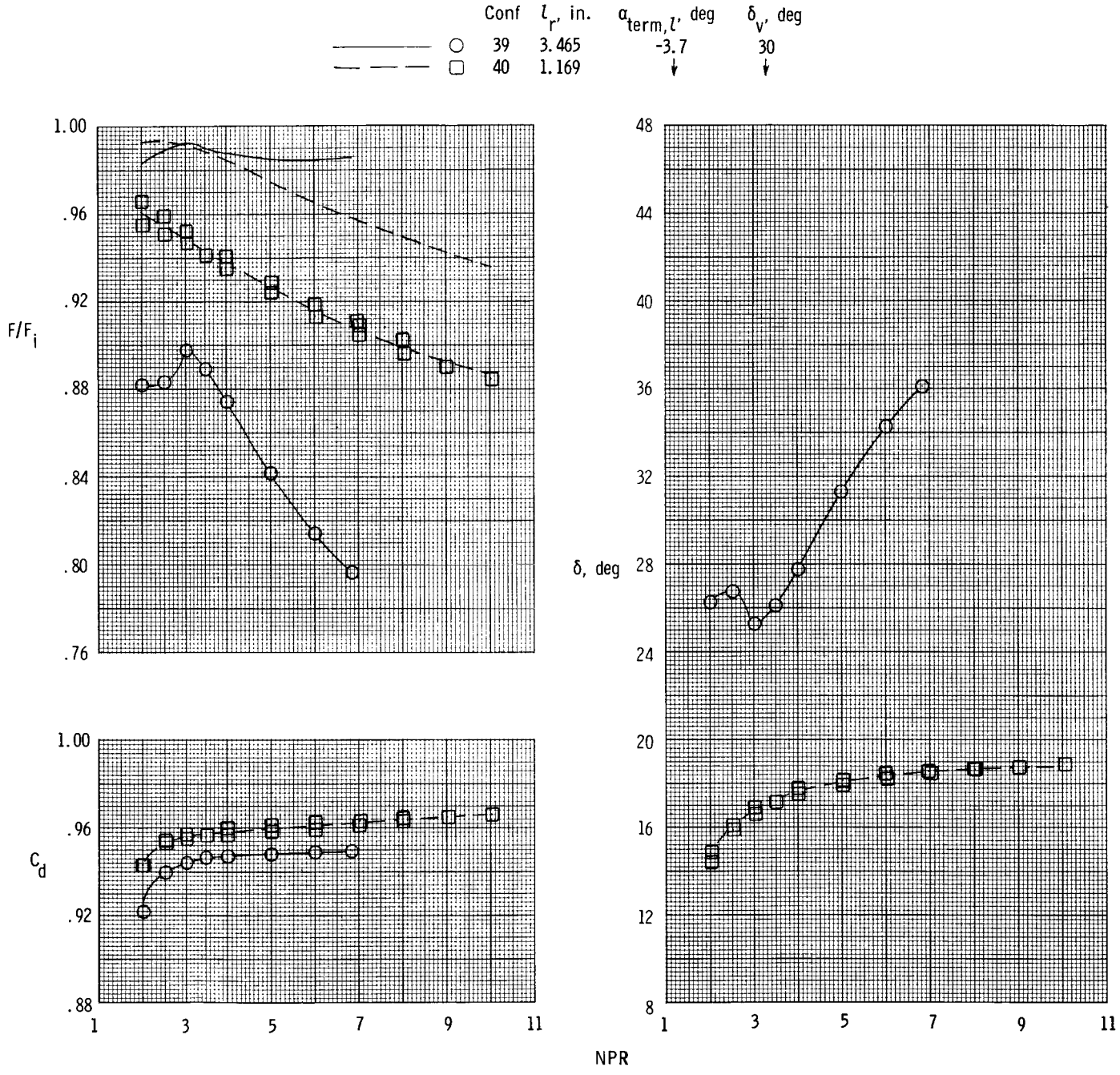

(q) Configurations 39 and 40.

Figure 5. Concluded.

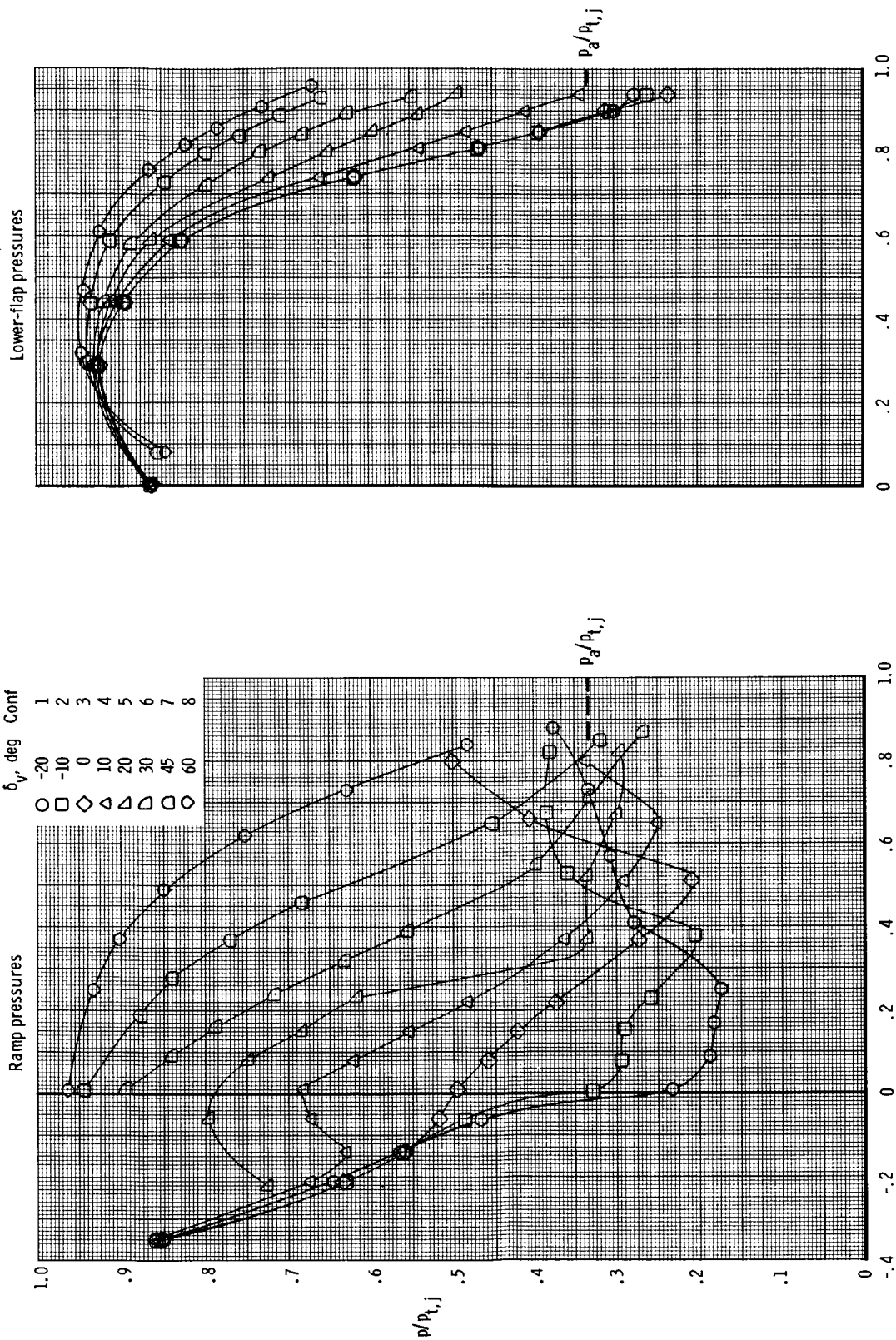

Figure 6. Effect of vector angle on flap centerline pressure distributions at NPR = 3.0.

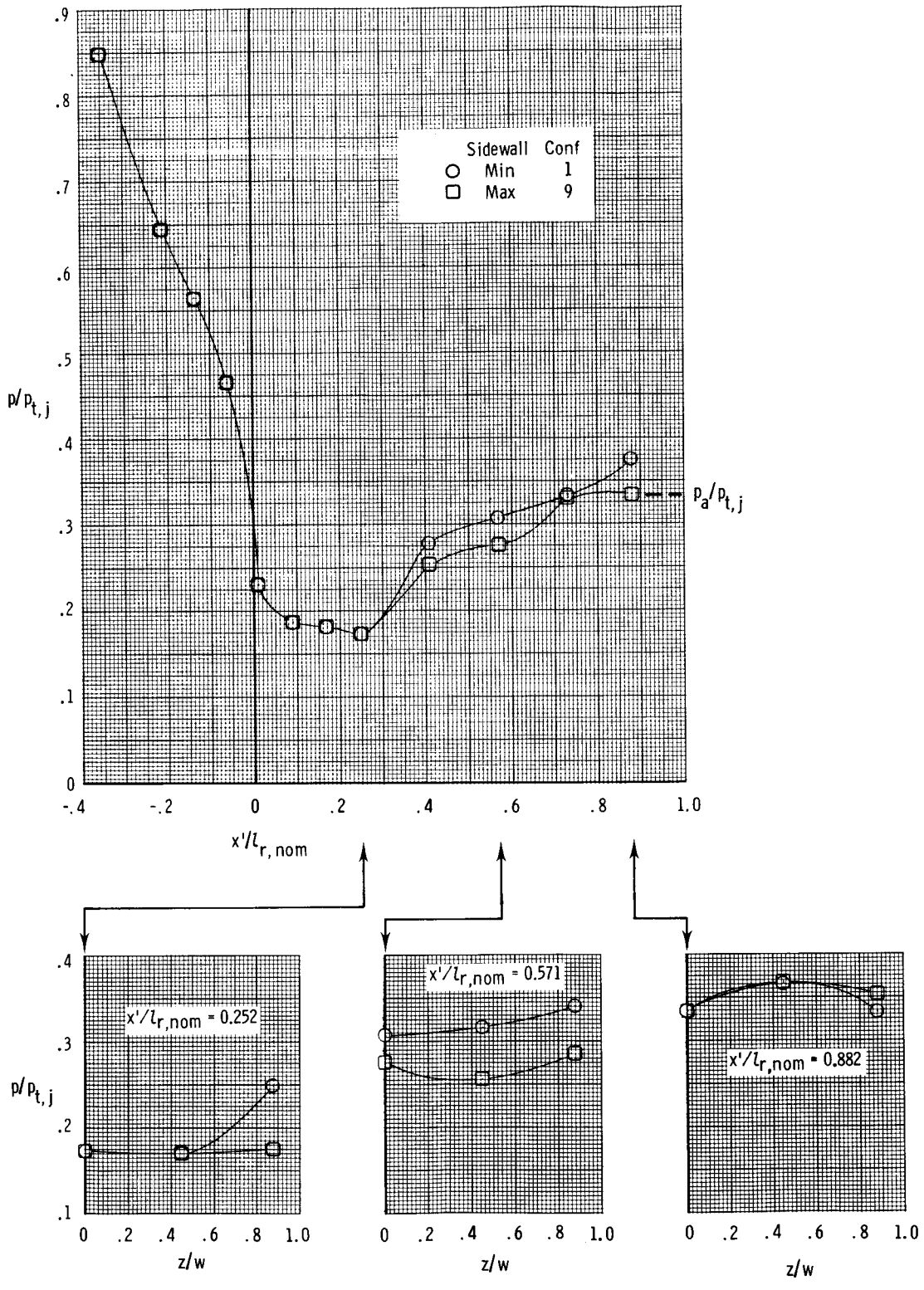

(a) $\delta_v = -20°$.

Figure 7. Effect of sidewall containment on ramp pressure distributions at NPR = 3.0.

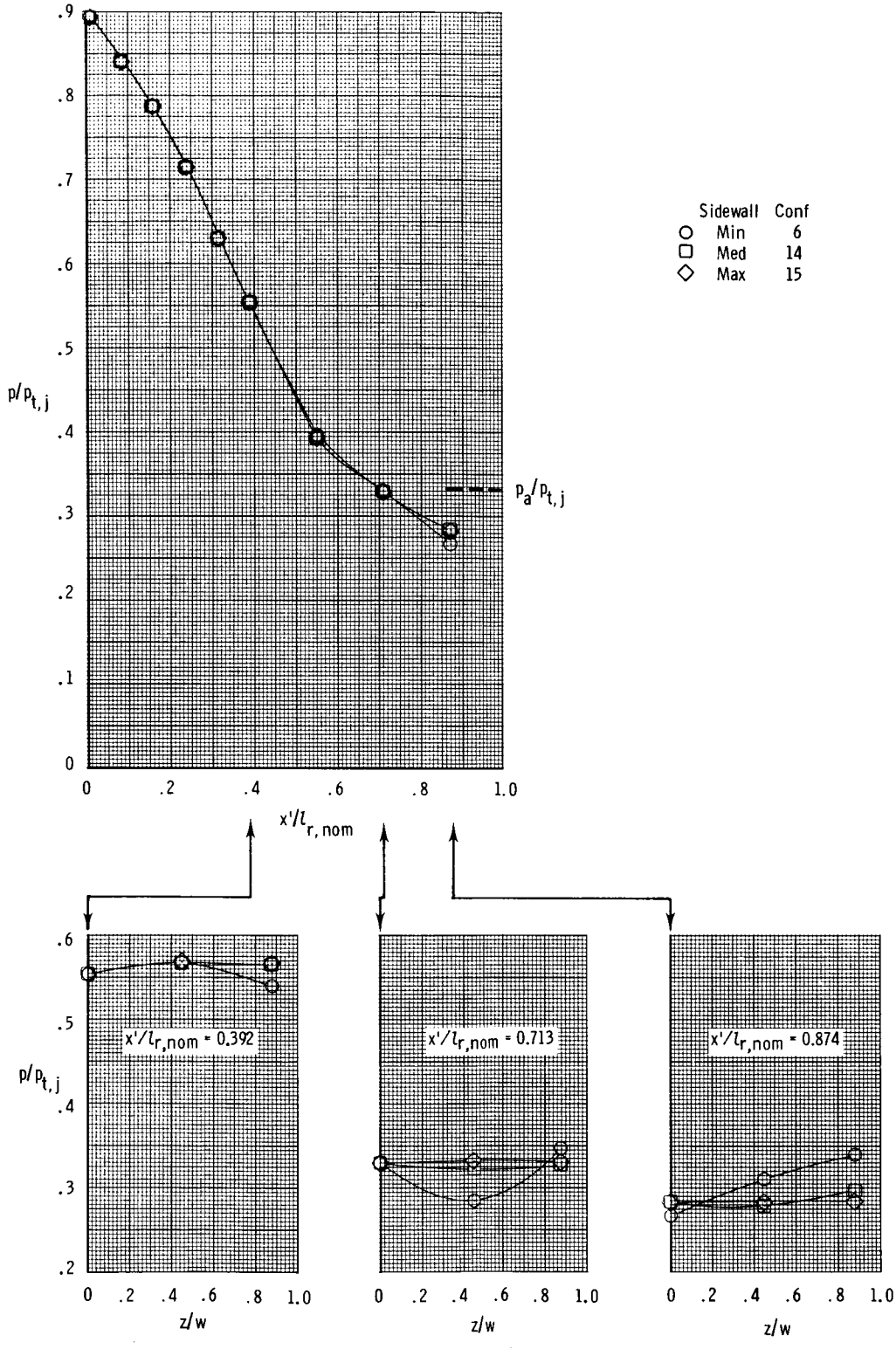

(b) $\delta_v = 30°$.

Figure 7. Concluded.

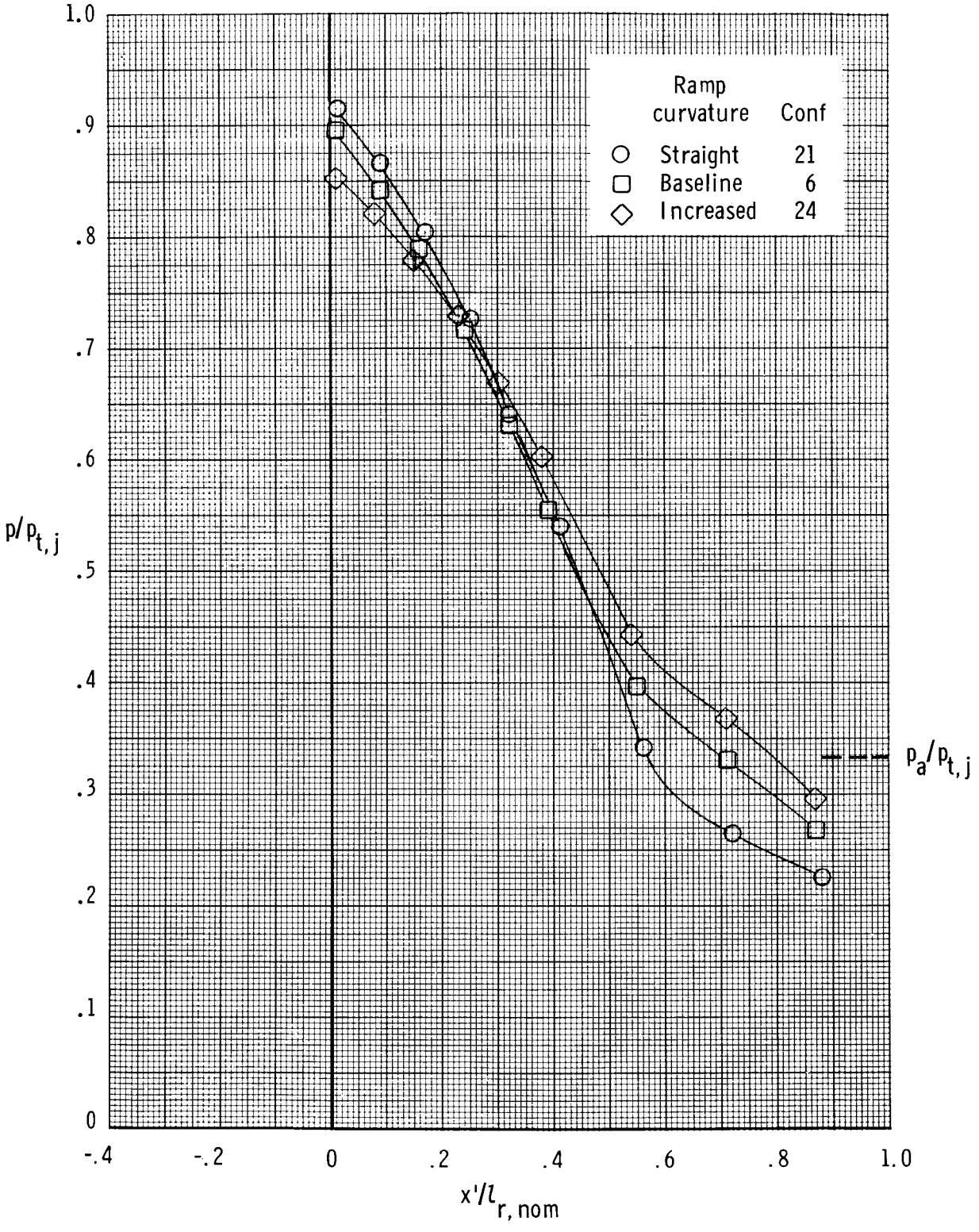

Figure 8. Effect of ramp curvature on ramp centerline pressure distributions for $\delta_v = 30°$ and NPR = 3.0.

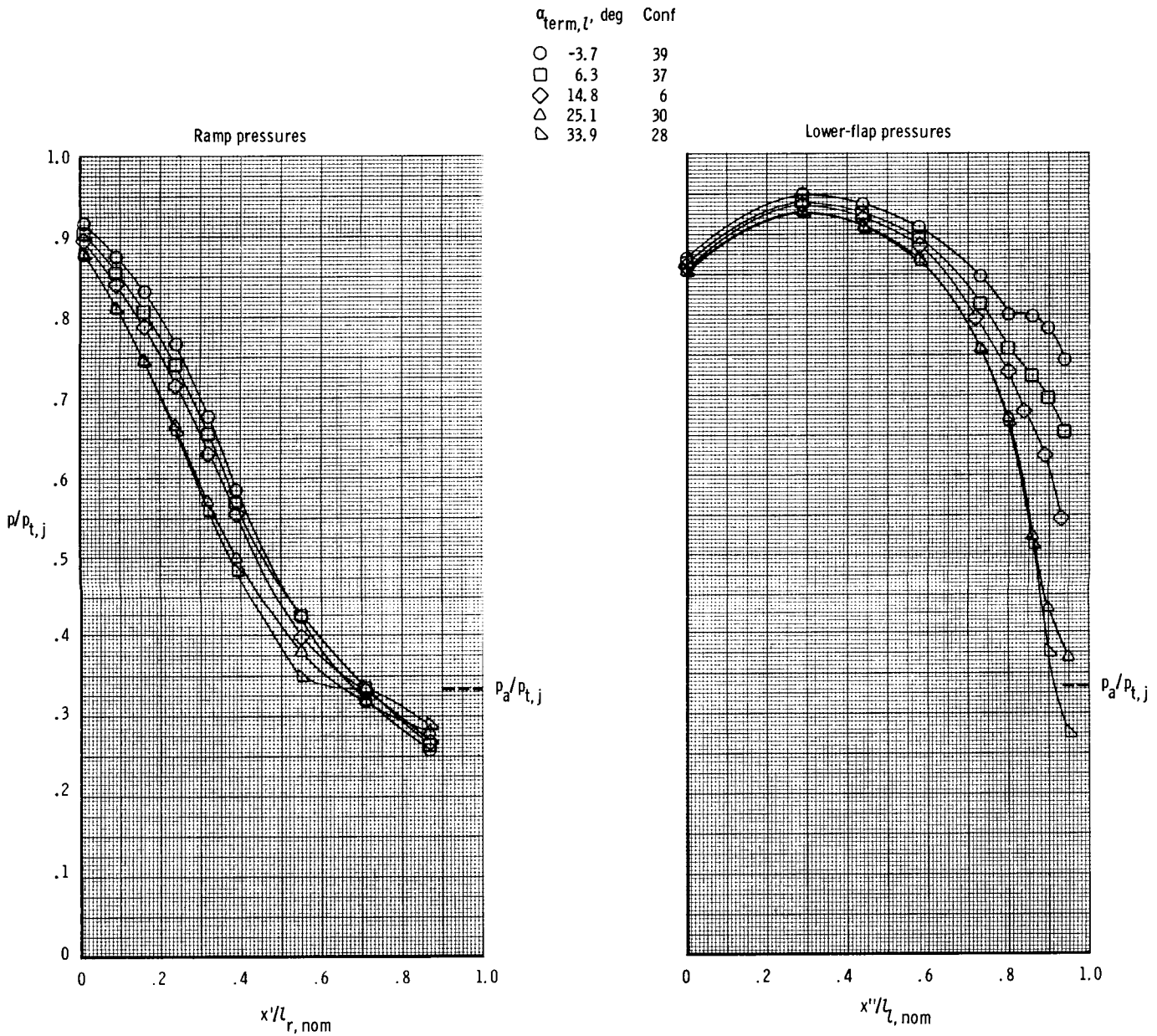

Figure 9. Effect of lower-flap terminal angle on flap centerline pressure distributions for $\delta_v = 30°$ and NPR = 3.0.

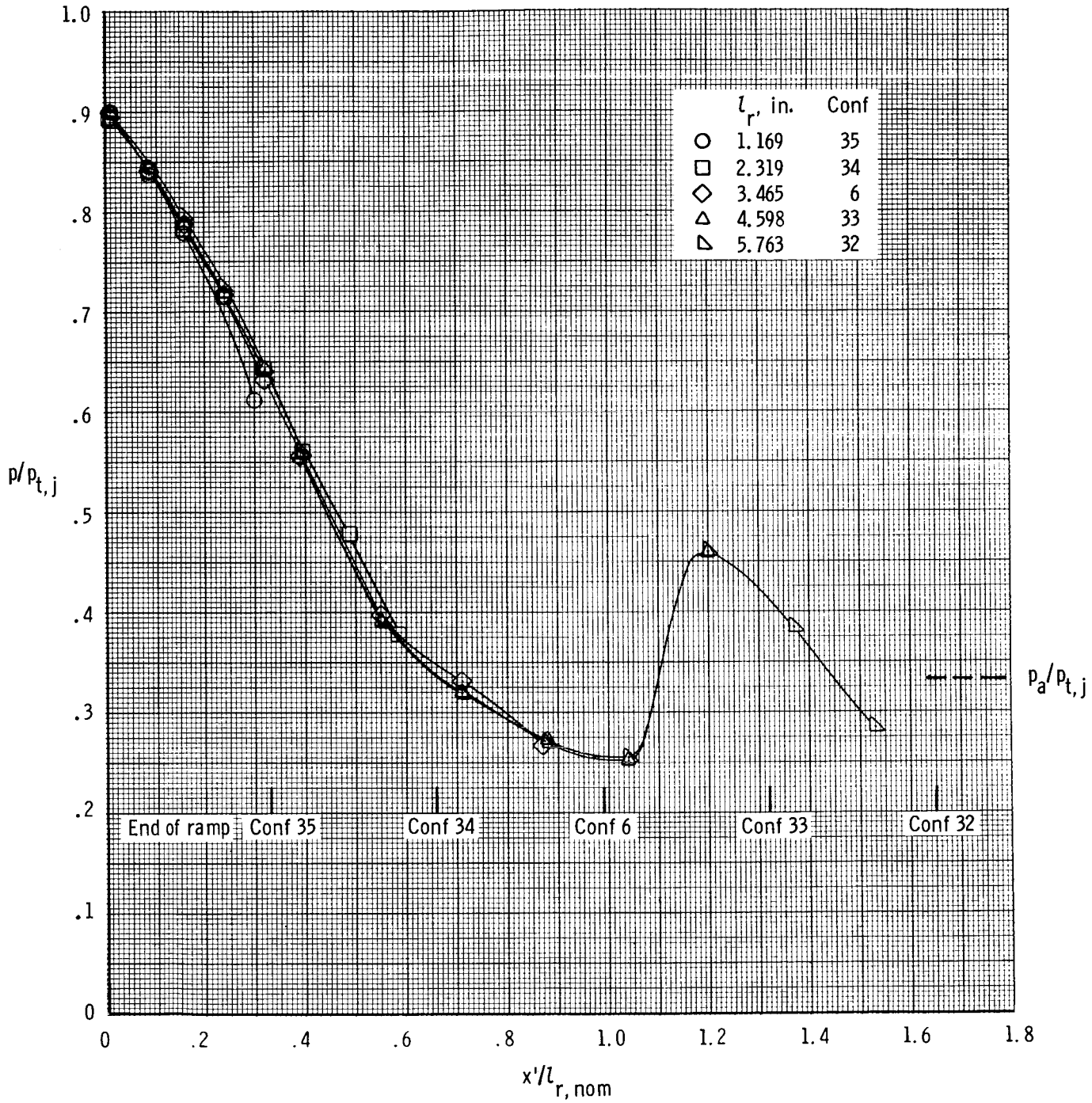

Figure 10 Effect of ramp length on ramp centerline pressure distributions for $\delta_v = 30°$ and NPR = 3.0.

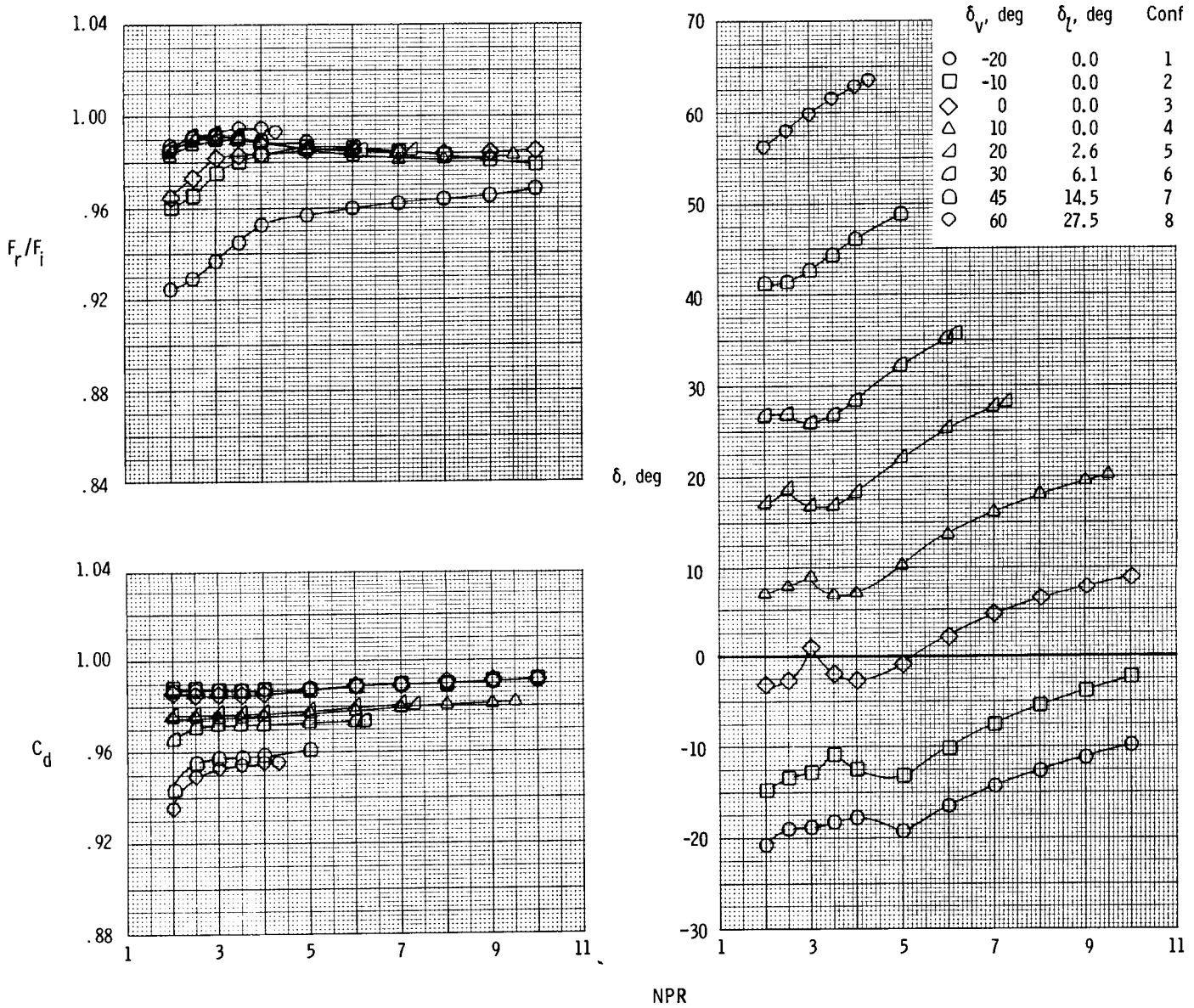

Figure 11. Effect of thrust vectoring on SERN performance as a function of nozzle pressure ratio. Minimum sidewall containment; baseline $l_{r,nom} = 3.48$ in.

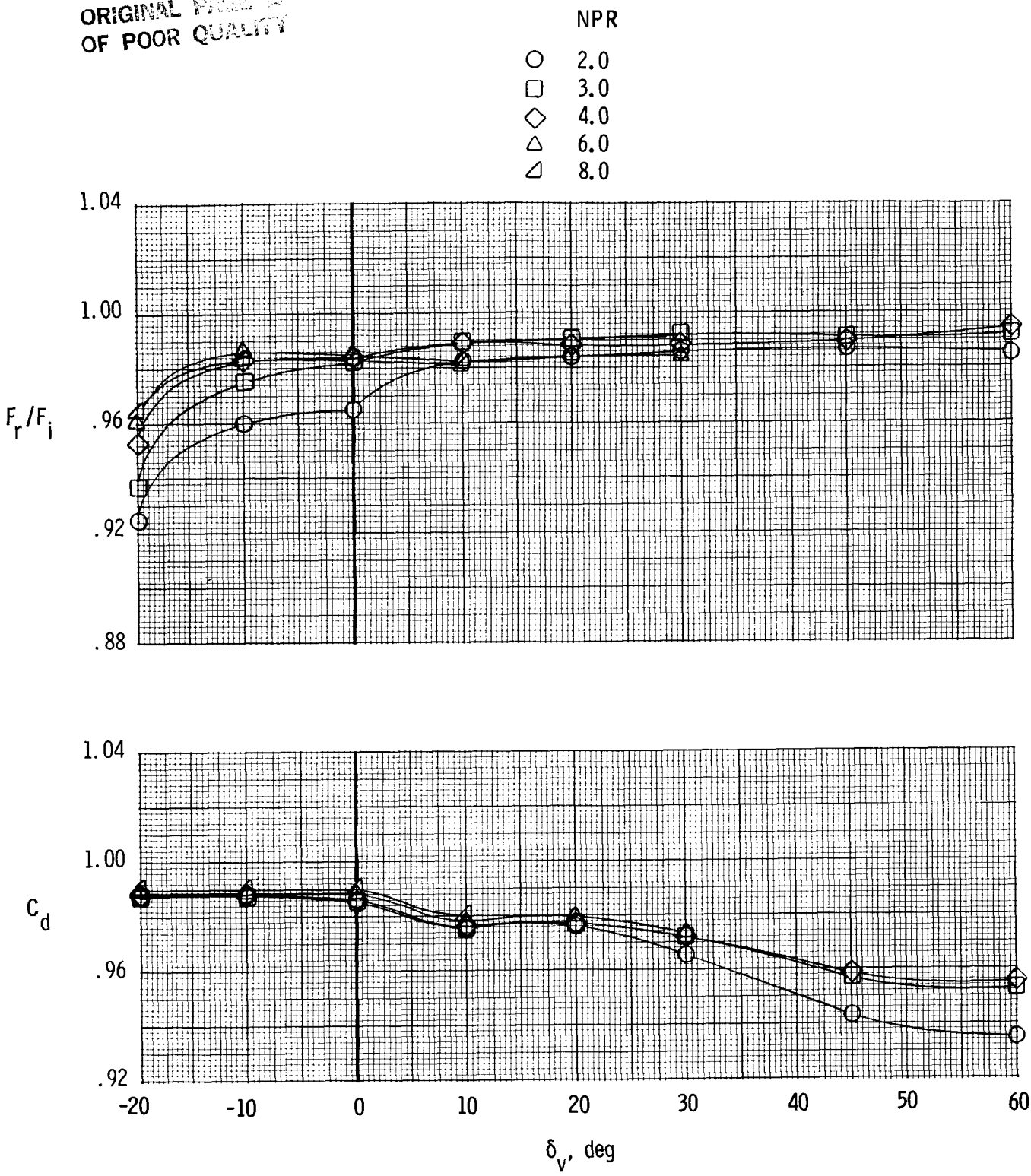

(a) Resultant thrust ratio and discharge coefficient.

Figure 12. Effect of thrust vectoring on SERN performance as a function of geometric thrust-vector angle. Minimum sidewall containment; baseline $l_{r,\mathrm{nom}} = 3.48$ in.

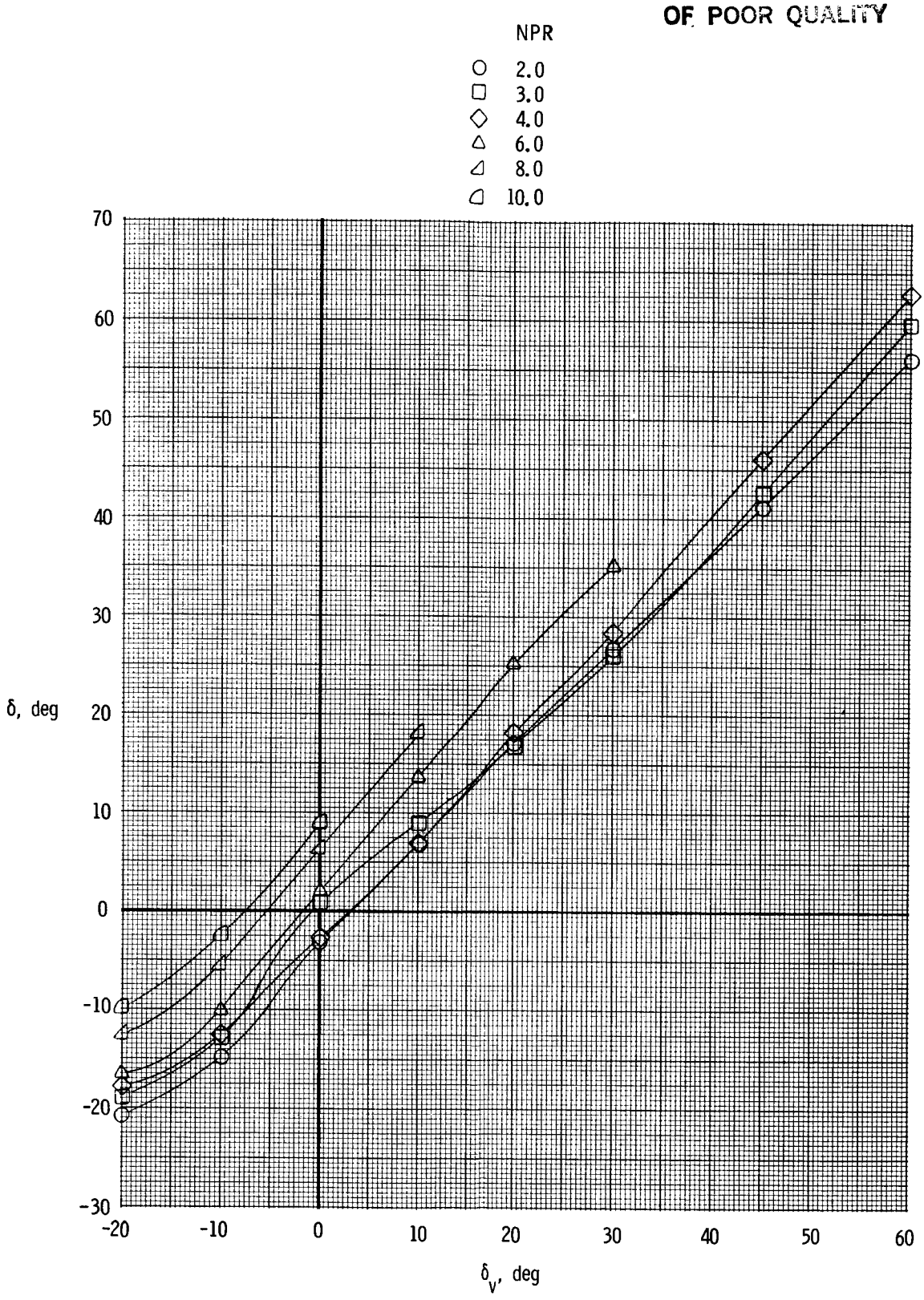

(b) Resultant thrust-vector angle.

Figure 12. Concluded.

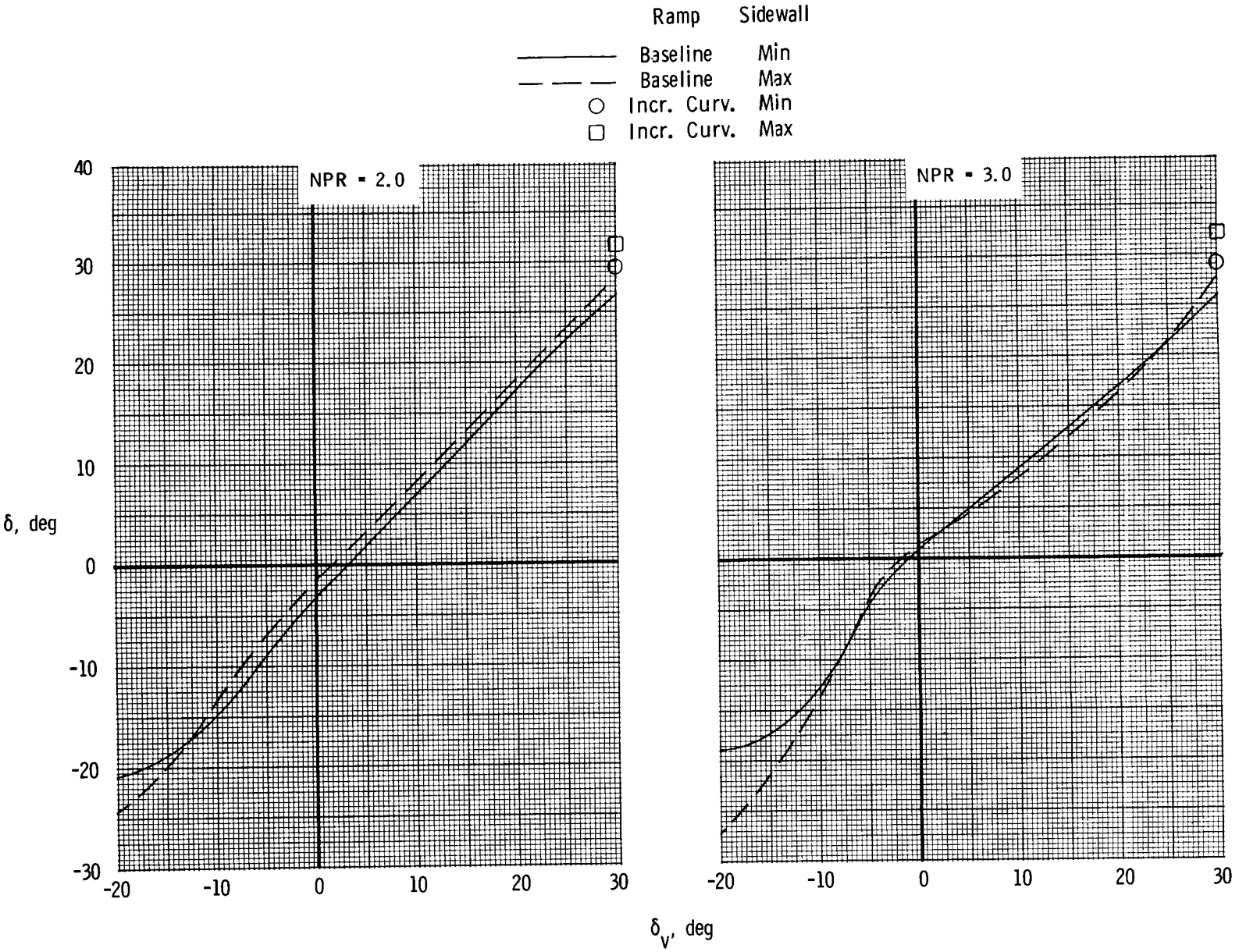

(a) NPR = 2.0 and 3.0.

Figure 13. Summary of sidewall containment effects on SERN resultant thrust-vector angle at constant nozzle pressure ratio.

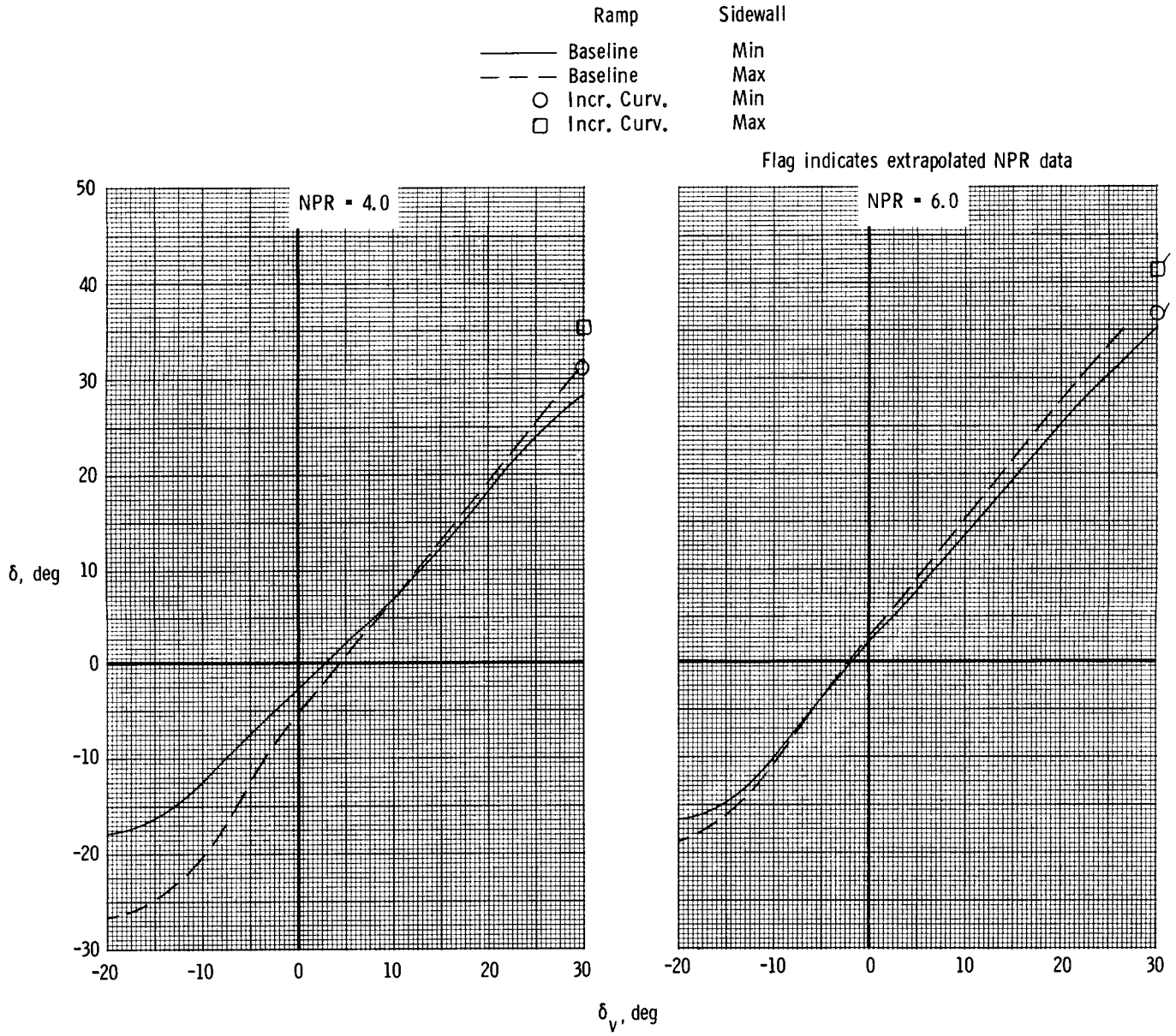

(b) NPR = 4.0 and 6.0.

Figure 13. Continued.

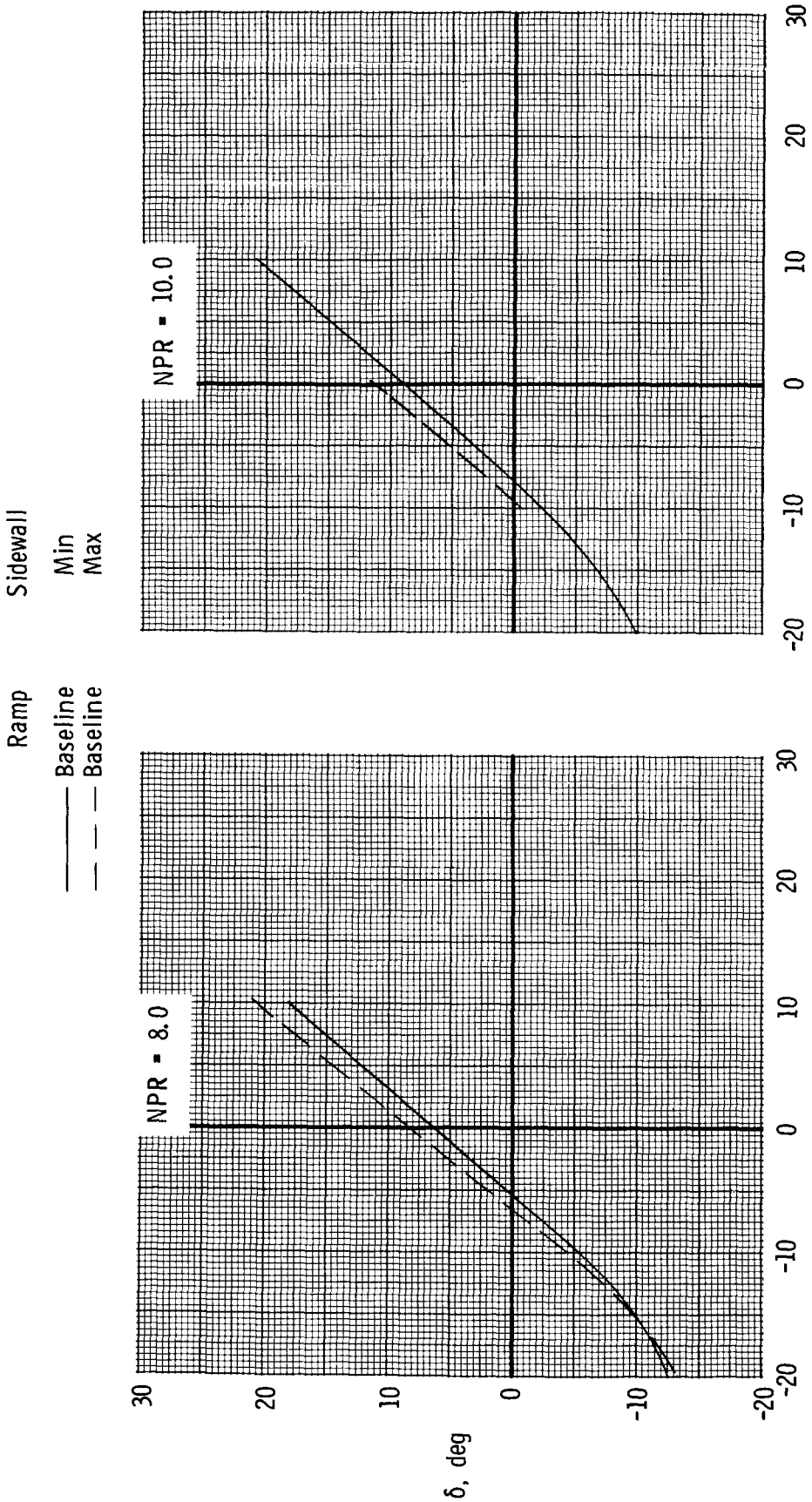

(c) NPR = 8.0 and 10.0.

Figure 13. Concluded.

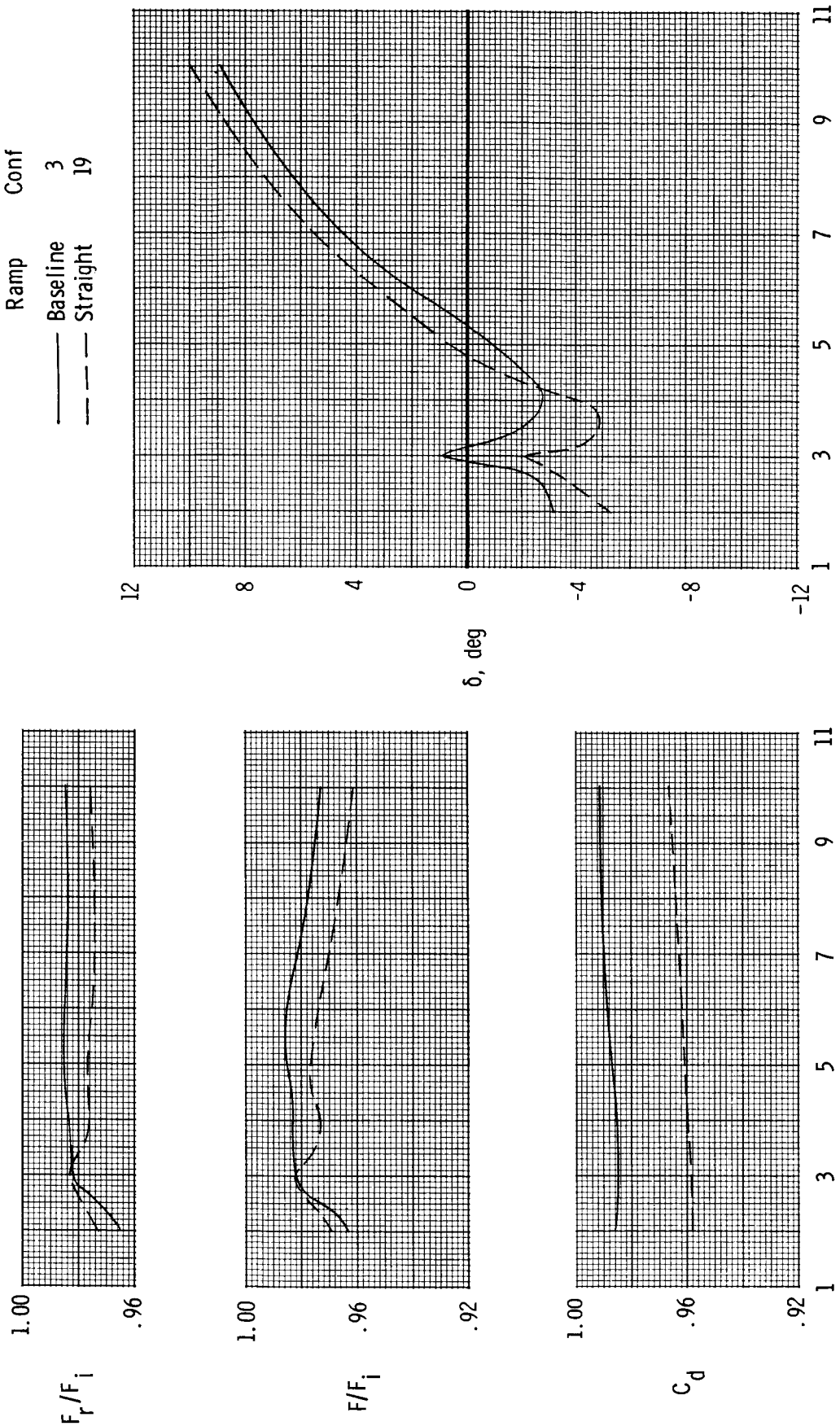

(a) $\delta_v = 0°$; $\alpha_{term,i} = 8.7°$; minimum sidewall.

Figure 14. Effect of ramp curvature on SERN performance.

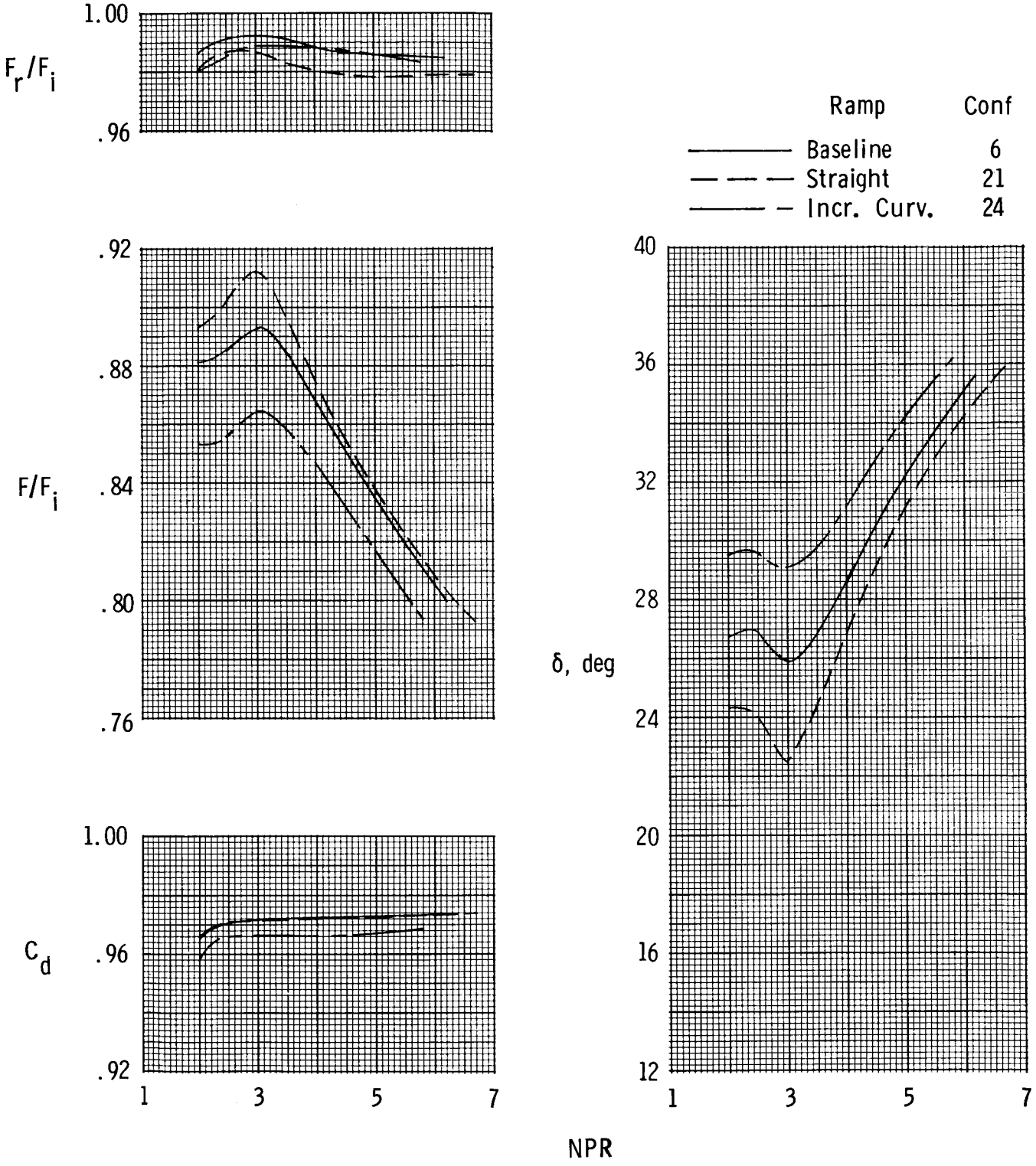

(b) $\delta_v = 30°$; $\alpha_{term,l} = 14.8°$; minimum sidewall.

Figure 14. Continued.

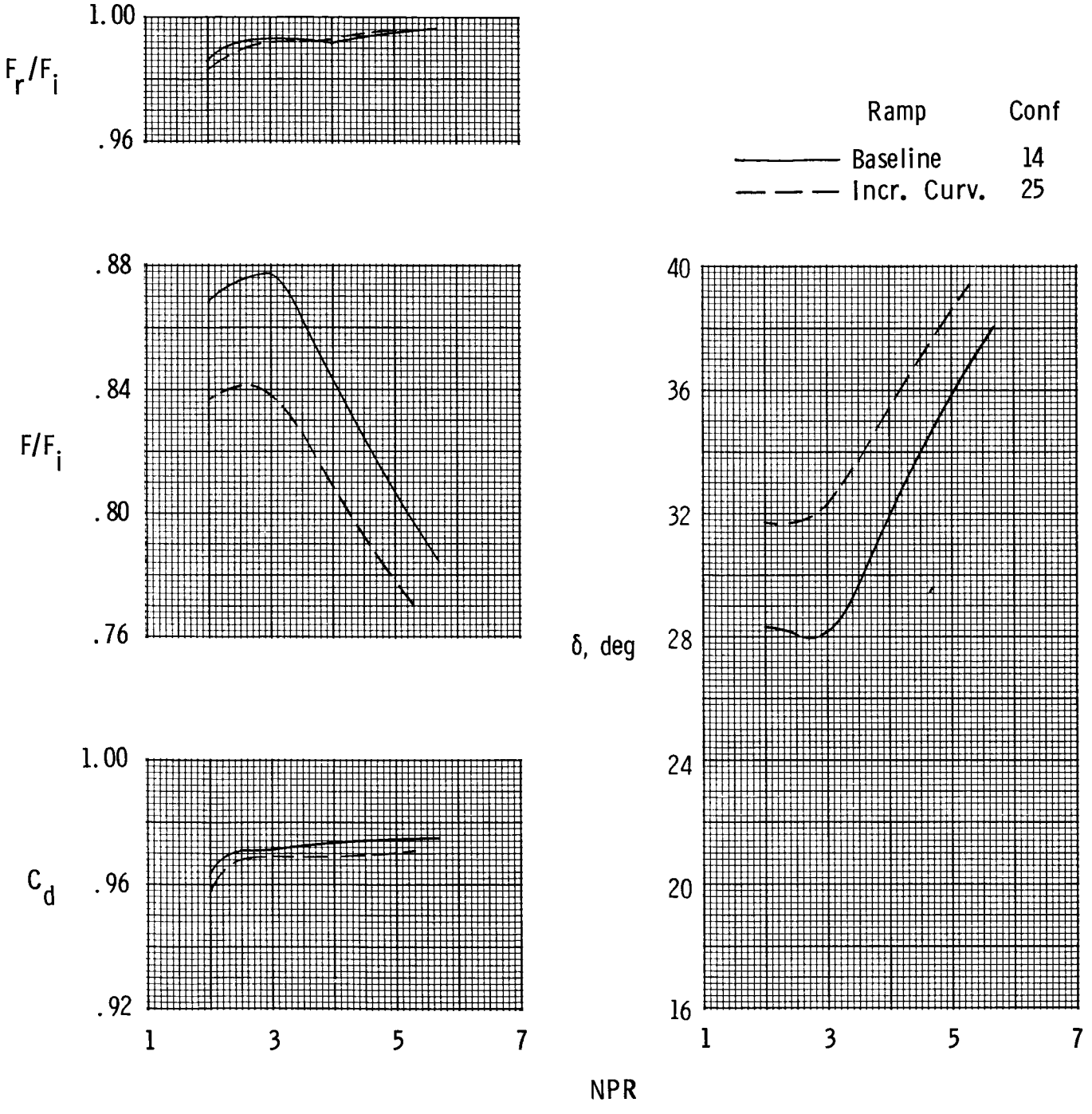

(c) $\delta_v = 30°$; $\alpha_{term,i} = 14.8°$; medium sidewall.

Figure 14. Continued.

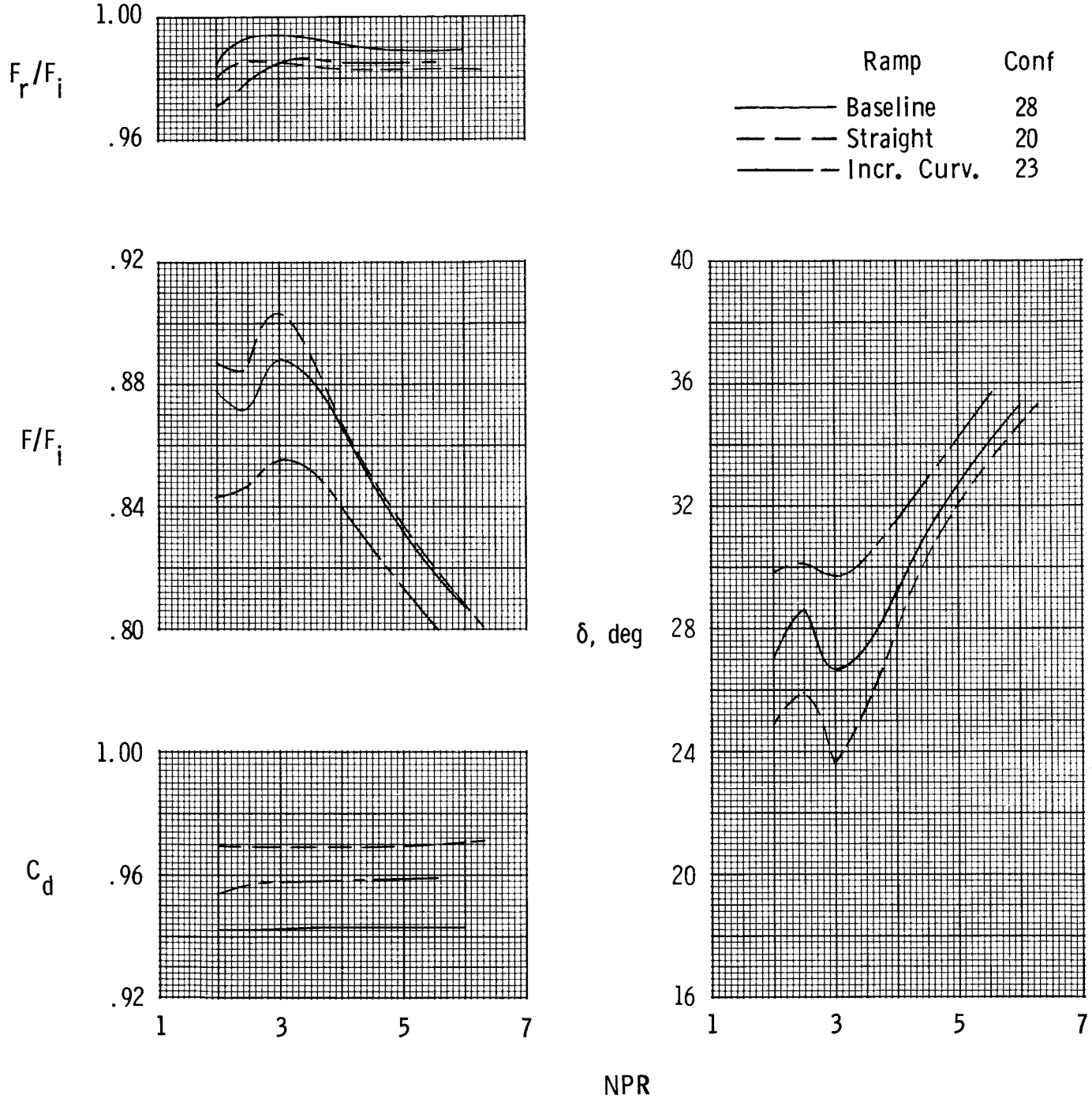

(d) $\delta_v = 30°$; $\alpha_{term,l} = 33.9°$; minimum sidewall.

Figure 14. Continued.

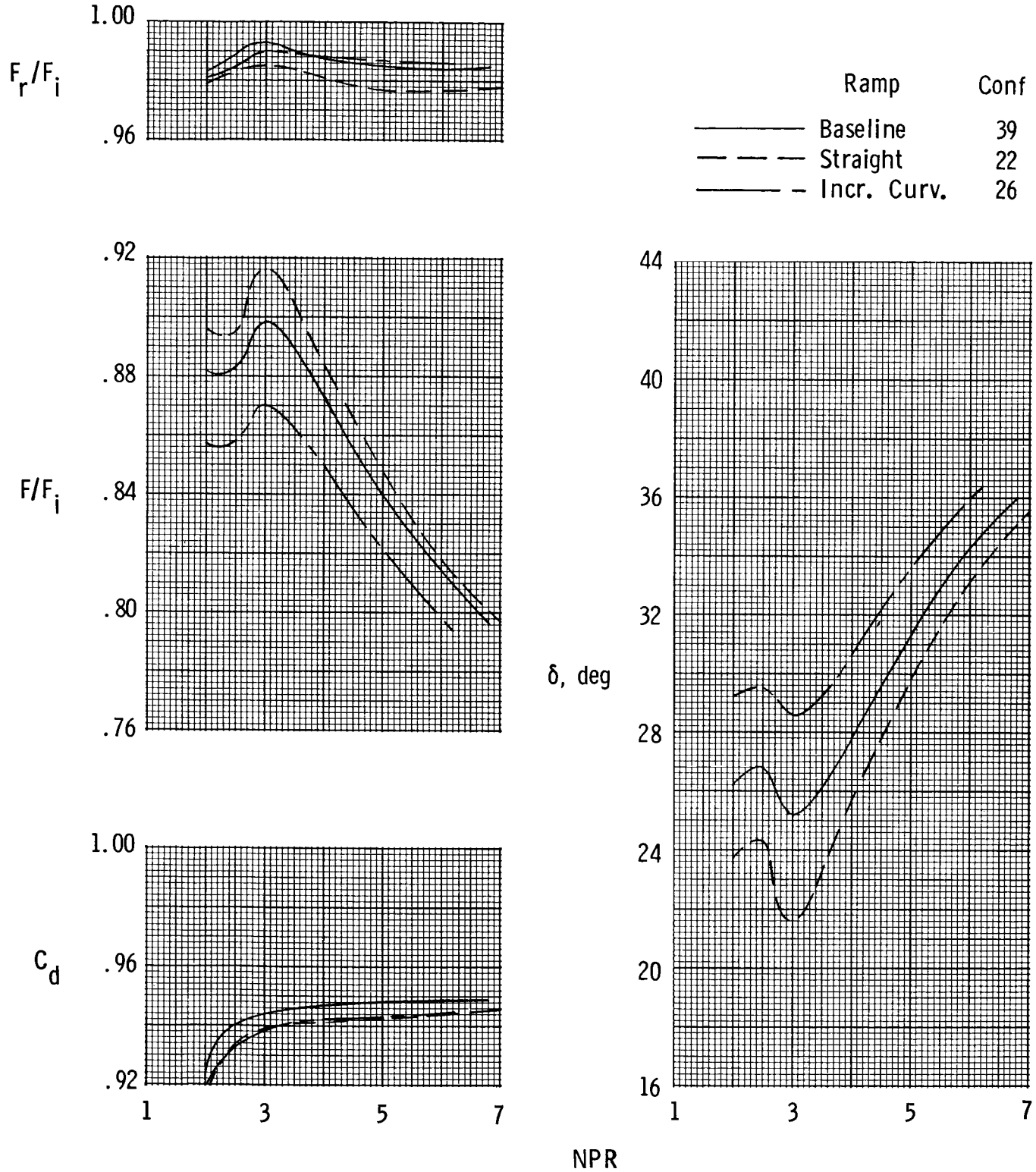

(e) $\delta_v = 30°$; $\alpha_{term,i} = -3.7°$; minimum sidewall.

Figure 14. Concluded.

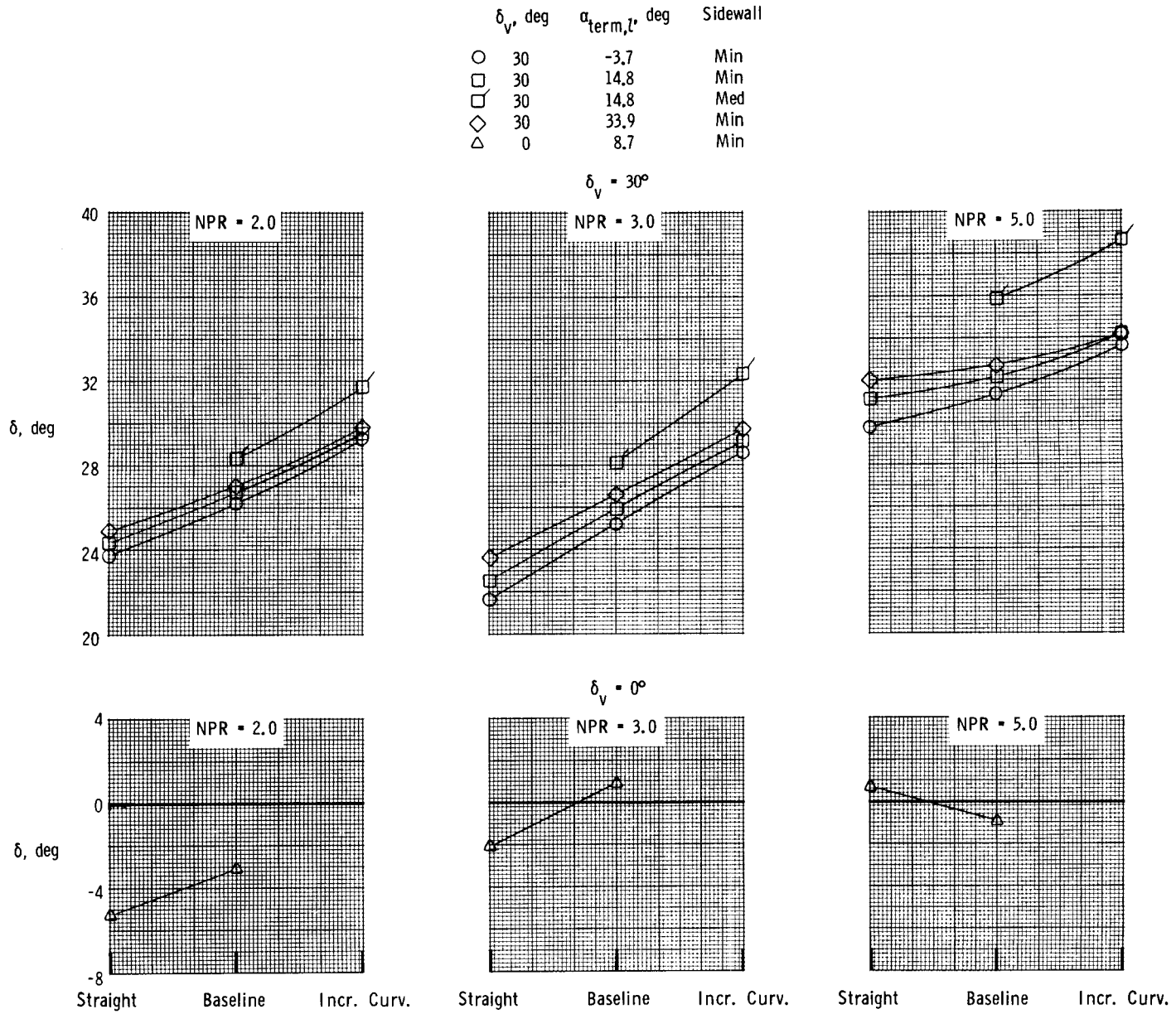

Figure 15. Summary of ramp curvature effects on SERN resultant thrust-vector angle at constant nozzle pressure ratio.

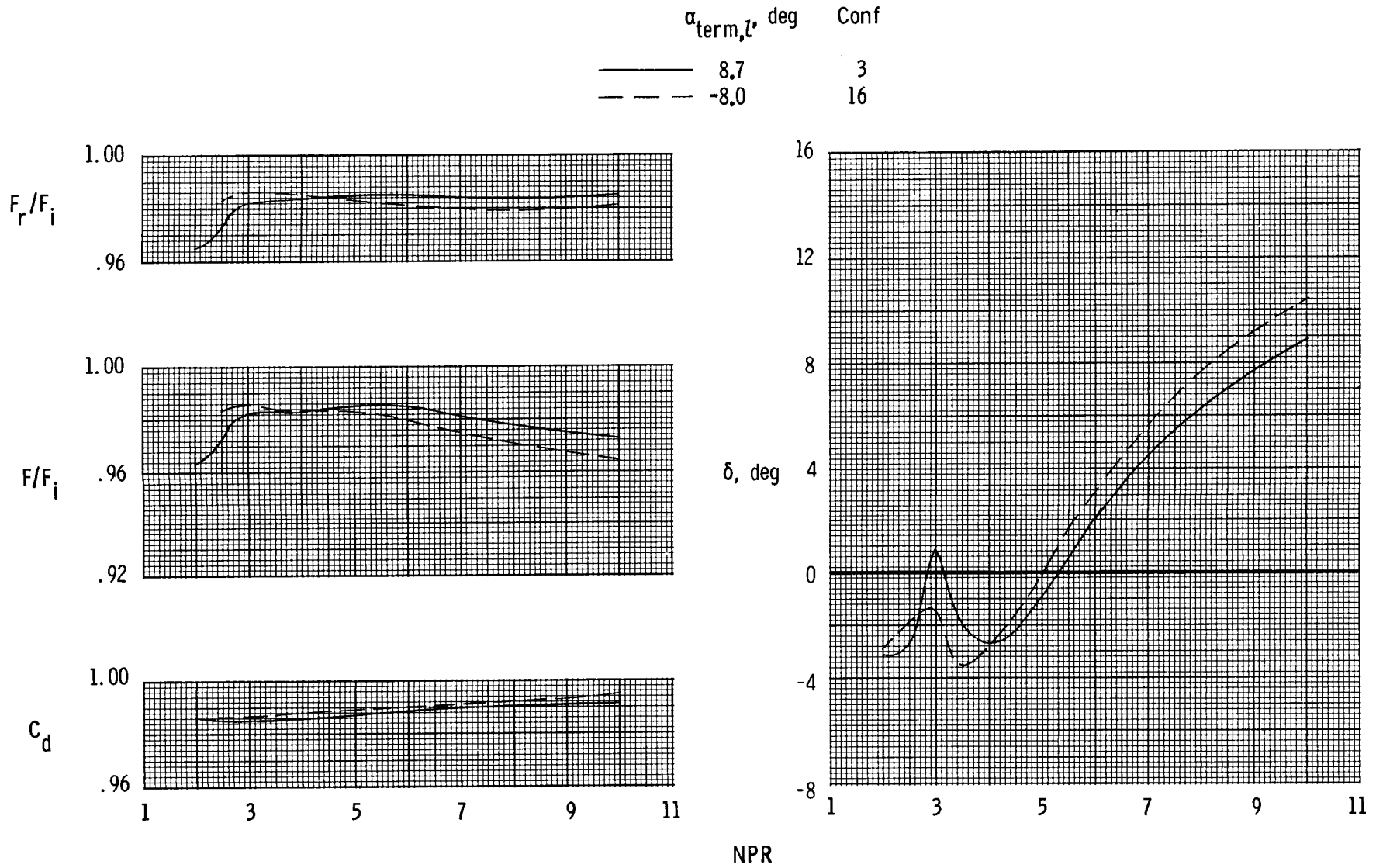

(a) $\delta_v = 0°$.

Figure 16. Effect of lower-flap lip angle on cruise and negative thrust-vectoring SERN performance.

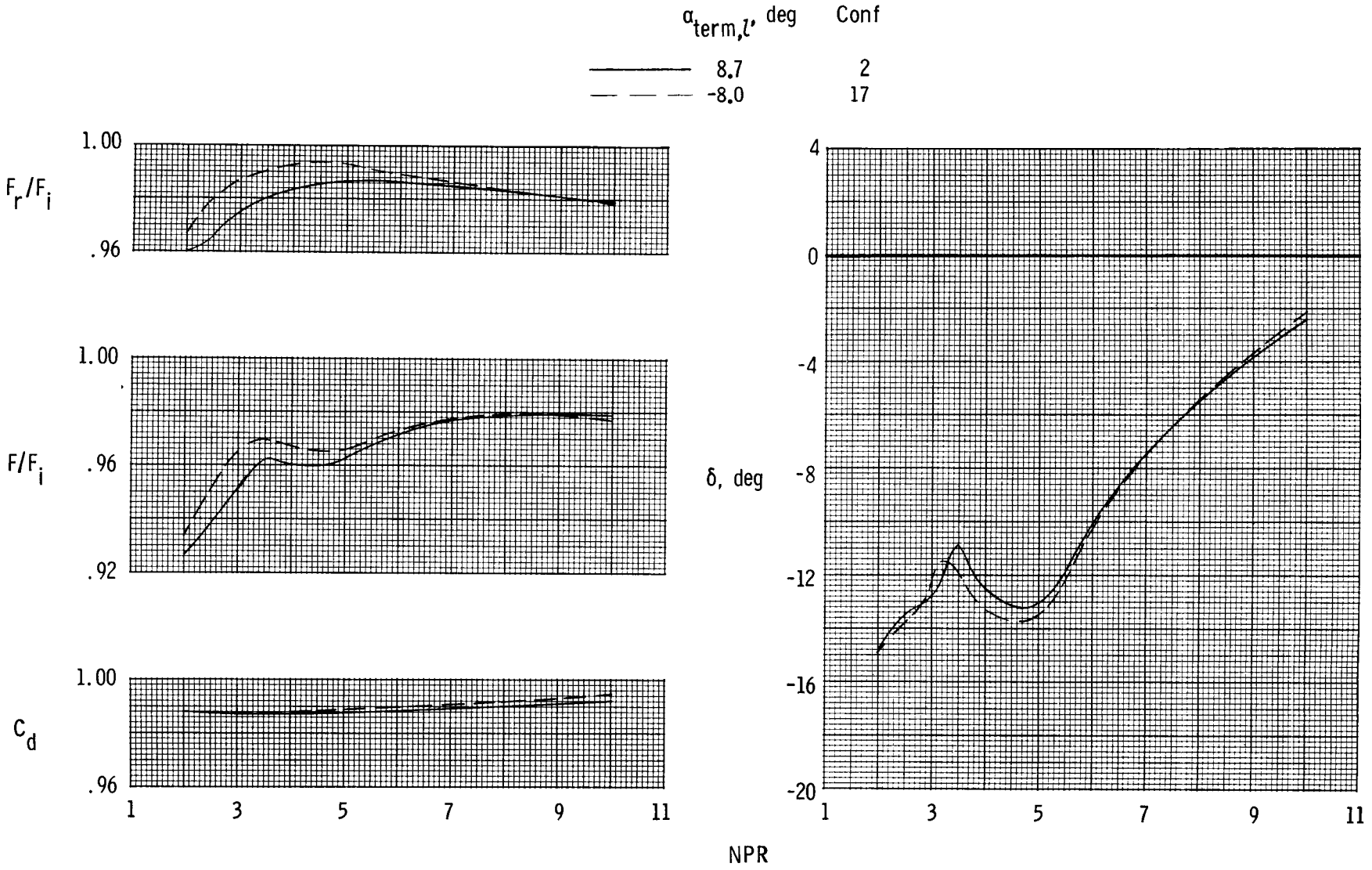

(b) $\delta_v = -10°$.

Figure 16. Continued.

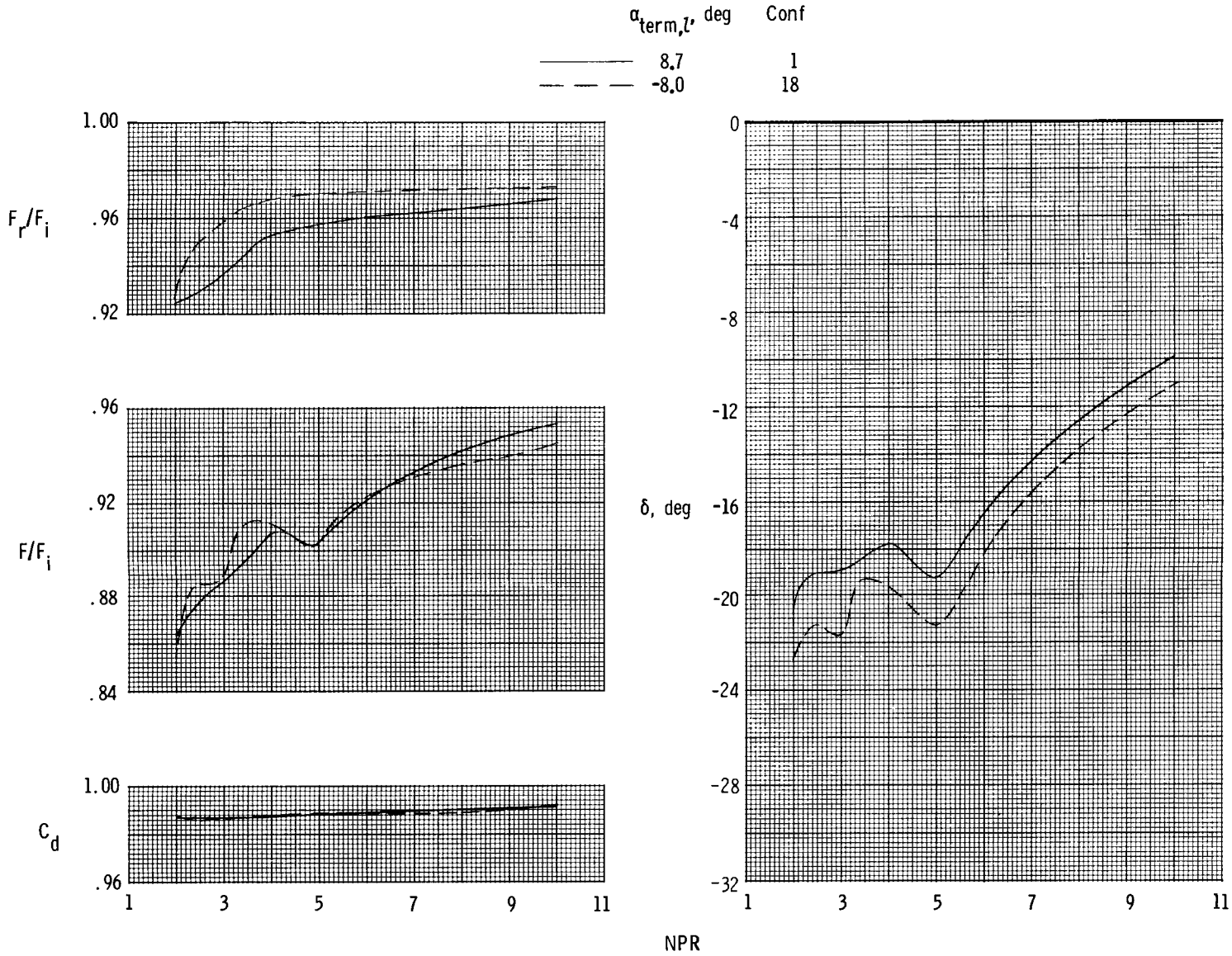

(c) $\delta_v = -20°$.

Figure 16. Concluded.

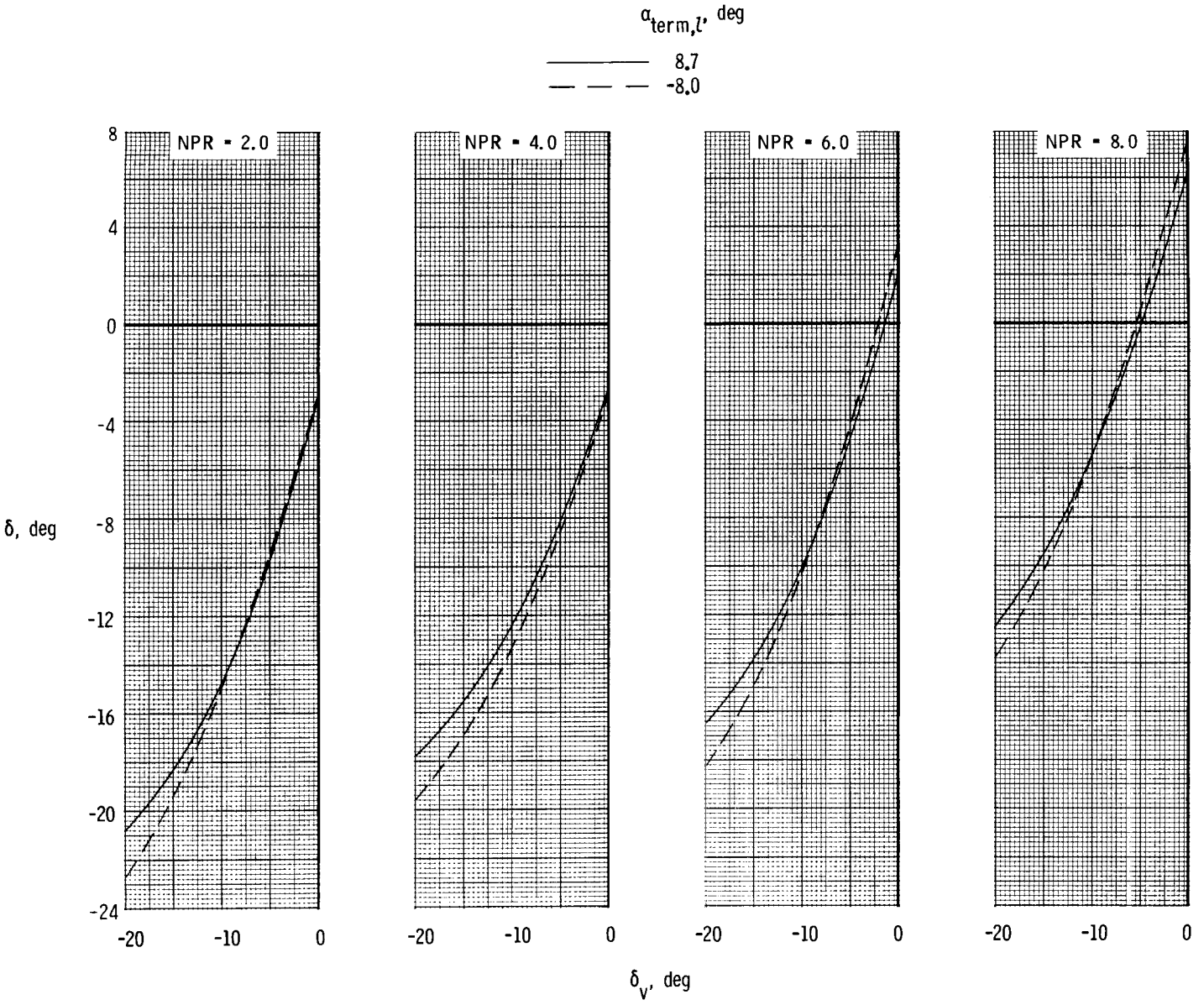

Figure 17. Summary of effects of lower-flap lip angle on cruise and negative thrust-vectoring SERN resultant thrust-vector angles at constant nozzle pressure ratio.

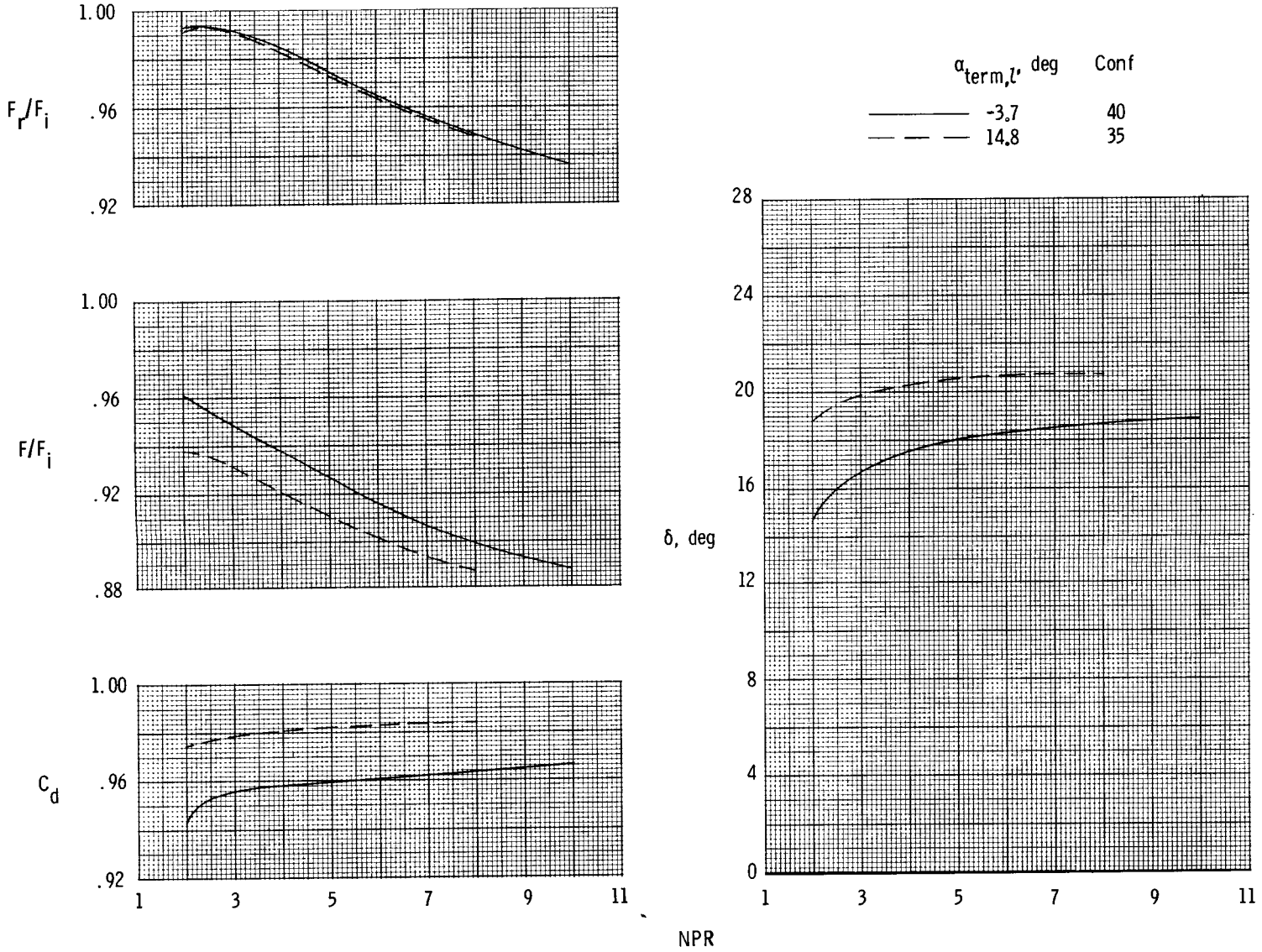

(a) $l_r = 1.17$ in., baseline ramp.

Figure 18. Effect of lower-flap lip angle and ramp length on $\delta_v = 30°$ SERN performance.

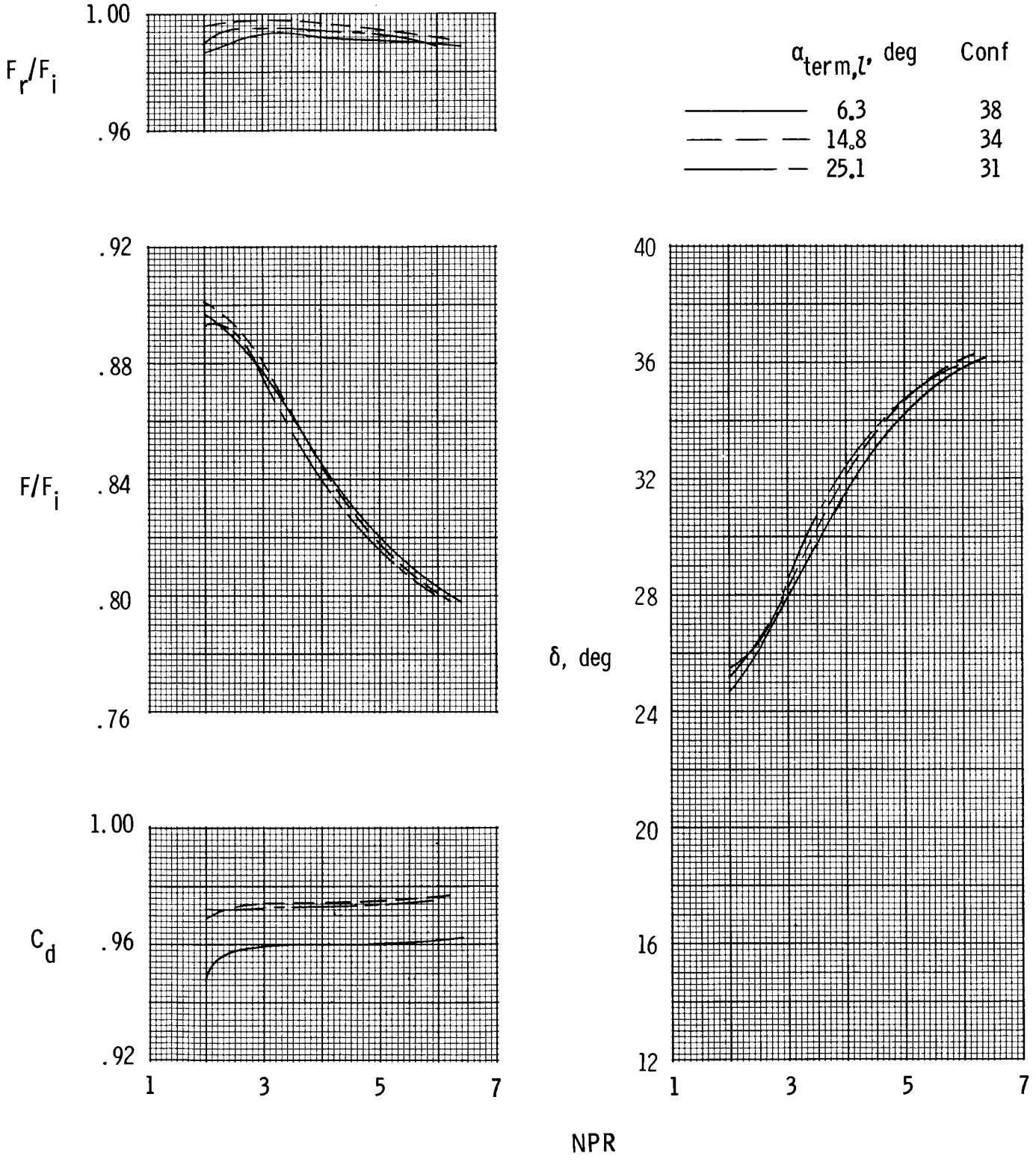

(b) $l_r = 2.32$ in., baseline ramp.

Figure 18. Continued.

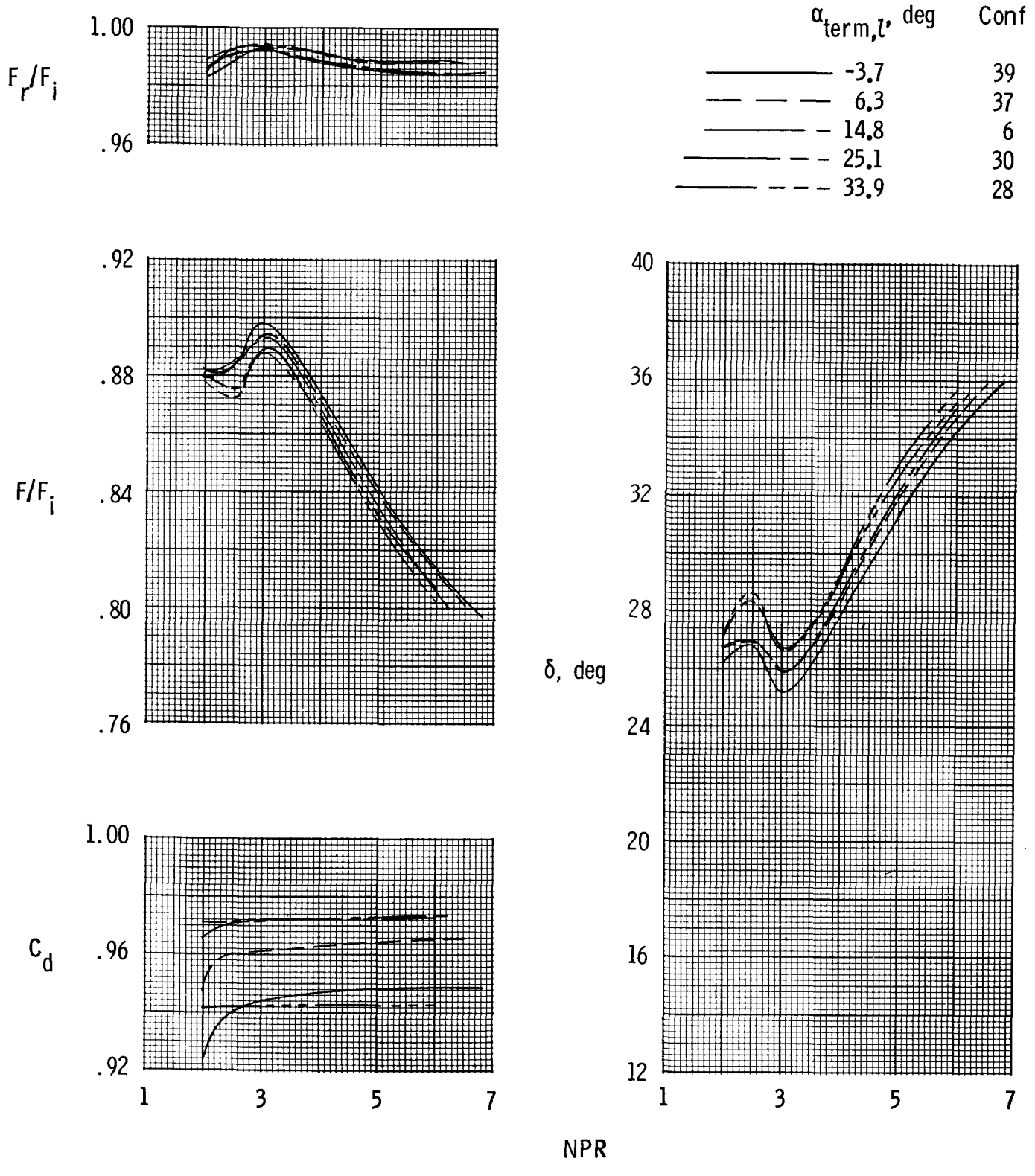

(c) $l_r = 3.46$ in., baseline ramp.

Figure 18. Continued.

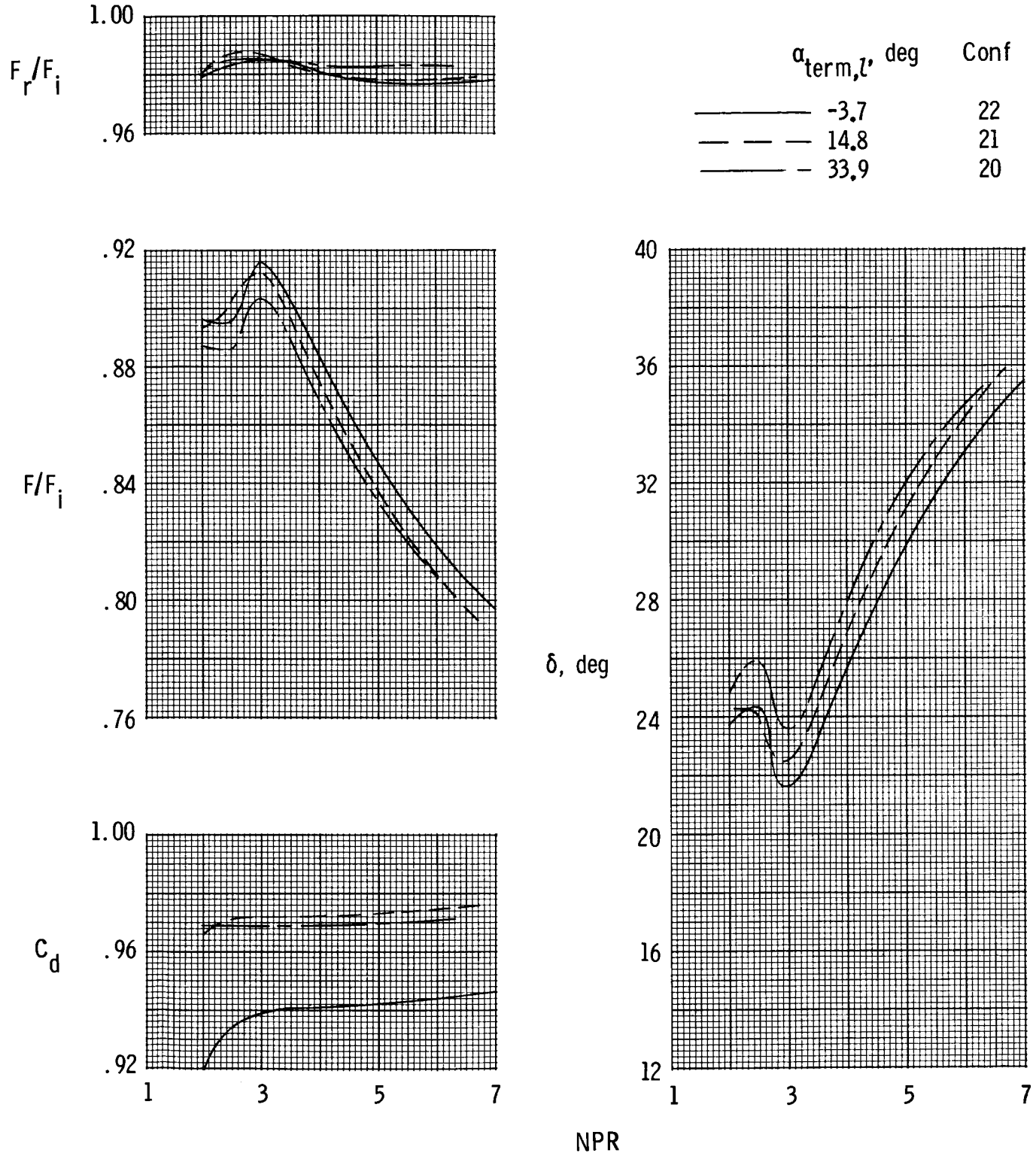

(d) $l_r = 3.46$ in., straight ramp.

Figure 18. Continued.

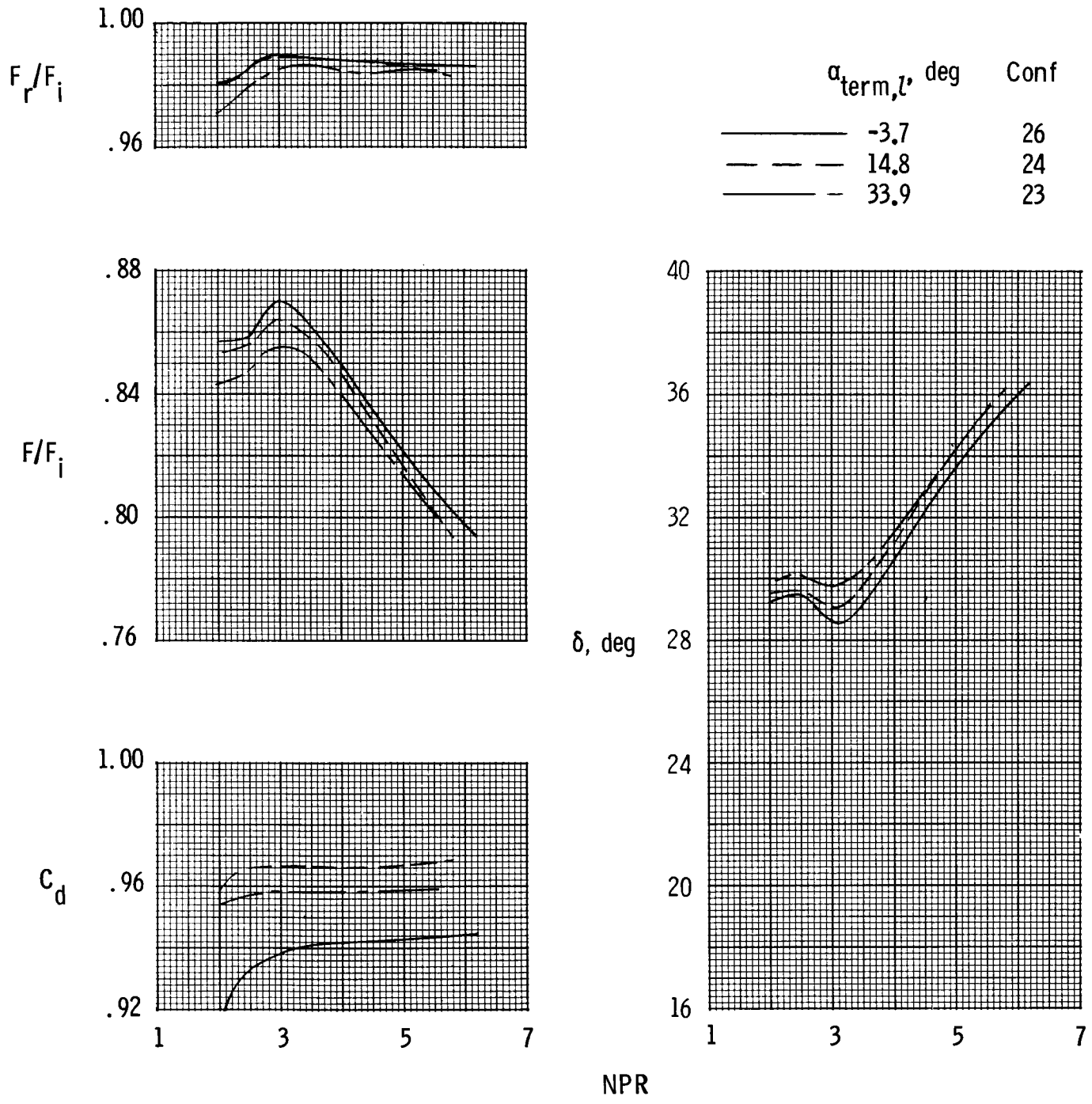

(e) $l_r = 3.46$ in., increased-curvature ramp.

Figure 18. Continued.

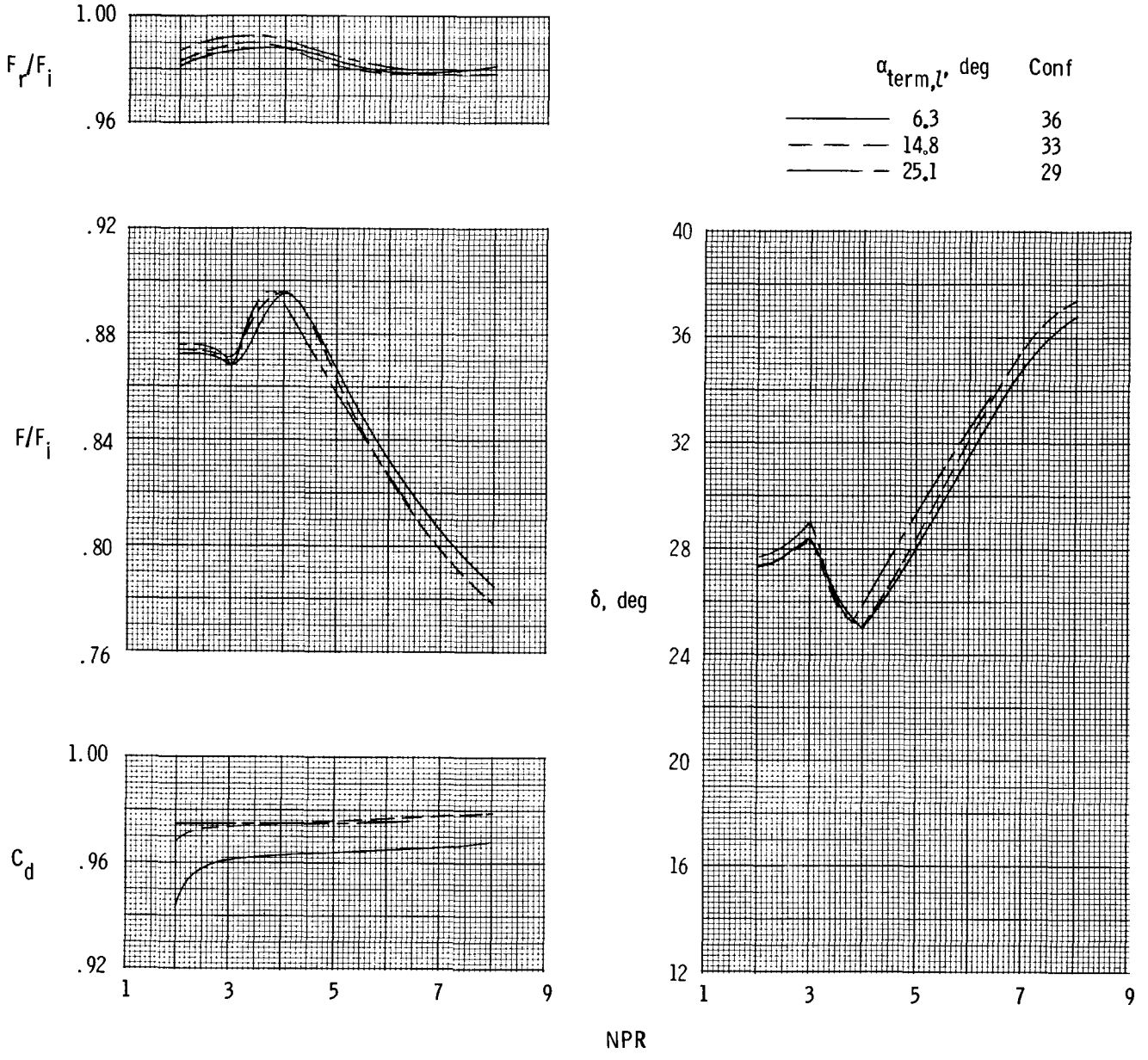

(f) $l_r = 4.60$ in., baseline ramp.

Figure 18. Continued.

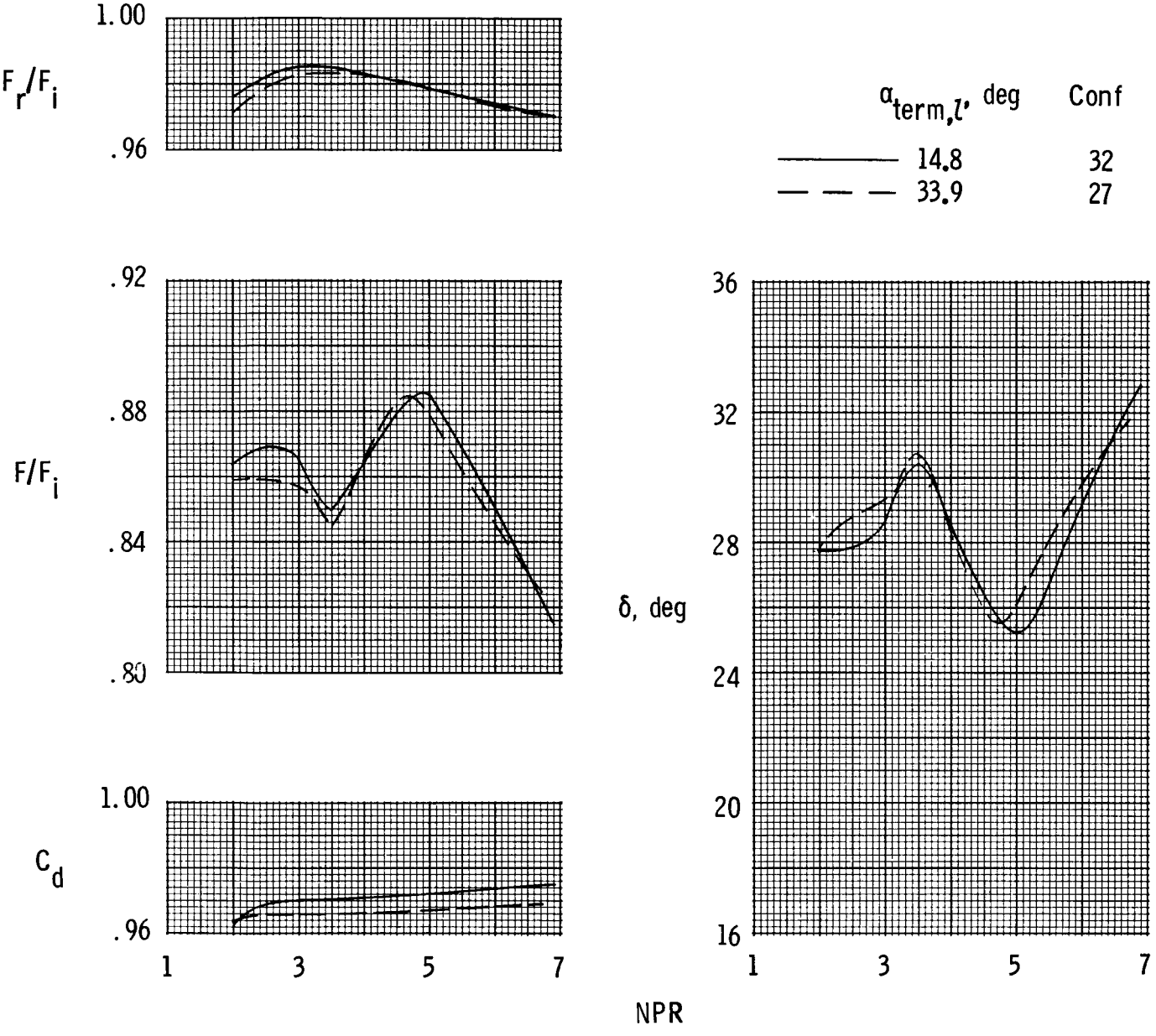

(g) $l_r = 5.74$ in., baseline ramp.

Figure 18. Concluded.

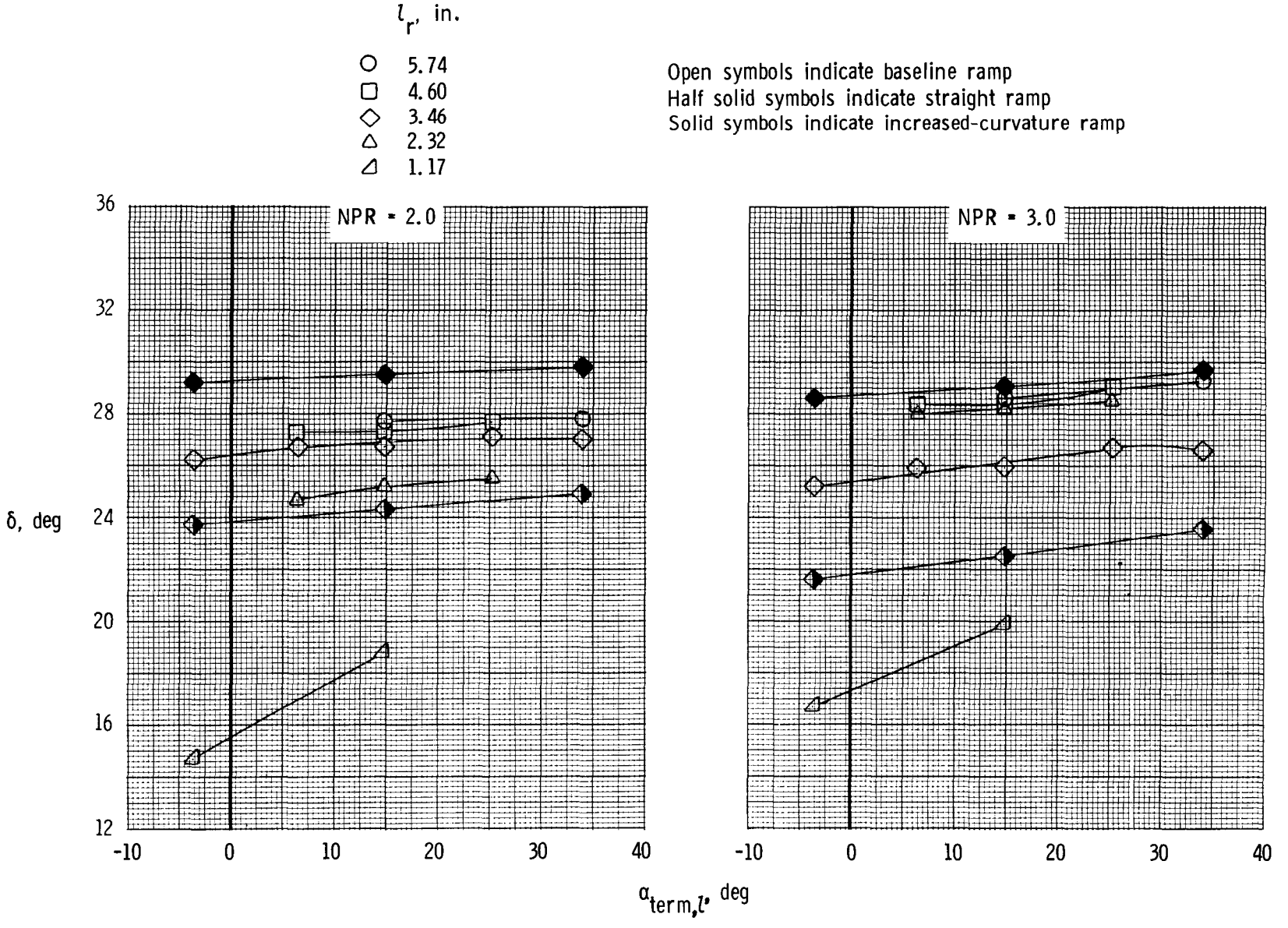

(a) NPR = 2.0 and 3.0.

Figure 19. Summary of lower-flap lip angle effects on $\delta_v = 30°$ SERN resultant thrust-vector angle at constant nozzle pressure ratio.

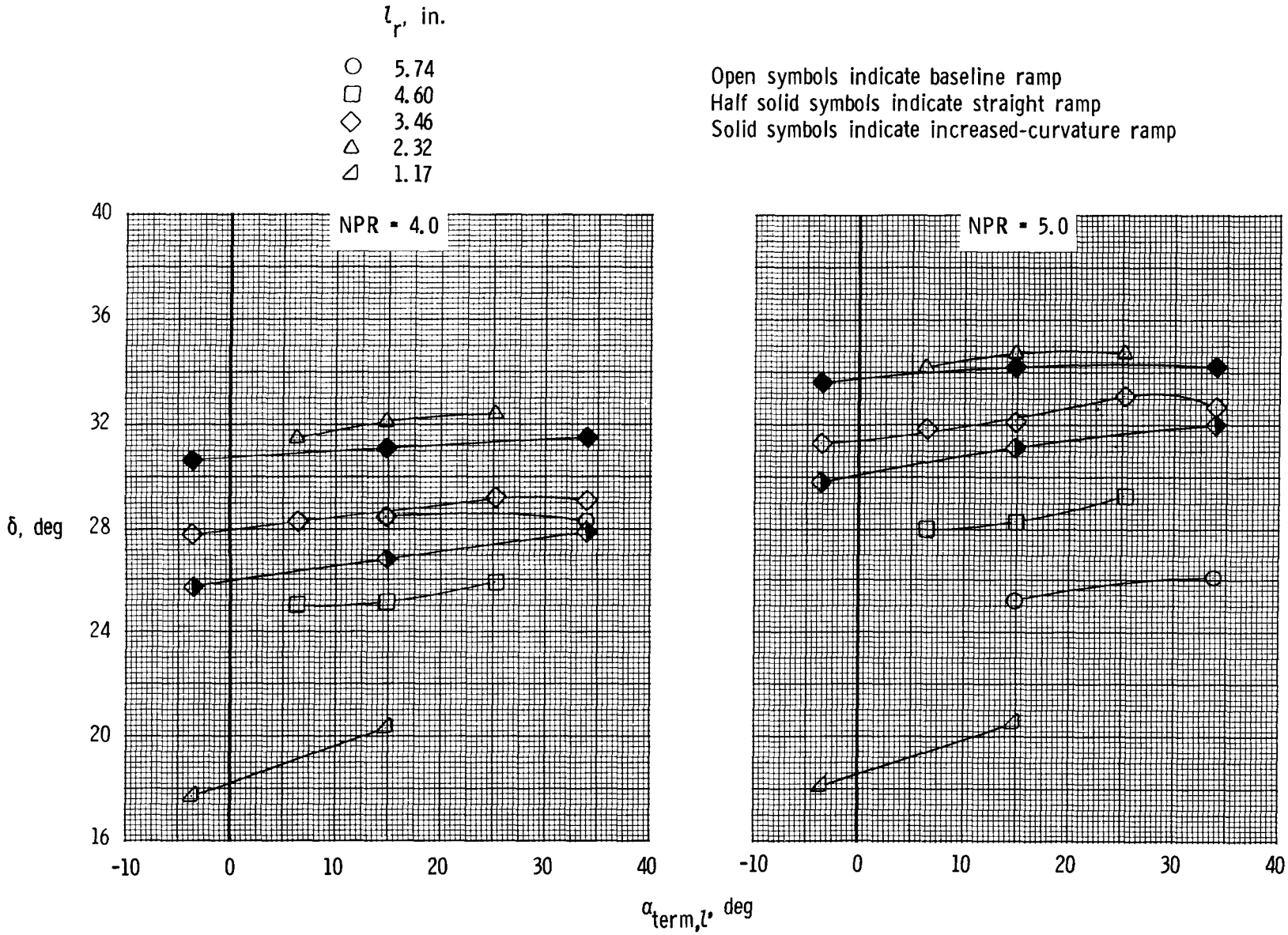

(b) NPR = 4.0 and 5.0.

Figure 19. Continued.

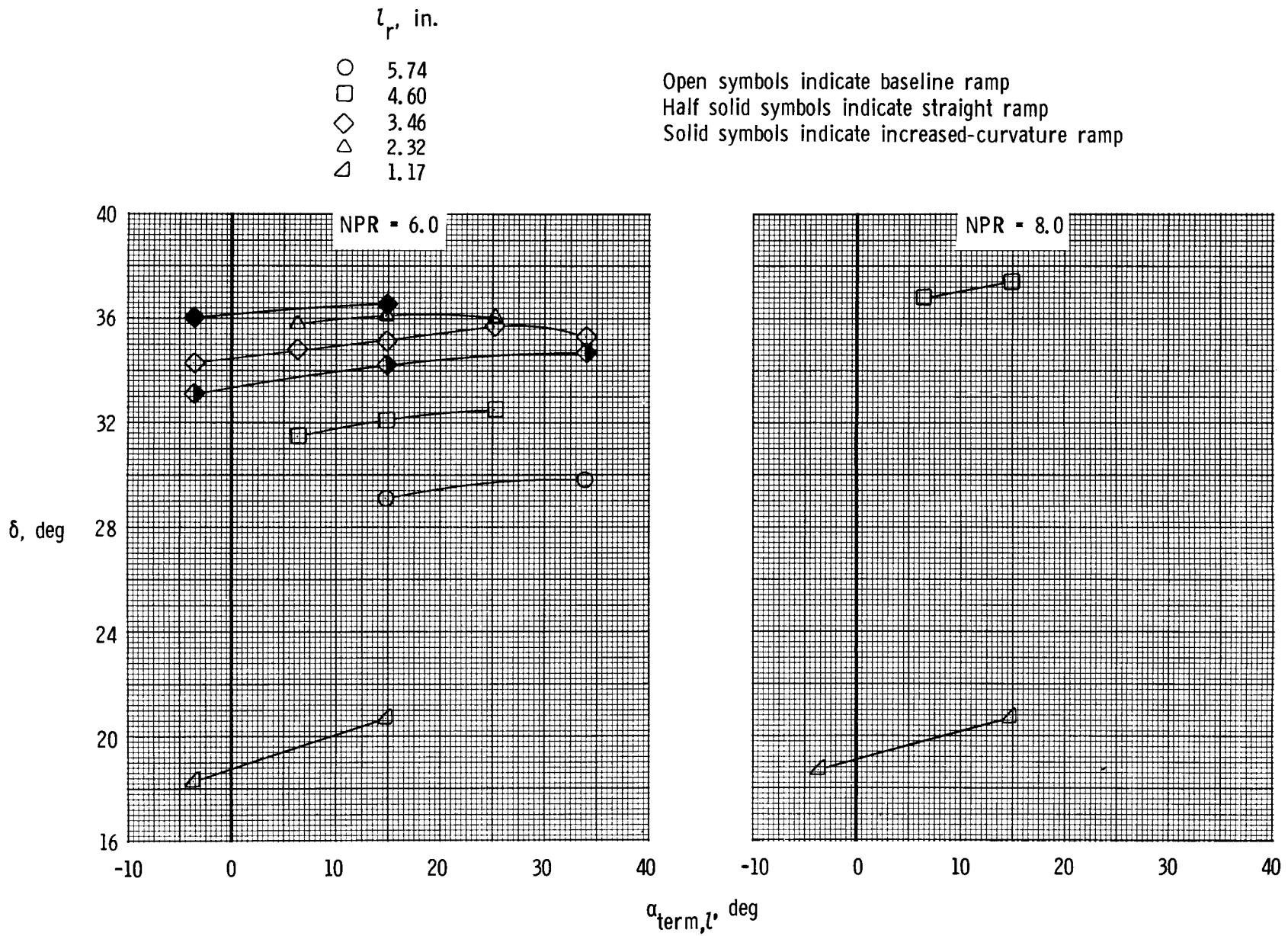

(c) NPR = 6.0 and 8.0.

Figure 19. Concluded.

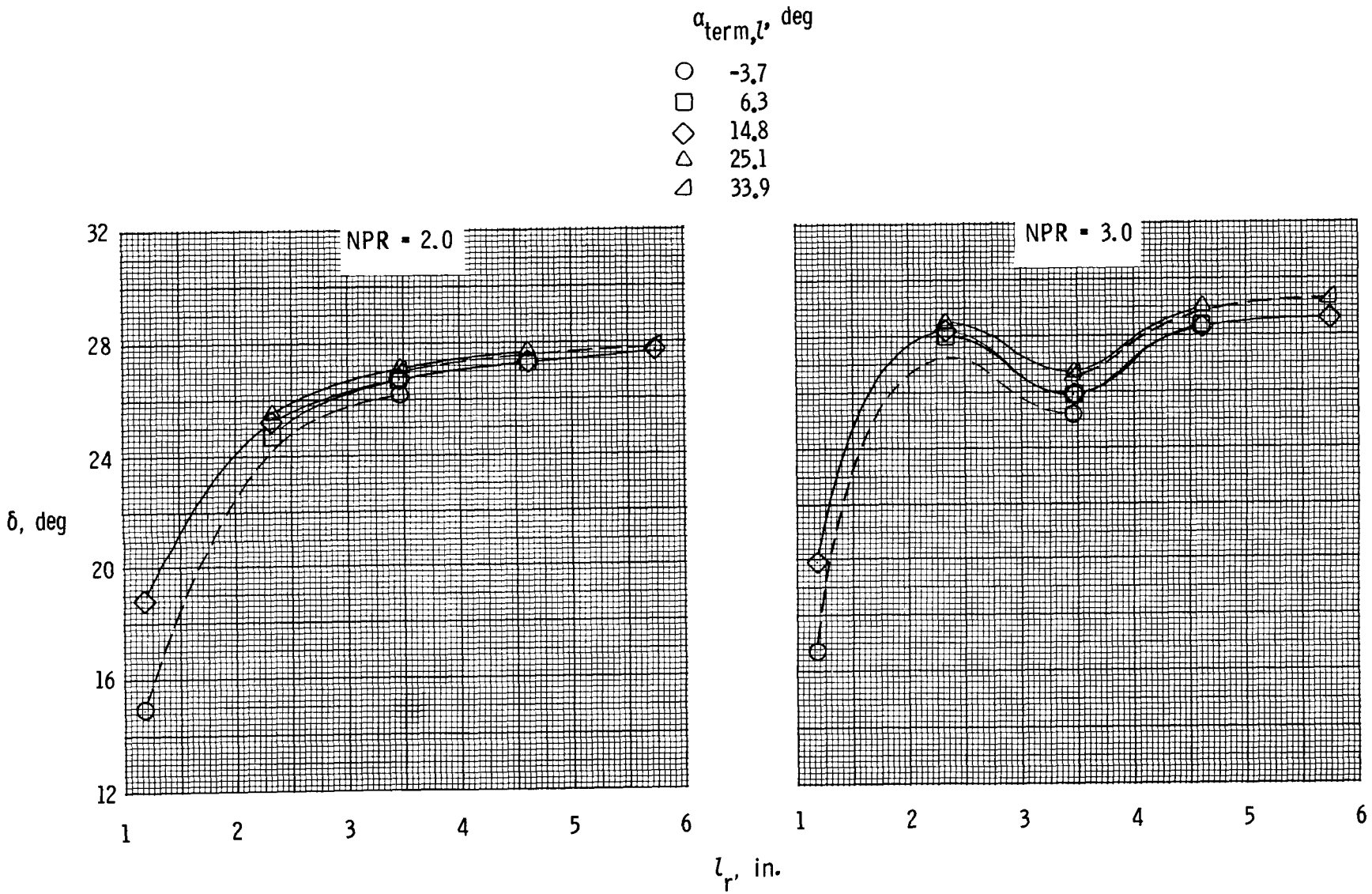

(a) NPR = 2.0 and 3.0.

Figure 20. Summary of ramp-length effects on $\delta_v = 30°$ SERN resultant thrust-vector angle at constant nozzle pressure ratio.

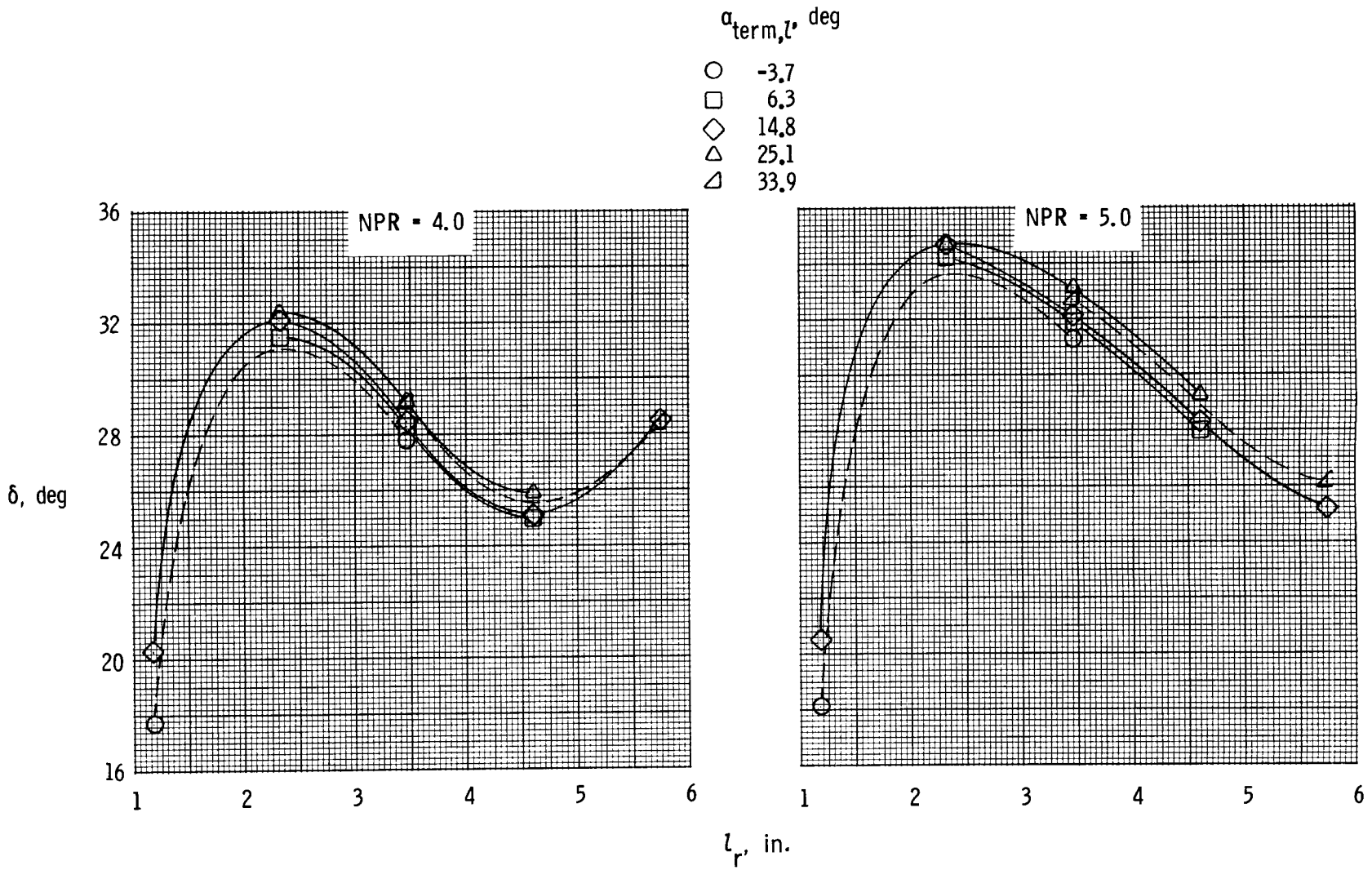

(b) NPR = 4.0 and 5.0.

Figure 20. Continued.

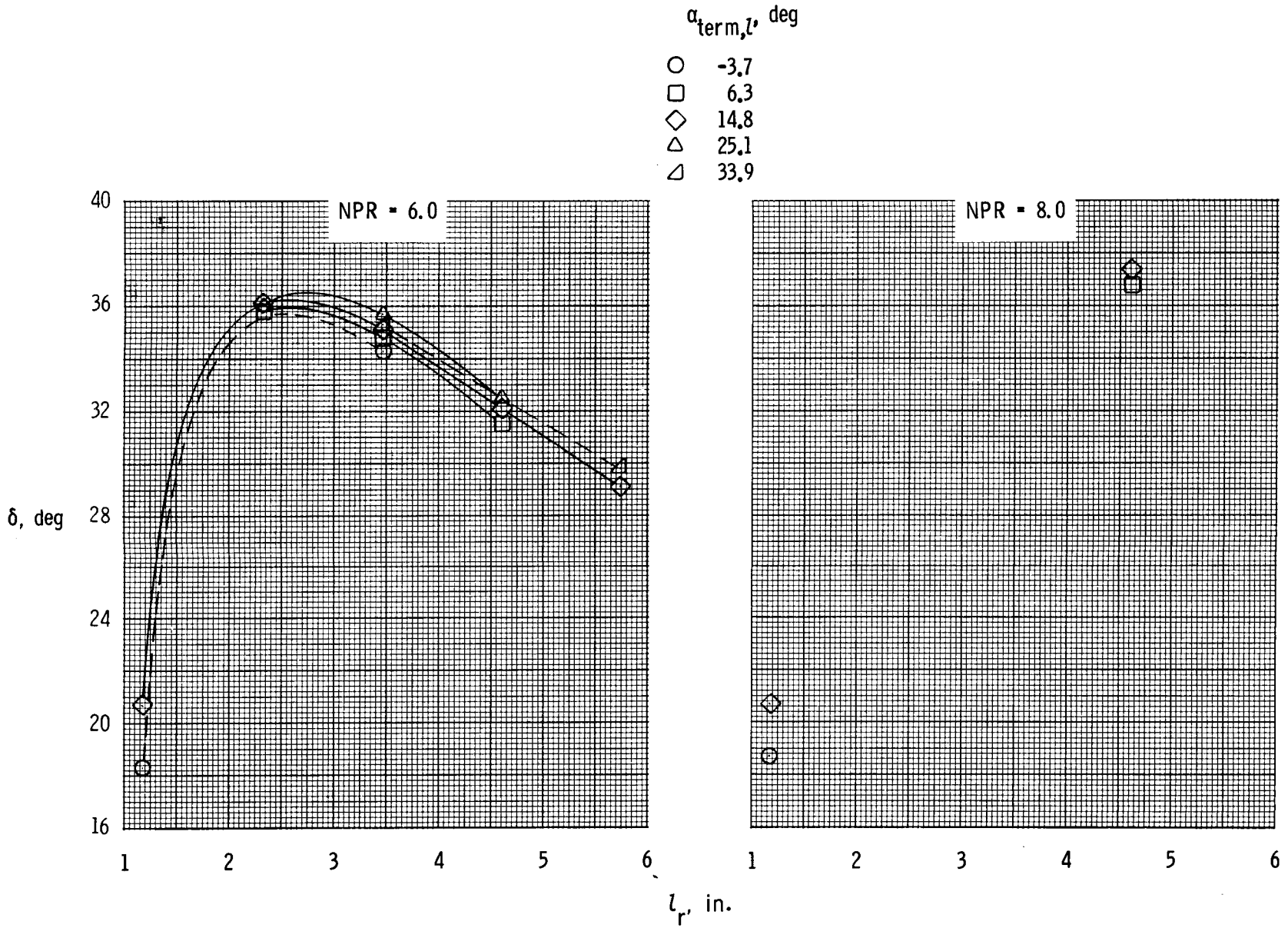

(c) NPR = 6.0 and 8.0.

Figure 20. Concluded.

1. Report No.	2. Government Accession No.	3. Recipient's Catalog No.
NASA TP-2364		

4. Title and Subtitle	5. Report Date
STATIC INTERNAL PERFORMANCE OF SINGLE-EXPANSION-RAMP NOZZLES WITH THRUST-VECTORING CAPABILITY UP TO 60°	October 1984
	6. Performing Organization Code: 505-43-90-07
7. Author(s): Bobby L. Berrier and Laurence D. Leavitt	8. Performing Organization Report No.: L-15766
9. Performing Organization Name and Address: NASA Langley Research Center, Hampton, VA 23665	10. Work Unit No.
	11. Contract or Grant No.
12. Sponsoring Agency Name and Address: National Aeronautics and Space Administration, Washington, DC 20546	13. Type of Report and Period Covered: Technical Paper
	14. Sponsoring Agency Code

15. Supplementary Notes

16. Abstract

An investigation has been conducted at static conditions (wind off) in the static-test facility of the Langley 16-Foot Transonic Tunnel. The effects of geometric thrust-vector angle, sidewall containment, ramp curvature, lower-flap lip angle, and ramp length on the internal performance of nonaxisymmetric single-expansion-ramp nozzles were investigated. Geometric thrust-vector angle was varied from $-20°$ to $60°$, and nozzle pressure ratio was varied from 1.0 (jet off) to approximately 10.0.

17. Key Words (Suggested by Authors(s))	18. Distribution Statement
Nonaxisymmetric nozzles Two-dimensional nozzles Single-expansion-ramp nozzles Internal performance Thrust vectoring	[redacted] Subject Category 02

19. Security Classif.(of this report)	20. Security Classif.(of this page)	21. No. of Pages	22. Price
Unclassified	Unclassified	142	

NASA-Langley, 1984